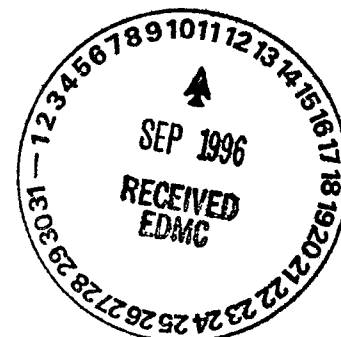# Safety Criteria for the Organic Watch List Tanks at the Hanford Site

Prepared for the U.S. Department of Energy
Assistant Secretary for Environmental Management

**Westinghouse
Hanford Company** Richland, Washington

Management and Operations Contractor for the
U.S. Department of Energy under Contract DE-AC06-87RL10930

SEP 1996
RECEIVED
EDMC

Safety Criteria for the Organic Watch List Tanks at the Hanford Site

J. E. Meacham
A. B. Webb
Westinghouse Hanford Company

M. G. Plys
S. J. Lee
Fauske and Associates, Inc.

J. M. Grigsby
G&P Consulting, Inc.

P. G. Heasler
J. L. Bryant
J. J. Toth
P. M. Daling
Pacific Northwest National Laboratory

Date Published
August 1996

ENGINEERING CHANGE NOTICE

Page 1 of 2

2. ECN Category (mark one)	3. Originator's Name, Organization, MSIN, and Telephone No. 373-1961	4. USQ Required?	5. Date
Supplemental [] Direct Revision [X] Change ECN [] Temporary [] Standby [] Supersedure [] Cancel/Void []	J. E. MEACHAM, W79300, S7-14	[] Yes [X] No	August 27, 1996

	6. Project Title/No./Work Order No.	7. Bldg./Sys./Fac. No.	8. Approval Designator
	Organic Safety Program	2704HV	N/A

	9. Document Numbers Changed by this ECN (includes sheet no. and rev.)	10. Related ECN No(s).	11. Related PO No.
	WHC-SD-WM-SARR-033, Rev. 0	NA	NA

12a. Modification Work	12b. Work Package No.	12c. Modification Work Complete	12d. Restored to Original Condition (Temp. or Standby ECN only)
[] Yes (fill out Blk. 12b) [X] No (NA Blks. 12b, 12c, 12d)	N/A	N/A _____ Design Authority/Cog. Engineer Signature & Date	N/A _____ Design Authority/Cog. Engineer Signature & Date

13a. Description of Change   13b. Design Baseline Document? [] Yes [] No

The most significant changes were the following: (1) Only tanks that had sufficient sample data (67 tanks) were categorized; the remaining tanks (82 tanks) were prioritized for further characterization using tank waste transfer histories and statistical modeling; (2) A model was developed to predict tank responses to an organic-nitrate combustion event; (3) Consequence analyses were added to the report; and (4) A more thorough discussion of controls was also added to the analysis.

14a. Justification (mark one)

Criteria Change [X]	Design Improvement []	Environmental []	Facility Deactivation []
As-Found []	Facilitate Const []	Const. Error/Omission []	Design Error/Omission []

14b. Justification Details

15. Distribution (include name, MSIN, and no. of copies)

See Document Distribution List

RELEASE STAMP

AUG 30 1996

DATE: HANFORD
STA: 37 RELEASE
ID: 20

A-7900-013-2 (05/96) GEF095

A-7900-013-1 (06/92)

16. Design Verification Required [ ] Yes [X] No	17. Cost Impact ENGINEERING	CONSTRUCTION	18. Schedule Impact (days)
	Additional [ ] $	Additional [ ] $	Improvement [ ]
	Savings [ ] $	Savings [ ] $	Delay [ ]

19. Change Impact Review: Indicate the related documents (other than the engineering documents identified on Side 1) that will be affected by the change described in Block 13. Enter the affected document number in Block 20.

SDD/DD	[ ]	Seismic/Stress Analysis	[ ]	Tank Calibration Manual	[ ]
Functional Design Criteria	[ ]	Stress/Design Report	[ ]	Health Physics Procedure	[ ]
Operating Specification	[ ]	Interface Control Drawing	[ ]	Spares Multiple Unit Listing	[ ]
Criticality Specification	[ ]	Calibration Procedure	[ ]	Test Procedures/Specification	[ ]
Conceptual Design Report	[ ]	Installation Procedure	[ ]	Component Index	[ ]
Equipment Spec.	[ ]	Maintenance Procedure	[ ]	ASME Coded Item	[ ]
Const. Spec.	[ ]	Engineering Procedure	[ ]	Human Factor Consideration	[ ]
Procurement Spec.	[ ]	Operating Instruction	[ ]	Computer Software	[ ]
Vendor Information	[ ]	Operating Procedure	[ ]	Electric Circuit Schedule	[ ]
OM Manual	[ ]	Operational Safety Requirement	[ ]	ICRS Procedure	[ ]
FSAR/SAR	[ ]	IEFD Drawing	[ ]	Process Control Manual/Plan	[ ]
Safety Equipment List	[ ]	Cell Arrangement Drawing	[ ]	Process Flow Chart	[ ]
Radiation Work Permit	[ ]	Essential Material Specification	[ ]	Purchase Requisition	[ ]
Environmental Impact Statement	[ ]	Fac. Proc. Samp. Schedule	[ ]	Tickler File	[ ]
Environmental Report	[ ]	Inspection Plan	[ ]		[ ]
Environmental Permit	[ ]	Inventory Adjustment Request	[ ]		[ ]

20. Other Affected Documents: (NOTE: Documents listed below will not be revised by this ECN.) Signatures below indicate that the signing organization has been notified of other affected documents listed below.

Document Number/Revision   Document Number/Revision   Document Number Revision

NA

21. Approvals

	Signature	Date		Signature	Date
Design Authority			Design Agent		
Cog. Eng. A. B. Webb	Q B Webb	8/29/86	PE		
Cog. Mgr. J. E. Meacham	J E Meacham	8/29/96	QA		
QA J. W. Hagan	J. W. Hagan	8/29/96	Safety		
Safety L. E. Thomas	L. E. Thomas	8/29/96	Design		
Environ.			Environ.		
Other			Other		
SEAC R. M. Marusich	Marusich	8/29/96			
TWRS SIR R. J. Cash	R. J. Cash	8/29/96			

DEPARTMENT OF ENERGY

Signature or a Control Number that
tracks the Approval Signature

ADDITIONAL

Safety Criteria for Organic Watch List Tanks at the Hanford Site

J. E. Meacham
Westinghouse Hanford Company, Richland, WA 99352
U.S. Department of Energy Contract DE-AC06-87RL10930

Abstract: This document reviews the hazards associated with the
storage of organic complexant salts in Hanford Site high-level waste
single-shell tanks.   The results of this analysis were used to
categorize tank wastes as *safe, conditionally safe*, or *unsafe*.
Sufficient data were available to categorize 67 tanks; 63 tanks were
categorized as *safe*, and four tanks were categorized as *conditionally
safe*. No tanks were categorized as *unsafe*. The remaining 82 SSTs lack
sufficient data to be categorized. Historic tank data and an analysis
of variance model were used to prioritize the remaining tanks for
characterization.

AUG 30 1996

DATE:

STA: 37

HANFORD
RELEASE

ID:

20

Release Approval   *Date*   *Release Stamp*
8-30-96

Approved for Public Release

RECORD OF REVISION		(1) Document Number WHC-SD-WM-SARR-033, ~~Rev. 0~~	Page 1

(2) Title
Safety Criteria for Organic Watch List Tanks at the Hanford Site

CHANGE CONTROL RECORD				
(3) Revision	(4) Description of Change - Replace, Add, and Delete Pages	Authorized for Release		
		(5) Cog. Engr.	(6) Cog. Mgr.	Date
0	(7) Preliminary Safety Criteria for Organic Watch List Tanks at the Hanford Site EDT 142232, 11/13/95			
1 RS	Document Revision ECN 609995	*JC Meal* JE Meacham	*JC Meal for* RJ Cash	8/30/96

SAFETY CRITERIA FOR ORGANIC
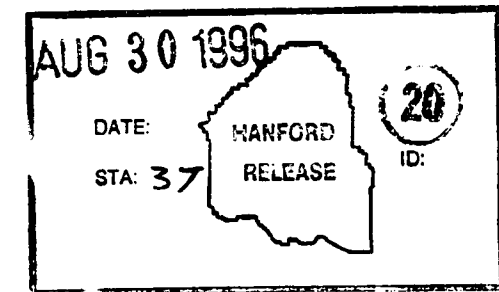# WATCH LIST TANKS AT THE HANFORD SITE

EXECUTIVE SUMMARY

This document reviews the hazards associated with the storage of organic complexant salts in Hanford Site high-level waste single-shell tanks (SSTs). Evaluations of Hanford Site double-shell tanks are not included because these tanks contain appreciable amounts of aqueous waste and cannot support organic complexant combustion under current storage conditions. Evaluation of double-contained receiver tanks and catch tanks are not included in this analysis because these tanks contain appreciable amounts of aqueous waste and cannot support organic complexant combustion under current storage conditions.

The results of this analysis were used to categorize tank wastes as *safe*, *conditionally safe*, or *unsafe*. Although total organic carbon is not a direct measure of chemical reactivity, conservative TOC criteria were used on an interim basis (until more direct measurements of chemical reactivity are available) to categorize the tanks. Sufficient data were available to categorize 67 tanks; 63 tanks were categorized as *safe*, and four tanks were categorized as *conditionally safe*. No tanks were categorized as *unsafe*. The remaining 82 SSTs lack sufficient data to be categorized. Historic tank data and an analysis of variance model were used to prioritize the remaining tanks for characterization.

A bounding consequence analysis showed dose consequences above risk evaluation guidelines for the organic-nitrate combustion hazard. Therefore, controls were described to reduce accident frequency and to maintain waste safety.

This page intentionally left blank.

TABLE OF CONTENTS

TABLE OF CONTENTS (Continued)

LIST OF FIGURES

LIST OF TABLES

LIST OF TERMS

DNFSB	Defense Nuclear Facilities Safety Board
DOE	U.S. Department of Energy
DBP	dibutyl phosphate
DQO	data quality objectives
DSC	differential scanning calorimetry
DST	double-shell tank
EA	environmental assessment
EBA	evaluation basis accident
EDTA	ethylenediaminetetraaceticacid
FAI	Fauske and Associates, Inc. (Burr Ridge, IL)
GRE	gas release event
HEDTA	hydroxyethylethylenediaminetriaceticacid
HTCE	historical tank content estimate
NPH	normal paraffinic hydrocarbons
NTA	nitrilotriaceticacid
RSST	reactive system screening tool (a small adiabatic calorimeter)
SA	safety assessment
SST	single-shell tank
TBP	tributyl phosphate
TC	thermocouple
TGA	thermogravimetric analysis
TOC	total organic carbon
UR	uranium recovery
USQ	unreviewed safety question
wt%	weight percent

1.0 INTRODUCTION

1.1 PURPOSE AND SCOPE

This document reviews the hazards associated with the storage of organic complexant salts in Hanford Site high-level waste single-shell tanks (SSTs). Evaluations of Hanford Site double-shell tanks (DSTs) are not included because these tanks contain appreciable amounts of aqueous waste and cannot support organic complexant combustion under current storage conditions. Evaluation of double-contained receiver tanks and catch tanks are not included in this analysis because these tanks contain appreciable amounts of aqueous waste and cannot support organic complexant combustion under current storage conditions.

The strategy of this document is to establish safety criteria for waste storage, and then to evaluate the tanks against the criteria using a statistical analysis. Although total organic carbon is not a direct measure of chemical reactivity, conservative TOC criteria were used on an interim basis (until more direct measurements of chemical reactivity are available) to categorize the tanks.

The tanks are categorized, and potential ignition sources are identified. Controls are identified to mitigate potential ignition sources, and the controls are applied in a graded fashion depending on tank category. This report also projects the potential consequences and frequency of an in-tank organic complexant combustion event.

1.2 BACKGROUND

Several waste generating processes have operated at the Hanford Site since 1944, including: the bismuth/phosphate process, the uranium recovery process, the REDOX process, the waste fractionization process, the PUREX process, and the processes conducted at the Plutonium Finishing Plant (PFP). The primary goal of these processes was to extract and/or process plutonium. The radioactive wastes from these processes are stored in underground tanks in alkaline slurries (Anderson 1990). There are a total of 177 storage tanks, 149 SSTs and 28 DSTs.

Each of the waste-generating processes had a rather wide variety of waste streams (at least 49 different types have been identified), but the following broad categories can be established: (1) cladding (or coating) waste from the removal of the fuel element cladding; (2) metal waste (MW) from the processing of the fuel itself to remove the plutonium or other fissile material; (3) decontamination waste from the clean-out of the systems (this includes N Reactor decontamination waste); (4) other miscellaneous waste, such as laboratory waste. Once the waste was generated and initially stored in the tanks, various other operations were performed, including removal/recovery of various materials (uranium, strontium, cesium), evaporation, solidification, and settling.

The principal organic compounds that were disposed to the storage tanks are divided into two classes: complexants (for chelating divalent, trivalent, and

tetravalent cations) and extraction solvents. This document focuses on the organic complexant hazard; the organic solvent hazard is discussed in other documents (Postma et al. 1994, Cowley and Postma 1996).

The principal organic complexants sent to the tanks are glycolic acid, citric acid, hydroxyethylethylenediaminetriaceticacid (HEDTA), and ethylenediamine-tetraaceticacid (EDTA). The quantities of complexants used are summarized in Table 1-1 (Allen 1976). In addition to these complexants, complexants such as nitrilotriaceticacid (NTA), di(2-ethylhexyl)phosphoric acid, and oxalic acid were also used, but the amounts of these complexants were relatively small and are not well quantified.

Table 1-1. Quantities of the Principal Organic Complexants Used at Hanford

Complexant	Quantity (Metric Tons)
Glycolic Acid	880
Citric Acid	850
Hydroxyethylethylenediaminetriaceticacid (HEDTA)	830
Ethylenediaminetetraaceticacid (EDTA)	220

1.3 CHANGES FROM PREVIOUS REVISION (Rev. 0)

This document uses the safety criteria from the previous revision (Webb et al 1995) but it also adds another, more stringent criterion for *safe* wastes. The *safe* waste category in the current document is now based only on fuel content. In the previous revision conditionally safe waste was defined as currently moist waste which had the potential to dry out to an *unsafe* state; *conditionally safe* waste in this revision includes any waste which exceeds the *safe* fuel criterion, but contains moisture. *Unsafe* waste remains the same for both revisions.

The most significant changes were the following:

- Only tanks that had sufficient sample data (67 tanks) were categorized; the remaining tanks (82 tanks) were prioritized for further characterization using tank waste transfer histories and statistical modeling.

- A model was developed to predict tank responses to an organic-nitrate combustion event.

- Consequence analyses were added to the report.

- A more thorough discussion of controls was also added to the analysis.

2.0 ORGANIC COMPLEXANT HAZARD

2.1 HAZARD PHENOMENOLOGY

During the defense mission at the Hanford Site, organic complexants including glycolic acid, citric acid, HEDTA, and EDTA were used during fuel reprocessing, metal recovery operations, and waste management separations. These materials were discharged to the tanks, where they mixed with sodium hydroxide, sodium nitrate and nitrite, and other inorganic diluents already present in the tanks. Organic complexants will react with oxidizing materials, such as nitrates or nitrites. This reaction can be accelerated to a rapid combustion by heating to high temperatures (above 220 °C) or by an initiator of sufficient energy (Fauske et al. 1995).

During the postulated combustion reaction, as product gases are being released, the tank headspace begins to heat and pressurize, assuming the venting capacity is not sufficient to provide pressure relief. Heat transfer occurs between the headspace and the tank dome, tank walls, and the uncombusted substrate surface. Condensation of water vapor, a major product, and minor species may also occur on these surfaces. As the pressure rises, pressure-driven flow would begin between the tank headspace and the environment; no credit is taken for flow through cascade lines between tanks since these lines are assumed to be shut. If the headspace were to attain sufficient pressure, cracks would develop in the concrete dome which then would allow further venting of combustion product gases and thus limit further pressure increases. Minor product gases may enter the headspace and cool down to form aerosols; the amount of aerosol formed depends upon the species vapor pressure at the given headspace temperature. Aerosols may co-agglomerate, fall out via gravitational sedimentation, or may be swept to surfaces by condensation. A certain portion of the vapors and aerosols of the minor products is carried out of the headspace by being entrained with the major gases, and transport of undesirable species to the environment then defines the source term from the tank for the postulated combustion reaction.

2.2 ORGANIC SOLVENTS

Various separation processes involving organic solvents have been used at the Hanford Site. These organic solvents were inadvertently and/or purposely sent to the underground storage tanks, and subsequent waste transfer operations might have distributed organic solvent among several of the 177 high-level waste tanks at the Hanford Site (Sederburg and Reddick 1994). The principal organic solvents were tributyl phosphate (TBP) and mixtures of normal paraffinic hydrocarbons (NPH). The solvents are only partially soluble in the aqueous wastes and can therefore exist either in separate phases dispersed among other liquid and solid phases or in a separate layer atop the aqueous phase.

Experiments with dibutyl phosphate (DBP), TBP, and NPH showed that the solvents do not exhibit condensed-phase combustion when mixed with nitrate oxidizers (Cowley and Postma 1996). The mixtures tested had theoretical chemical energy releases well in excess of that required for condensed-phase

organic complexant-nitrate combustions. Adding DBP, TBP, and NPH to fuel-lean mixtures (i.e., mixtures containing less organic complexant than was necessary to sustain a propagating combustion) of organic complexants and nitrate, did not make an otherwise non-reactive waste into a combustible condition.

Testing of waste from tank C-204 corroborated the simulant experiment results (Conner 1996). Waste samples from this tank contained over 25 weight percent (wt%) TBP (dry basis), and did not exhibit condensed-phase combustion when tested by adiabatic calorimetry.

Although the solvents do not exhibit condensed-phase combustion, they could combust in air. If a portion of the organic solvent were heated to the flash point by a large initiator, combustion in air would ensue. This hazard is outside the scope of this analysis and is discussed in Cowley and Postma (1996).

2.3 ORGANIC-NITRATE REACTION PHENOMENOLOGY

Two reaction phenomena have been examined: (1) spontaneous chemical runaway (self heating) reactions occurring throughout the waste mass; and (2) ignition of propagating exothermic chemical reactions (combustion) typified by a moving reaction front.

2.3.1 Spontaneous Chemical Runaway

The rate of heating must exceed the rate of cooling for a spontaneous chemical runaway reaction to occur (Gygax 1990). If the temperature is not controlled, then undesirable deflagrations can occur when the large activation energy barriers are exceeded. Preventing spontaneous chemical runaway has been thoroughly studied in the chemical and petroleum industries (American Institute of Chemical Engineers 1989, 1992, 1995a, 1995b, 1995c, 1995d, and 1995e). Hanford Site tank wastes have been assessed using similar methodology, and the results show that spontaneous conditions leading to a chemical runaway in the passively ventilated tanks are highly unlikely under current storage conditions (Fauske 1996a). However, the waste in seven SSTs (C-106, SX-107, -108, -110, -111, -112 and -114) has high enough decay heat to require active cooling to maintain waste temperatures within acceptable limits. Temperature monitoring and waste cooling controls (see Section 6.2) are currently required for these tanks.

The potential for spontaneous chemical runaway reactions was evaluated by comparing the characteristic time of cooling (i.e., the time required to reach a new equilibrium temperature following an instantaneous change in heating rate) with the waste storage time. Calculations indicate that the characteristic time of cooling ranges from a few hours to 3.1 years for the Hanford Site tanks (Fauske 1996a). Some waste has been stored for more than 40 years, and there have been no transfers of waste into the SSTs for about 15 years. Several characteristic times of cooling have passed during the last 15 years of storage; consequently, bulk runaway reactions are not credible.

In addition, no credible mechanisms to increase tank temperatures to chemical runaway reaction levels have been identified for the passively ventilated

tanks. Drying the wastes can decrease the thermal conductivity; however, this decrease would not be sufficient to lead to spontaneous chemical runaway (Fauske 1996a). Waste temperatures after removal of the pumpable liquid (interim stabilization) have continued to decline consistent with the principal heat load from radioactive decay rates. One hundred fourteen of the 149 SSTs have been interim stabilized.

2.3.2 Ignition of Organic Complexants

If enough fuel is present and the waste is sufficiently dry, an organic-nitrate/nitrite propagating combustion event could be initiated by a variety of sources. However, it is important to note that all of the waste sampling and testing to date indicate no waste that meet these conditions.

Potential credible ignition sources include hot metal objects, rotary core upsets, burning gasoline spills from a ruptured vehicular fuel tank, or lightning (see Section 4.0). However, fuel, oxidizers, and temperature (initiators) are all important parameters. Specific conditions of fuel, moisture, and temperature (initiators) are all required to support a propagating combustion. Fuel and moisture criteria are discussed in Section 2.4 and ignition source requirements are discussed in Section 2.5.

2.4 SAFETY CRITERIA

The minimum required fuel concentration has been determined using a contact-temperature ignition model (Fauske et al. 1995). Theory indicates that a necessary (but not sufficient) condition for a condensed-phase propagating combustion is that the fuel concentration be greater than 4.5 wt% total organic carbon (TOC), or that fuel concentration exceed 1.2 MJ/kg on an energy equivalent basis. For fuel concentrations between 4.5 and 7.9 wt% TOC, the waste moisture concentration required to prevent a propagating combustion varies linearly from 0 to 20 wt%. Above 20 wt%, the fuel-moisture linear relationship no longer holds because the mixture becomes liquid continuous. A stoichiometric fuel-oxidizer mixture will not propagate when the moisture concentration exceeds 20 wt% (Fauske et al. 1995).

If a waste lacks sufficient fuel to support a propagating combustion (even if the waste were hypothetically dried), the waste is categorized as *safe*. That is, the waste is *safe* if the following inequalities are met (Equations 2-1 and 2-3):

$$wt\% \, TOC \leq 4.5 \qquad (2\text{-}1)$$

On a wet TOC basis, the fuel criterion would be the dry TOC multiplied by $(1-x_w)$

$$TOC(wet) < (4.5 - 4.5 x_w) \qquad (2\text{-}3)$$

In terms of energy (ΔH) the criterion for dry waste is

$$\Delta H \, (MJ/kg) \leq 1.2 \qquad\qquad (2\text{-}3)$$

If waste contains sufficient fuel (i.e., greater than 4.5 wt% TOC or 1.2 MJ/kg), but is too moist to support a propagating combustion, the waste is categorized as *conditionally safe*. In summary, the waste cannot combust if the following inequalities are met (Equations 2-3 and 2-4):

$$wt\% \, TOC \leq (4.5 + 17 \, x_w) \qquad\qquad (2\text{-}4)$$

or in terms of energy (ΔH)

$$\Delta H \, (MJ/kg) \leq (1.2 + 4.5 \, x_w) \qquad\qquad (2\text{-}5)$$

where x_w is the mass fraction of free water for values less than 0.2 (20 wt%).

Waste that does not meet the criteria for the *safe* or *conditionally safe* categories is defined as *unsafe*. The criteria are shown graphically in Figure 2-1. Analysis of variance (ANOVA) models have been used to compare TOC and moisture tank waste data to the safety criteria. Results and assumptions are reviewed in Section 3.0.

Experiments with waste simulants (Fauske et al. 1995, Fauske 1996a, Fauske 1996b, Fauske 1996c) show that significantly more than 4.5 wt% TOC is required to support a propagating combustion. Mixtures of sodium nitrate/nitrite oxidizer with sodium acetate, sodium citrate dihydrate, and HEDTA dihydrate have been tested. The lower limit concentrations were 6, 8, and 6 wt% TOC, respectively. Two energetic surrogates were found not to have a lower flammability limit, i.e., even stoichiometric concentrations could not sustain a propagating combustion. These were sodium acetate trihydrate and sodium oxalate.

Additional data were taken with varying amounts of water for those simulants that could sustain a propagating combustion. A comparison of the simulant experiments results against the safety criteria is shown in Figure 2-2. All of the empirical data from simulant testing indicate that the criteria are bounding. It was found in all cases that 20 wt% free water was sufficient to prevent even a stoichiometric mixture of these surrogates from sustaining a propagating combustion. The free water equivalent maximum was 15% for sodium HEDTA dihydrate.

Figure 2-1.   Safety Criteria for Organic Waste

Figure 2-1.   Safety Criteria for Organic Waste

The chart axes and regions:
- Y-axis: Total Organic Carbon (Weight % Wet), scale 1 to 8
- X-axis: Free Water (Weight %), scale 0 to 30

Regions labeled:
- UNSAFE (COMBUSTIBLE)
- CONDITIONALLY SAFE
- SAFE

Boundary equations:
$$TOC = 4.5 + 0.17 (WT \% \text{ Free } H20)$$
$$TOC = 4.5 - 0.045 (WT \% \text{ Free } H2O)$$

AAAACRTE.GAL/960826/ABW
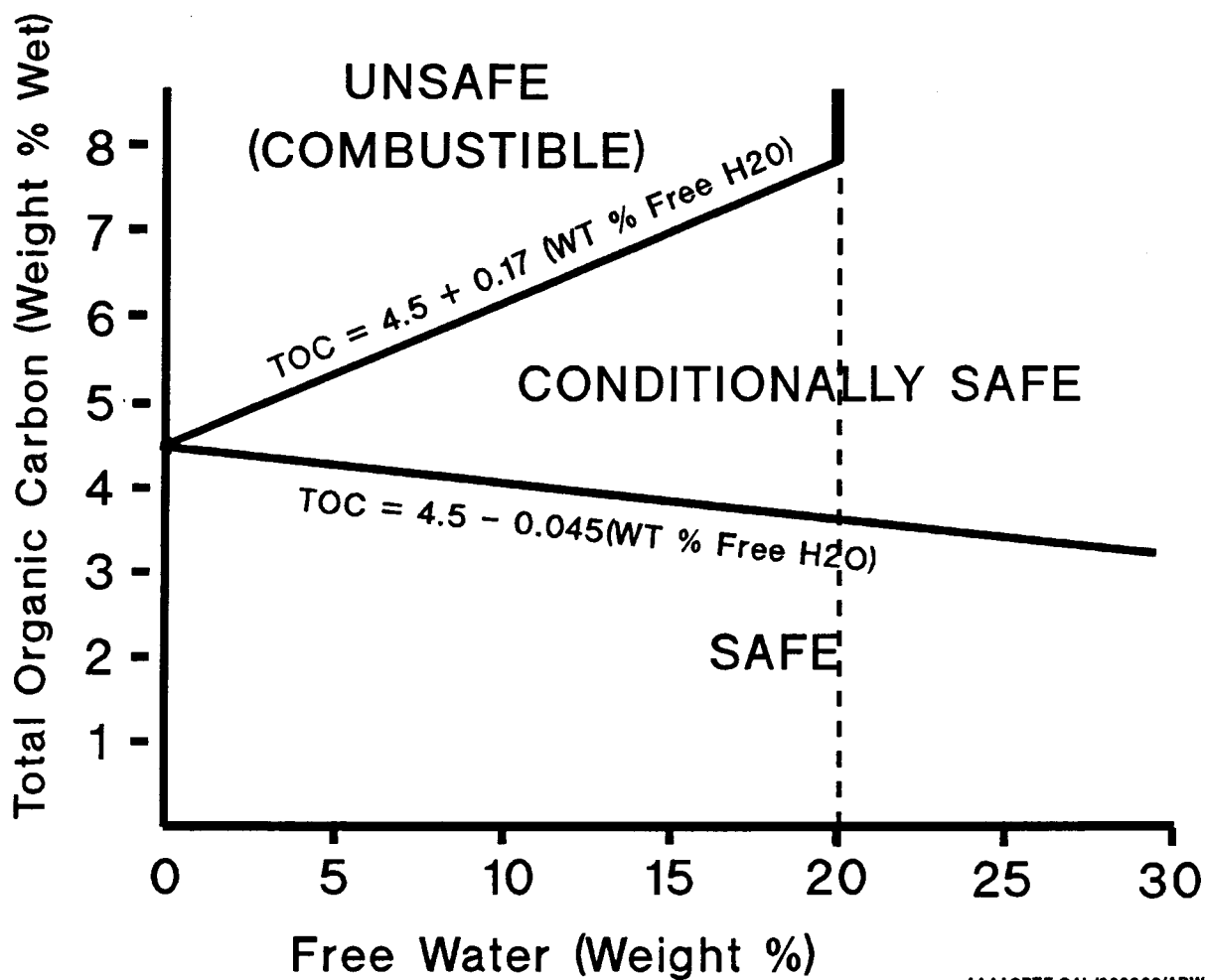
Figure 2-2.   Comparison of Experimental Results to Safety Criteria

No Burn	Burn	
○	●	Na Acetate
□	■	Na HEDTA · $2H_2O$
△	▲	Na Citrate · $2H_2O$
▽	▼	Na Butyrate
◇		Aℓ Dibutyl Phosphate
S		Stoichiometric

$$wt. \% \ TOC = 4.5 + 17x_w$$

HF951081.CDR 8-1-95
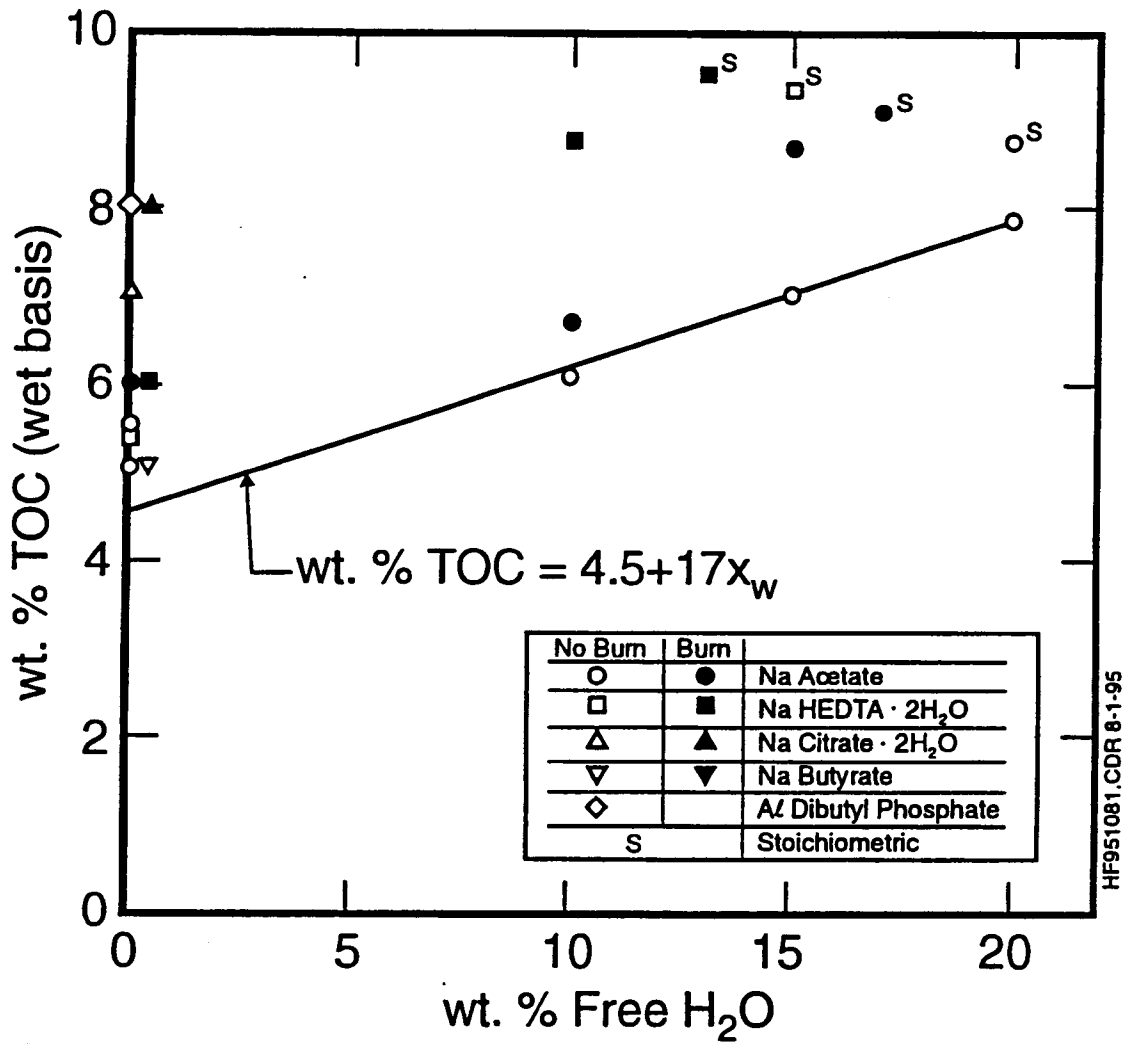
2.5 IGNITION PHENOMENOLOGY

The minimum amount of energy required to ignite an organic complexant combustion was derived using theory (Fauske 1996a). For a dry (zero total water) stoichiometric mixture of organic fuel and oxidizer, the minimum ignition energy is 3.3 Joules. This value is about four orders of magnitude larger than for flammable gas mixtures.

Experiments with waste simulants indicate significantly more energy is actually required to ignite an organic combustion. Ignition sources utilized to date include a pyrotechnic "electrical match" which releases (when supplied with 110 VAC) about 140 J over a 3-5 msec period, and various size steel particles (1/16, 3/32 and 3/16 inch) heated to about 1300 °C (corresponding energy contents of 10, 35 and 270 J).

Experimental results indicate that greater than 10 J is required to ignite dry (zero total water) stoichiometric organic-nitrate mixtures. Experiments also showed that ignition sources larger than 270 J are required if a small amount of free moisture (~5 wt%) is present, even for stoichiometric organic-nitrate mixtures (Fauske 1996a).

2.6 ORGANIC DECOMPOSITION (AGING)

Studies indicate that organic complexants undergo hydrolytic and radiolytic decomposition (aging) under tank waste conditions (Camaioni et al. 1994, 1995, Bryan et al. 1996). As the organic waste ages, some intermediate byproducts can be more energetic, but most of these byproducts are unstable and quickly convert to other less reactive materials by radiolysis or hydrolysis. The net effect of aging decreases the potential chemical energy of the waste.

The influence of temperature and radiation dose on the rate of aging is not sufficiently defined to quantify the effect aging has had on safe storage. Therefore, no credit for aging was assumed in this safety analysis. Kinetic data.for aging are being investigated using waste simulants, and the composition of actual waste will be examined in an effort to quantify aging in the future. The organic in the waste will be speciated to develop a reliable indicator of aging, such as the ratio of the unaged constituents to the resultant aging byproducts (e.g., oxalate).

2.7 ORGANIC SOLUBILITY

The solubility properties of organic complexants are being investigated (Barney 1994, 1996). Tests with waste simulants indicate that with the important exception of sodium oxalate, all the other sodium carboxylate salts and their principal decomposition products are very soluble in the alkaline aqueous in the tanks. If the energetic complexants are present in the non-combustible aqueous phase, then most of the fuel could be removed by interim stabilization (pumping of the liquid from the tanks).

The measured solubility limit for the energetic complexants (EDTA, NTA, glycolate, succinate, DBP, and citrate) is approximately 100 g/L. Aqueous samples from 61 tanks have been analyzed for TOC concentration. Only five of these tank aqueous samples had TOC concentrations greater than 14 g/L (Van Vleet 1993a, 1993b). Since the highest measured value for TOC (approximately 40 g/L) is substantially below the measured limit of 100 g/L, it is anticipated that most or all of the energetic complexants are contained in the aqueous phase.

3.0 TANK WASTE FUEL AND MOISTURE ANALYSIS

The methodology developed for estimating the quantities of combustible waste in the Hanford high level waste tanks is discussed here. The methodology uses as inputs, tank characterization data for fuel and moisture, waste tank volumes, tank process history (historical tank transfer records) and selected physical property data. This information is integrated into a statistical analytical technique to estimate the current conditions of tank wastes that have been sampled for TOC and/or moisture. Using the estimate of fuel/moisture for sampled wastes, and a tank grouping scheme derived from historical tank records, fuel/moisture estimates are produced for the unsampled tanks.

3.1 ASSUMPTIONS AND CONSERVATISMS IN THE ANALYSIS

The validity of the combustible waste estimates produced in this chapter rests on several assumptions. If these assumptions were altered the estimates of combustible waste could change substantially. Below is a list of the most important assumptions:

(1) TOC and moisture concentrations are log-normally distributed within tank layers and their bivariate distribution is log-normal.

(2) The spatial variability of both TOC and moisture (on the log scale) is roughly the same in all tanks and can be pooled together across tanks.

(3) The tanks that have been sampled for TOC and moisture are representative tanks, particularly with respect to the TOC and moisture tank groupings that have been defined.

(4) The errors present in the TOC and moisture measurements are much smaller than the spatial variabilities and can be ignored.

(5) The samples taken from each tank are representative of the waste within the tank.

(6) The uncertainty distributions on moisture and TOC are assumed to be independent.

The first two assumptions are most important to the validity of this analysis. In fact, these assumptions are critical for ANY analysis that uses sampling data; the sampling data must be representative of the properties to be measured. Most particularly, the predictions for unsampled tanks are only valid if the sampled tanks (in each group) are representative of all the tanks in that group.

Furthermore, it should be pointed out that the validity of the first two assumptions can not easily be checked without taking more data. This is not the case with the other assumptions in the list, which can be checked with existing data.

Existing data shows that assumptions (3) and (4) are reasonable; a few tanks seem to show significantly more spatial variability in moisture/TOC than others. Whether this is because of measurement bias, atypical sampling, or real differences in spatial variability is unclear at this time. Also, existing data shows that the log-normal distribution sometimes does not adequately describe the tail of the TOC distribution. Sometimes the spatial distribution of TOC has a heavier tail than predicted by the log-normal distribution. Even though there are deficiencies with these assumptions, we do not believe the deficiencies are severe enough at this time to warrant changes in the methodology.

The methodology actually uses data to calculate spatial variability plus measurement error. To calculate the fraction of combustible waste, an estimate for spatial variability, uncontaminated by measurement error, is required and this is obtained by subtracting out estimates for measurement error obtained from the labs. The current estimate is 10%. If measurement error is over-estimated, then combustible waste fractions will be too small, if it is under-estimated, the combustible waste fractions will be too large.

Several conservatisms also exist in this analysis and the current model will be refined when these conservatisms can be better quantified. Below is a list of the major conservatisms:

(1) The combustible fraction of the waste is contiguous.

(2) The waste contains sufficient nitrate/nitrite oxidizer for combustion, and the fuel and oxidizer are intimately mixed.

(3) The TOC measured in the tank waste is not aged and is still combustible.

(4) The measured TOC is assumed to be organic complexant unless demonstrated otherwise. [The current TOC analyses do not distinguish between organic solvent and organic complexant TOC. This is a conservative assumption because testing with simulants and actual waste samples show that the organic solvents do not combust with the nitrate/nitrite salts under tank conditions (Cowley and Postma 1996, Conner 1996)].

(5) The minimum TOC concentration (dry basis) required to support a propagating combustion is 4.5 wt% (experiments with waste simulants indicate the actual value is closer to 6.0 wt%).

(6) Most of the combustible TOC is not contained in the aqueous phase.

When evaluating the safety consequences of a particular combustive waste fraction, it is assumed that all the combustible waste is contiguous (1), and therefore would burn. It is most likely that only a proportion of the combustible waste would be contiguous, and if this proportion was known, the present combustible waste fractions should be multiplied by it to produce the fraction of combustible waste that can participate in a burn. Conservatisms (2) through (4) deal with the present definition of combustible waste. If tank organic carbon heat of reaction were better known, the combustible waste fraction would most likely be smaller. Also, the present calculation assumes that the combustion is fuel limited and not oxidant limited, a reasonable

assumption for saltcake waste. However, the calculation is also applied to sludge tanks where this may not be the case.

This methodology produces an estimate for the dry combustible waste fraction, which is probably more conservative than the state of the waste after jet-pumping. If one equates the dry waste fraction to the state after jet-pumping, one is assuming no combustible TOC is in the liquid phase (6).

3.2 OVERVIEW AND INTERPRETATION OF AVAILABLE DATA

This section gives a brief overview of the information used to estimate the combustible waste volumes in each tank: analytical sample data and chemical flowsheet process history. The analytical data and chemical flowsheet process history are used to group tanks that have waste with similar TOC and moisture properties, allowing the combustible fraction of waste in the unsampled tanks to be estimated.

Sampling of the tank is carried out based on the type and quantity of waste in each individual tank. Three techniques were used: push-mode and rotary-mode core sampling, and auger sampling. When core sampling, segments for the entire vertical depth of the tank waste below the riser are collected. Auger sampling retrieves only a surface sample, approximately the top 0.4 m (40 cm) of waste. Before laboratory analysis, core samples are extruded and sub-sampled, while auger samples are not.

Drainable liquid is separated from the solid sample before analysis of the solid phase constituents. However, given that liquid remains in the sample solid phase within the interstitial pore volume, analysis reports of core and auger solid TOC measurements are actually measurements of the composite solid plus any undrained liquid that remains with the solid.

Several sources of data were considered for the analyte and physical property data. These include tank characterization reports, the tank waste information network, and documented process aids reports. These three sources of data represent a majority of the analytical results from Hanford tank farm analysis. Data available through December 1995 were used in this effort.

3.2.1 TOC Measurements

TOC is the analyte used to estimate the fuel content of the waste, with the measured concentration of carbon materials providing possible fuel for an organic-nitrate combustion. Many of the SSTs have been sampled and TOC concentrations measured, making TOC a good analyte for this purpose.

TOC is measured in the laboratory by first oxidizing the organic species to carbon dioxide, and then using a carbon dioxide gas analyzer to detect and quantify the amount of CO_2 produced. Only the amount CO_2 produced is measured, and information pertaining to the species cannot be recovered. Three different oxidation techniques were used to measure TOC. These methods included: (1) silver-catalyzed hot persulfate wet oxidation (direct), (2) high temperature furnace combustion with coulometry detection, and (3) ultraviolet catalyzed persulfate with nondispersive infrared detection. The

direct persulfate oxidation and furnace oxidation methods are in use at the WHC 222-S laboratory.

3.2.2 Moisture Measurements

The *conditionally safe* category for Hanford tank wastes includes the presence of water because water has been shown to prevent propagating combustions in mixtures of organic fuel and oxidizer. The moisture content of tank waste sample is determined using thermogravimetric analysis (TGA) and gravimetric analysis. In TGA, a small sample of waste (10 to 30 milligrams) is collected on a platinum pan and placed in the TGA analyzer. The sample is sealed in an inert environment of nitrogen gas and heated at 10°C per minute, while the total mass of the sample is recorded on a plot of temperature versus mass. The mass loss inflection points are noted, and the mass loss between the inflection points are recorded. Mass loss is recorded, converted to a percent basis, and reported as percent moisture of the sample. Water of hydration is generally released at temperatures above 120°C, and would not be recorded as moisture loss in the moisture data set.

Gravimetric analysis involves heating the waste sample at a constant temperature in a small furnace for a period of 18 to 24 hours. In the case of gravimetric analysis, the sample weight is about one half to two grams. In the case of the 222-S laboratory, the constant temperature of the sample drying is usually 105 °C. The loss of mass during the drying is converted to a wt% basis and reported as percent moisture.

3.2.3 Tank Grouping Information

The two characteristics used for tank moisture grouping are the following: (1) absence or presence of visible liquid on the tank waste surface, and (2) large or small particle size distribution of the solid. Visible liquid on the waste surface suggests that the waste is saturated with liquid. Waste particle size is important because waste simulant experiments, theoretical analyses, and actual waste testing indicate that the large particle size wastes (saltcakes) tend to drain liquid more readily than the small particle wastes (sludges) (Atherton 1974, Handy 1975, Metz 1975a, 1975b, and 1976, Kirk 1980, Jeppson and Wong 1993, Epstein et al. 1994, and Simpson 1994). Therefore, the large particle wastes could potentially be drier than the small particle wastes. Particle sizes for the tank wastes were assigned using the information in Agnew (1996).

The designation of the absence or presence of visible liquid on the tank surface is provided from the initial organic-nitrate screening of 149 SSTs. Photographs of the tank waste indicate that fifty tanks have visible liquid on the surface. Small particle size is characterized by less than a 150 micron mean particle size diameter. SSTs are then grouped into one of the following four groups: (I) Dry surface, large particle size; (II) Dry surface, small particle size (III) Wet surface, large particle size or (IV) Wet surface, small particle size.

Chemical flowsheet and process history information are used for tank TOC grouping. The TOC groupings are described in the *History of Organic Carbon in Hanford HLW Tanks: HDW Model Rev. 3* (Agnew 1996). The Hanford defined waste

model uses three methods to account for the organics: (1) knowledge of process, (2) chemicals used and waste volumes produced, and (3) chemical analysis of characteristic waste types. Tank waste fuel conditions were grouped into one of the following three groups: solvent TOC, complexant TOC, or non-TOC wastes. The solvent TOC tanks mostly received organic solvents (e.g., TBP and NPH); the complexant TOC tanks mostly received organic complexants (e.g., glycolate, citrate, EDTA, and HEDTA); and the non-TOC tanks are suspected of receiving little or no TOC.

When combining the moisture and TOC groups together, each SST waste belongs to one of 12 possible groups (one of the four moisture groups, and one of the three TOC groups). However, some groups do not contain tank waste types, and only eight groups are populated with tank wastes, as shown on Table 3-1.

3.3 ANALYSIS OF VARIANCE MODEL

It should be noted that this estimation problem is fundamentally different than most waste estimation problems in that no direct measurements on the variable of interest have been taken; only measurements that are indirectly related to combustible waste are available, and these can only be used by postulating a relationship between the desired quantities. The measured variables indirectly related to combustible waste are TOC and moisture content (wt% H_2O) of the waste. A relationship, the safety criteria, was presented in Section 2.3.

If a distribution of H_2O and TOC concentrations can be established for a tank, then an "estimate" of combustible waste can be made. Mathematically, this strategy is expressed by the integral equation;

$$R = \int_{(X_{H_2O}, X_{TOC}) \in A} f(X_{H_2O}, X_{TOC}) \, dX_{H_2O} dX_{TOC} \qquad (3\text{-}1)$$

where $f(X_{H2O}, X_{TOC})$ represents the distribution of (H_2O, TOC) values in the tank, the set A defines combustible waste in terms of (H_2O, TOC), W_{tot} represents the total amount of waste in the tank, and R is the desired estimate of combustible waste in the tank.

Sample data from the tanks are used to estimate the distribution $f(X_{H2O}, X_{TOC})$ of moisture and TOC in the tanks. Sufficient data do not exist to produce an estimate that is entirely empirical; an estimate that relied on no distributional assumptions would require hundreds of measurements per tank. Therefore, to obtain this distribution, it was assumed that both moisture and TOC are lognormally distributed. An analysis of variance (ANOVA) was used to estimate the distribution parameters. The assumption of lognormality seems to be justified from the available data.

Table 3-1. TOC and Moisture Grouping for 149 Single-Shell Tanks

TOC and Moisture Group	Tank(s)
Dry Surface, Large Particle Size, Solvent Waste	A-101, AX-101, BX-111, BY-101, BY-102, BY-103, BY-104, BY-105, BY-106, BY-107, BY-108, BY-109, BY-110, BY-111, BY-112, S-102, S-105, S-108, S-109, S-110, S-112, SX-103, SX-109, TX-109, TX-116, U-111
Dry Surface, Small Particle Size, Solvent Waste	A-104, A-105, A-106, AX-102, AX-103, B-101, B-105, BX-109, C-101, C-102, C-104, C-105, C-107, C-108, C-112, C-201, C-202, C-203, C-204, S-104, TX-101, TX-102 , TX-104, TX-105, TX-106, TX-107, TX-108, TX-110, TX-111, TX-112, TX-113, TX-114, TX-115, TX-117, TX-118, TY-102, TY-103, TY-105, TY-106, U-104
Wet Surface, Large Particle Size, Solvent Waste	A-102, S-101, S-103, S-106, S-111, SX-101, SX-102, SX-104, SX-105, SX-106, U-103, U-105, U-106, U-107, U-108, U-109
Wet Surface, Small Particle Size, Solvent Waste	A-103, B-102, BX-104, C-103, C-106, C-109, C-110, S-107, T-110, T-111, TY-104, U-102
Dry Surface, Large Particle Size, Complexant Waste	No tanks in group
Dry Surface, Small Particle Size, Complexant Waste	B-103, B-106, B-108, B-109, BX-101, BX-102, BX-112, SX-107, SX-108, SX-110, SX-111, SX-113, SX-114, SX-115, T-101, T-105, T-106, T-108, T-109, T-201, T-202, T-203, T-204, TX-103, TY-101, U-110
Wet Surface, Large Particle Size, Complexant Waste	No tanks in group
Wet Surface, Small Particle Size, Complexant Waste	B-112, B-201, B-203, B-204, BX-103, BX-105, BX-106, BX-110, T-102, T-103, T-107, U-101, U-112, U-201, U-202, U-203, U-204
Dry Surface, Large Particle Size, non-TOC Waste	No tanks in group
Dry Surface, Small Particle Size, non-TOC Waste	AX-104, B-104, B-107, BX-107, BX-108, C-111, SX-112
Wet Surface, Large Particle Size, non-TOC Waste	No tanks in group
Wet Surface, Small Particle Size, non-TOC waste	B-110, B-111, B-202, T-104, T-112

Using a lognormal distribution, the volume of combustible waste was calculated using Equation 3-1 for each tank with sample data. Estimates of combustible waste volumes for the unsampled tanks were calculated by extrapolating data from the sampled tanks.

The methodology employed here produces uncertainty distributions for combustible waste. The ANOVA descriptions of parametric uncertainty can be used to produce posterior distributions on the lognormal distributions parameters, which can be propagated to produce an uncertainty distribution for the combustible waste.

Using the assumption of lognormality (or equivalently, normality on the log scale), the estimate for combustible waste becomes:

$$Y = (\log(X_{H2O}), \log(X_{TOC})) \qquad \mu = (\mu_{H2O}, \mu_{TOC}) \tag{3-2}$$

$$C_0 = \frac{W_{tot}}{2\pi\sqrt{1-\rho^2}\sigma_{H2O}\sigma_{TOC}} \qquad \Gamma = \begin{bmatrix} \sigma_{H_2O}^2 & \rho\,\sigma_{H2O}\sigma_{TOC} \\ \rho\,\sigma_{H2O}\sigma_{TOC} & \sigma_{TOC}^2 \end{bmatrix} \tag{3-3}$$

$$R = C_0 \int_{Y \in \log(A)} \exp\left[-\frac{1}{2}(Y-\mu)^T \Gamma^{-1}(Y-\mu)\right] \tag{3-4}$$

The means and standard deviations (i.e., μ's and σ's) appearing in this formula define the distribution and are estimated using ANOVA. The fact that these parameters are not exactly known means that the resulting combustible waste R is not perfectly known. The posterior distribution of R is determined by a Monte Carlo calculation that utilizes all the ANOVA-derived uncertainty distributions on the μ's and σ's.

3.3.1 TOC ANOVA Model

Approximately 400 locations have been sampled and evaluated for TOC in Hanford SSTs in the past eight years. These measurements allow estimates to be made of the TOC in the tanks, and more importantly, determination of the distribution of TOC within a tank. The data is analyzed using a random effects ANOVA model, which produces estimates of TOC in the tank and also statements of variability.

The TOC measurements have been fit to an ANOVA model of the form:

$$Y_{ijkl} = \mu + D_i + G_j + DG_{ij} + T_{jk} + DT_{ijk} + E_{ijkl} \tag{3-5}$$

The individual terms in the ANOVA model are defined in terms of the indices.

Therefore, U in the model represents mean tank-farm TOC (or H_2O), while the terms D_i represents the deviation of the (i=surface, i=subsurface) layer from this mean. The term G_j represents the deviation of group j from the tank farm mean, while DG_{ij} represents the deviation of that group's layers from the tank farm average for the layers. The terms involving T explain deviations of tank averages from the Group averages.

The measurement, Y_{ijkl}, represents a log_{10} TOC measurement (expressed in wt%) taken under conditions $ijkl$. The indices $ijkl$ describe important conditions that influence the TOC measurements. These are defined as:

i: describes the vertical location of the measurement (i=surface layer, subsurface layer),

j: identifies a tank group,

k: represents the tank associated with the measurement,

l: identifies "replicate" measurements that occur within a layer in a specific tank.

This particular model was chosen to describe TOC for two principal reasons. First, it incorporates the most important variables thought to affect TOC that are available for all measurements/tanks. Secondly, the model is simple enough to allow all its terms to be estimated with the data available.

The model error term E_{ijkl} describes all variability within a layer, which includes horizontal and vertical variability within the layers. The variability associated with the error term also includes measurement error, a fact that can have important consequences for the calculation of combustible waste. Since integral calculation requires the distribution of TOC as input, the spatial variability (denoted by σ.toc) is required. Parameter Var(E) from the ANOVA estimates this, if measurement variability is not too large. The calculation assumes that Var(E) represents spatial variability, a reasonable assumption, assuming the measurement variability presented in (3-5) are appropriate for these data.

With the current model, spatial effects within a tank are described by four terms, D_i, DG_{ij}, DT_{ijk} and E_{ijkl}. The terms D_i and DG_{ij} play a fundamentally different role in the model than the last two terms when the model is used predictively. Enough data exists in the data set to estimate the first set of terms for all tanks, so these terms will always be available for the purposes of prediction. However, in tanks with no data, the last two terms will not be available and will be set to zero. For these tanks, having good values for Var (DT_{ijk}) and Var (E_{ijkl}) are important, so that the uncertainty of the estimate can be assessed.

For a tank with data, the "best estimate" for TOC in layer i=(top,bottom) is

$$\mu_i = \mu + D_i + DG_{ij} + T_{jk} + DT_{ijk} \qquad (3\text{-}6)$$

while for a tank without data, the "best estimate" is

$$\mu_i = \mu + D_i + DG_{ij} \qquad (3\text{-}7)$$

This last estimate is much less certain than the previous estimate, and its uncertainty is inflated by the amount *Var (T) + Var (DT)*.

3.3.2 Moisture ANOVA Model

Approximately 1000 locations have been sampled and evaluated for moisture in Hanford SSTs in the past eight years. These measurements are not necessarily at the same sample locations that produced TOC measurements discussed in the last section. In fact, about half of the (H_2O, TOC) measurements originate from a common sample. The moisture measurements are evaluated using an ANOVA model that is almost exactly like the model developed for TOC. Since this model has been discussed in detail in the previous section, the description here will be abbreviated.

The moisture measurements have been fit to an ANOVA model having exactly the same form as the TOC model:

$$Y_{ijkl} = \mu + D_i + G_j + DG_{ij} + T_{jk} + DT_{ijk} + E_{ijkl} \qquad (3\text{-}8)$$

The measurement, Y_{ijkl}, represents a $\log_{10}(H_2O)$ measurement (expressed in wt percent) taken under conditions *ijkl*. The indices *ijkl* describe important conditions that influence the H_2O measurements. These are defined as;

i: describes the vertical location of the measurement (i=surface layer, subsurface layer),

j: identifies a tank group,

k: represents the tank associated with the measurement,

l: identifies the "replicate" measurements that occur within a layer in a specific tank.

The tank grouping used for moisture is not the same as the grouping used for TOC. For moisture prediction, tanks are grouped according to the particle size of their waste. Two categories are used, large and small. Since there are only two groups, sufficient data exists to characterize each group.

3.3.3 Calculation of the Correlation Between Moisture and TOC

One required parameter not supplied by the moisture and TOC ANOVA analysis is the correlation coefficient between the two quantities. To obtain an estimate for p, the correlation between the last term in the ANOVA model was used (i.e., E_{ijkl}). A single correlation coefficient was computed for all samples that had both TOC and moisture analyses (i.e., H_2O,TOC pairs). This resulted in an estimate based upon 162 pairs, resulting in a value for correlation of 18%. This parameter also has measurement errors associated with it, but because of the relatively large number of observations associated with the estimate, it was decided to assume that this parameter was perfectly known.

3.4 ESTIMATION OF COMBUSTIBLE WASTE

The likelihood of an organic-nitrate combustion and its severity can be directly related to the amount of combustible waste in a tank. In this section, tanks that have sufficient waste data are categorized as *safe*, *conditionally safe*, or *unsafe*. For tanks that lack sufficient data, the ANOVA analysis is used to estimate the amount of combustible waste. The ANOVA results and tank history data are combined to prioritize the remaining tanks for further characterization.

3.4.1 Quantity and Confidence for the Estimates

For all of the tank waste sample data collected thus far, no waste measurements have exceeded the *conditionally safe* criteria (see calculation notes in Appendix A). However, it is important to note that each tank waste contains a distribution of organic complexants, and that there is a small probability that some fraction of waste exceeds the safety criteria. For this evaluation, 95% of the waste must be below the *safe* or *conditionally safe* criteria to categorize a tank as *safe* or *conditionally safe*.

When determining the safety category of a tank, it is tempting to ignore statistical uncertainties and state that whenever five percent of the waste exceeds the criteria, it will be concluded with 100% confidence that the tank is either *conditionally safe* or *unsafe*. However, statistical uncertainties cannot be ignored, and acceptable probabilities of making decision errors must be specified. For this evaluation, comparisons with the safety criteria will be made using one-sided 95% confidence limits. For example, for a tank to be categorized as *safe*, there must be 95% confidence that 95% of the waste has a TOC (dry) concentration less than 4.5 wt%.

3.4.2 Categorization of Tanks

Table 3-2 lists the 43 tanks that meet the *safe* category from the ANOVA analysis of the TOC data. In addition to these 43 tanks, 20 tanks have been categorized as *safe* because they received little or no organic material (Table 3-3). Careful examination of waste histories (Agnew 1996) showed that these tanks received minimal (less than 0.53 wt%) or no organic waste, and differential scanning calorimetry (DSC) analyses of all the samples from these tanks corroborate that the waste has no exothermic energy. Because these tanks were suspected of receiving minimal organic waste, and all the DSC

screening showed only endothermic reactions, TOC analyses were not performed on these wastes.

Four tanks were placed in the *conditionally safe* category from the analysis of TOC and moisture data (Table 3-4), and no tanks were categorized as *unsafe*. It is important to note that the waste histories of the four tanks categorized as *conditionally safe* (AX-102, C-201, C-202, and U-105) indicate solvent TOC. If organic speciation confirms that the TOC is indeed solvent, this might allow these tanks to be categorized as *safe*.

Table 3-2. Safe Tanks Based on TOC data (dry) at 95% Confidence.

Tank	Percentage of Safe Waste (TOC < 4.5)	Tank	Percentage of Safe Waste (TOC < 4.5)	Tank	Percentage of Safe Waste (TOC < 4.5)
A-101	99.5	C-103	99.0	T-104	>99.9
A-102	96.7	C-104	99.6	T-105	>99.9
A-103	99.0	C-105	99.9	T-107	>99.9
A-106	98.9	C-106	>99.9	T-111	>99.9
B-103	99.9	C-108	>99.9	TX-102	99.8
B-110	99.9	C-109	>99.9	TX-118	99.1
B-111	99.9	C-110	>99.9	TY-101	>99.9
BX-104	99.8	C-111	>99.9	TY-102	>99.9
BX-105	99.5	C-112	99.7	TY-103	>99.9
BX-107	99.9	C-204	NA*	TY-105	>99.9
BX-110	>99.9	S-104	>99.9	TY-106	>99.9
BX-111	99.9	S-109	>99.9	U-103	98.6
BX-112	99.6	S-111	98.9	U-110	>99.9
BY-106	>99.9	SX-102	99.1	U-111	99.8
---	---	T-102	>99.9	---	---

NA = Not Applicable; chemical speciation of the organic in C-204 showed that the TOC was TBP organic solvent (Conner 1996). Experiments with TBP waste simulants (Cowley and Postma 1996) and tests with the C-204 TBP saturated waste (Conner 1996) showed that condensed-phase combustions are not credible (see Section 2.2).

Table 3-3. Safe Tanks that Received Minimal Organic Waste and
Showed No Exothermic Energy During DSC Analysis

Tank	Tank	Tank
B-104	BX-109	TX-107
B-106	C-101	TY-104
B-201	SX-108	U-201
B-204	SX-113	U-202
BX-101	T-106	U-203
BX-106	T-108	U-204
BX-108	T-109	-----

Table 3-4. Conditionally Safe Tanks Based on TOC and Moisture Data at
95% Confidence

Tank	Percentage of Conditionally Safe Waste $(TOC < 4.5 + 17x_w)$
AX-102	97.3
C-201	---*
C-202	---*
U-105	98.4

* The C-200 series tanks received various small (and possibly unique)
  transfers of waste and are not included in the ANOVA run in
  Appendix A. Only a small amount of waste was obtained during sampling
  of tanks C-201 and C-202, so sufficient sample was not available for
  complete TOC and moisture analyses. Analyses of the waste sample from
  C-201 indicate TOC and moisture concentrations of 4.2 and 10.6 wt%,
  respectively. Differential scanning calorimetry analysis of the
  sample from C-202 indicated exothermic energy. Tanks C-201 and C-202
  were categorized as *conditionally safe* as a prudent measure until more
  sampling and characterization are completed.

3.4.3 Prioritization of the Unsampled Tanks

Three factors were considered to prioritize future characterization efforts:
plans for interim stabilization, tank TOC history, and estimates of
combustible waste using the ANOVA model. Each factor is discussed in the
following sections.

Interim stabilization is important to the organic complexant hazard because
moisture will be removed as a result of pumping. Even if a tank were not
interim stabilized, eventually the SST would leak, leading to the same end.
Table 3-5 lists the eighteen unsampled tanks (in sequence) that are scheduled
for interim stabilization. Because moisture is the determining factor between
the *conditionally safe* and *unsafe* categories, the tanks suspected of
containing high TOC that are scheduled for interim stabilization are a high
priority for characterization. Characterization of the unsampled tanks will
permit the tanks to be categorized in accordance with the criteria in this
sectionr. The controls applicable to each category of tank are addressed in
Section 6.0.

Table 3-5. Unsampled Tanks Scheduled for Interim Stabilization

Sequence	Tank	Sequence	Tank	Sequence	Tank
1	T-110	7	S-103	13	S-101
2	SX-103	8	S-106	14	SX-101
3	SX-104	9	U-107	15	S-107
4	SX-105	10	U-108	16	U-102
5	SX-106	11	AX-101	17	U-109
6	S-102	12	S-112	18	U-106

Transaction and process information have been used to account for the
disposition of soluble organic materials throughout the history of Hanford
(Agnew 1996). Results are presented in Agnew (1996) and are summarized in
Table 3-6. From Table 3-6, none of the unsampled tanks are expected to
contain average TOC concentrations higher than the fuel criterion. Tanks in
U, AX, and SX Farms received significant organic material and will be
prioritized accordingly.

The ANOVA model was used to estimate the percentage of *safe* waste [i.e., the
amount containing less than 4.5 wt% (dry) TOC] and the volume of combustible
waste for the tanks with insufficient or no data (see Appendix A). Results
are shown in Table 3-7. The percentage of *safe* waste is given at 95%
confidence on a dry basis, and estimates of combustible waste volumes are
given at 95% confidence on a wet basis. From the ANOVA estimates, all of the
unsampled tanks fall into the *safe* category. Consequently, interim
stabilization and TOC histories have more influence over sampling priority.

Comparing Tables 3-5 and 3-6, 17 of the 18 tanks scheduled for interim
stabilization are suspected of receiving organic waste. Therefore, these 17
tanks are a high priority for additional characterization, as shown in
Table 3-8. The eighteenth tank, T-110, listed first on Table 3-5 is not a
driver for characterization in Table 3-8 because it has no organic waste as
shown in Table 3-6. The priority for the remaining 66 tanks are from the
ANOVA extrapolation to the unsampled tanks.

Table 3-6. Mean TOC Concentration Estimates From Tank Waste Histories

Tank	Mean TOC (wt%)	Tank	Mean TOC (wt%)	Tank	Mean TOC (wt%)
AX-101	1.35	BY-105	0.45	AX-104	0.00
AX-103	1.20	BY-107	0.45	B-101	0.00
U-106	1.13	BY-108	0.45	B-105	0.00
U-109	1.13	BY-109	0.45	B-108	0.00
SX-103	1.01	BY-110	0.45	B-202	0.00
U-108	0.98	BY-111	0.45	B-203	0.00
BY-102	0.98	BY-112	0.45	BX-102	0.00
SX-105	0.96	SX-101	0.44	C-102	0.00
U-102	0.98	TX-103	0.37	C-107	0.00
S-107	0.94	S-106	0.37	C-203	0.00
TX-104	0.94	S-112	0.36	SX-107	0.00
SX-104	0.92	T-101	0.35	SX-109	0.00
TX-101	0.88	TX-105	0.35	SX-110	0.00
S-103	0.87	S-108	0.35	SX-111	0.00
U-107	0.84	TX-115	0.34	SX-112	0.00
SX-106	0.81	TX-108	0.32	SX-114	0.00
S-101	0.73	TX-112	0.32	SX-115	0.00
B-109	0.73	S-105	0.29	U-101	0.00
TX-111	0.68	TX-114	0.28	U-112	0.00
S-102	0.67	TX-113	0.26	T-110	0.00
TX-106	0.62	U-104	0.20	T-112	0.00
S-110	0.61	TX-117	0.14	T-201	0.00
TX-110	0.60	TX-116	0.09	T-202	0.00
BX-103	0.58	B-102	0.09	T-203	0.00
B-112	0.53	T-103	0.04	T-204	0.00
BY-101	0.45	B-107	0.00	TX-109	0.00
BY-103	0.45	A-104	0.00	---	----
BY-104	0.45	A-105	0.00	---	----

Table 3-7.   ANOVA Estimates for Percentage of Safe Waste and
Combustible Waste Volumes for the Unsampled Tanks

Tank	Percentage of safe waste	Combustible Waste (m^3)	Tank	Percentage of safe waste	Combustible Waste (m^3)	Tank	Percentage of safe waste	Combustible Waste (m^3)
SX-101	99.1	1.1	SX-109	99.4	0.25	AX-104	97.7	0.01
SX-106	99.5	0.76	TX-110	99.9	0.25	C-203	99.0	0.01
SX-105	99.0	0.75	TX-117	99.6	0.24	SX-114	99.7	<0.01
U-109	99.4	0.71	BY-102	99.4	0.22	SX-112	99.4	<0.01
SX-104	99.5	0.68	TX-113	99.3	0.22	SX-111	99.8	<0.01
AX-101	99.2	0.67	TX-109	99.6	0.22	TX-103	99.7	<0.01
S-106	99.5	0.66	BY-101	99.7	0.21	T-101	>99.9	<0.01
U-108	99.4	0.61	TX-111	99.7	0.20	SX-107	99.5	<0.01
S-101	99.5	0.60	TX-105	99.2	0.19	SX-110	99.6	<0.01
S-110	99.4	0.53	B-101	99.1	0.19	U-112	>99.9	<0.01
BY-103	99.9	0.46	B-105	99.4	0.19	T-103	>99.9	<0.01
S-102	99.5	0.45	AX-103	99.6	0.18	U-101	>99.9	<0.01
U-106	99.4	0.45	BY-107	99.8	0.18	T-203	>99.9	<0.01
BY-110	99.4	0.44	TX-116	99.4	0.17	T-204	>99.9	<0.01
U-107	99.3	0.44	TX-112	99.5	0.16	BX-102	>99.9	<0.01
SX-103	99.5	0.41	C-107	99.4	0.16	T-201	>99.9	<0.01
BY-105	99.9	0.41	U-102	99.4	0.16	SX-115	99.2	<0.01
S-108	99.5	0.40	TX-115	99.4	0.16	B-108	>99.9	<0.01
BY-108	99.0	0.39	B-102	98.0	0.16	B-109	>99.9	<0.01
BY-111	99.3	0.38	C-102	99.5	0.15	T-202	>99.9	<0.01
A-105	96.6	0.35	TX-114	99.6	0.12	T-112	>99.9	<0.01
BY-109	99.2	0.33	T-110	99.4	0.08	B-107	>99.9	<0.01
TX-106	99.9	0.31	TX-101	98.1	0.08	B-203	>99.9	<0.01
S-103	99.1	0.31	TX-108	99.3	0.08	B-202	>99.9	<0.01
S-112	99.6	0.31	U-104	99.1	0.08	B-112	>99.9	<0.01
S-105	99.4	0.28	S-107	99.3	0.08	BX-103	99.8	<0.01
BY-104	99.0	0.26	A-104	98.6	0.07	--	---	----
BY-112	99.3	0.26	TX-104	98.6	0.06	--	---	----

Table 3-8. Characterization Priority for the Unsampled Tanks.

Priority	Tank	Priority	Tank	Priority	Tank
1	SX-103	29	BY-104	57	AX-104
2	SX-104	30	BY-112	58	C-203
3	SX-105	31	SX-109	59	SX-114
4	SX-106	32	TX-110	60	SX-112
5	S-102	33	TX-117	61	SX-111
6	S-103	34	BY-102	62	TX-103
7	S-106	35	TX-113	63	T-101
8	U-107	36	TX-109	64	SX-107
9	U-108	37	BY-101	65	SX-110
10	S-112	38	TX-111	66	U-112
11	AX-101	39	TX-105	67	T-103
12	S-101	40	B-101	68	U-101
13	SX-101	41	B-105	69	T-203
14	S-107	42	AX-103	70	T-204
15	U-102	43	BY-107	71	BX-102
16	U-109	44	TX-116	72	T-201
17	U-106	45	TX-112	73	SX-115
18	S-110	46	C-107	74	B-108
19	BY-103	47	TX-115	75	B-109
20	BY-110	48	B-102	76	T-202
21	BY-105	49	C-102	77	T-112
22	S-108	50	TX-114	78	B-107
23	BY-108	51	T-110	79	B-203
24	BY-111	52	TX-101	80	B-202
25	A-105	53	TX-108	81	B-112
26	BY-109	54	U-104	82	BX-103
27	TX-106	55	A-104	--	--
28	S-105	56	TX-104	--	--

4.0 EVALUATION OF POTENTIAL ORGANIC-NITRATE COMBUSTION INITIATORS

The purpose of this section is to identify potential ignition sources that might accelerate an organic-nitrate reaction to a rapid combustion, and to estimate the frequencies that these various sources would occur. Situations considered include normal operations and activities, operational upsets and equipment failures, and natural phenomena.

4.1 SCREENING OF EVENTS

Tank farm operations and activities (Bajwa and Farley 1994) were reviewed to determine which equipment and activities could lead to moderate strength ignition sources (i.e., greater than 3 Joules) being present at the waste surface or within the waste. The potential for organic complexant ignition by rotary-mode core sampling is not assessed in this report, but is addressed in a separate safety analysis (Kubic 1996). Rotary-mode core sampling is included in Table 4-1 (and elsewhere in the document) for completeness.

Table 4-1. Summary of Operations Evaluation

Operation	Incident Conditions	Heating Potential
In-tank instrumentation	Electrical overcurrent	Negligible, ignition not credible
Grinding and drilling operations	Sparks from grinding and drilling operations on or near a riser	Negligible, ignition not credible
Still camera photography	Dropping flash unit onto the waste surface, hot filament contacts waste	Ignition temperatures are possible
Video camera	Dropping light unit onto the waste surface, hot filament contacts waste	Ignition temperatures are possible
Hot metal from welding and torching operations	Hot steel particles or pieces drop and contact the waste	Ignition temperatures are possible
Vehicle operation above the tank	Rupture of fuel tank on aboveground equipment, fuel leakage into the tank, subsequent fire	Ignition temperatures are possible
Rotary-mode core sampling	Loss of bit cooling, failure to shut down drill sampler causes frictional heating of the waste	Ignition temperatures are possible
Lightning strikes	Lightning strike on or near a tank or equipment causes lightning current to reach the waste	Ignition temperatures are possible
Flammable gas burn	Flammable gas burn in an organic tank or adjacent tank ignites the waste	Ignition temperatures are possible

Electrostatic discharges and instrumentation circuit faults would deposit insufficient energy in the waste to ignite an organic complexant combustion. Mechanical sparks from grinding and drilling operations on or near a riser would cool as they fell through the headspace and would have insufficient energy to cause ignition of solid phase organics. Potential ignition sources

resulting from video or photography lighting, welding or torching, vehicle operations, and rotary-mode core sampling are discussed in Section 4.2.

A review of natural phenomena hazards was also performed to identify potential organic-nitrate ignitors. Lightning was determined to be the only natural phenomenon with sufficient energy in ignition sources to ignite solid organics. Other effects were evaluated such as seismic-induced collisions between in-tank equipment and resultant sparking of equipment, and it was determined that these would not produce capable ignitors. Nearby facility or range fires could produce flaming brands and sparks that could affect the top of the tank but it was assumed that these phenomena could not enter the tank and fall directly onto the waste surface.

4.2 EVENT FREQUENCIES

The following summarizes the estimation of event frequencies. The events are defined as the ignition source being present at the waste surface or within the waste. The ignition source frequencies were based on "order-of-magnitude" estimates obtained from the best available information and informed engineering judgement. These estimates are based on unmitigated conditions. It is first assumed that no controls are in place to exclude the ignition source. These values are considered good "order-of-magnitude" estimates to indicate the impacts of basic controls that might be used to mitigate these accidents (reduce the frequency of ignition sources).

4.2.1 Frequency of Hot Filaments

Video and still cameras are periodically placed into waste storage tanks to photograph the waste or internal structures in the tanks. The camera and lights represent potential sources of electrical and thermal energy that could apply enough energy to the waste surface to initiate an organic-nitrate combustion. The cameras and lights are typically placed in the tank through a riser and are suspended above the waste surface.

Three possible mechanisms were postulated that result in the camera or light contacting the waste surface: (1) the light impacts against the riser or other installed equipment during installation, the housing breaks, the bulb breaks and a hot filament from the light source falls onto the waste surface; (2) the structural support for the camera or light fails, the light falls to the waste surface breaking the housing and the bulb, the hot filament drops to the waste surface; and (3) the power cable to the camera or light fails, falls onto the waste surface, and electrical shorts create hot molten metal or arcs which contact the waste surface. All three are judged to be unlikely events.

The frequency of these scenarios can be reduced by: (1) de-energizing the lights and camera during installation or using an impact resistent housing for the light, (2) using a light support system that can not fall through the riser (e.g., use a "top hat" which seats against the riser flange), (3) limit the length of the power cables so that they can not extend to the waste surface and still be energized.

4.2.2 Frequency of Welding and Torch Cutting

Occasionally, tank farm operators are required to weld or cut material on or near a riser. This introduces an opportunity to allow weld slag or hot metal pieces to enter the tank, thereby creating the conditions necessary to initiate an organic-nitrate combustion.

Three conditions must be met for weld slag or hot metal to enter a riser and contact the waste surface. First, the riser must be open. Second, weld slag or hot metal must be directed towards the open riser, although the riser cover is assumed to be ineffective in stopping hot material created when working directly on the riser. Third, the slag or hot metal must be large enough that it will not cool down to below the ignition energy requirement as it falls to the waste surface 6 to 12 meters below. Because the conditions that could allow this scenario would be expected if no restrictions were in place, the unmitigated scenario is judged to be anticipated.

The frequency of welding slag or hot metal reaching the waste surface can be reduced by restricting welding activities such that (1) welding is not performed near an open riser or pit drain, and (2) welding that must be performed directly on a riser has a barrier installed to prevent slag and hot metal from falling to the waste surface.

4.2.3 Frequency of Vehicle Fuel Fires

Vehicles often enter the tank farms for various support activities. Although perimeter roads around the tanks exist, trucks may need to drive over the top of a tank for a variety of reasons (access to risers, pump pits, etc.). This introduces an opportunity for vehicle accidents and, of most concern, fuel leaks and subsequent fires.

The accident scenario examined here involves the following sequence of events. First, a vehicle backs into or strikes a riser. This causes the fuel tank to rupture, resulting in a fuel spill into the riser (either the riser fails or is uncovered, allowing fuel to enter the tank). Next, the fuel is assumed to ignite and the burning fuel enters the riser. Finally, the burning fuel ignites the organic-nitrate waste. The frequencies and conditional probabilities of these events are evaluated below.

The frequency of vehicular accidents resulting in fuel tank ruptures was evaluated based on two off normal (ON) reports in two subsequent years as described below.

- ON #WHC-TANKFARM-1992-29 -- In this event a drywell monitoring van backed over a riser at 104-SX and punctured its gas tank. Two gallons of gas spilled onto the ground and five more gallons were caught in a bucket while spilling. It is important to note that the driver did a 360 degree walk-around prior to backing up and noticed the riser, but still hit the riser anyway. The riser was not opened in the accident.

- ON #WHC-TANKFARM-1993-76 -- In this event, a drywell monitoring vehicle backed into a riser at 108-S. A pinhole leak in the vehicle's gas tank resulted, but the riser was not opened in the accident.

Frequencies for vehicle accidents that could cause fuel fires in SSTs were evaluated in Lindberg (1996). Two possible scenarios were considered in assessing the safety of the waste tanks with respect to fuel spills from vehicles. The first scenario modelled accounted for a leak from a ruptured fuel tank due to an accident. The accident also breaks a riser that enters the waste tank, allowing an opening in the top of the waste tank. The fuel leaking from the fuel tank enters the waste tank through the broken riser. The fuel vapor in the waste tank then builds to the lower flammability limit and is ignited by an ignition source in the tank. This ignition results in a rapid burn or deflagration. The second scenario describes a leak from the vehicle similar to that described above, except that the leaking fuel would ignite due to a source of sparks from the accident or contact with hot elements of the vehicle's engine or exhaust system. The burning fuel would enter the waste tank through the broken riser and ignite the contents of the tank.

The results of the quantifications of an event tree for this scenario in SSTs indicated the frequency of a gasoline fire in any of the SSTs (the sum of vapor phase fires and gasoline pool fires for the SSTs) was 3.8×10^{-4}/yr (Lindberg 1996). A rough "per-tank" estimate is this number divided by 149 SSTs or 2.6×10^{-6}/tank-yr.

The final event that occurs is that the fuel initiates the organic-nitrate combustion, if combustible waste is present. It is assumed that ignition is probable, even though ignition may not occur except under relatively severe circumstances. A gasoline spill burns vapors and relatively little actual liquid fuel burns. As a result, most of the heat from a gasoline burn is generated above the liquid pool and only a relatively small fraction of the thermal energy is directed towards the liquid pool. Therefore, there is some question about whether or not the temperature rise in the pool would exceed the ignition temperature for an organic-nitrate combustion. However, without detailed modeling of the gasoline fire and spill volumes, it is difficult to predict the severity of the gasoline fire and subsequent thermal input to the waste surface.

Given this evaluation, the unmitigated frequency of burning gasoline at the waste surface is judged to be extremely unlikely.

The frequency of these condensed-phase organic combustion events can be reduced by following vehicle access controls including:

- Protecting the fuel tanks (e.g., skid plates)

- Using a spotter to reduce the likelihood of running the vehicle into the riser

- Placing barriers around risers to prevent vehicle approach

4.2.4 Frequency of Rotary Mode Core Drilling Failure

Rotary mode core drilling was not evaluated in this report, but is covered in a separate safety assessment (Kubic 1996). Rotary-mode core drilling of organic tanks is discussed in Kubic (1996).

4.2.5 Frequency of Lightning

Thunderstorms can produce lightning strikes that discharge the electrical potential between the atmosphere and the ground. Although rare, ash fall, range fires, and dust storms can also produce lightning. Lightning strikes at the tank farms are a safety concern because they could cause an in-tank ignition of flammable gases, or a fire involving organic solvents or organic nitrates. In addition, lightning strikes may cause the conduction of large electrical currents through systems, structures or components important to safety, putting personnel and operations at risk. Operational records report no incidence of lightning strikes on a tank riser or appurtenance during the 50-year history of the Hanford Site, whereas a number of lightning strikes have hit 200 Area structures, power poles, and transformers.

Recent research on mitigation of natural phenomena hazards has led to a better focus of the issues surrounding lightning at the tank farms as reported in Zach (1996). The report discusses a number of factors necessary for a fire to result from a lightning strike including the following:

- Lightning must strike a tank riser, appurtenance, or the ground in the immediate vicinity of a tank farm.

- At the time of the strike, the tank must contain a flammable gas above the lower flammability limit (LFL) or a concentration of organic nitrate sufficient to support combustion.

- The discharge must pass from the riser or appurtenance into the tank through conduction paths such as instrumentation lines or other equipment connected to the tank riser or by arcing across non-conductive segments.

- The discharge must have sufficient energy to create an arc or cause ohmic heating to temperatures high enough to ignite the materials.

As discussed below, analyses of these factors resulted in a determination that significant waste heating as a result of a lightning strike is an extremely unlikely event for a given tank.

A number of studies have been performed to assess the likelihood of lightning striking the ground or facilities at the Hanford Site. The most appropriate methodology for determining lightning frequency is to use data from the National Lightning Detection Network (NLDN[tm]) and the Bureau of Land Management for the region around the tank farms. This was done for the 10 years ending in January 1996. After accounting for detection frequency and uncertainties, the observed rate was conservatively determined to be 0.06 strikes/yr/km^2 (Zach 1996).

Assuming lightning strikes the vicinity of a tank farm, the outcome is uncertain. Because the tanks are interconnected with instrument, ventilation, and transfer lines, the entire farm may act as a grounding electrode. However, for those strikes that are not direct on a riser (e.g., a ventilation duct), the energy would be dispersed throughout the farm and it is incredible that a path would exist to the waste that would carry sufficient energy to

cause an organic combustion. To ignite organic waste forms, an electrical arc must occur in or near combustible materials. For SSTs, the path of the electrical currents depends on factors such as whether the riser is grounded (to rebar in the dome or to the earth), and whether the riser has conductive equipment reaching to or near the waste surface.

For the ignition of organic nitrates in tanks, the lightning must strike a tank that can sustain an organics fire. Using the observed 0.06 strikes/yr/km^2 as a best estimate of lightning strike frequency, and considering the cross-sectional area of a large underground tank to be bounded by 500 m^2, the likelihood of a direct strike over a particular tank is 3×10^{-5}/yr (one strike in 33,000 yr) and can be characterized as extremely unlikely. This value is considered appropriate for use as a condensed phase organic combustion initiator where a comparatively high energy is required to ignite the material. The value may be conservative for the following reasons:

- The average strike frequency in the tank farms is less than 0.06 strikes/yr/km^2 because the study area included higher elevations where observed frequencies were higher than the immediate vicinity of the tank farms.

- It is assumed that a strike anywhere over a tank will hit a riser or appurtenance, and there are no other nearby preferential paths such as light poles that could dissipate the energy outside of the tank wastes.

- The equivalent target area of the zone immediately around the riser of a typical tank is less than 50 m^2 or one tenth the tank area. Strikes outside the 50 m^2 may dissipate without causing an ignition.

A direct strike over a particular tank is conservatively assessed at 3×10^{-5}/yr. The conditional probability of point source ignition resulting from a strike to the tank is less than unity because (1) data show lightning strikes at the Hanford Site are less energetic than lightning strikes around the world (Zach 1996), (2) the tank geometry must be favorable to arcing in or near the waste surface, and (3) most energy would preferentially dissipate through the comparatively conductive concrete and rebar.

Given the above, the frequency of lightning creating ignition condition on the waste surface or within the waste is judged to be no more than extremely unlikely per tank per year.

The frequency of point source ignition caused by lightning could be reduced by installing lightning protection.

4.2.6 Frequency of Flammable Gas Deflagrations

A postulated scenario for organic-nitrate ignition is a flammable gas deflagration that heats the waste to ignition temperatures. Two potential mechanisms for ignition of flammable gas followed by ignition of organic-nitrate salts were investigated. The first involves the release and ignition of the flammable gas by various spontaneous or operational waste disturbing mechanisms. The second involves a seismic event, which results in liberation of flammable gases plus an ignition source for the gases.

It is recognized that not all flammable gas burns would deliver enough energy to the waste surface to initiate an organic-nitrate reaction. Preliminary calculations of the likelihood of saltcake being ignited by a flammable gas burn were performed to support this study. It was determined that a threshold gas temperature for this event (headspace temperature) is about 1400°K (1130°C) (Plys 1996). Deflagration accidents that could create such high temperatures are larger than those that are analyzed to cause severe structural damage to the tank and could result in significant radiological consequences.

No scenario has been postulated for such a large release, where a relatively dry waste surface (i.e., potentially combustible and ignitable) could exist following the release. Scenarios that allow for a large amount of gas bearing, wet waste to release its gas (e.g., rollovers, and seismic events) are not consistent with a dry post-GRE waste surface. Therefore, it is judged that a flammable gas induced condensed phase organic propagating reaction is significantly less likely than a large flammable gas deflagration itself. Therefore such a scenario is judged to have a frequency of no more than extremely unlikely, and is not a significant factor in establishing the frequency of condensed phase organic propagating reactions. However, controls that have been imposed to address flammable gas hazards (Leach and Grigsby 1996), and those that will be proposed for technical safety requirements (TSRs) are also effective in reducing the risk of flammable gas induced condensed phase organic combustion events.

This page intentionally left blank.

5.0 CONSEQUENCE ANALYSIS

5.1 BOUNDING ACCIDENT ANALYSIS

The ANOVA analysis was used to postulate the maximum volume of waste that could participate in an organic complexant combustion event (see Appendix A for calculations). The volume of combustible waste was taken to be the amount of waste that could statistically exceed the *conditionally safe* criterion. Tank U-105 had the greatest postulated amount of combustible waste for all the SSTs. The best statistical estimate (at 50% confidence) of combustible waste in U-105 was 0.92 m^3, and the bounding statistical estimate (at 95% confidence) was 25 m^3. These volumes were used in the consequence calculations that follow.

5.2 ASSUMPTIONS AND CONSERVATISMS

The validity of the consequence calculations summarized in this chapter rests on several assumptions. If these assumptions were altered, the consequence estimates could change. Below is a list of the most important assumptions:

- The ANOVA model prediction of combustible waste for U-105 bounds the amount of combustible waste for all SSTs.

- When the gas pressure in the tank exceeds the HEPA filter pressure capabilities, the HEPA filter will rupture and disperse a significant fraction of its burden. The rupture pressure of the HEPA filter is taken to be 0.1 atm overpressure (10 kPa or 1.47 psig).

- The SST dome will crack at 0.75 atm (76 kPa or 11 psig) overpressure and will vent gases through these cracks (Han 1996).

- The hazard is confined to SSTs. The DSTs, double contained receiver tanks, and catch tanks contain too much moisture to be combustive.

- The specific heat of the waste is 2,000 J/Kg-°K. This value was derived from handbook values for sodium acetate salts reacting with sodium nitrates.

- The vertical spread rate of the combustion is 0.6 mm/sec, and the horizontal spread rate is 1.2 mm/sec. These values were based on the highest spread rates observed during simulant experiments (Fauske et al. 1995).

- From thermodynamic calculations (Fauske 1996a), a combustion temperature of 800 °C was used for this analysis. A large fraction of the cesium, mercury, and sodium hydroxides are volatilized at this temperature. These compounds dominate the radiological, toxicological, and corrosives releases.

- Mechanical entrainment of non-volatile radionuclides and toxics by the escaping hot gases and vapors was assumed to be negligible when compared

to the releases of cesium, mercury, and sodium hydroxide. This was based on an earlier estimate that entrainment of non-volatiles would be less than 1E-5. More recent evaluations indicate that this mechanical entrainment may be in the range of 1E-3 to 1E-5. A comparison calculation with 1E-4 for non-volatile radionuclides showed that approximately 5% more dose would be added to that currently calculated for the cesium release. In the present analysis, this mechanical entrainment effect is neglected.

• The average TOC and moisture concentrations in the combustible waste were assumed to be 7.0 wt% and 10 wt%, respectively.

Several conservatisms also exist in this analysis and the consequence analysis will be refined when these conservatisms can be better quantified. Below is a list of the major conservatisms:

• Sufficient oxidizer (nitrates and nitrites) are assumed to be present, and are well mixed with the organic fuel.

• The combustible waste is contiguous and is burned completely.

• An ignition source is present and is in the same location as the combustible waste.

• All the ignition sources identified in Section 4 are strong enough to ignite an organic-nitrate combustion.

• Bounding radionuclide and toxic concentrations were assumed for U-105 (Tables 5-1 and 5-2, respectively). The radionuclide concentrations are from Cowley (1996), and the toxic concentrations are from Van Keuren (1996).

Table 5-1.   Bounding Radionuclide Concentrations and Conversion Factors.

Isotope	Dose Conversion Factor (Sv/Bq)	Concentration (Bq/L)	Sv/L
Cs-137	8.63E-09	1.01E+11	8.72E+02
Sr-90	6.47E-08	1.63E+12	1.05E+05
Y-90	2.28E-09	1.63E+12	3.72E+03
Co-60	5.91E-08	4.18E+08	2.47E+01
Tc-99	2.25E-09	1.20E+10	2.70E+01
Sb-125	3.30E-09	2.80E+08	9.24E-01
Eu-154	7.73E-08	5.75E+09	4.44E+02
Pu-239	1.16E-04	4.40E+08	5.10E+04

Table 5-2. Bounding Toxic Concentrations

Analyte	Concentration (g/L)
Cadmium	1.7
Mercury	54
Sodium Hydroxide	210
Uranium	280

5.3 ACCIDENT FREQUENCIES

Section 4.0 summarizes the credible ignition sources. The frequencies of these ignition sources are for the **unmitigated** accident. That is, this is how often these ignition sources might occur (on a per tank-year basis) if no restrictive controls or safety class equipment were in place.

The activities described in Section 4.0 are not expected to be applied equally to all tanks each year, nor are all tanks equally vulnerable to ignitors. However, for purposes of this safety evaluation, it is conservatively assumed that on an **unmitigated** basis, all activities would be conducted frequently on all tanks during any given year. The introduction of ignitors to tank waste is estimated to have a frequency of unlikely each year (1E-2).

Application of controls discussed in Section 6.0 activities would reduce the ignition source frequencies. The controls vary in their effectiveness, but in general, an overall reduction of at least 1E-2 is expected. When these controls are applied as mitigation, the **mitigated** frequency of ignitors is then expected to be extremely unlikely (1E-4). With the ignition controls described in Section 6.0, the ignition source frequency for any tank is estimated to be less than or equal to 1E-4 per SST-year.

The accident frequency is dependent on ignition source frequency, whether the subject tank contains combustible waste, whether the ignition source contacts the combustible waste, and whether the ignition source is strong enough to ignite the combustible waste. Estimates of combustible waste volumes are provided in Section 3.4 and Appendix A. The frequencies assumed for ignition source contact (with combustible waste), and ignitor success (once in contact) are discussed below.

5.3.1 Frequency of Ignition Source Contact with Combustible Waste

All ignitors described for this accident have access to the surface of the waste. Only lightning and rotary core drilling (which is discussed in Kubic 1996) would have access to the waste below the surface. Because the fraction of combustible waste in the tanks is low (less than 3%), any ignition source would most likely not contact combustible waste. The probability of an ignitor finding combustible waste is less than unity.

5.3.2 Ignitor Success

Testing suggests that about 5 wt% moisture can suppress ignition of an organic-nitrate combustion (Fauske 1996a). Experiments with waste simulants and actual waste samples indicate that more than 5 wt% moisture would be retained even if the waste were exposed to dry Hanford Site air (Scheele et al. 1996). Therefore, many of the ignition sources reviewed in Section 4.0 would not ignite an organic-nitrate combustion in the tanks and the probability of ignitor success would also be less than unity.

5.3.3 Frequency of Organic Salt-Nitrate Combustions

The likelihood that an organic salt-nitrate combustion will occur in a particular tank is determined by whether there is combustible waste present, and is proportional to the likelihood that an ignitor will be introduced into that particular tank. As discussed above, the likelihoods of ignitors being introduced to SST is taken to be the same for all of tanks, and is governed by the effectiveness of controls to exclude ignitors from tanks.

Of the 67 tanks with measured TOC values, none were categorized as *unsafe*, and extrapolation of the data to the unsampled tanks (using the ANOVA results) indicates the unsampled tanks would only contain modest amounts of combustive waste. Historical records of processing and waste transfers also suggest none of the 82 unsampled tanks would be categorized as *unsafe*.

A bounding estimate on the number of tanks at risk can be made using simple statistics. Given that 67 tanks have already been sampled and found to be not at risk, no more than six of the remaining 82 tanks should be at risk (Dixon and Massey 1957). Although this is believed to be conservative, uncertainties about the waste character in the 82 unsampled tanks suggest that this conservatism is justified. Therefore, the number of tanks that are vulnerable is taken to be less than ten for the purpose of risk calculations.

Combining the frequency of ignition sources, frequency of ignition source contact, frequency of ignitor success, and the number of vulnerable tanks (taken to be less than ten) the facility wide unmitigated accident frequency is judged to be unlikely (less than 1E-2) and the mitigated accident frequency is judged to be extremely unlikely (less than 1E-4).

5.4 ORGANIC-NITRATE COMBUSTION MODEL

The consequences from an organic salt-nitrate combustion event are dominated by releases occurring as a result of the high temperatures and pressures that are generated. Volatile radionuclides and other chemicals are driven off as vapors at the high combustion temperatures. The principal elements (usually driven off as hydroxide compounds) released are cesium, mercury, and sodium which condense into particulates as the exiting gases cool to respective condensation temperatures. A computer program, Organic Nitrate (ORNATE), was written to study the dynamic effects of this organic salt-nitrate combustion. The development and details of this program are presented in Appendix B.

5.4.1 Tank Response

The response of tank U-105 to a condensed phase reaction and the corresponding fission product aerosol behavior were analyzed. This tank has a headspace volume of 1657 m^3 and a total waste volume of 1582 m^3. Two cases were analyzed. In the first case, 0.058% of the waste, or 0.92 m^3 is assumed to combust. In the second case, 1.6% of the total waste, or 25 m^3, is assumed to combust. The average TOC and moisture content of the reactive portion of the waste were assumed to be 7.0% and 10.0%, respectively for both cases. The model assumptions and its validation are presented in Appendix B.

For the 0.92 m^3 case, the HEPA filter fails at 570 seconds (10 min). The pressure keeps increasing and reaches the peak pressure of 1.36E+05 Pa (5.04 psig) when the reactive waste is exhausted and the reaction stops at 1,010 seconds (17 min). Subsequently the tank de-pressurizes because of gas outflow and heat transfer to the dome wall and the saltcake. The depressurization slows down when the fog starts to form at 1,120 seconds (19 min). The peak temperatures reached during the transient in the headspace gas, on the wall, and on the saltcake surface are 396°K, 324°K and 318°K, respectively. The airborne aerosol builds up monotonically in the tank until the reaction stops. Some airborne aerosols are settled in the tank and some are released. The aerosol settlement potential is determined by total suspended mass, and until the water fog forms, both sodium and cesium hydroxide dominate aerosol. Leakage continues and stops only when the tank is fully de-pressurized. Note that when steam fog starts to form, it coagglomerates with aerosols from the reaction and the total deposition rate is increased. At the end of the transient, 3.8E-03 kg of CsOH remains airborne in the tank, 3.8E-03 kg has been settled in the tank, and 1.6E-03 kg has been released to the ambient. Hence, the fraction of CsOH released to the environment is about 0.17 of cesium contained in the combusted 0.92 m^3.

For the 25 m^3 case, there is enough combustible waste to cause dome failure; the tank pressure reaches the dome failure pressure of 1.75E+05 Pa (11 psig) at 1,350 seconds (22 min). The dome starts to crack, creating more flow openings just enough to relieve the excess pressure in the tank. Hence, the pressure is maintained constant at the tank failure pressure up until all reactive waste is exhausted and the reaction stops at 2,770 seconds (46 min). The tank quickly de-pressurizes. The headspace heats up because the effluent gases enter the headspace at the reaction temperature of 1,137°K. The hot headspace gas in turn transfers heat to the dome and unreacted saltcake by radiation and convection. The peak temperatures predicted for the headspace and the dome wall are 1,030°K and 580°K, respectively.

It should be noted that after the dome starts to crack, the airborne aerosol concentration remains nearly constant. Also, fallout of airborne aerosol is minuscule compared to leakage to the environment. Because of the high outflow, the aerosols do not have sufficient time to age and fall out. At the end of the transient, 1.1E-02 kg of CsOH remains airborne in the tank, 2.2E-03 kg has settled in the tank, and 2.3E-01 kg has been released to the environment. Hence, the fraction of CsOH released is 0.95 of the cesium contained in the combusted 25 m^3.

5.4.2 Release Fraction

The release fractions for toxic and radiological species are summarized below and are detailed in Appendix B. It should be noted that the release fractions shown in Table 5-3 are based on the total tank inventory, not on the combusted portion of the waste.

Table 5-3. Release Fractions for Tank U-105

Analyte	Release Fraction (0.92 m³ Combusted)	Release Fraction (25 m³ Combusted)
Cs-137	3.6E-05	5.5E-03
Sr-90	1.5E-12	2.3E-10
Y-90	4.9E-14	7.5E-12
Co-60	1.6E-12	2.4E-10
Tc-99	5.5E-12	8.4E-10
Sb-125	3.4E-06	5.3E-04
Eu-154	3.9E-07	5.9E-05
Pu-239	5.5E-14	8.5E-12
Cd	1.2E-08	1.9E-06
Hg	9.9E-05	1.5E-02
NaOH	1.2E-08	1.9E-06

5.5 DOSE CONSEQUENCES

The dose calculations were performed according to standard methods based upon the quantities of released radionuclides and toxicological chemicals. These methods are briefly described below.

5.5.1 Radiological Dose Calculation Process

The dose to an onsite or offsite receptor for an isotope is given by the equation:

$$Dose = \frac{X}{Q} * BR * V * (RF_i * Q_i * DCF_i) * 1000 \frac{L}{m^3} * 1000 \frac{mSv}{Sv} * Rs \quad (5-1)$$

where,

X/Q = atmospheric dispersion coefficient (0.034 s/m³ for the onsite receptor; 2.8E-5 s/m³ for the offsite receptor). These X/Q values are calculated for the tank farm areas relative to the nearest boundary, now taken as the south shoreline of the Columbia River to the north of the tank farms.

BR = breathing rate (3.3E-04 m³/s)

V = volume of waste in tank (m³)

Rf_i = Release fraction for i_{th} isotope

Q_i = Activity concentration for i_{th} isotope in Bq/L based on the bounding tank source term for all SST solids (bounding value from Table 5-1)

DCF_i= dose conversion factor for i_{th} isotope (Sv/Bq) (dose due to inhalation of unit activity; bounding value from Table 5-1).

Rs = respirable fraction (assumed to be 1.0).

The respirable fraction is the fraction of the material which is released that is in the respirable range. Because this material is formed as a vapor at high temperatures and will eventually condense to form aerosols as it leaves the tank, or shortly thereafter, it is expected that a majority of the material will be in the respirable particle size range. For the purposes of this calculation, the respirable fraction is taken as 1.0. That is, it is assumed that all of the radionuclides of interest reach the maximum exposed individual as respirable particles. Total radiological doses reported in Tables 5-4 and 5-5 are the sum of dose for the radionuclides of interest.

5.5.2 Toxicological Exposure Calculation Process

A method of comparison to guidelines for individual toxic chemicals is given by the equation:

$$FC = C * RF * RR * \frac{X}{Q} * \frac{1000}{ERPG} \qquad (5-2)$$

where,

FC = Fraction of risk acceptance guideline

C = Concentration of toxic material in waste (g/L)

RF = Release fraction

RR = rate of material being released from tank (L/s)

X/Q = atmospheric dispersion coefficient (s/m3)

ERPG = Emergency Response Planning Guideline (mg/m3)

The 1000 is a unit conversion (mg/g).

Each toxic chemical has three ERPGs, ERPG-1, ERPG-2 and ERPG-3 plus a fourth limit PEL-TWA. The limit used depends on the frequency class of the receptor and whether the onsite or offsite receptor is being considered. ERPG-1 is a level at which most people will experience no permanent effects, exceeding ERPG-2 can result in permanent damage, and exceeding ERPG-3 can result in life threatening effects.

The toxic evaluation requires adding up the sum of the concentration of the toxics (Cd, Hg, U) divided by their appropriate limits, the sum of the corrosives (NaOH) divided by its appropriate limit, and the particulate concentration divided by its appropriate limit. Particulates are evaluated since it is possible that a large enough concentration of even nontoxic particulates can cause choking. The particulates are compared to the limits by the following equation:

$$SOF = d*Q'*\frac{X}{Q'}*\frac{1E+06}{RG} \qquad (5-3)$$

where,

SOF = Sum of fractions

d = density of solids (usually taken as 1.6 g/cm^3)

Q' = release rate (L/s)

X/Q' = atmospheric dispersion coefficient (s/m^3).

RG = risk guideline (appropriate PEL or ERPG, mg/m^3)

The 1E+06 is a unit conversion.

The limits for particulates are:

$$
\begin{array}{lll}
\text{PEL-TWA} & = & 10 \text{ mg/m}^3 \\
\text{ERPG-1} & = & 30 \text{ mg/m}^3 \\
\text{ERPG-2} & = & 50 \text{ mg/m}^3 \\
\text{ERPG-3} & = & 100 \text{ mg/m}^3
\end{array}
$$

The procedure requires that the largest sum of fractions in the three categories be examined. If the largest is less than 1, the Risk Guidelines are met.

5.5.3 Summary of Dose Consequences for U-105

The consequences for the U-105 combustion scenarios are shown in Table 5-4, and Table 5-5. The radiological and toxicological consequences exceed risk acceptance guidelines (Figures 5-1 and 5-2). Mitigated and unmitigated consequences are identical because there are no practical means to limit the amount of radionuclides and chemical compounds released, should the combustion start. Therefore, the focus is on prevention of ignition sources to reduce the frequency of the accident.

Table 5-4. Tank U-105 Radiological and Toxicological Consequences for 0.92 m^3 Combustion and Comparison to Risk Acceptance Guidelines

Consequences	Onsite Dose/Exposure		Offsite Dose/Exposure	
	Calculated Dose	Risk Guideline	Calculated Dose	Risk Guideline
Radiological	5.8E+02 mSv (5.8E+01 rem)	5 mSv (0.5 rem)	4.8E-01 (4.8E-02 rem)	1 mSv (0.1 rem)
Toxicological (SOF)	2.9E+03	1 (ERPG-2)	3.2	1 (ERPG-1)

Notes:
The above table is based on the following: Total waste volume = 1582 m^3, Head Space volume = 1657 m^3, TOC = 7.0 wt%, H_2O = 10 wt%, and amount of combustible waste is 0.92 m^3 (50% confidence on the upper bound of combustible waste = 0.058% for U-105).

Table 5-5. Tank U-105 Radiological and Toxicological Consequences for 25 m^3 Combustion and Comparison to Risk Acceptance Guidelines

Consequences	Onsite Dose/Exposure		Offsite Dose/Exposure	
	Calculated Dose	Risk Guideline	Calculated Dose	Risk Guideline
Radiological	86 Sv (8.6E+03 rem)	5 mSv (0.5 rem)	71 mSv (7.1 rem)	1 mSv (0.1 rem)
Toxicological (SOF)	1.4E+05	1 (ERPG-2)	160	1 (ERPG-1)

Notes:
The above table is based on the following: Total waste volume = 1582 m^3, Head Space volume = 1657 m^3, TOC = 7.0 wt%, H_2O = 10 wt%, and amount of combustible waste is 25 m^3 (95% confidence on the upper bound of combustible waste = 1.6% for U-105).

Figure 5-1. Comparison of Consequences to Radiological Guidelines for 0.92 m^3 Combustion Event in Tank U-105
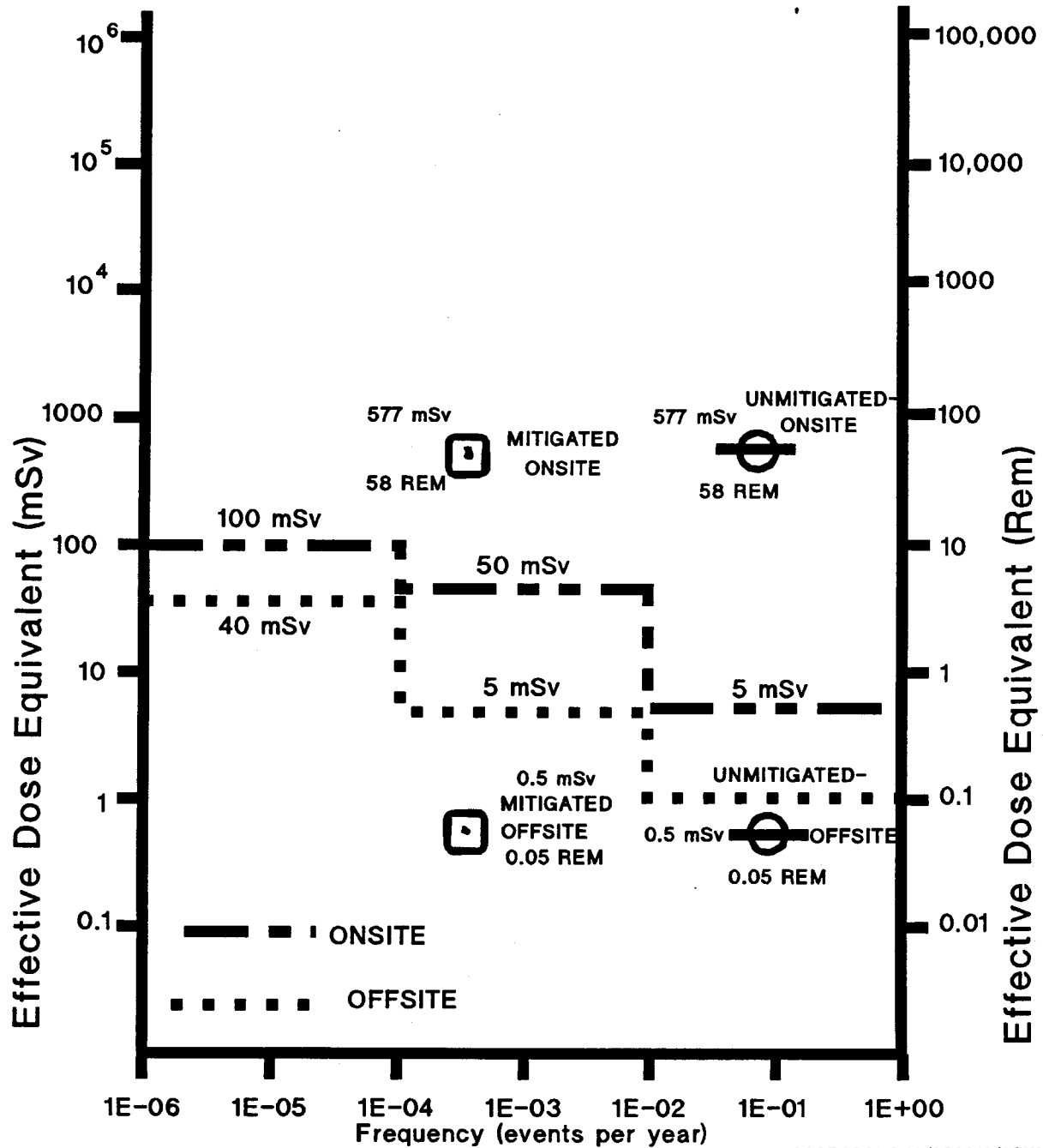
Figure 5-2. Comparison of Consequences to Radiological Guidelines for 25 m³ Combustion Event in Tank U-105

AAARAG14.GAL/960826/ABW
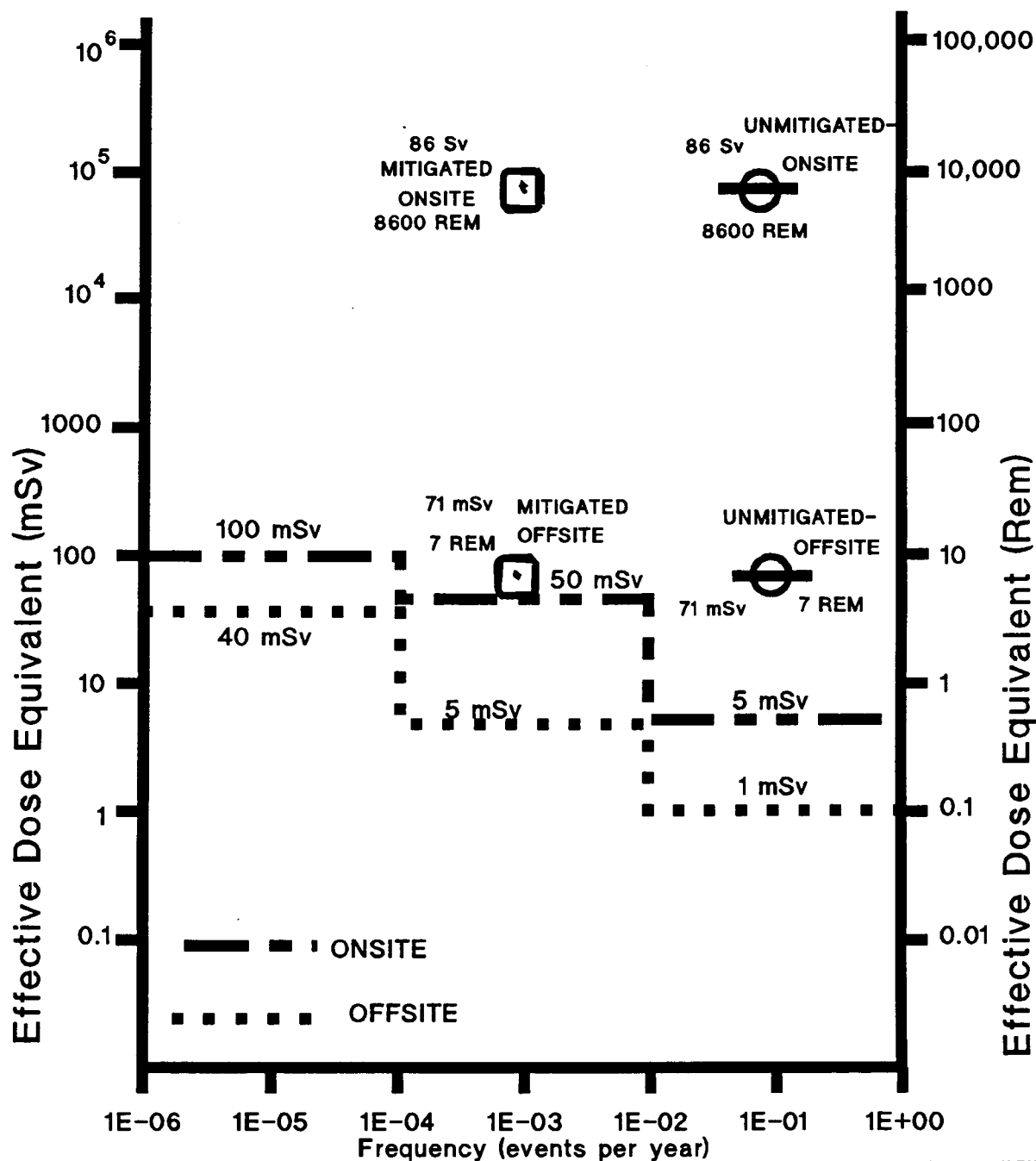
5.4.3 Conclusions of Consequence Assessment

The onsite consequences are excessive from both organic combustion scenarios, even when controls on ignitors have been considered. The offsite radiological consequences are acceptable only for 0.92 m^3 combustion scenario. It is therefore important that controls be used to prevent this accident, as no practical means exist to stop the accident if it starts, nor to limit the release of radioactive and toxic materials to the environment. Potential controls for organic tanks are discussed in Section 6.0.

6.0 CONTROLS

The potential controls for organic salt-nitrate reactions are listed below. These controls will become Technical Safety Requirement or other operating controls as appropriate.

6.1 IGNITION CONTROLS

Theoretical analysis indicates that the threshold energy for ignition of dry organic salt-nitrate wastes is more than 3.3 Joules (Fauske 1996a). Evaluations of potential ignition sources (see Section 4) have shown that there are six types of ignitors which could exceed this ignition threshold: hot lamp filaments, hot pieces of metal or slag from torch cutting or welding, vehicle fuel fires, rotary-mode core drilling, lightning strikes, and flammable gas burns. Controls are discussed below for each type of ignitor.

6.1.1 Hot Filaments from Failed Camera Lights

6.1.1.1   Restraints (e.g. "Top hats") will be used for power cord installations for lights.

Controls: Restraints (known as "top hats") shall be used on the power supply cables for lights to prevent a failed light from dropping to the level of the waste.

6.1.2 Welding and Torch Cutting

6.1.2.1   A component was assumed to be installed in open risers prior to welding and cutting activities that prevents hot metal from falling onto the waste surface.

Controls: The procedures, design, and work controls for maintenance, modification, and equipment removal/installation shall prevent hot metal pieces and slag from entering the tank and falling to the waste surface. Appropriate equipment, such as plugs or covers shall be used to ensure that hot metal pieces do not enter the tank and fall to the waste surface.

6.1.3 Vehicle Fuel Fire

6.1.3.1   Credit may be taken for prevention of this accident scenario through the use of spotters to assist drivers when maneuvering around in the tank farm. This was not included in the frequency calculations. This is a conservatism in the analysis.

Controls: An administrative control program shall be in place to ensure that spotters are used whenever vehicles will be maneuvering around or near tank projections. The duty of the spotter is to assure that the vehicle does not collide with tank projections.

6.1.3.2   Engineering design and evaluation shall assure that vehicle tanks are protected from collisions with tank appurtenances.

Controls: An administrative control program shall be used for all waste tanks which limits vehicles operating above the tanks to the following requirements:

The vehicle must have a protective plate (skid plate) protecting the fuel tank and any reservoir tanks from contacting risers protruding above grade, or

The fuel tanks should not project below the bumpers or main structural members of the vehicle, or

The fuel tank (and any reservoir tank) must be physically located at a height greater than the highest riser that would impact a tank located at a lower level.

6.1.4 Rotary Mode Core Drilling

6.1.4.1   Rotary mode core drilling was not evaluated in this report, but is covered in a separate safety assessment (Kubic 1996).

6.1.5 Lightning Strikes

6.1.5.1   **Controls:** If lightning storm activity is reported within 80 km (50 miles) of the tank farm, all activities will cease, tall objects will be lowered (secured in lowest position practicable), and the tank and equipment will be secured until the storm has passed. This control requires that securing the tank and equipment begins when the storm is at 80 km and is completed by the time the storm reaches 8 km (5 mi).

6.1.6 Flammable Gas Burn

6.1.6.1   Plausible scenarios for ignition of organic-nitrate containing wastes due to flammable gas deflagrations have not been identified, but are not ruled out. Controls, that have been imposed to address flammable gas hazards (Leach and Grigsby 1996), and those that will be proposed for TSRs, however, are also effective in reducing the risk of flammable gas induced condensed phase organic combustion events.

Controls: The control requirements specified for reducing the frequency of flammable gas burns are considered to be adequate to reduce the likelihood of this method of igniting an organic salt – nitrate combustion to acceptable levels.

6.2 TEMPERATURE CONTROLS

6.2.1 Temperature Monitoring

6.2.1.1   There are 7 tanks which potentially have enough decay heat to raise waste temperatures to the ignition temperature if cooling was disrupted for long periods. These tanks are C-106, SX-107,

-108, -110, -111, -112, and -114. Though measurements of waste samples show that TOC is relatively low in these tanks and the quantities of combustible waste at 95% confidence are predicted to be less than 2 m^3 for the worst one, it would not be prudent to allow a tank to heat up to the temperature at which an accelerated chemical reaction might occur. The effect of active cooling on bulk runaway has not yet been analyzed for these tanks.

Controls: Temperature monitoring is required for C-106, SX-107, -108, -110, -111, -112, and -114. Active cooling is required and cannot be permanently removed unless analyses show that bulk runaway cannot occur in these tanks.

6.2.2 Bulk Heatup (C-106 only)

6.2.2.1   It would not be prudent to allow C-106 to heat up to the temperature at which an accelerated chemical reaction might occur. Therefore, controls are required. Credit was taken for detection of and recovery actions for loss of evaporative cooling and loss of ventilation in tank C-106.

Controls: Monitor the waste temperature in C-106. Appropriate actions (such as moisture addition or restoration of ventilation) shall be taken to return the waste temperature to within the limits.

6.3 WASTE TRANSFER CONTROLS

If a waste contains TOC in excess of the *safe* criterion, moisture enhances safety of the tank. Therefore, the following controls apply:

6.3.1 Unsampled, Leaking Tank

6.3.1.1   **Controls:** When an unsampled tank is determined to be leaking, attempts shall be made to assess the TOC concentration to determine if the tank can be categorized as *safe*. If this cannot be done in time or if the answer should prove negative, then salt well pumping will be evaluated and a waiver sought from DOE to pursue salt well pumping if a comparison of risks indicates that this is the best course.

6.3.2 Prior to Interim Stabilization

6.3.2.1   In order to minimize future leakage of tank wastes to the environment, tank waste characterization should be pursued for tanks that have not been interim stabilized to determine which of these tanks can be categorized as *safe*.

Controls: An assessment of tank waste must be made before interim stabilization to ensure that the post pumped waste state would be *safe* or *conditionally safe*.

6.3.3 Moisture Monitoring

Moisture monitoring is important for Unsafe tanks (currently none identified), Conditionally Safe tanks, and Unsampled tanks. In all of these tank categories maintaining the moisture in the waste helps to maintain safety. A baseline surveillance should be performed visually to determine whether there is visible moisture near the solids surface. Additional means should be used depending upon available instrumentation and waste samples to provide measurements to correlate with the visual observations or to establish baseline moisture where visual observation does not show surface moisture. Techniques which may be used include manual tape, ENRAF, or FIC instruments. Neutron scans in LOW or electromagnetic induction (EMI) in LOW may also be used as well as neutron and EMI in the Surface Moisture Monitoring System (SMMS) as it becomes available and practicality is demonstrated.

Periodic moisture monitoring (e.g., quarterly) using additional waste samples, the same measurements or other measurements which have been suitably cross-correlated to the original should be used to verify continuing waste moisture. As long as the level does not change by more than a nominal amount to allow for instrument error (e.g., 5% of original value), the tank waste moisture can be regarded as remaining static.

The visual appearance of the surface should be reconfirmed at some longer interval (e.g. each 5 years).

6.3.3.1   **Controls:** Periodic surveillance or evaluation of moisture shall be performed to determine moisture concentration in those tanks categorized as *conditionally safe*.

6.3.3.2   **Controls:** For the *conditionally safe* tanks, proposed changes to the SST ventilation systems design or operations shall be evaluated to guard against unacceptable waste dryout. This is to prevent a tank moving from the *conditionally safe* to *unsafe* category.

6.4 CONTROLS APPLIED TO SAFE TANKS

A small organic-nitrate combustion event ($\sim$0.1 m^3) could exceed risk acceptance guidelines. Currently, it is difficult to definitively show that 0.1 m^3 of combustible waste does not exist in the SSTs (some tanks contain more than 1000 m^3 of waste). Therefore, ignition controls will be applied to all tanks, including tanks categorized as *safe*. Temperature controls will be applied to the seven tanks identified in Section 6.2 (even if they are categorized as *safe*) until analyses can demonstrate bulk runaway is not credible.

6.5 CONTROLS APPLIED TO CONDITIONALLY SAFE TANKS

Ignition controls are appropriate for *conditionally safe* tanks for the same reasons discussed in Section 6.4 above. Waste moisture is the principal control in maintaining safety for these tanks, therefore, waste transfer controls are applied to the *conditionally safe* tanks.

6.6 CONTROLS APPLIED TO UNSAMPLED TANKS

Tanks that have insufficient or no characterization data were not categorized in Section 3. However, tank histories and the ANOVA model extrapolation suggest that all of the remaining tanks will be categorized as *safe* once characterized. As a prudent measure, unsampled tanks will be treated as *conditionally safe* until characterized. Therefore, ignition controls and waste transfer controls are applied to the unsampled tanks.

6.7 CONTROLS APPLIED TO UNSAFE TANKS

Unsafe tanks contain waste which exceeds the safety criteria and therefore prevention of ignition by all sources is essential. No operations that could produce ignition sources (e.g., photography, welding, and torch cutting) are allowed in tanks categorized as *unsafe*. In addition, physical barriers are required around the tank risers to minimize the potential for a vehicle gasoline tank rupture over a riser. Temperature and waste transfer controls are also required on *unsafe* tanks.

This page intentionally left blank.

7.0 FUTURE WORK

7.1 OBTAIN ADDITIONAL TOC AND MOISTURE DATA

Total organic carbon and moisture data will continue to be obtained to assess the safety status of the tanks. These data will be inserted into the ANOVA model and tanks will be categorized as *safe, conditionally safe,* or *unsafe* as the data become available.

7.2 CONFIRM AND REFINE TANK GROUPING MODELS

Modeling activities will continue to examine tank grouping schemes and organic concentration estimates. Generalized conclusions on waste conditions may be appropriate within a waste type, within a tank, or across a family of similar tanks, depending on the model and the confidence in the model. Models will be benchmarked through sampling and characterization.

7.3 QUANTIFY THE EFFECTS OF ORGANIC AGING AND SOLUBILITY

Studies and tank waste data indicate that organic complexants and solvents undergo hydrolytic and radiolytic decomposition (aging) under tank waste conditions (Camaioni et al. 1994, 1995; Bryan et al. 1996). However, the influence of temperature and radiation dose on the rate of these reactions is not sufficiently defined to quantify aging. Kinetic data for these decomposition reactions are being investigated using waste simulants. Temperature data archives will be searched to better quantify waste temperature histories. The composition of selected waste samples will also be examined to determine the extent of aging in the waste tanks. The combustion characteristics of actual waste will continue to be examined using adiabatic calorimetry (Meacham 1996).

A byproduct of organic aging is the generation of flammable gas. Therefore, the relationship between the tanks suspected of containing organic and of generating substantial quantities of flammable gas will be examined.

Additional work on organic solubility is needed to corroborate organic solubility in actual organic waste. Results with waste simulants will be confirmed through analysis (organic speciation) of selected waste samples. Once organic aging and solubility can be quantified, these effects will be factored into an overall risk analysis for the organic complexant hazard.

7.4 FURTHER QUANTIFICATION OF IGNITION SOURCE REQUIREMENTS

Laboratory tests using waste simulants will be conducted to empirically define the energy requirements for ignition of the dry wastes, and to determine the minimum waste moisture concentrations required to preclude initiation of organic complexant propagating combustions. Once the effect of fuel and moisture concentration on ignition source requirements are better quantified, it may be possible to eliminate some ignition sources as credible (reducing the burden of ignition controls).

7.5 REVISION OF SAFETY DOCUMENTATION

Information from historical records, characterization, organic aging experiments, and organic solubility testing will be critically evaluated in a risk based assessment. This risk analysis will be used to determine the safety status of the waste and to direct any necessary monitoring or mitigation activities.

8.0 REFERENCES

Agnew, S. F., 1996, *History of Organic Carbon in Hanford HLW Tanks: HDW Model Rev. 3*, LA-UR-96-989, Los Alamos National Laboratory, Los Alamos, New Mexico.

Allen, G.K., 1976, *Estimated Inventory of Chemicals Added to the Underground Waste Tanks, 1944 Through 1975*, ARH-CD-6108, Atlantic Richfield Hanford Company, Richland, Washington.

American Institute of Chemical Engineers, 1989, *Plant Guidelines for Technical Management of Chemical Process Safety*, American Institute of Chemical Engineers, New York, New York.

American Institute of Chemical Engineers, 1992, *Plant Guidelines for Technical Management of Chemical Process Safety*, American Institute of Chemical Engineers, New York, New York.

American Institute of Chemical Engineers, 1995a, *Guidelines for Chemical Reactivity and Applications to Process Design*, American Institute of Chemical Engineers, New York, New York.

American Institute of Chemical Engineers, 1995b, *Tools for Making Acute Risk Decisions: With Chemical Process Applications*, American Institute of Chemical Engineers, New York, New York.

American Institute of Chemical Engineers, 1995c, *Guidelines for Process Safety Management*, American Institute of Chemical Engineers, New York, New York.

American Institute of Chemical Engineers, 1995d, *Guidelines for Process Safety Fundamentals for General Plan Operation*, American Institute of Chemical Engineers, New York, New York.

American Institute of Chemical Engineers, 1995e, *Guidelines for Safe Process Operations and Maintenance*, American Institute of Chemical Engineers, New York, New York.

Anderson, J. D., 1990, *A History of the 200 Area Tank Farms*, WHC-MR-0132, Westinghouse Hanford Company, Richland, Washington.

Atherton, J. A., 1974, *Prediction of Liquor Retention in Saltcakes and Sludges*, ARH-CD-230, Atlantic Richfield Hanford Company, Richland, Washington.

Bajwa, J. K., W. G. Farley, 1994, *Construction, Maintenance, and Operational Activities Analysis Summaries*, WHC-SD-WM-SARR-009, Rev. 0, Westinghouse Hanford Company, Richland, Washington.

Barney, G. S., 1994, *The Solubilities of Significant Organic Compounds in HLW Tank Supernatant Solutions*, WHC-SA-2565-FP, Westinghouse Hanford Company, Richland, Washington.

Barney, G. S., 1996, *The Solubilities of Significant Organic Compounds in HLW Tank Supernatant Solutions--FY1995 Progress Report*, WHC-EP-0899, Westinghouse Hanford Company, Richland, Washington.

Bryan, S. A., C. M. King, L. R. Pederson, and S. V. Forbes, 1996, *Thermal and Radiolytic Gas Generation from Tank 241-SY-103 Waste: Progress Report*, TWSFG96.17, Pacific Northwest National Laboratory, Richland, Washington.

Camaioni, D. M., W. D. Samuels, B. D. Lenihan, S. A. Clauss, K. L. Wahl, and J. A. Campbell, 1994, *Organic Tanks Safety Program Waste Aging Studies*, PNL-10161, Pacific Northwest Laboratory, Richland, Washington.

Camaioni, D. M., W. D. Samuels, S. A. Clauss, B. D. Lenihan, K. L. Wahl, J. A. Campbell, and W. J. Shaw, 1995, *Organic Tanks Safety Program FY95 Waste Aging Studies*, PNL-10794, Pacific Northwest Laboratory, Richland, Washington.

Connor, J. M., 1996, *Tank Characterization Report for Single-Shell Tank 241-C-204*, WHC-SD-WM-ER-488, Rev. 0, Westinghouse Hanford Company, Richland, Washington.

Cowley, W. L., 1996, *Development of Radiological Concentrations and Unit Liter Doses for TWRS FSAR Radiological Consequence Calculations*, WHC-SD-WM-SARR-037, Rev 0, Westinghouse Hanford Company, Richland, Washington.

Cowley, W. L., and A. K. Postma, 1996, *Analysis of Consequences of Postulated Solvent Fires in Hanford Site Waste Tanks*, WHC-SD-WM-CN-032, Rev. 0B, Westinghouse Hanford Company, Richland, Washington.

Dixon and Massey, 1957, *Introduction to Statistical Analysis*, Second Edition, Appendix, Table A-9c Confidence Belts for Proportions (Confidence Coefficient .95), McGraw Hill Book Company, New York, New York.

Epstein, M., H. K. Fauske, M. D. Crippen, D. R. Dickinson, J. D. McCormack, R. J. Cash, J. E. Meacham, and C. S. Simmons, 1994, *Ferrocyanide Safety Program: An Assessment of the Possibility of Ferrocyanide Sludge Dryout*, WHC-EP-0816, Westinghouse Hanford Company, Richland, Washington.

Fauske, H. K., 1996a, *Assessment of Chemical Vulnerabilities in the Hanford High-Level Waste Tanks*, WHC-SD-WM-ER-543, Rev. 0, Westinghouse Hanford Company, Richland, Washington.

Fauske, H. K., 1996b, *An Assessment of Requirements for Organic-Nitrate Propagating Reactions Including RSST and Tube Propagation Test Results With Waste Simulants*, FAI/96-48, Rev. 0, Fauske and Associates, Inc., Burr Ridge, Illinois.

Fauske, H. K., 1996c, *Propagation Scale-Up Tests with Organic-Nitrate/Nitrite Mixtures*, FAI/96-45, Rev. 0, Fauske and Associates, Inc., Burr Ridge, Illinois.

Fauske, H. K., D. R. Dickinson, R. J. Cash, and J. E. Meacham, 1995, *The Contact Ignition (CTI) Criteria for Propagating Chemical Reactions Including the Effect of Moisture and Application to Hanford Waste*, WHC-SD-WM-ER-496, Rev. 0, Westinghouse Hanford Company, Richland, Washington.

Gygax, R. W., 1990, "Scaleup Principles for Assessing Thermal Runaway Risks," *Chemical Engineering Progress*, February 1990.

Han, F. C., 1996, *Structural Integrity and Potential Failure Modes of Hanford High Level Waste Tanks*, WHC-SD-WM-TWR-RPT-002, Rev. 0, Westinghouse Hanford Company, Richland, Washington.

Handy, L. L, 1975, *Flow Properties of Saltcake for Interstitial Liquid Removal/Immobilization Development Program*, ARH-C-6, Atlantic Richfield Hanford Company, Richland, Washington.

Jeppson, D. W., and J. J. Wong, 1993, *Ferrocyanide Waste Simulant Characterization*, WHC-EP-0631, Westinghouse Hanford Company, Richland, Washington.

Kirk, J. J., 1980, *Permeability, Porosity, and Capillarity of Hanford Waste Material and Its Limits of Pumpability*, RHO-CD-925, Rev. 2, Rockwell Hanford Operations, Richland, Washington.

Kubic, W. L., 1996, *An Evaluation of Reactive Chemical Hazards During Rotary Mode Core Sampling*, TSA10-CN-WT-SA-CH-001, Rev. 1, Los Alamos National Laboratory, Los Alamos, New Mexico.

Leach, C. E., J.M. Grigsby, 1996, *Flammable Gas/Slurry Growth Unreviewed Safety Question: Justification for Continued Operation for the Tank Farms at the Hanford Site*, WHC-SD-WM-JCO-007, Westinghouse Hanford Company, Richland, Washington.

Lindberg, S. E., 1996, *Frequency Analysis of Vehicle Fuel Release Resulting in Waste Tank Fire*, WHC-SD-WM-CN-037, Rev. 0, Westinghouse Hanford Company, Richland, Washington.

Meacham, J. E., 1996, *Strategy for Resolution of the Organic Complexant and Organic Solvent Safety Issues*, WHC-EP-0908, Westinghouse Hanford Company, Richland, Washington.

Metz, W. P., 1975a, *Capillarity Demonstration*, (internal memorandum to R. C. Roal, March 26), Atlantic Richfield Hanford Company, Richland, Washington.

Metz, W. P., 1975b, *Preliminary Evaluation of the Affects of Capillary Forces on Stabilizing Hanford Waste Saltcakes and Sludges*, (internal memorandum to R. J. Thompson, September 9), Atlantic Richfield Hanford Company, Richland, Washington.

Metz, W. P., 1976, *A Topical Report on Interstitial Liquid Removal From Hanford Saltcakes*, ARH-CD-545, Atlantic Richfield Hanford Company, Richland, Washington.

Plys, M., 1996, *Organic-Nitrate Reaction & Headspace Burns*, (internal memorandum to Allen Webb, May 8), Fauske and Associates, Inc., Burr Ridge, Illinois.

Postma, A. K., D. B. Bechtold, G. L. Borsheim, J. M. Grigsby, R. L. Guthrie, M. Kummerer, M. G. Plys, and D. A. Turner, 1994, *Safety Analysis of Exothermic Reaction Hazards Associated with the Organic Liquid Layer in Tank 241-C-103*, WHC-SD-WM-SARR-001, Rev. 0, Westinghouse Hanford Company, Richland, Washington.

Scheele, R. D., P. R. Bredt, and R. L. Sell, 1996, *Organic Tank Safety Project: Development of a Method to Measure the Equilibrium Water Content of Hanford Organic Tank Wastes and Demonstration of Method on Actual Waste*, PNNL-11227, Pacific Northwest National Laboratory, Richland, Washington.

Sederberg, J. P., J. A. Reddick, 1994, *TBP and Diluent Mass Balances in the Purex Plant at Hanford 1955-1991*, WHC-MR-0483, Rev. 0, Westinghouse Hanford Company, Richland, Washington.

Simpson, B. C., 1994, *Tank 241-T-111 Characterization Report*, WHC-EP-0806, Westinghouse Hanford Company, Richland, Washington.

Van Keuren, J. C., 1996, *Toxic Chemical Considerations for Tank Farm Releases*, WHC-SD-WM-SARR-011, Rev. 2, Westinghouse Hanford Company, Richland, Washington.

Van Vleet, R. J., 1993a, *Radionuclide and Chemical Inventories for the Single Shell Tanks*, WHC-SD-WM-TI-565, Rev. 0, Westinghouse Hanford Company, Richland, Washington.

Van Vleet, R. J., 1993b, *Radionuclide and Chemical Inventories for the Double Shell Tanks*, WHC-SD-WM-TI-543, Rev. 1, Westinghouse Hanford Company, Richland, Washington.

Webb, A. B., D. M. Camaioni, J. M. Grigsby, P. G. Heasler, B. Malinovic, M. G. Plys, J. L. Stewart, J. J. Toth, and D. A. Turner, 1995, *Preliminary Safety Criteria for Organic Watch List Tanks at the Hanford Site*, WHC-SD-WM-SARR-033, Rev. 0, Westinghouse Hanford Company, Richland, Washington.

Zach, J. J., 1996, *Probability, Consequences, and Mitigation for Lightning Strikes to Hanford Site High-Level Waste Tanks*, WHC-SD-WM-ES-387, Rev. 1, Westinghouse Hanford Company, Richland, Washington.

APPENDIX A

CALCULATION NOTES FOR TOC AND MOISTURE ANOVA ANALYSIS

This page intentionally left blank.

APPENDIX A

CALCULATION NOTES FOR TOC AND MOISTURE ANALYSIS

A.1.0 PURPOSE

This appendix describes combustible waste estimation calculations performed by a collection of Splus subroutines and command files. The calculations use sampling data to determine the moisture and TOC distributions in all Hanford SSTs and thereby statistically estimate combustible waste. Combustible waste is defined as waste that can burn (roughly, waste with *TOC > 4.5%* and moisture less than 20%). Two types of combustible waste are calculated; the combustible waste currently in the tanks (current combustible waste fraction), and the combustible waste that would be in the tanks after complete dry-out (dry combustible waste fraction).

A.2.0 METHODOLOGY

Combustible waste that is currently in a tank is defined as waste that meets the following criteria:

$$TOC > 4.5\% + 0.17 \; H_2O \; and \; H_2O < 20\% \tag{A-1}$$

The variable, *TOC*, represents the weight concentration of total organic carbon in the sample, (percent wet basis), while H_2O represents the concentration of moisture. If all moisture were to be removed from the tank, the criteria for (dry) combustible waste is:

$$TOC > 4.5\% - 0.045 \; H_2O \tag{A-2}$$

Since combustible waste is defined in terms of TOC and moisture, it is possible to use this relationship to determine combustible waste in a tank from moisture and TOC measurements.

The strategy employed to calculate combustible waste requires that the concentration distribution of TOC and H2O in a tank be estimated. A concentration distribution describes what fraction of the waste that has TOC (or H_2O) concentration above 1%, 5%, 10%, etc. Integrating the (H_2O,TOC) concentration distribution over the combustible region defined in Equation A-1 or A-2 determines the fraction of combustible waste in the tank.

To estimate the distribution of (H_2O,TOC) in the tanks, a statistical procedure suited to the structure of the available data has been chosen. The

distribution of (H_2O,TOC) has been assumed to have a bivariate log-normal distribution and the five unknown parameters that define such a distribution are estimated using ANOVA (Analysis of Variance) procedures (the unknown parameters consist of 2 log-means, 2 standard deviations, and the correlation between moisture and TOC). A simple parametric form has been chosen because sufficient data does not exist to fit the distribution empirically. Dozens of observations per tank would be required for an empirical fit.

ANOVA is also employed for the same reason; only about 20% of the tank waste layers have been sampled, and the typical sampled tank contains only 2 or 3 measurements, not enough data to estimate even a simple parametric distribution like the log-normal. ANOVA combines information from similar tanks so that it is possible to construct the desired distributions. ANOVA also allows reasonable distributions to be constructed for unsampled tanks.

Of course, with so little data, many of the ANOVA tank estimates are quite extrapolative. Fortunately, the ANOVA procedure also provides uncertainties for the extrapolated parameters, so that one can evaluate just how good the extrapolations are. The uncertainties provided by the ANOVA are a very important component of this calculation because we desire more than a "best estimate" of combustible waste; the risk calculation requires an uncertainty distribution for combustible waste as its input and the uncertainties provided by the ANOVA fits are propagated to form an uncertainty distribution for combustible waste.

This uncertainty distribution describes how close the calculated values are to the true combustible waste and represents the adequacy of the existing data to estimate combustible waste.

A.2.1 QUANTITIES TO BE ESTIMATED

Four different combustible waste fractions are actually estimated for the risk analysis. The four types of combustible waste are:

$R_{cur,sur}$ = Current combustible waste fraction in the tank surface layer (within 20 cm of the surface),

$R_{cur,bot}$ = Current combustible waste fraction in the tank subsurface layer,

$R_{dry,surf}$ = Dry combustible waste fraction in the tank surface,

$R_{dry,bot}$ = Dry combustible waste fraction in the tank subsurface layer.

In other words, combustible waste is actually estimated at two locations in the tank; it is estimated for the surface layer, and in the sub-surface layer. This categorization of combustible waste is made because waste at the surface is more likely to have a different (H_2O,TOC) distribution than sub-surface waste. There are also risk analysis motivations for distinguishing between surface and subsurface waste because surface waste is more likely to be exposed to an initiator than sub-surface waste.

Although four combustible waste portions are actually calculated by the methodology, only two are reported: the total current fraction of combustible waste and the total dry fraction of combustible waste. These are calculated by averaging together the appropriate surface and subsurface fractions. Of course the average requires the correct weights. The appropriate formulas are:

$$R_{cur} = \frac{V_{surf}}{V_{surf}+V_{bot}} R_{cur,surf} + \frac{V_{bot}}{V_{surf}+V_{bot}} R_{cur,bot} \qquad \text{(A-3)}$$

and

$$R_{dry} = \frac{V_{surf}}{V_{surf}+V_{bot}} R_{dry,surf} + \frac{V_{bot}}{V_{surf}+V_{bot}} R_{dry,bot} \qquad \text{(A-4)}$$

where V_{surf} and V_{bot} are the surface and subsurface waste volumes.

A.2.2 H2O/TOC ANOVA MODEL

Approximately 1400 H_2O and TOC measurements are available for all 149 SSTs. The data is analyzed using a random effects ANOVA model, which produces estimates of H_2O (or TOC) in the tanks as well as statements of uncertainty. The formula for the specific ANOVA model utilized on TOC is:

$$Y_{ijkl} = \mu + D_i + G_j + DG_{ij} + T_{jk} + DT_{ijk} + E_{ijkl} \quad \text{(5)}$$

The measurement, Y_{ijkl}, represents a *log10(H2O)* or TOC measurement (expressed in percent) taken under conditions *i j k l*. The indices *i j k l* describe the conditions that the measurements were taken under. These are defined as:

i: describes the layer the measurement was taken in (i=surface layer, subsurface layer).

j: identifies a tank group. There are 3 tank groups for TOC and 4 groups for H_2O.

k: represents the tank associated with the measurement.

l: identifies the "replicate" measurements that occur within a layer in a specific tank.

The ANOVA fitting procedure will produce estimates for all the unknown terms present in the above equation. Since the terms are considered to be random variables, it also calculates their variances (such as *Var(E_{ijkl})* = σ_E^2,

$Var(T_{ik}) = \sigma_T^2$, etc.). These variances are used by the ANOVA procedure to calculate uncertainty in the TOC estimates.

For a tank with data, the "best estimate" for TOC in layer i is:

$$\mu_i = \mu + D_i + G_j + DG_{ij} + T_{jk} + DT_{ijk} \qquad \text{(A-6)}$$

while for a tank without data, the "best estimate" is:

$$\mu_i = \mu + D_i + G_j + DG_{ij} \qquad \text{(A-7)}$$

This last estimate is much less certain than the previous estimate, and its uncertainty is inflated by the amount $Var(T) + Var(DT)$. The log-normal distribution for the concentration in the layer therefore has a log-mean of μ_i and the standard deviation of the concentration is estimated by the ANOVA component σ_E, the within-layer standard deviation.

The actual estimates for all tanks are automatically produced by the Splus (Chambers and Hastie 1992 and S-Plus 1991) ANOVA subroutine Vcsas, a subroutine that produces restricted maximum likelihood estimates for the specified ANOVA model (see Corbeil and Searle 1976 for a description of REML). This routine produces the best estimate (i.e., log-mean) for each tank layer, as well as the standard errors of the estimates (i.e., uncertainties).

The ANOVA model chosen to describe H_2O and TOC is not unique; its form depends heavily on the amount and type of data available to the fit. Using the present ANOVA model, only about 20% of the tank layers contain data, indicating that it is not possible to include anything more complex than the two-layer model presently employed. The two layers in the model introduce three terms into the model (D_i, DG_{ij}, and DT_{ijk}) and create a model that is considerably more complex than the original ANOVA model which was:

$$Y_{ijk} = \mu + G_i + T_{ij} + E_{ijk} \qquad \text{(A-8)}$$

These layer terms are not very important for tanks that have data. For tanks with data in both layers, the ANOVA basically fits log-means to each layer. However, for layers that contain no data, these terms determine how the extrapolation is done.

A.2.3 TOC TANK GROUPING

Tank groups (as identified by index j) have been introduced into the ANOVA model to allow TOC to be predicted in unmeasured tanks. Tanks have been grouped into three logical categories, based on the waste chemistry of the principal waste stream used to fill the tank (as defined by Agnew 1996). The three categories are: complexant series tanks, solvent series tanks, and finally non-TOC series tanks.

Three categorizations cannot perfectly predict TOC. For example, a "'non-TOC" tank may still contain TOC because secondary waste streams contain TOC, or because of errors in the historical records. Splitting the tanks into more categories will decrease the within group variations, but also decrease the amount of data available to estimate TOC for each group. Given this constraint (i.e., data must exist to describe TOC in each group), we decided to limit the categories to the three above.

A.2.4 H2O TANK GROUPING

For moisture prediction, tanks are grouped according to the particle size of their waste and the wetness of the waste surface. Two particle size categorizations are used, large and small and photographs have been used to categorize the tank into wet (visible standing water on the surface) and dry. This results in four moisture groups:

Group I: Dry surface, large particle size,

Group II: Dry surface, small particle size,

Group III: Wet surface, large particle size,

Group IV: Wet surface, small particle size.

A.2.5 CALCULATION OF THE CORRELATION BETWEEN MOISTURE AND TOC

One required parameter not supplied by the moisture and TOC ANOVA's is the correlation coefficient between the two quantities. To obtain an estimate for ρ, the correlation between the ANOVA residuals was used (i.e., E_{ijkl}). A single correlation coefficient was computed for all available E_{ijkl}(H_2O,TOC) pairs. This resulted in an estimate based upon 162 pairs. The value for correlation obtained from this calculation was 35%. This parameter also has uncertainty associated with it, but because of the relatively large number of observations associated with the estimate, it was decided to assume that this parameter was perfectly known.

A.2.6 ESTIMATION OF COMBUSTIBLE WASTE

The ANOVA results described in the last two sections produce a description of the individual moisture and TOC distributions of waste in a tank. In this section, these ANOVA estimates will be used to calculate the four combustible

waste fractions in a tank ($R_{dry,surf}$, $R_{cur,surf}$, $R_{dry,bot}$, and $R_{cur,bot}$). The estimates for these quantities are not given as a single "best estimate," but as a Bayesian probability distribution that describes our state of uncertainty about the true value.

A.2.6.1 Calculation of Combustible Waste Amounts

It should be noted that this estimation problem is fundamentally different than most waste estimation problems in that no direct measurements on the variable of interest have been taken; only measurements that are indirectly related to combustible waste are available, and can only be used by postulating a relationship between the quantities. The measured variables indirectly related to combustible waste are total organic carbon (TOC) and moisture (% H_2O) of the waste. This section presents a relationship between (H_2O,TOC) concentrations in a unit of tank waste and its reactivity.

Therefore if one can "estimate" the distribution of (H_2O,TOC) concentrations in a tank, an application of this relationship gives the combustible waste in the tank. Mathematically, this strategy is expressed by the integral formula:

$$R = \int_{(X_{H2O}, X_{TOC}) \in A} f(X_{H2O}, X_{TOC}) \, dX_{H2O} dX_{TOC} \qquad \text{(A-9)}$$

where $f(X_{H2O}, X_{TOC})$ represents the distribution of (H_2O, TOC) values in the tank, the set A defines combustible waste in terms of (H_2O, TOC), and R is the estimate of combustible waste fraction in the tank.

Using the assumption of lognormality (or equivalently, normality on the log scale), the estimate for combustible waste becomes:

$$R = C_0 \int_{Y \in log(A)} exp \left[-\frac{1}{2} (Y - \mu)^T \Gamma^{-1} (Y - \mu) \right] dY \qquad \text{(A-10)}$$

with

$$Y = (\log(X_{H2O}), \log(X_{TOC})) \qquad \mu = (\mu_{H2O}, \mu_{TOC}) \qquad \text{(A-11)}$$

$$C_0 = \frac{1}{2\pi\sqrt{1 - \rho^2} \sigma_{H2O} \sigma_{TOC}} \qquad \Gamma = \begin{bmatrix} \sigma_{H2O}^2 & \rho \sigma_{H2O} \sigma_{TOC} \\ \rho \sigma_{H2O} \sigma_{TOC} & \sigma_{TOC}^2 \end{bmatrix} \qquad \text{(A-12)}$$

The means and standard deviations (i.e., μ's and σ's) appearing in this formula define the distribution and are produced by the ANOVA fits. The fact that these parameters are not exactly known means that the resulting combustible waste R is not perfectly known. The posterior distribution of R is determined by a Monte Carlo calculation that utilizes all the ANOVA-derived uncertainty distributions on the μ's and σ's.

To be more specific, the ANOVA results are used to produce Bayesian posterior distributions as described in (Dempster et al. 1981). The Monte Carlo then propagates these distributions to combustible waste using Equation A-8.

As mentioned earlier, four different types of combustible waste are to be calculated. Each type is calculated using Equation A-8, using appropriate values for A, μ_{H2O}, and μ_{TOC}. How these parameters are defined for each of the four types of combustible waste is:

$R_{cur,surf}$: A is defined as $X_{H2O} < 20\%$ and $X_{TOC} > 4.5\% + 0.17\ X_{H2O}$. The means, μ_{H2O} and μ_{TOC}, represent ($H2O,TOC$) concentrations of waste at the surface.

$R_{dry,surf}$: A is defined as $X_{TOC} > 4.5\% - 0.045\ X_{H2O}$. The means, μ_{H2O} and μ_{TOC}, represent ($H2O,TOC$) concentrations of waste at the surface.

$R_{cur,bot}$: A is defined as $X_{H2O} < 20\%$ and $X_{TOC} > 4.5\% + 0.17\ X_{H2O}$. The means, μ_{H2O} and μ_{TOC}, represent ($H2O,TOC$) concentrations of waste below the surface.

$R_{dry,bot}$: A is defined as $X_{TOC} > 4.5\% + 0.045\ X_{H2O}$. The means, μ_{H2O} and μ_{TOC}, represent ($H2O,TOC$) concentrations of waste below the surface.

A.2.7   MONTE CARLO CALCULATIONS TO DETERMINE UNCERTAINTY DISTRIBUTIONS

Equation 10 basically expresses combustible waste in terms of five distributional parameters, μ_{H2O}, μ_{TOC}, σ_{H2O}, σ_{TOC}, and ρ. To calculate a distribution of combustible waste that expresses the uncertainty in this estimate, a Monte Carlo calculation is performed that assumes the parameters have a standard Bayesian posterior distribution (Dempster et al. 1981). The input parameters (μ_{H2O}, μ_{TOC}, σ_{H2O}, σ_{TOC}) that define combustible waste are simulated in the following manner by the Monte Carlo:

1. Simulate σ^2_{TOC} from a Chi-squared variate using the formula:

$$\sigma^2_{TOC} = \frac{DOF\,\hat{\sigma}^2_{TOC}}{\chi^2_{DOF}} \tag{A-13}$$

where $_2\hat{\sigma}_{TOC}$ represents the estimate produced by the ANOVA and χ_N represents a random Chi-squared variate with N degrees of freedom. The variable *DOF* represents the degrees of freedom associated with the sigma.

2. Substitute the simulated σ_{TOC} from the previous step into the following formula that is used to simulate μ_{TOC}:

$$\mu_{TOC} = \hat{\mu}_{TOC} + \sigma_{TOC}Z \tag{A-14}$$

Z represents a standard normal variate and $\hat{\mu}_{TOC}$ is the estimate produced by the ANOVA.

3. Simulate σ^2_{TOC} and μ_{H_2O} using steps similar to those described for TOC.

The Monte Carlo produces 1000 simulated sets of combustible waste volumes for a tank and these values are then used to form empirical distributions and discrete state space probabilities of the 4 combustible waste fractions. The surface and subsurface fractions are averaged together to produce the dry and current combustible waste fractions.

A.3.0 INPUT DATA

The Table A-1 contains the TOC data used in the H_2O and TOC ANOVAs. The measurements are identified by the 2 main factors used in the ANOVAs: tank and sample layer.

Table A-1. Input Data for the ANOVA Model

#	tank.id	riser.id	sample.layer	H_2O, wt%	TOC, wt%
11	a101	NA	sub-surface	34.19	0.8437838
15	a101	NA	sub-surface	42.37	0.5763636
19	a102	a19	surface	30.66	NA
20	a102	NA	sub-surface	40.92	0.7200000
21	a102	NA	sub-surface	29.40	0.7940000
22	a102	19	surface	33.59	NA
23	a103	NA	sub-surface	40.30	0.7730000
25	a103	NA	sub-surface	40.10	0.8040000
28	a106	NA	sub-surface	43.00	0.7150000
29	a106	NA	sub-surface	45.10	0.6230000
36	ax102	9e	surface	31.12	NA
37	ax102	9e	surface	NA	6.3500000
38	ax102	3a	surface	28.01	NA
40	ax102	9e	surface	33.30	NA
41	ax102	9e	surface	NA	4.8100000
42	ax102	3a	surface	NA	6.1200000
43	ax102	3a	surface	29.57	NA
45	ax102	3a	surface	NA	5.3400000
47	b102	1	surface	22.83	NA
48	b102	1	surface	13.07	NA
49	b102	1	surface	18.17	NA
50	b102	1	surface	17.82	NA
51	b102	1	surface	15.15	NA
52	b102	1	surface	16.98	NA

#	tank.id	riser.id	sample.layer	H$_2$O, wt%	TOC, wt%
53	b103	2	surface	40.31	NA
54	b103	7	surface	50.08	NA
55	b103	7	surface	NA	0.0645000
56	b103	7	surface	NA	0.0710000
57	b103	2	surface	38.76	NA
58	b103	7	surface	50.26	NA
59	b104	2	surface	61.19	NA
60	b104	2	sub-surface	44.37	NA
61	b104	7	sub-surface	47.40	NA
62	b104	7	sub-surface	47.55	NA
63	b104	7	sub-surface	47.63	NA
64	b104	2	sub-surface	47.65	NA
65	b104	7	sub-surface	47.07	NA
66	b104	2	sub-surface	44.72	NA
67	b104	7	sub-surface	47.82	NA
68	b104	7	surface	47.84	NA
69	b104	7	sub-surface	47.88	NA
70	b104	7	sub-surface	47.93	NA
71	b104	2	sub-surface	46.11	NA
72	b104	2	sub-surface	44.75	NA
73	b104	2	sub-surface	45.15	NA
74	b104	2	sub-surface	47.98	NA
75	b104	7	sub-surface	48.02	NA
76	b104	7	surface	45.46	NA
77	b104	2	sub-surface	44.64	NA
78	b104	7	sub-surface	47.16	NA
79	b104	7	sub-surface	48.13	NA
80	b104	7	sub-surface	47.09	NA
81	b104	7	sub-surface	47.12	NA

#	tank.id	riser.id	sample.layer	H$_2$O, wt%	TOC, wt%
82	b104	7	surface	47.14	NA
83	b104	2	sub-surface	42.50	NA
84	b104	7	sub-surface	46.98	NA
85	b104	2	surface	42.34	NA
86	b104	2	sub-surface	40.90	NA
87	b104	7	sub-surface	47.23	NA
88	b104	2	sub-surface	46.69	NA
89	b104	2	sub-surface	46.15	NA
90	b104	2	sub-surface	46.69	NA
91	b104	2	sub-surface	40.79	NA
92	b104	7	surface	46.64	NA
93	b104	7	sub-surface	46.62	NA
94	b104	7	sub-surface	46.56	NA
95	b104	2	sub-surface	44.18	NA
96	b104	2	sub-surface	46.26	NA
97	b104	2	sub-surface	44.24	NA
98	b104	7	sub-surface	46.20	NA
99	b104	2	sub-surface	46.20	NA
100	b104	7	sub-surface	46.97	NA
102	b104	7	sub-surface	50.27	NA
104	b104	2	sub-surface	28.08	NA
105	b104	7	sub-surface	48.24	NA
106	b104	2	sub-surface	49.84	NA
107	b104	2	sub-surface	49.93	NA
109	b104	2	sub-surface	48.39	NA
110	b104	7	sub-surface	48.32	NA
113	b104	7	sub-surface	49.80	NA
114	b104	2	sub-surface	48.98	NA
115	b104	7	sub-surface	49.08	NA

#	tank.id	riser.id	sample.layer	H₂O, wt%	TOC, wt%
116	b104	2	sub-surface	49.14	NA
118	b104	7	sub-surface	48.17	NA
119	b110	NA	sub-surface	NA	0.0300000
120	b110	NA	sub-surface	NA	0.0312000
121	b110	NA	sub-surface	NA	0.0456000
122	b110	NA	sub-surface	NA	0.0298000
123	b110	NA	sub-surface	NA	0.0304000
124	b110	NA	sub-surface	NA	0.0421000
125	b110	NA	sub-surface	NA	0.0457000
126	b110	NA	sub-surface	NA	0.0439000
127	b110	NA	sub-surface	NA	0.0328000
128	b110	NA	sub-surface	NA	0.0463000
129	b110	NA	sub-surface	NA	0.0407000
130	b110	NA	sub-surface	NA	0.0398000
131	b110	NA	sub-surface	NA	0.0396000
132	b110	NA	sub-surface	NA	0.0358000
133	b111	3	sub-surface	NA	0.0750000
134	b111	NA	sub-surface	NA	0.1320000
135	b111	NA	sub-surface	NA	0.1340000
136	b111	5	sub-surface	NA	0.1250000
137	b111	3	sub-surface	NA	0.0530000
138	b111	5	sub-surface	NA	0.1340000
139	b111	NA	sub-surface	NA	0.1340000
140	b111	NA	sub-surface	NA	0.0820000
141	b111	3	sub-surface	NA	0.0820000
142	b111	3	sub-surface	NA	0.0560000
143	b111	NA	sub-surface	NA	0.1320000
144	b111	5	sub-surface	NA	0.1590000
145	b111	NA	sub-surface	NA	0.0670000

#	tank.id	riser.id	sample.layer	H$_2$O, wt%	TOC, wt%
146	b111	5	sub-surface	NA	0.1330000
147	b111	NA	sub-surface	NA	0.1590000
148	b111	NA	sub-surface	NA	0.1620000
149	b111	NA	sub-surface	NA	0.0680000
150	b111	NA	sub-surface	NA	0.0560000
151	b111	NA	sub-surface	NA	0.1590000
152	b112	7	surface	40.04	NA
153	b112	7	surface	40.19	NA
154	b112	3	surface	47.14	NA
155	b112	3	surface	45.57	NA
156	b112	7	surface	43.26	NA
157	b112	7	surface	21.08	NA
158	bx101	7	surface	23.83	NA
159	bx101	7	surface	21.98	NA
160	bx101	1	surface	14.21	NA
161	bx101	1	surface	13.14	NA
162	bx101	1	surface	14.14	NA
163	bx101	7	surface	18.36	NA
164	bx101	1	surface	27.77	NA
165	bx101	7	surface	15.35	NA
166	bx101	7	surface	15.76	NA
167	bx101	1	surface	24.80	NA
168	bx101	7	surface	16.37	NA
170	bx103	2	surface	59.61	NA
175	bx103	2	sub-surface	23.40	NA
176	bx103	2	sub-surface	23.60	NA
177	bx103	7	sub-surface	40.75	NA
179	bx103	7	sub-surface	40.68	NA
182	bx103	2	sub-surface	25.01	NA

#	tank.id	riser.id	sample.layer	H$_2$O, wt%	TOC, wt%
183	bx103	7	sub-surface	39.25	NA
184	bx103	2	sub-surface	24.14	NA
185	bx103	2	surface	55.20	NA
186	bx103	2	surface	57.21	NA
187	bx103	7	surface	63.17	NA
188	bx103	7	sub-surface	44.91	NA
189	bx103	2	sub-surface	29.60	NA
190	bx103	7	surface	60.65	NA
191	bx103	2	surface	62.98	NA
192	bx103	2	sub-surface	22.14	NA
193	bx104	NA	sub-surface	NA	0.2710000
196	bx104	NA	sub-surface	NA	0.4400000
197	bx104	NA	sub-surface	NA	0.1780000
199	bx105	2	surface	NA	NA
201	bx105	6	surface	4.91	NA
203	bx105	2	surface	NA	NA
204	bx105	6	surface	5.54	NA
205	bx105	6	surface	14.78	NA
206	bx105	2	surface	15.74	NA
207	bx105	2	surface	NA	NA
208	bx105	2	surface	NA	NA
209	bx105	2	surface	NA	NA
210	bx105	6	surface	16.18	NA
211	bx105	6	surface	NA	NA
212	bx105	6	surface	NA	NA
213	bx105	6	surface	NA	NA
214	bx105	NA	sub-surface	NA	0.1800000
215	bx105	6	surface	18.77	NA
216	bx105	6	surface	18.97	NA

#	tank.id	riser.id	sample.layer	H$_2$O, wt%	TOC, wt%
217	bx105	6	surface	NA	NA
218	bx105	2	surface	NA	NA
219	bx105	2	surface	9.86	NA
220	bx105	2	surface	11.53	NA
221	bx105	2	surface	13.76	NA
222	bx105	2	surface	7.24	NA
223	bx105	2	surface	13.43	NA
225	bx107	NA	sub-surface	55.95	0.0500000
226	bx107	3	sub-surface	48.70	NA
227	bx107	NA	sub-surface	53.70	0.0730000
228	bx107	3	sub-surface	35.20	NA
229	bx107	7	sub-surface	54.68	NA
230	bx107	7	sub-surface	51.40	NA
231	bx107	7	sub-surface	54.70	NA
232	bx107	NA	sub-surface	NA	0.0700000
233	bx107	3	sub-surface	48.72	NA
234	bx107	7	sub-surface	50.80	NA
235	bx107	7	sub-surface	54.90	NA
236	bx107	NA	sub-surface	NA	0.0796000
237	bx107	7	sub-surface	55.15	NA
238	bx107	3	sub-surface	52.50	NA
239	bx107	7	sub-surface	55.20	NA
240	bx107	3	sub-surface	55.90	NA
241	bx107	3	sub-surface	56.00	NA
242	bx107	7	sub-surface	48.80	NA
243	bx107	3	sub-surface	49.10	NA
244	bx107	3	sub-surface	34.00	NA
245	bx107	3	sub-surface	50.16	NA
246	bx107	7	sub-surface	NA	0.0700000

#	tank.id	riser.id	sample.layer	H$_2$O, wt%	TOC, wt%
247	bx107	NA	sub-surface	NA	0.0700000
248	bx107	3	sub-surface	54.30	NA
249	bx107	7	sub-surface	50.40	NA
250	bx107	7	sub-surface	52.90	NA
251	bx107	3	sub-surface	54.10	NA
252	bx107	7	sub-surface	51.20	NA
253	bx107	3	sub-surface	50.70	NA
254	bx107	3	sub-surface	56.00	NA
255	bx107	7	sub-surface	50.80	NA
256	bx107	3	sub-surface	27.90	NA
257	bx107	NA	sub-surface	NA	0.0550000
258	bx107	NA	sub-surface	NA	0.0550000
259	bx107	NA	sub-surface	NA	0.0550000
260	bx107	7	sub-surface	53.40	NA
261	bx107	3	sub-surface	50.34	NA
262	bx107	NA	sub-surface	49.60	0.0550000
263	bx107	3	sub-surface	56.89	NA
264	bx107	7	sub-surface	44.30	NA
265	bx107	7	sub-surface	43.00	NA
266	bx107	3	sub-surface	38.40	NA
267	bx107	7	sub-surface	46.20	NA
268	bx107	3	sub-surface	39.40	NA
269	bx107	3	sub-surface	39.60	NA
271	bx107	3	sub-surface	66.30	NA
272	bx107	3	sub-surface	56.80	NA
273	bx107	7	sub-surface	56.60	NA
274	bx107	7	sub-surface	56.20	NA
275	bx107	7	sub-surface	56.90	NA
276	bx107	7	sub-surface	57.30	NA

#	tank.id	riser.id	sample.layer	H_2O, wt%	TOC, wt%
277	bx107	3	sub-surface	44.00	NA
278	bx107	7	sub-surface	57.50	NA
279	bx107	7	sub-surface	58.00	NA
280	bx107	7	sub-surface	43.70	NA
281	bx107	7	sub-surface	43.00	NA
282	bx107	7	sub-surface	57.70	NA
283	bx107	3	sub-surface	NA	0.0997000
284	bx107	7	sub-surface	63.70	NA
285	bx107	NA	sub-surface	52.50	0.0897000
286	bx107	7	sub-surface	46.00	NA
287	bx107	7	sub-surface	56.20	NA
288	bx107	7	sub-surface	63.30	NA
289	bx107	7	sub-surface	56.50	NA
290	bx107	7	sub-surface	45.00	NA
291	bx107	3	sub-surface	61.80	NA
292	bx107	3	sub-surface	36.40	NA
293	bx107	7	sub-surface	56.30	NA
294	bx107	7	sub-surface	56.30	NA
295	bx107	3	sub-surface	56.30	NA
296	bx107	7	sub-surface	44.30	NA
297	bx107	7	sub-surface	56.40	NA
298	bx108	2	surface	52.78	NA
299	bx108	6	surface	9.19	NA
300	bx108	2	surface	51.80	NA
301	bx108	6	surface	4.74	NA
302	bx108	6	surface	4.57	NA
303	bx108	6	surface	4.42	NA
304	bx108	6	surface	3.29	NA
305	bx108	6	surface	6.59	NA

#	tank.id	riser.id	sample.layer	H₂O, wt%	TOC, wt%
307	bx110	6	surface	NA	0.3470000
308	bx110	NA	sub-surface	51.90	0.0169000
309	bx110	3	surface	NA	0.4100000
310	bx110	3	surface	10.42	NA
312	bx110	6	surface	45.22	NA
313	bx110	NA	sub-surface	NA	0.0700000
314	bx110	6	surface	NA	0.3480000
315	bx110	3	surface	NA	0.3890000
316	bx110	6	surface	43.67	NA
318	bx111	NA	sub-surface	51.90	0.0600000
320	bx112	NA	sub-surface	57.47	0.1220000
321	bx112	NA	sub-surface	57.47	0.8930000
324	by103	12a	surface	11.63	NA
325	by103	12a	surface	19.49	NA
327	by103	10b	surface	14.06	NA
328	by103	10b	surface	33.59	NA
335	by106	NA	sub-surface	26.83	0.1860000
336	by106	NA	sub-surface	10.15	0.0123000
337	by106	NA	sub-surface	11.57	0.1050000
338	by106	NA	sub-surface	32.20	0.2280000
340	by106	NA	sub-surface	25.39	0.1700000
341	by106	NA	sub-surface	20.47	0.0823000
342	by106	NA	sub-surface	18.01	0.0948000
343	by106	NA	sub-surface	43.45	0.3020000
344	by106	NA	sub-surface	18.38	0.0403000
345	by106	NA	sub-surface	14.94	0.0464000
346	by106	NA	sub-surface	12.26	0.0111000
347	by106	NA	sub-surface	17.65	0.0940000
348	by106	NA	sub-surface	15.64	0.0898000

#	tank.id	riser.id	sample.layer	H$_2$O, wt%	TOC, wt%
349	by106	NA	sub-surface	17.41	0.0674000
350	by106	NA	sub-surface	14.37	0.0733000
351	by106	NA	sub-surface	14.24	0.0994000
353	by106	NA	sub-surface	47.26	0.2280000
355	by106	NA	sub-surface	14.24	0.1200000
358	by106	NA	sub-surface	38.31	0.2310000
359	by106	NA	sub-surface	27.76	0.1220000
360	by106	NA	sub-surface	NA	1.9200000
362	by106	NA	sub-surface	25.62	0.4410000
363	by106	NA	sub-surface	NA	1.9900000
364	by106	NA	sub-surface	38.01	2.0800000
365	by106	NA	sub-surface	36.62	2.1700000
366	by106	NA	sub-surface	21.07	0.4180000
367	by106	NA	sub-surface	46.65	0.2310000
368	by106	NA	sub-surface	43.17	0.2860000
369	by106	NA	sub-surface	20.10	0.1340000
375	c101	8	surface	10.46	NA
377	c101	8	surface	21.80	NA
378	c101	8	surface	33.63	NA
380	c101	8	surface	23.35	NA
382	c101	8	surface	34.20	NA
383	c101	8	surface	20.40	NA
385	c103	2	sub-surface	51.26	NA
386	c103	2	sub-surface	NA	1.0700000
387	c103	2	sub-surface	49.75	NA
389	c103	2	sub-surface	43.23	NA
392	c103	7	sub-surface	76.46	NA
394	c103	7	sub-surface	79.15	NA
395	c103	2	sub-surface	30.82	NA

#	tank.id	riser.id	sample.layer	H₂O, wt%	TOC, wt%
398	c103	7	sub-surface	73.49	NA
400	c103	2	sub-surface	54.05	NA
401	c103	2	sub-surface	56.63	NA
402	c103	7	sub-surface	69.13	NA
404	c103	2	sub-surface	63.09	NA
410	c103	2	sub-surface	61.30	NA
411	c103	2	sub-surface	44.04	NA
413	c103	7	sub-surface	NA	0.9930000
414	c103	2	sub-surface	27.20	NA
416	c103	NA	sub-surface	NA	0.3900000
420	c103	2	sub-surface	26.37	NA
423	c103	2	sub-surface	25.00	NA
428	c103	2	sub-surface	25.30	NA
429	c103	2	sub-surface	NA	0.9790000
432	c103	NA	sub-surface	NA	0.2630000
436	c103	2	sub-surface	NA	0.4360000
439	c103	2	sub-surface	NA	0.9330000
440	c103	7	sub-surface	NA	0.9050000
441	c103	2	sub-surface	NA	0.8940000
442	c103	2	sub-surface	NA	0.8860000
443	c103	7	sub-surface	NA	0.8760000
444	c103	2	sub-surface	NA	0.4650000
445	c103	2	sub-surface	NA	0.7340000
446	c103	7	sub-surface	NA	0.8460000
448	c103	2	sub-surface	13.47	NA
451	c103	2	sub-surface	NA	0.7650000
454	c103	2	sub-surface	NA	0.7850000
456	c104	NA	sub-surface	NA	0.4410000
457	c105	2	sub-surface	NA	0.5400000

#	tank.id	riser.id	sample.layer	H$_2$O, wt%	TOC, wt%
458	c105	NA	sub-surface	NA	0.0999000
460	c105	2	sub-surface	14.05	NA
461	c105	2	surface	33.28	NA
466	c105	2	sub-surface	NA	0.5460000
467	c105	2	sub-surface	NA	0.6700000
469	c105	8	sub-surface	20.56	NA
470	c105	2	sub-surface	36.54	NA
471	c105	2	surface	36.59	NA
472	c105	8	surface	41.64	NA
474	c105	8	surface	42.75	NA
476	c105	2	sub-surface	NA	0.6760000
478	c105	2	sub-surface	12.91	NA
479	c105	2	sub-surface	19.48	NA
480	c105	2	sub-surface	21.04	NA
482	c105	8	sub-surface	30.71	NA
483	c105	2	sub-surface	37.88	NA
484	c105	8	sub-surface	21.54	NA
486	c105	8	sub-surface	12.50	NA
487	c106	NA	sub-surface	NA	0.0800000
489	c106	NA	sub-surface	NA	0.4620000
491	c108	3	surface	NA	0.3400000
492	c108	7	surface	NA	0.1840000
493	c108	3	surface	22.10	NA
494	c108	3	surface	NA	0.3550000
495	c108	4	surface	NA	0.0923000
496	c108	4	surface	52.97	NA
497	c108	4	surface	52.41	NA
498	c108	4	surface	48.57	NA
499	c108	7	surface	15.35	NA

#	tank.id	riser.id	sample.layer	H₂O, wt%	TOC, wt%
500	c108	4	surface	51.85	NA
501	c108	NA	surface	NA	0.1460000
502	c108	7	surface	46.28	NA
503	c108	7	surface	45.76	NA
504	c108	4	surface	50.45	NA
505	c108	7	surface	27.66	NA
506	c108	7	surface	NA	0.0188000
507	c108	4	surface	46.80	NA
508	c108	NA	surface	NA	0.1270000
509	c108	3	surface	19.90	NA
510	c108	4	surface	NA	0.0805000
511	c108	7	surface	39.15	NA
512	c108	7	surface	NA	0.0379000
513	c108	7	surface	NA	0.1540000
514	c108	7	surface	32.97	NA
515	c108	NA	surface	NA	0.0493000
516	c108	4	surface	49.23	NA
517	c108	4	surface	NA	0.0758000
518	c108	NA	surface	NA	0.1770000
519	c108	4	surface	47.79	NA
520	c108	4	surface	NA	0.1130000
521	c109	6	surface	NA	0.2000000
522	c109	7	sub-surface	57.70	NA
523	c109	8	surface	19.60	NA
524	c109	7	surface	NA	0.3200000
525	c109	NA	sub-surface	NA	0.3300000
526	c109	6	sub-surface	NA	0.3300000
527	c109	6	sub-surface	NA	0.2150000
528	c109	NA	sub-surface	NA	0.2100000

#	tank.id	riser.id	sample.layer	H$_2$O, wt%	TOC, wt%
529	c109	7	surface	NA	0.3100000
530	c109	6	surface	NA	0.2100000
531	c109	7	sub-surface	NA	0.2830000
533	c109	6	surface	NA	0.2200000
534	c109	6	surface	28.40	NA
535	c109	8	surface	NA	0.2300000
536	c109	NA	sub-surface	NA	0.3000000
537	c109	8	surface	38.30	NA
538	c109	7	surface	52.80	NA
539	c109	6	surface	19.30	NA
540	c109	8	surface	NA	0.1900000
541	c109	8	sub-surface	NA	0.2440000
542	c109	7	surface	51.60	NA
543	c109	8	surface	NA	0.2500000
544	c109	8	sub-surface	NA	0.2800000
545	c109	7	sub-surface	NA	0.3000000
546	c109	7	surface	NA	0.3800000
547	c109	NA	sub-surface	NA	0.2900000
548	c109	6	sub-surface	21.50	NA
549	c109	NA	sub-surface	NA	0.3000000
550	c109	6	surface	39.40	NA
551	c109	8	surface	39.60	NA
552	c109	NA	sub-surface	NA	0.2800000
553	c109	8	sub-surface	27.80	NA
554	c110	2	sub-surface	57.20	NA
555	c110	2	sub-surface	55.30	NA
556	c110	5	sub-surface	56.80	NA
557	c110	2	sub-surface	55.30	NA
558	c110	5	sub-surface	NA	0.1047000

#	tank.id	riser.id	sample.layer	H$_2$O, wt%	TOC, wt%
559	c110	2	sub-surface	56.60	NA
560	c110	7	sub-surface	65.24	NA
561	c110	NA	sub-surface	NA	0.1050000
563	c110	7	sub-surface	62.00	NA
564	c110	7	sub-surface	61.90	NA
567	c110	2	sub-surface	62.70	NA
568	c110	2	sub-surface	60.90	NA
569	c110	5	sub-surface	50.60	NA
570	c110	2	sub-surface	60.80	NA
571	c110	7	surface	62.50	NA
572	c110	5	sub-surface	50.40	NA
573	c110	2	sub-surface	61.90	NA
575	c110	2	sub-surface	60.40	NA
576	c110	2	sub-surface	60.40	NA
577	c110	5	sub-surface	50.10	NA
578	c110	5	sub-surface	60.40	NA
579	c110	2	sub-surface	60.30	NA
580	c110	2	sub-surface	49.30	NA
581	c110	5	sub-surface	59.60	NA
582	c110	5	sub-surface	59.80	NA
583	c110	7	surface	59.80	NA
584	c110	7	sub-surface	50.51	NA
585	c110	7	sub-surface	53.80	NA
586	c110	7	surface	54.20	NA
587	c110	5	sub-surface	NA	0.1090000
588	c110	5	sub-surface	NA	0.1090000
589	c110	7	sub-surface	64.50	NA
590	c110	5	sub-surface	61.10	NA
592	c110	7	sub-surface	62.50	NA

#	tank.id	riser.id	sample.layer	H$_2$O, wt%	TOC, wt%
593	c110	5	sub-surface	57.60	NA
595	c110	NA	sub-surface	NA	0.0528000
596	c110	NA	sub-surface	NA	0.0500000
597	c110	2	sub-surface	53.20	NA
598	c110	2	sub-surface	NA	0.0528000
599	c110	2	sub-surface	48.60	NA
602	c110	2	sub-surface	52.60	NA
603	c110	5	sub-surface	57.80	NA
604	c110	NA	sub-surface	NA	0.1090000
605	c111	6	surface	NA	0.1220000
606	c111	6	surface	44.74	0.1220000
607	c111	6	surface	NA	0.0893000
608	c111	6	surface	44.25	0.0893000
609	c111	6	surface	NA	0.1280000
610	c111	6	surface	44.25	NA
611	c111	6	surface	44.23	NA
612	c111	6	surface	44.74	NA
614	c111	6	surface	44.23	0.0909000
615	c111	6	surface	NA	0.0909000
616	c111	6	surface	38.58	0.1280000
617	c111	6	surface	NA	0.0709000
618	c111	6	surface	NA	0.0738000
619	c111	6	surface	28.01	0.0639000
620	c111	6	surface	38.58	NA
621	c111	6	surface	28.24	0.0724000
622	c111	6	surface	28.24	NA
623	c111	6	surface	NA	0.0724000
624	c111	6	surface	28.01	NA
625	c111	6	surface	30.80	NA

#	tank.id	riser.id	sample.layer	H$_2$O, wt%	TOC, wt%
626	c111	2	surface	35.50	NA
627	c111	6	surface	NA	0.0639000
628	c111	2	surface	26.54	NA
630	c111	6	surface	32.50	NA
631	c112	2	sub-surface	NA	0.3200000
632	c112	2	sub-surface	NA	0.3200000
633	c112	8	sub-surface	NA	0.3800000
634	c112	2	sub-surface	NA	0.3200000
636	c112	NA	sub-surface	NA	0.3200000
637	c112	NA	sub-surface	NA	0.2200000
638	c112	2	sub-surface	NA	0.3800000
639	c112	8	sub-surface	NA	0.2100000
640	c112	NA	sub-surface	45.00	0.1400000
642	c112	8	sub-surface	NA	0.1600000
643	c112	8	surface	NA	0.5000000
644	c112	NA	surface	45.00	0.4900000
645	c112	NA	surface	58.00	0.4900000
646	c112	NA	sub-surface	53.00	0.3000000
648	c112	NA	sub-surface	58.00	0.3100000
649	c112	2	surface	NA	0.5900000
650	c112	7	sub-surface	NA	0.1300000
651	c112	NA	sub-surface	52.00	0.4000000
652	c112	NA	sub-surface	57.00	0.3900000
653	c112	8	sub-surface	NA	0.3900000
654	c112	8	sub-surface	NA	0.1100000
656	c112	8	surface	NA	0.4800000
657	c112	7	sub-surface	NA	0.1000000
658	c112	NA	sub-surface	64.00	0.2900000
659	c112	8	sub-surface	NA	0.2500000

#	tank.id	riser.id	sample.layer	H$_2$O, wt%	TOC, wt%
660	c112	NA	surface	49.00	0.8200000
661	c112	8	sub-surface	NA	0.3000000
662	c112	8	sub-surface	NA	0.3100000
663	c112	NA	sub-surface	38.00	0.3100000
664	c112	NA	sub-surface	34.00	0.2500000
665	c112	NA	sub-surface	NA	0.2900000
666	c112	7	sub-surface	NA	0.2900000
667	c112	NA	sub-surface	56.00	0.2300000
668	c112	8	sub-surface	NA	0.2800000
669	c112	8	surface	NA	0.8600000
670	c112	2	sub-surface	NA	0.3050000
671	c112	NA	sub-surface	41.00	0.2700000
672	c112	8	surface	NA	0.7700000
673	c112	8	sub-surface	NA	0.2700000
674	c112	8	sub-surface	NA	0.2700000
676	c112	8	sub-surface	NA	0.3000000
679	s104	2	surface	9.10	NA
680	s104	3	sub-surface	50.10	NA
681	s104	2	surface	7.66	NA
684	s104	7	sub-surface	33.80	0.1190000
686	s104	2	sub-surface	20.50	NA
690	s104	7	sub-surface	17.99	NA
693	s104	3	sub-surface	35.60	0.2380000
694	s104	7	sub-surface	NA	0.1090000
695	s104	2	sub-surface	NA	0.1100000
696	s104	NA	sub-surface	55.70	0.0677000
698	s104	7	sub-surface	53.80	NA
700	s104	NA	sub-surface	54.30	0.0600000
701	s104	2	sub-surface	53.10	NA

#	tank.id	riser.id	sample.layer	H$_2$O, wt%	TOC, wt%
702	s104	2	sub-surface	37.80	0.1100000
703	s104	2	sub-surface	58.10	NA
705	s104	NA	sub-surface	55.10	0.0517000
706	s104	7	sub-surface	52.40	NA
708	s104	7	sub-surface	31.60	0.1140000
709	s104	NA	sub-surface	NA	0.1090000
710	s104	2	sub-surface	24.90	NA
711	s104	7	sub-surface	26.30	NA
712	s104	2	sub-surface	24.20	NA
713	s104	7	sub-surface	25.60	NA
714	s104	3	sub-surface	34.50	NA
715	s104	3	sub-surface	25.50	NA
716	s104	7	sub-surface	34.60	NA
717	s104	7	sub-surface	34.70	NA
718	s104	2	sub-surface	25.30	NA
719	s104	2	sub-surface	25.20	NA
720	s104	7	sub-surface	34.90	NA
721	s104	2	sub-surface	34.90	NA
722	s104	3	sub-surface	36.20	NA
723	s104	2	sub-surface	35.20	NA
724	s104	3	sub-surface	33.90	NA
725	s104	2	sub-surface	24.90	NA
726	s104	3	sub-surface	35.20	NA
727	s104	2	sub-surface	35.50	NA
728	s104	2	sub-surface	36.20	NA
729	s104	2	surface	36.20	NA
730	s104	3	sub-surface	36.20	NA
731	s104	7	sub-surface	36.30	NA
732	s104	2	sub-surface	37.10	NA

#	tank.id	riser.id	sample.layer	H_2O, wt%	TOC, wt%
733	s104	2	sub-surface	37.20	NA
734	s104	2	sub-surface	37.70	NA
735	s104	2	sub-surface	37.80	NA
736	s104	2	sub-surface	38.30	NA
737	s104	2	sub-surface	38.30	NA
738	s104	3	sub-surface	34.90	NA
739	s104	7	sub-surface	30.80	NA
740	s104	7	sub-surface	28.50	NA
741	s104	7	sub-surface	28.60	NA
742	s104	7	sub-surface	29.30	NA
743	s104	7	sub-surface	29.40	NA
744	s104	3	sub-surface	29.50	NA
745	s104	3	sub-surface	29.60	NA
746	s104	2	surface	29.70	NA
747	s104	7	sub-surface	29.70	NA
748	s104	7	sub-surface	30.00	NA
749	s104	7	sub-surface	30.30	NA
750	s104	3	sub-surface	30.32	NA
751	s104	2	sub-surface	25.70	NA
752	s104	3	sub-surface	30.60	NA
753	s104	7	sub-surface	26.30	NA
754	s104	7	sub-surface	30.80	NA
755	s104	7	surface	31.10	NA
756	s104	2	sub-surface	31.60	NA
757	s104	3	sub-surface	31.60	NA
758	s104	2	sub-surface	80.30	NA
759	s104	2	sub-surface	31.90	NA
760	s104	7	surface	32.00	NA
761	s104	7	sub-surface	32.80	NA

#	tank.id	riser.id	sample.layer	H$_2$O, wt%	TOC, wt%
762	s104	3	sub-surface	27.10	NA
763	s104	7	sub-surface	26.40	NA
764	s104	3	sub-surface	33.40	NA
765	s104	7	sub-surface	33.50	NA
766	s104	7	sub-surface	33.90	NA
767	s104	2	sub-surface	30.40	NA
768	s104	7	surface	42.90	NA
769	s104	NA	sub-surface	NA	0.2060000
770	s104	3	sub-surface	38.50	NA
771	s104	2	sub-surface	64.60	NA
772	s104	NA	sub-surface	NA	0.2190000
773	s104	3	sub-surface	42.80	NA
774	s104	2	sub-surface	23.70	NA
775	s104	7	sub-surface	29.00	0.2210000
776	s104	3	sub-surface	NA	0.2380000
777	s104	7	surface	44.20	NA
778	s104	7	sub-surface	42.30	NA
779	s104	2	surface	67.00	NA
780	s104	3	sub-surface	43.30	NA
781	s104	3	sub-surface	43.30	NA
782	s104	7	surface	43.40	NA
783	s104	2	sub-surface	43.90	NA
784	s104	3	surface	43.40	NA
785	s104	7	sub-surface	29.30	0.2350000
786	s104	3	surface	43.50	NA
787	s104	7	sub-surface	22.90	NA
788	s104	3	sub-surface	24.70	0.2280000
789	s104	3	sub-surface	35.00	0.1300000
790	s104	3	sub-surface	NA	0.1300000

#	tank.id	riser.id	sample.layer	H_2O, wt%	TOC, wt%
791	s104	3	surface	39.30	NA
792	s104	3	surface	40.60	NA
793	s104	3	sub-surface	NA	0.1300000
794	s104	3	sub-surface	23.80	NA
795	s104	7	surface	44.80	NA
796	s104	2	sub-surface	23.70	NA
797	s104	7	sub-surface	NA	0.2060000
798	s104	3	sub-surface	20.90	NA
799	s104	3	sub-surface	21.60	NA
800	s104	7	sub-surface	41.30	NA
801	s104	2	surface	63.30	NA
802	s104	2	sub-surface	41.30	NA
803	s104	3	sub-surface	45.00	NA
804	s104	7	sub-surface	41.60	NA
805	s104	7	sub-surface	41.60	NA
806	s104	3	sub-surface	42.00	NA
807	s104	3	sub-surface	42.30	NA
812	s109	NA	sub-surface	NA	0.0470000
813	s109	NA	sub-surface	NA	0.0470000
815	s111	NA	sub-surface	18.10	2.3352778
817	s111	NA	sub-surface	10.70	0.1015748
819	s111	NA	sub-surface	17.40	1.5400000
825	sx102	NA	surface	NA	0.8167203
826	sx102	NA	sub-surface	NA	0.1980000
831	sx113	7	surface	52.11	NA
832	sx113	6	surface	47.77	NA
833	sx113	6	surface	37.15	NA
834	sx113	6	surface	46.81	NA
835	sx113	7	surface	53.80	NA

#	tank.id	riser.id	sample.layer	H₂O, wt%	TOC, wt%
836	sx113	7	surface	46.07	NA
837	sx113	6	surface	46.41	NA
838	sx113	7	surface	42.71	NA
840	t102	2	sub-surface	NA	0.0680000
841	t102	2	sub-surface	NA	0.0660000
842	t104	3	sub-surface	41.10	NA
843	t104	3	surface	40.90	NA
844	t104	3	sub-surface	70.10	NA
845	t104	3	sub-surface	48.70	NA
846	t104	3	sub-surface	42.70	NA
847	t104	3	sub-surface	43.80	NA
848	t104	3	surface	9.52	NA
849	t104	3	sub-surface	40.60	NA
850	t104	3	surface	9.72	NA
851	t104	3	sub-surface	48.60	NA
852	t104	6	sub-surface	69.80	NA
853	t104	6	sub-surface	68.90	NA
854	t104	3	sub-surface	70.30	NA
855	t104	3	sub-surface	69.30	NA
856	t104	6	sub-surface	69.40	NA
857	t104	3	sub-surface	69.50	NA
858	t104	6	sub-surface	70.30	NA
859	t104	6	sub-surface	69.70	NA
860	t104	6	sub-surface	68.80	NA
861	t104	3	sub-surface	NA	0.0706000
862	t104	6	sub-surface	69.90	NA
863	t104	6	sub-surface	70.10	NA
864	t104	3	sub-surface	70.10	NA
865	t104	3	sub-surface	70.10	NA

#	tank.id	riser.id	sample.layer	H$_2$O, wt%	TOC, wt%
866	t104	3	sub-surface	70.10	NA
867	t104	6	sub-surface	70.10	NA
868	t104	6	sub-surface	65.10	NA
869	t104	6	sub-surface	69.70	NA
870	t104	3	sub-surface	67.00	NA
871	t104	3	sub-surface	65.10	NA
872	t104	3	sub-surface	65.50	NA
873	t104	6	sub-surface	66.30	NA
874	t104	3	sub-surface	66.30	NA
875	t104	6	sub-surface	66.40	NA
876	t104	6	sub-surface	69.00	NA
877	t104	6	sub-surface	67.00	NA
878	t104	6	sub-surface	68.80	NA
879	t104	3	sub-surface	67.20	NA
880	t104	6	sub-surface	67.40	NA
881	t104	6	sub-surface	67.60	NA
882	t104	6	sub-surface	68.10	NA
883	t104	6	sub-surface	68.30	NA
884	t104	6	sub-surface	68.40	NA
885	t104	3	sub-surface	68.50	NA
886	t104	3	sub-surface	68.70	NA
887	t104	3	sub-surface	66.90	NA
888	t104	6	sub-surface	73.62	NA
889	t104	3	sub-surface	70.20	NA
890	t104	NA	sub-surface	NA	0.0100000
891	t104	3	sub-surface	72.50	NA
892	t104	3	sub-surface	72.50	NA
893	t104	6	sub-surface	73.10	NA
894	t104	3	sub-surface	71.50	NA

#	tank.id	riser.id	sample.layer	H$_2$O, wt%	TOC, wt%
895	t104	6	sub-surface	73.60	NA
896	t104	3	sub-surface	71.50	NA
897	t104	6	sub-surface	73.90	NA
898	t104	6	sub-surface	74.70	NA
899	t104	6	sub-surface	76.30	NA
903	t104	NA	surface	62.20	0.2900000
904	t104	6	sub-surface	69.90	NA
905	t104	6	sub-surface	73.30	NA
906	t104	6	sub-surface	70.90	NA
907	t104	3	sub-surface	70.40	NA
908	t104	6	sub-surface	70.40	NA
909	t104	3	sub-surface	70.40	NA
910	t104	3	sub-surface	70.40	NA
911	t104	3	sub-surface	70.50	NA
912	t104	3	sub-surface	70.60	NA
914	t104	6	sub-surface	70.90	NA
915	t104	6	sub-surface	70.60	NA
916	t104	3	sub-surface	71.00	NA
917	t104	NA	sub-surface	NA	0.0760000
918	t104	6	sub-surface	71.00	NA
919	t104	NA	sub-surface	NA	0.0760000
920	t104	3	sub-surface	71.10	NA
921	t104	6	sub-surface	71.10	NA
922	t104	3	sub-surface	71.40	NA
923	t104	6	sub-surface	71.40	NA
924	t104	6	sub-surface	70.80	NA
925	t104	6	sub-surface	51.60	NA
926	t104	6	sub-surface	60.70	NA
927	t104	3	sub-surface	60.50	NA

#	tank.id	riser.id	sample.layer	H$_2$O, wt%	TOC, wt%
928	t104	3	sub-surface	58.10	NA
929	t104	NA	sub-surface	NA	0.0550000
930	t104	6	sub-surface	57.20	NA
931	t104	3	sub-surface	60.20	NA
932	t104	3	surface	54.50	NA
933	t104	6	sub-surface	59.70	NA
934	t104	3	sub-surface	54.20	NA
935	t104	3	sub-surface	59.60	NA
936	t104	6	sub-surface	60.40	NA
937	t104	NA	sub-surface	NA	0.0550000
938	t104	6	sub-surface	55.40	NA
939	t104	3	sub-surface	52.70	NA
940	t104	6	sub-surface	58.90	NA
941	t104	NA	sub-surface	NA	0.0550000
942	t104	3	sub-surface	52.50	NA
943	t104	3	sub-surface	52.90	NA
944	t104	3	sub-surface	56.10	NA
945	t104	3	sub-surface	57.70	NA
946	t104	3	sub-surface	57.50	NA
947	t104	3	sub-surface	54.50	NA
948	t104	6	sub-surface	63.60	NA
949	t104	3	sub-surface	64.80	NA
950	t104	3	sub-surface	64.90	NA
951	t104	6	sub-surface	64.50	NA
952	t104	6	sub-surface	64.40	NA
953	t104	3	sub-surface	64.20	NA
954	t104	3	sub-surface	64.20	NA
955	t104	3	sub-surface	64.00	NA
956	t104	3	sub-surface	63.90	NA

#	tank.id	riser.id	sample.layer	H₂O, wt%	TOC, wt%
957	t104	6	sub-surface	60.20	NA
958	t104	3	sub-surface	63.60	NA
959	t104	6	sub-surface	61.00	NA
960	t104	6	sub-surface	53.70	NA
961	t104	3	sub-surface	53.80	NA
962	t104	6	sub-surface	61.60	NA
963	t104	6	sub-surface	61.90	NA
964	t104	6	sub-surface	63.90	NA
965	t104	6	sub-surface	70.80	NA
966	t104	3	sub-surface	62.50	NA
967	t104	6	sub-surface	62.50	NA
968	t104	6	sub-surface	62.60	NA
969	t104	3	sub-surface	62.70	NA
970	t105	NA	surface	NA	0.0528000
972	t105	NA	surface	NA	0.2620000
973	t105	2	surface	NA	0.2440000
974	t105	5	sub-surface	NA	0.1630000
976	t105·	5	surface	NA	0.5180000
978	t105	2	surface	NA	0.3892308
980	t105	8	surface	NA	0.4290000
981	t105	8·	surface	51.97	NA
982	t105	8	sub-surface	NA	0.4130000
983	t106	3	surface	14.45	NA
984	t106	3	surface	18.56	NA
985	t106	3	surface	15.62	NA
986	t106	5	surface	23.28	NA
987	t106	3	surface	20.49	NA
988	t106	5	surface	14.59	NA
989	t106	3	surface	18.38	NA

#	tank.id	riser.id	sample.layer	H₂O, wt%	TOC, wt%
990	t106	5	surface	14.18	NA
991	t106	3	surface	14.27	NA
992	t106	5	surface	22.57	NA
993	t106	3	surface	19.39	NA
994	t106	3	surface	19.91	NA
995	t106	3	surface	17.83	NA
996	t106	5	surface	21.24	NA
997	t106	5	surface	11.85	NA
998	t106	5	surface	12.06	NA
999	t106	5	surface	17.48	NA
1000	t106	3	surface	14.08	NA
1001	t107	NA	sub-surface	NA	0.1690000
1002	t107	NA	surface	75.30	0.1950000
1003	t107	NA	sub-surface	95.60	0.1100000
1004	t107	3	sub-surface	NA	0.1920000
1005	t107	2	surface	5.65	NA
1006	t107	NA	sub-surface	16.70	0.0970000
1007	t107	5	sub-surface	NA	0.1350000
1008	t107	NA	surface	5.76	0.0505000
1009	t107	NA	sub-surface	60.20	0.1270000
1010	t107	5	sub-surface	NA	0.1200000
1011	t107	5	sub-surface	NA	0.1230000
1012	t107	NA	sub-surface	18.00	0.0655000
1013	t107	NA	sub-surface	51.90	0.1440000
1014	t107	2	sub-surface	29.60	NA
1015	t107	2	surface	27.00	NA
1016	t107	3	sub-surface	NA	0.0270000
1017	t107	NA	sub-surface	55.00	0.0270000
1018	t107	2	surface	25.40	NA

#	tank.id	riser.id	sample.layer	H₂O, wt%	TOC, wt%
1019	t107	NA	sub-surface	51.40	0.0265000
1020	t107	NA	sub-surface	52.90	0.0265000
1021	t107	3	sub-surface	49.70	NA
1023	t107	2	surface	5.87	NA
1024	t107	5	sub-surface	NA	0.0240000
1025	t107	3	surface	NA	0.2000000
1026	t107	2	sub-surface	29.90	NA
1027	t107	NA	sub-surface	95.60	0.1100000
1030	t107	3	sub-surface	NA	0.0310000
1032	t107	NA	sub-surface	47.80	0.0320000
1035	t107	NA	sub-surface	49.50	0.0400000
1036	t107	5	sub-surface	NA	0.0280000
1037	t107	5	sub-surface	58.50	NA
1038	t107	5	sub-surface	54.60	NA
1039	t107	3	sub-surface	54.60	NA
1040	t107	3	sub-surface	54.60	NA
1041	t107	5	sub-surface	54.80	NA
1042	t107	3	sub-surface	54.80	NA
1045	t107	3	sub-surface	55.40	NA
1046	t107	3	sub-surface	55.60	NA
1047	t107	2	sub-surface	40.30	NA
1048	t107	5	sub-surface	54.30	NA
1049	t107	3	sub-surface	57.70	NA
1050	t107	NA	sub-surface	48.50	0.0685000
1051	t107	3	surface	15.30	NA
1052	t107	2	sub-surface	59.00	NA
1053	t107	3	sub-surface	59.30	NA
1054	t107	5	sub-surface	59.40	NA
1055	t107	3	surface	15.20	NA

#	tank.id	riser.id	sample.layer	H₂O, wt%	TOC, wt%
1056	t107	2	sub-surface	NA	0.0710000
1057	t107	5	sub-surface	59.90	NA
1058	t107	2	sub-surface	42.10	NA
1059	t107	5	sub-surface	60.10	NA
1060	t107	2	sub-surface	45.80	NA
1062	t107	2	sub-surface	44.40	NA
1063	t107	2	sub-surface	57.20	NA
1064	t107	NA	sub-surface	55.10	0.0905000
1065	t107	5	sub-surface	54.20	NA
1066	t107	5	sub-surface	52.80	NA
1069	t107	5	sub-surface	NA	0.0410000
1071	t107	NA	sub-surface	55.10	0.0905000
1072	t107	3	sub-surface	NA	0.0650000
1074	t107	5	sub-surface	53.40	NA
1075	t107	3	sub-surface	NA	0.0910000
1077	t107	5	sub-surface	NA	0.1000000
1078	t107	2	surface	NA	0.0500000
1080	t108	5	surface	0.77	NA
1081	t108	5	surface	1.12	NA
1082	t108	2	surface	1.68	NA
1083	t108	5	surface	2.48	NA
1084	t108	2	surface	19.66	NA
1085	t108	5	surface	2.43	NA
1086	t108	2	surface	38.68	NA
1087	t108	5	surface	0.54	NA
1088	t108	5	surface	0.83	NA
1089	t108	2	surface	35.93	NA
1090	t108	2	surface	24.44	NA
1091	t108	5	surface	0.56	NA

#	tank.id	riser.id	sample.layer	H₂O, wt%	TOC, wt%
1092	t108	2	surface	39.36	NA
1093	t108	5	surface	4.32	NA
1094	t111	NA	sub-surface	NA	0.3300000
1095	t111	NA	sub-surface	NA	0.3680000
1096	t111	6	sub-surface	NA	0.3300000
1097	t111	NA	sub-surface	NA	0.3000000
1098	t111	NA	sub-surface	NA	0.2000000
1099	t111	6	sub-surface	NA	0.4120000
1100	t111	NA	sub-surface	NA	0.4120000
1101	t111	3	sub-surface	NA	0.3000000
1102	t111	3	sub-surface	81.00	NA
1103	t111	3	sub-surface	NA	0.2000000
1104	t111	NA	sub-surface	NA	0.3850000
1105	t111	3	sub-surface	80.50	NA
1106	t111	6	sub-surface	69.20	NA
1107	t111	3	surface	79.60	NA
1108	t111	6	surface	79.80	NA
1109	t111	3	sub-surface	80.40	NA
1110	t111	3	sub-surface	79.30	NA
1111	t111	6	sub-surface	75.90	NA
1112	t111	3	sub-surface	79.30	NA
1113	t111	3	sub-surface	80.60	NA
1114	t111	3	sub-surface	77.20	NA
1115	t111	6	sub-surface	52.60	NA
1116	t111	3	sub-surface	77.80	NA
1117	t111	3	surface	81.10	NA
1118	t111	6	sub-surface	74.80	NA
1119	t111	3	sub-surface	68.60	NA
1120	t111	6	sub-surface	75.90	NA

#	tank.id	riser.id	sample.layer	H$_2$O, wt%	TOC, wt%
1121	t111	6	sub-surface	78.40	NA
1122	t111	3	surface	77.80	NA
1123	t111	6	sub-surface	59.60	NA
1124	t111	6	sub-surface	77.20	NA
1125	t111	3	sub-surface	77.00	NA
1126	t111	3	sub-surface	77.00	NA
1127	t111	6	sub-surface	76.40	NA
1128	t111	3	sub-surface	78.30	NA
1129	t111	6	surface	80.80	NA
1131	t111	3	sub-surface	78.60	NA
1132	t111	3	sub-surface	81.70	NA
1133	t111	6	sub-surface	76.90	NA
1134	t111	6	sub-surface	76.70	NA
1135	t111	3	sub-surface	78.60	NA
1136	t111	6	sub-surface	76.40	NA
1137	t111	6	sub-surface	61.30	NA
1138	t111	3	sub-surface	84.70	NA
1139	t111	3	sub-surface	74.90	NA
1140	t111	6	sub-surface	72.10	NA
1141	t111	6	sub-surface	74.40	NA
1142	t111	6	sub-surface	74.70	NA
1143	t111	3	sub-surface	82.20	NA
1144	t111	6	sub-surface	72.00	NA
1145	t111	6	sub-surface	84.40	NA
1146	t111	3	sub-surface	84.00	NA
1147	t111	3	sub-surface	83.00	NA
1148	t111	3	sub-surface	74.70	NA
1149	t111	6	sub-surface	69.50	NA
1150	t111	6	sub-surface	71.20	NA

#	tank.id	riser.id	sample.layer	H₂O, wt%	TOC, wt%
1151	t111	6	sub-surface	71.20	NA
1152	t111	6	sub-surface	71.00	NA
1153	t111	3	sub-surface	84.80	NA
1157	tx102	NA	surface	44.51	0.1908714
1173	tx118	NA	surface	NA	1.0600000
1178	ty101	NA	sub-surface	NA	0.0663000
1180	ty102	NA	surface	58.00	0.2360000
1181	ty102	NA	sub-surface	NA	0.0327000
1182	ty103	NA	surface	52.67	0.1100000
1184	ty103	NA	sub-surface	NA	0.0715000
1185	ty103	NA	sub-surface	51.20	0.1490000
1186	ty104	NA	sub-surface	55.50	0.0907000
1187	ty104	15	surface	51.67	NA
1188	ty104	NA	sub-surface	NA	0.2780000
1189	ty104	15	surface	NA	0.0826000
1190	ty104	NA	sub-surface	51.00	0.2100000
1191	ty104	15	surface	51.42	NA
1192	ty104	18	surface	NA	0.0895000
1193	ty104	18	surface	49.95	NA
1194	ty104	NA	surface	NA	0.4000000
1195	ty104	18	surface	NA	0.6520000
1196	ty104	18	surface	NA	0.6520000
1197	ty104	15	surface	49.75	NA
1198	ty104	18	surface	NA	0.0774000
1199	ty104	15	surface	NA	0.5510000
1200	ty104	15	surface	NA	0.6940000
1201	ty104	15	surface	NA	0.0971000
1204	ty104	15	surface	55.23	NA
1205	ty104	NA	sub-surface	NA	0.1950000

#	tank.id	riser.id	sample.layer	H$_2$O, wt%	TOC, wt%
1206	ty104	18	surface	53.23	NA
1207	ty104	NA	surface	52.73	0.0600000
1209	ty105	NA	sub-surface	39.40	0.0805000
1210	ty106	6	surface	39.16	NA
1211	ty106	6	surface	39.18	NA
1212	ty106	NA	sub-surface	39.20	0.0780000
1213	ty106	NA	sub-surface	NA	0.2480000
1214	ty106	6	surface	37.17	NA
1215	ty106	NA	surface	35.50	0.0920000
1216	ty106	NA	sub-surface	NA	0.2090000
1217	ty106	6	surface	32.20	NA
1218	ty106	NA	sub-surface	39.20	0.1700000
1219	ty106	7	surface	30.28	NA
1220	ty106	7	surface	30.80	NA
1221	u103	NA	sub-surface	8.70	0.6862857
1222	u105	NA	surface	20.80	2.7500000
1223	u105	NA	sub-surface	NA	2.7500000
1226	u110	NA	sub-surface	26.90	0.0653000
1227	u110	NA	sub-surface	42.64	0.0540000
1228	u110	NA	sub-surface	37.27	0.1110000
1229	u110	NA	sub-surface	37.30	0.0693000
1230	u110	NA	sub-surface	44.36	0.0715000
1231	u110	NA	sub-surface	39.06	0.0713000
1232	u110	NA	sub-surface	39.06	0.0554000
1233	u110	NA	sub-surface	42.98	0.0708000
1234	u110	NA	sub-surface	29.10	0.0599000
1235	u110	NA	sub-surface	38.50	0.0726000
1236	u110	NA	surface	5.59	0.0494000
1237	u110	NA	surface	8.04	0.0828000

#	tank.id	riser.id	sample.layer	H_2O, wt%	TOC, wt%
1238	u110	NA	surface	8.73	0.0878000
1239	u110	NA	sub-surface	34.50	0.1610000
1240	u110	NA	sub-surface	39.10	0.1100000
1241	u110	NA	surface	3.08	0.0605000
1242	u110	NA	sub-surface	39.04	0.0734000
1243	u110	NA	sub-surface	37.30	0.1100000
1244	u110	NA	sub-surface	44.10	0.0898000
1245	u110	NA	surface	4.16	0.0740000
1246	u110	NA	sub-surface	38.80	0.0859000
1247	u110	NA	sub-surface	37.30	0.1410000
1248	u110	NA	sub-surface	43.18	0.0409000
1249	u110	NA	surface	4.75	0.0361000
1250	u110	NA	sub-surface	42.51	0.0352000
1251	u110	NA	sub-surface	39.20	0.0530000
1252	u110	NA	sub-surface	42.50	0.6750000
1253	u110	NA	sub-surface	38.19	0.0794000
1254	u110	NA	sub-surface	46.78	0.0785000
1255	u110	NA	sub-surface	42.50	0.6750000
1256	u110	NA	sub-surface	43.60	0.0779000
1257	u110	NA	sub-surface	40.60	0.6430000
1258	u110	NA	sub-surface	44.68	0.0896000
1259	u111	NA	surface	NA	0.5400000
1260	u111	NA	surface	39.12	0.5200000
1262	b201	7	sub-surface	31.90	NA
1263	b201	7	sub-surface	54.20	NA
1264	b201	2	sub-surface	NA	0.0470000
1265	b201	7	sub-surface	NA	0.0300000
1266	b201	2	sub-surface	NA	0.1900000
1267	b201	7	sub-surface	NA	0.0660000

#	tank.id	riser.id	sample.layer	H$_2$O, wt%	TOC, wt%
1268	b201	7	sub-surface	52.90	NA
1269	b201	2	sub-surface	NA	0.4000000
1270	b201	7	sub-surface	68.60	NA
1271	b201	7	surface	67.70	NA
1272	b201	2	sub-surface	NA	0.4200000
1273	b201	7	sub-surface	53.40	NA
1274	b201	7	sub-surface	35.40	NA
1275	b201	7	sub-surface	35.30	NA
1276	b201	7	sub-surface	NA	0.0760000
1277	b201	7	sub-surface	74.70	NA
1278	b201	7	sub-surface	60.20	NA
1279	b201	7	sub-surface	19.40	NA
1280	b201	7	sub-surface	28.10	NA
1281	b201	7	sub-surface	NA	0.0600000
1282	b201	7	sub-surface	15.50	NA
1283	b201	7	surface	65.40	NA
1284	b202	NA	sub-surface	NA	0.2200000
1285	b202	2	sub-surface	NA	0.2200000
1286	b202	5	surface	62.66	NA
1287	b202	NA	sub-surface	NA	0.2200000
1288	b202	5	sub-surface	78.65	NA
1289	b202	2	sub-surface	64.90	NA
1290	b202	NA	sub-surface	NA	0.1900000
1291	b202	5	sub-surface	83.09	NA
1292	b202	NA	sub-surface	NA	0.2300000
1293	b202	5	sub-surface	NA	0.2100000
1294	b202	5	sub-surface	NA	0.2300000
1295	b202	5	sub-surface	NA	NA
1296	b202	5	sub-surface	84.40	NA

#	tank.id	riser.id	sample.layer	H₂O, wt%	TOC, wt%
1297	b202	5	sub-surface	63.10	NA
1298	b202	5	sub-surface	67.10	NA
1300	b202	2	sub-surface	NA	NA
1301	b202	5	surface	63.70	NA
1302	b202	2	sub-surface	63.04	NA
1303	b202	5	sub-surface	NA	0.3800000
1304	b202	2	sub-surface	74.60	NA
1305	b202	2	sub-surface	70.34	NA
1306	b202	2	sub-surface	74.70	NA
1307	b202	5	sub-surface	NA	0.3650000
1308	b202	NA	sub-surface	NA	0.3650000
1309	b202	2	sub-surface	74.70	NA
1310	b202	2	sub-surface	NA	0.3770000
1311	b202	NA	sub-surface	NA	0.3770000
1312	b202	5	sub-surface	77.30	NA
1313	b202	2	sub-surface	NA	0.1900000
1314	b202	2	sub-surface	67.30	NA
1315	b202	2	sub-surface	74.81	NA
1316	b202	NA	sub-surface	NA	0.3360000
1317	b202	NA	sub-surface	NA	0.3800000
1318	b202	2	sub-surface	74.81	NA
1319	b202	5	sub-surface	77.18	NA
1321	b202	2	sub-surface	76.66	NA
1322	b202	5	sub-surface	74.97	NA
1323	b202	5	sub-surface	75.35	NA
1324	b202	2	sub-surface	75.40	NA
1325	b202	2	sub-surface	75.50	NA
1326	b202	2	sub-surface	75.60	NA
1327	b202	2	sub-surface	75.60	NA

#	tank.id	riser.id	sample.layer	H_2O, wt%	TOC, wt%
1328	b202	2	sub-surface	75.98	NA
1329	b202	5	surface	76.02	NA
1330	b202	2	sub-surface	35.20	NA
1331	b202	5	sub-surface	72.61	NA
1332	b202	2	sub-surface	68.70	NA
1333	b202	2	sub-surface	80.90	NA
1334	b202	2	sub-surface	41.60	NA
1335	b202	2	sub-surface	80.10	NA
1336	b202	5	sub-surface	80.04	NA
1337	b202	5	sub-surface	78.69	NA
1338	b202	5	sub-surface	71.48	NA
1339	b202	5	sub-surface	71.60	NA
1340	b202	5	sub-surface	71.60	NA
1341	b202	2	sub-surface	71.99	NA
1342	b202	5	sub-surface	74.63	NA
1343	b202	2	sub-surface	37.13	NA
1344	b202	5	sub-surface	NA	0.3360000
1345	b202	5	sub-surface	78.29	NA
1346	b202	5	sub-surface	72.90	NA
1347	b202	2	sub-surface	73.10	NA
1348	b202	5	sub-surface	78.20	NA
1349	b202	2	sub-surface	78.00	NA
1350	b202	5	sub-surface	73.99	NA
1351	b202	5	sub-surface	74.10	NA
1352	b202	2	sub-surface	74.10	NA
1353	b202	5	surface	74.20	NA
1354	b202	5	sub-surface	77.97	NA
1355	b202	5	sub-surface	77.73	NA
1356	b202	2	sub-surface	74.40	NA

#	tank.id	riser.id	sample.layer	H_2O, wt%	TOC, wt%
1357	b202	5	sub-surface	77.30	NA
1358	b202	5	sub-surface	37.60	NA
1359	b202	5	sub-surface	52.30	NA
1361	b202	2	sub-surface	13.70	NA
1363	b202	NA	sub-surface	NA	0.1900000
1365	b202	2	sub-surface	56.75	NA
1366	b202	2	sub-surface	14.66	NA
1367	b202	2	sub-surface	57.22	NA
1368	b202	2	sub-surface	10.97	NA
1369	b202	5	sub-surface	60.00	NA
1370	b204	NA	sub-surface	NA	0.1011368
1371	c201	7	surface	10.69	3.7700000
1372	c201	7	surface	10.53	4.1000000
1373	c201	7	surface	11.46	4.5700000
1374	c202	7w	surface	6.49	NA
1375	c202	7e	surface	4.88	NA
1376	c202	7e	surface	5.39	NA
1377	c202	7w	surface	6.96	NA
1378	c203	7e	surface	30.98	NA
1379	c203	7e	surface	31.78	NA
1380	c203	7w	surface	49.03	NA
1381	c203	7e	surface	33.26	NA
1382	c203	7w	surface	52.12	NA
1383	c203	7e	surface	41.04	NA
1384	c203	7w	surface	36.66	NA
1385	c203	7w	surface	33.67	NA
1386	c204	7	surface	NA	9.1800000
1387	c204	7	surface	NA	13.0000000
1388	c204	7	surface	NA	1.3800000

#	tank.id	riser.id	sample.layer	H_2O, wt%	TOC, wt%
1389	c204	7	surface	NA	14.8000000
1390	t204	NA	sub-surface	73.00	0.6734579
1392	u201	6	surface	35.74	NA
1394	u201	6	surface	36.29	NA
1397	u201	6	sub-surface	38.99	NA
1398	u201	6	sub-surface	33.80	NA
1403	u202	2	sub-surface	36.24	NA
1406	u202	2	surface	26.24	NA
1407	u202	2	surface	25.49	NA
1409	u202	2	surface	18.90	NA
1410	u202	2	sub-surface	24.43	NA
1411	u202	2	surface	24.11	NA
1412	u202	2	sub-surface	23.96	NA
1414	u202	2	sub-surface	22.90	NA
1415	u202	2	sub-surface	22.87	NA
1416	u202	2	surface	22.24	NA
1419	u202	2	sub-surface	38.71	NA
1420	u202	2	sub-surface	41.50	NA
1421	u202	2	sub-surface	43.64	NA
1422	u202	2	surface	24.45	NA
1423	u203	6	surface	31.51	NA
1424	u203	6	surface	24.50	NA
1425	u203	6	surface	22.94	NA
1426	u203	6	surface	33.25	NA
1427	u204	6	surface	NA	0.0120000
1429	u204	2	surface	29.12	0.0800000
1431	u204	2	surface	NA	0.0807000
1434	u204	2	surface	NA	0.0823000
1437	u204	6	surface	21.84	NA

#	tank.id	riser.id	sample.layer	H_2O, wt%	TOC, wt%
1438	u204	6	surface	24.18	0.0120000
1439	u204	6	surface	NA	0.0128000
1440	u204	6	surface	21.84	0.0128000
1441	u204	6	surface	24.18	NA
1442	u204	2	surface	29.56	NA
1446	u204	2	surface	29.12	NA
1447	u204	2	surface	29.56	0.0823000

A.4.0 ORGANIZATION OF CALCULATIONS

The calculations are performed within a package called Splus and include a library of Splus functions, which are called by command files. Because the software is developed within the Splus data analysis package, it is easily modified. Consequently, several variants of this software are being used in the Organics project for various side calculations. This documentation refers to one version of the software, Version **Reynolds**. This identifier is simply the name of the directory containing the command files.

The calculations are produced by running 5 command files in the sequence listed below:

1.input: This inputs all required data into Splus.

2.anova.h2o: This performs the ANOVA fits on the moisture data.

2.anova.toc: This performs the ANOVA fits on the TOC data.

3.correlations: This calculates the correlations between the H_2O and TOC ANOVA residuals.

4.tank.summary: This merges TOC and H_2O ANOVA results into a single table suitable for the combustible waste calculations.

5.state.space: This calculates the uncertainty distributions for combustible waste using a Monte Carlo simulation.

The uncertainty distributions on combustible waste are the fundamental output of these calculations. However, it should be noted that many intermediate results are calculated and are available to the user in the Splus working directory. This documentation does not attempt to describe these intermediate results in detail.

A.5.0 OUTPUT DATA

The principal result of these calculations is a file that contains current and dry combustible waste fractions. For each combustible waste fraction, two estimates are given, the "best estimate" which is the median from the uncertainty distribution, and an upper 95% confidence bound, which is the 95% quantile from the uncertainty distribution. The estimates of most immediate concern for the risk analysis are the 95% bounds.

TABLE A-2. COMBUSTIBLE WASTE OUTPUT DATA

Tank No.	Waste Volume (m³)	Combustible Fraction (50% Est, wet)	Combustible Fraction (95% Est, wet)	Combustible Fraction (50% Est, dry)	Combustible Fraction (95% Est, dry)
A-101	3607	9.61E-07	0.00015214	0.000263181	0.005471661
A-102	155	5.16E-06	0.0008218	0.001373322	0.033642968
A-103	1404	5.90E-07	0.000164355	0.000481381	0.010728451
A-104	106	1.33E-07	0.000622649	6.26E-05	0.013847014
A-105	72	2.90E-08	0.000485607	3.55E-05	0.033946969
A-106	473	8.77E-07	0.000352622	0.000449947	0.01123701
AX-101	2831	5.07E-08	0.000236291	2.25E-05	0.007539763
AX-102	148	0.001819523	0.026541025	0.082154989	0.278904125
AX-103	424	7.83E-08	0.000420728	4.06E-05	0.004116791
AX-104	26	2.24E-08	0.000380467	2.97E-05	0.022945602
B-101	428	6.29E-08	0.000436709	4.02E-05	0.009012786
B-102	121	5.41E-07	0.001313564	7.85E-05	0.020275575
B-103	223	7.52E-14	7.19E-10	1.55E-09	2.35E-06
B-104	1404	6.11E-14	5.60E-09	3.99E-09	1.72E-05
B-105	1158	5.61E-08	0.000166287	2.32E-05	0.005537089
B-106	443	8.11E-11	3.34E-06	1.45E-07	0.00012682
B-107	625	2.36E-12	4.14E-07	1.51E-08	6.70E-05
B-108	356	8.55E-11	4.61E-06	2.38E-07	0.000878584
B-109	481	4.68E-11	2.95E-06	1.24E-07	0.000200233
B-110	931	5.92E-17	5.17E-11	4.55E-12	9.33E-09
B-111	897	1.68E-12	7.58E-09	8.06E-09	2.50E-06
B-112	125	1.77E-11	3.28E-07	1.76E-07	0.000439469
B-201	110	1.99E-11	9.77E-07	3.76E-08	0.000161958
B-202	102	7.42E-12	5.10E-07	5.73E-08	0.000107291
B-203	193	9.80E-12	4.54E-07	4.62E-08	8.10E-05
B-204	189	6.07E-12	4.91E-07	3.93E-08	7.01E-05
BX101	163	8.57E-10	1.89E-05	4.24E-07	0.000594426
BX-102	363	6.94E-11	4.72E-06	2.03E-07	0.00037519
BX-103	257	3.75E-12	1.12E-07	1.07E-07	0.001991838

Tank No.	Waste Volume (m³)	Combustible Fraction (50% Est, wet)	Combustible Fraction (95% Est, wet)	Combustible Fraction (50% Est, dry)	Combustible Fraction (95% Est, dry)
BX-104	363	1.93E-08	2.54E-05	2.15E-05	0.001541724
BX-105	193	1.36E-08	3.12E-05	1.27E-06	0.004556989
BX-106	174	2.87E-11	3.17E-06	1.92E-07	0.003272717
BX-107	1306	1.24E-14	6.26E-10	1.71E-10	2.04E-07
BX-108	98	9.24E-11	4.19E-06	3.82E-08	0.002125805
BX-109	731	5.32E-08	0.000243474	3.77E-05	0.008553825
BX-110	783	1.30E-10	9.00E-08	6.80E-08	6.18E-06
BX-111	613	1.78E-10	1.05E-06	1.58E-07	0.00101796
BX-112	625	8.90E-10	4.83E-06	4.82E-06	0.003859455
BY-112	1465	9.28E-08	0.000141196	2.94E-05	0.003859455
BY-102	1048	9.29E-08	0.000213895	3.21E-05	0.006405585
BY-103	1514	2.43E-07	0.00030695	3.31E-05	0.001053587
BY-104	1537	8.51E-08	0.000168439	.3.17E-05	0.009920771
BY-105	1904	5.77E-08	0.000215235	2.74E-05	0.001081765
BY-106	2430	3.25E-09	1.38E-06	7.57E-07	3.62E-05
BY-107	1007	7.19E-08	0.000176926	3.23E-05	0.001623011
BY-108	863	1.14E-07	0.000452707	3.42E-05	0.009648538
BY-109	161	7.09E-08	0.00020639	3.11E-05	0.00801857
BY-110	1506	4.82E-08	0.000294665	2.79E-05	0.00641854
BY-111	1737	6.12E-08	0.000217619	2.97E-05	0.006615516
BY-112	1101	6.38E-08	0.000234141	3.01E-05	0.007386385
C-101	333	1.91E-07	0.000350966	6.70E-05	0.011885672
C-102	1196	4.41E-08	0.00012182	2.21E-05	0.004910553
C-103	738	1.25E-07	0.000328797	0.000227004	0.009832012
C-104	1117	1.65E-07	7.74E-05	8.56E-05	0.003615411
C-105	511	3.84E-08	1.47E-05	2.00E-05	0.001061979
C-106	867	2.01E-09	3.57E-06	3.91E-06	0.000749267
C-107	897	6.25E-08	0.000181375	3.40E-05	0.005924789
C-108	250	7.24E-12	3.76E-09	3.05E-08	2.94E-06
C-109	235	2.66E-09	1.67E-07	6.87E-06	7.69E-05
C-110	670	3.54E-14	7.19E-10	5.96E-09	3.36E-06
C-111	216	3.29E-13	3.52E-09	3.21E-09	1.74E-06
C-112	394	2.79E-09	2.40E-07	2.18E-05	0.002859856
S-101	1616	1.49E-07	0.000370533	4.82E-05	0.005341905
S-102	2078	5.74E-08	0.000216755	2.15E-05	0.005379307
S-103	939	2.85E-07	0.000330618	5.82E-05	0.008703919
S-104	1113	5.96E-12	1.27E-08	5.83E-08	9.25E-06
S-105	1726	6.26E-08	0.000164019	2.38E-05	0.005570106
S-106	1813	2.19E-07	0.000362032	3.86E-05	0.005471729

Tank No.	Waste Volume (m³)	Combustible Fraction (50% Est, wet)	Combustible Fraction (95% Est, wet)	Combustible Fraction (50% Est, dry)	Combustible Fraction (95% Est, dry)
S-107	1423	1.39E-08	5.54E-05	2.22E-05	0.006755398
S-108	2286	5.60E-08	0.000174379	1.93E-05	0.005154502
S-109	2150	5.89E-12	6.65E-08	6.64E-09	3.67E-06
S-110	1476	9.20E-08	0.000360826	2.37E-05	0.00594553
S-111	2256	6.41E-05	0.001570459	0.001205011	0.011281114
S-112	1980	7.47E-08	0.000154787	2.62E-05	3.00E+16
SX-101	1726	2.26E+00	0.000626	3.39E+00	0.00902
SX-102	2055	4.45E-07	7.87E-05	3.41E-05	0.00907109
SX-103	2468	4.23E-08	0.000167228	2.01E-05	0.005312744
SX-104	2324	1.91E-07	0.0002937	2.95E-05	0.005240872
SX-105	2585	1.74E-07	0.00028907	2.53E-05	0.009526875
SX-106	2036	2.26E-07	0.000374	3.48E-05	0.004743229
SX-107	394	3.60E-11	1.99E-06	1.32E-07	0.004544771
SX-108	329	6.28E-11	1.97E-06	1.93E-07	0.004117578
SX-109	924	8.06E-08	0.000273458	4.62E-05	0.005715409
SX-110	235	6.89E-11	2.58E-06	1.78E-07	0.003754536
SX-111	473	7.60E-11	1.99E-06	1.27E-07	0.002032169
SX-112	348	4.74E-11	3.08E-06	1.96E-07	0.005888691
SX-113	98	1.19E-11	9.76E-07	1.37E-07	0.003344418
SX-114	685	4.11E-11	3.02E-06	1.12E-07	0.0027756
SX-115	45	1.07E-11	3.69E-06	4.94E-08	0.008420116
T-101	386	5.81E-11	2.22E-06	1.65E-07	8.68E-05
T-102	121	1.00E-12	2.69E-07	6.31E-09	2.26E-05
T-103	102	3.53E-11	3.80E-06	1.40E-07	0.000921809
T-104	1684	1.00E-14	3.91E-11	2.45E-10	1.28E-07
T-105	371	1.97E-10	1.10E-07	8.27E-07	2.39E-05
T-106	79	6.57E-10	2.95E-05	1.15E-07	0.001902965
T-107	655	2.22E-12	8.61E-10	1.02E-09	9.83E-08
T-108	167	2.81E-08	0.000160526	6.69E-07	0.000567356
T-109	220	1.30E-10	3.53E-06	2.27E-07	0.000153819
T-110	1435	1.55E-08	5.88E-05	1.50E-05	0.005852415
T-111	1688	1.78E-11	1.26E-08	3.74E-06	0.000337559
T-112	254	1.87E-12	3.07E-07	1.69E-08	9.79E-05
T-201	110	2.05E-11	1.51E-06	7.62E-08	0.000385959
T-202	79	5.10E-11	1.58E-06	8.51E-08	0.000252548
T-203	132	3.34E-11	2.83E-06	5.60E-08	0.000238859
T-204	144	1.94E-11	1.47E-06	5.41E-08	8.09E-05
TX-101	329	8.90E-08	0.000251317	6.05E-05	0.018588031
TX-102	821	4.21E-10	8.99E-07	1.50E-06	0.002076066

Tank No.	Waste Volume (m³)	Combustible Fraction (50% Est. wet)	Combustible Fraction (95% Est. wet)	Combustible Fraction (50% Est. dry)	Combustible Fraction (95% Est. dry)
TX-103	594	4.15E-11	1.53E-06	1.79E-07	0.002967337
TX-104	246	7.06E-08	0.000258997	6.38E-05	0.013552725
TX-105	2305	2.08E-08	8.12E-05	2.51E-05	0.008200344
TX-106	1715	5.19E-08	0.000182932	1.94E-05	0.001250269
TX-107	136	1.08E-07	0.000696449	7.58E-05	0.020744716
TX-108	507	7.79E-08	0.000161642	3.65E-05	3.65315797
TX-109	1453	4.66E+00	0.000148079	3.22E+00	0.00413
TX-110	1749	2.59E-08	0.000140525	1.65E-05	0.001209832
TX-111	1400	3.31E-08	0.000139595	2.01E-05	0.002552611
TX-112	2456	2.29E-08	6.66E-05	2.04E-05	0.004571219
TX-113	2297	3.22E-08	9.70E-05	1.63E-05	0.00709281
TX-114	2025	2.25E-08	5.72E-05	2.01E-05	0.004023461
TX-115	2422	3.12E-08	6.57E-05	2.13E-05	0.005863646
TX-116	2388	3.97E-08	7.21E-05	1.44E-05	0.005656652
TX-117	2369	1.56E-08	0.000101349	1.47E-05	0.004003695
TX-118	1313	1.01E-06	0.000331558	0.000200857	0.008574575
TY-101	447	3.60E-12	5.97E-08	9.33E-09	9.81E-06
TY-102	242	4.45E-12	7.84E-09	6.53E-08	1.37E-05
TY-103	613	1.26E-12	5.06E-09	2.45E-08	4.26E-06
TY-104	174	1.57E-11	3.63E-09	5.65E-07	1.50E-05
TY-105	874	1.62E-10	6.92E-07	4.51E-07	0.000357615
TY-106	64	4.00E-11	6.65E-08	1.47E-07	3.91E-05
U-101	95	1.67E-11	4.08E-06	9.37E-08	0.000810161
U-102	1416	1.41E-08	0.000113226	2.39E-05	0.006391953
U-103	1771	3.29E-05	0.002687207	0.00050957	0.01448096
U-104	462	6.74E-08	0.0001706	3.61E-05	0.009064336
U-105	1582	0.00058337	0.016236071	0.012856246	0.126621606
U-106	855	3.57E-07	0.000523435	4.23E-05	0.005754748
U-107	1537	3.34E-07	0.000283894	3.55E-05	0.006767966
U-108	1771	1.96E-07	0.00034276	3.23E-05	0.00557904
U-109	1752	2.39E-07	0.000403793	4.00E-05	0.006009354
U-110	704	2.14E-11	2.97E-09	1.50E-09	3.17E-08
U-111	1245	7.02E-08	2.78E-05	3.65E-05	0.002801074
U-112	185	2.96E-11	2.83E-06	1.66E-07	0.00043996
U-201	19	2.50E-11	5.19E-06	1.45E-07	0.00065029
U-202	19	3.09E-11	4.12E-06	1.92E-07	0.000877741
U-203	11	3.68E-11	6.18E-06	1.74E-07	0.000798753
U-204	11	2.60E-11	4.26E-06	2.42E-07	0.00040764

A.6.0 REFERENCES

Agnew, S. F., 1996, *History of Organic Carbon in Hanford HLW Tanks: HDW Model, Rev. 3*, LA-UR-96-989, Los Alamos National Laboratory, Los Alamos, New Mexico.

Chambers J. M., and T. J. Hastie, 1992, *Statistical Models in S*, Wadsworth, 1992.

Corbeil, R. R., and S. R. Searle, 1976, *Restricted Maximum Likelihood (REML) Estimation of Variance Components in the Mixed Model*, Technometrics, vol. 18, pp. 31-38.

Dempster A. P., D. B. Rubin, and R. K. Tsutakawa, 1981, *Estimation in Covariance Components Models*, JASA Vol 76, # 374, p. 341.

S-PLUS Reference Manual, 1991, Statistical Sciences, Inc., Seattle, Washington.

This page intentionally left blank.

APPENDIX B

ORGANIC-NITRATE COMBUSTION MODEL (ORNATE)

This page intentionally left blank.

TABLE OF CONTENTS

TABLE OF CONTENTS (Continued)

LIST OF FIGURES

LIST OF TABLES

APPENDIX B

ORGANIC-NITRATE COMBUSTION MODEL (ORNATE)

B.1 SUMMARY

A mechanistic model of organic-nitrate reactions initiated in hypothetically reactive waste in Hanford underground storage tanks is presented here. The model considers experimental data for the type of waste that can sustain a propagating reaction and the reaction rate. It also contains a thermal-hydraulic assessment of tank transient pressure and temperature to yield flows of gases to the environment, a release model to predict vaporization of volatile materials from reacted waste, and an aerosol transport and deposition model to provide the source term to the environment. The various phenomena models are integrated in a computer program called ORNATE (ORganic-NitrATE).

Reactions are modeled as if initiated on the waste surface and propagating with given velocities on the surface and normal to the surface (into the waste) yielding a conical reacting wavefront. A surrogate reaction of sodium acetate with sodium nitrate, with tank-specific fuel and moisture estimates, is used to model the post-reaction waste temperature and gaseous products. Major gaseous products include steam, nitrogen, and carbon dioxide. Toxic and radioactive species are released as minor gaseous products and include sodium hydroxide, cesium hydroxide, technetium oxide, and antimony. Most elements (strontium, transuranics) are highly involatile under the oxidizing conditions.

Example cases are selected in accord with a more broad risk assessment structure which requires hypothetical consequences of various reacting volumes corresponding to threshold events. HEPA failure and dome collapse are the two primary threshold events, and cases are defined so that just enough reactive waste exists to achieve these states. The reactive volume predicted by this model will be used by another part of the risk assessment to assess the probability of the scenario, and the consequences predicted by this model will be used by another part of the risk assessment in conjunction with the probability to define risk. Cases are also presented here for different reacted volumes to provide the basis for a finer-grain risk curve.

Tank pressure and temperature response is a slow but accelerating increase as the surface area of the reaction front grows. Since cases are defined by threshold reacting volumes, the pressure and temperature reach peaks when the volume is consumed and then quickly decline. Material release occurs during the entire time the tank pressure exceeds the ambient value. During depressurization, water fog formation causes aerosol fallout, and overall about half the vaporized material is retained within the tank. Generally, HEPA failure may be caused by a reacted volume on the order of a cubic meter, while dome collapse requires an order of magnitude greater volume. Tank response is sensitive to venting capacity: many tanks have riser covers that would lift early during an event, so that larger reacted volumes are required for a given damage level, but larger releases occur.

This page intentionally left blank.

B.2 SCOPE AND PURPOSE

A model for hypothetical organic-nitrate reactions in Hanford waste tanks is presented here commensurate with the current level of phenomenological understanding of these reactions and the potential for fission product release. The scope of this study includes:

- Brief review of the organic-nitrate experimental background,
- Modeling of the reaction·rate and fission product release rate,
- Modeling of tank response including aerosol behavior,
- Integration of models into a computer program, and
- Quantification of release potential for hypothetical cases.

Experimental data are used as the basis for the reaction rate, and these data are extrapolated to account for features not explicitly observed, such as propagation of a surface reaction. Chemical equilibrium is used to define releases because at the low propagation velocities mechanical aerosol formation mechanisms appear unimportant. A surrogate chemical reaction is used to define the temperature of the combustion products because the actual reactions that could take place in the tanks are unknown but likely bounded by the surrogate. Since the reaction product gases are highly oxidizing, the choice of surrogate does not affect calculated releases.

The purpose of this study is to provide a portion of a risk assessment of single shell tanks at Hanford. Thus the various phenomena models are integrated into a computer program called ORNATE (ORganic-NitrATE) for repeated application. Example cases are selected in this report in accord with the methodology of the larger study, and are designed to capture perceived distinct consequence thresholds. The ORNATE model is used in the larger study on a tank-by-tank basis to find: the volume reacted to achieve a given threshold (the larger study uses this to assess the probability of the scenario), and the amount of each toxic or radioactive compound released (the larger study uses this source term).

This page intentionally left blank.

B.3 ORGANIC-NITRATE REACTION PHENOMENA REVIEW

A brief review of the experimental background on organic-nitrate reactions pertinent to the Hanford waste tanks is presented here. For details of experiments and the criteria for propagation of a reaction, see (Fauske and Epstein, 1995; Fauske, 1996). No attempt is made here to describe Hanford waste constituents.

The reaction of concern is a self-sustaining, i.e., propagating reaction between dominant oxidizers present in the Hanford tanks (sodium nitrate, sodium nitrite, and sodium hydroxide) and organic salt fuels which were originally present as tetrasodium ethylenediamine tetraacetate (EDTA), trisodium hydroxyethlyenediamine triacetate (HEDTA), sodium citrate, sodium hydroxyacetate, and others. Such a reaction requires a high-energy initiator, but the characteristics or plausibilities of initiators are not considered here (they are considered in evaluating scenario probability). The real consitutents of Hanford waste tanks are more complex because more organic source materials and their aging products are involved, as are numerous trace species.

Experiments conducted with surrogate compounds have allowed definition of a composition criterion for a propagating reaction in terms of the fuel content (measured as TOC, or total organic carbon) and moisture content (which includes chemically bound water as well). Surrogate here refers to the fact that off-the-shelf mixtures of the species mentioned above were tested, rather than mixtures formed by simulating the chemical processes used to generate Hanford waste.

A conservative criterion for the fuel content required to sustain a propagating reaction in such mixtures is:

$$TOC (wt\%) > [4.5 + 0.17 (H_2O wt\%)] \tag{B-1}$$

where % TOC refers to the weight percent of carbon and % H_2O refers to the weight percent of water. In addition, it is impossible to sustain a reaction when

$$H_2O (wt\%) \geq 20 \tag{B-2}$$

even for stoichiometric mixtures. The criterion is illustrated in Figure B-1. Data points on this figure were taken using a propagation tube with a large, sustained ignition source.

Experiments were also conducted with small, limited duration ignition sources to explore the effects of initiator size and moisture content. A stoichiometric mixture of sodium acetate trihydrate could not be ignited by a 140 J electric match discharged over a 3-5 msec period. A free (not chemically bound) water content of 5% was sufficient to prevent ignition of other surrogates, leading to the conclusion that small amounts of free water are highly effective to prevent ignition from small sources.

When a reaction can propagate, the reaction products just behind the reaction boundary attain a high temperature which is essentially the adiabatic reaction temperature. Temperature histories measured by thermocouples placed at various distances from the ignition source in a propagation tube in Figure B-2 illustrate the progress of a propagating reaction and quantify the reaction temperature. A propagation velocity of about 0.33-0.6 mm/s and reaction temperatures between 700 and 1000°C are observed. The reacted waste itself is a fused solid because excess oxidizers melt during the reaction. Mechanical aerosol formation is not readily observed and believed to be negligible, a fact attributable to the slow propagation velocity.

It is noted here that the average composition of waste in the Hanford tanks is far too lean in fuel to support a propagating reaction even if the waste were dry, and further, most tanks currently contain too much moisture to allow a reaction. Thus two key issues are, the distribution of fuel in tanks and the loss of moisture from tanks; these issues are addressed by the larger risk study. Obviously, the only realistic scenarios for calculation are those with high enough fuel and low enough moisture to sustain a reaction. The larger risk study supplies these input composition values and keeps track of the probability of their existence.

Figure B-1. Comparison Between Measured TOC Values and
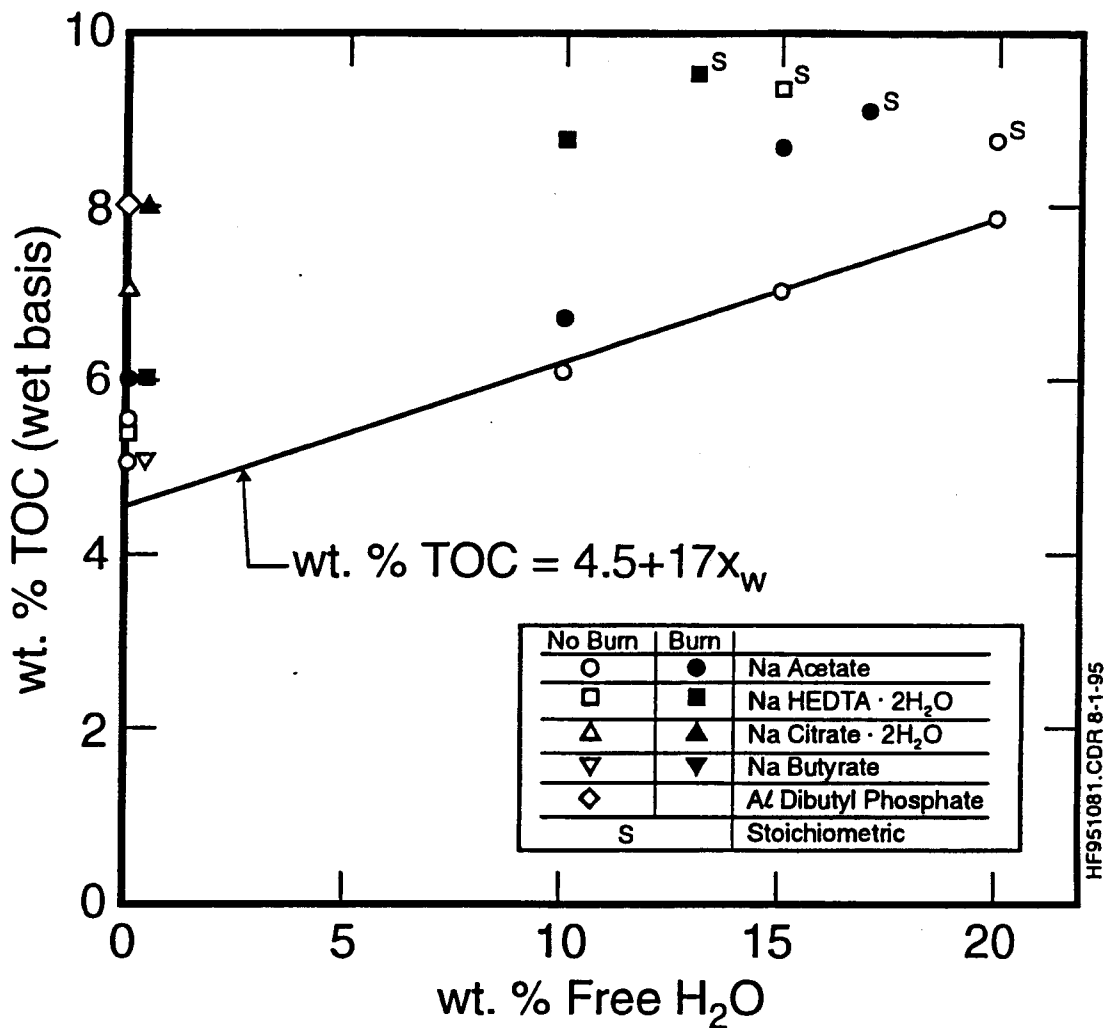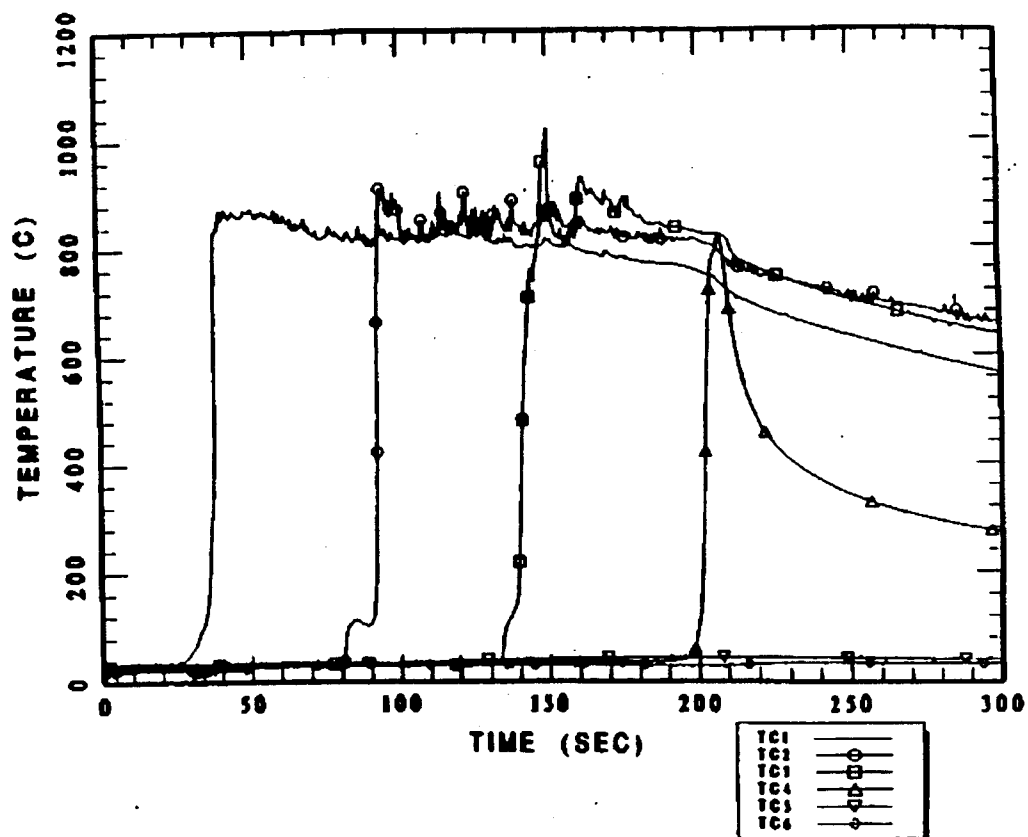the Proposed Safety Criteria

Figure B-2.   Illustration of Combustion Temperatures for a 28 wt%
NaAc (dry basis) With 15% Moisture (wet basis)

B.4 REACTION RATE AND RELEASE MODELS

B.4.1 REACTION RATE MODEL

B.4.1.1 Propagating Reaction Model

A surrogate reaction of sodium acetate with sodium nitrate models post-reaction waste temperature and gaseous products. Major gaseous products include steam, nitrogen, and carbon dioxide. Minor gaseous products include sodium hydroxide and cesium hydroxide. The reaction of sodium acetate with sodium nitrate is:

$$NaCH_3CO_2 + 1.6\,NaNO_3 \rightarrow 1.3\,NaCO_2 + 0.7\,CO_2 + 1.5\,H_2O + 0.8\,N_2 \quad \text{(B-3)}$$
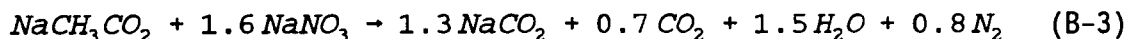
Release rates for major and minor products are proportional to the rate at which sodium acetate is consumed:

$$W_i = f_i\,\rho_s\,x_{ac}\frac{dV}{dt} \quad \text{(B-4)}$$

where the subscript i denotes any of the five species considered, f is a proportionality constant to be determined, ρ_s is the saltcake density, x_{ac} is the mass fraction of sodium acetate, and V is the volume of saltcake reacted as a function of time, t. The mass fraction of sodium acetate is expressed as a function of the known mass fraction of total organic carbon, x_{toc}:

$$x_{ac} = x_{toc}\frac{MW_{ac}}{2MW_c} \quad \text{(B-5)}$$

where MW_{ac} is the molecular weight of sodium acetate and MW_c is the molecular weight of carbon. Equation (B-1) yields f_i for nitrogen and carbon dioxide:

$$f_{N2} = 0.8\frac{MW_{N2}}{MW_{ac}} \quad \text{(B-6a)}$$

and

$$f_{CO2} = 0.7\frac{MW_{CO2}}{MW_{ac}} \quad \text{(B-6b)}$$

The proportionality constant for water must also take into account the mass fraction of water in the saltcake x_w, in addition to the water vapor generated by the reaction. Assuming the reaction front vaporizes all water:

$$f_{H2O} = 1.5\frac{MW_{H2O}}{MW_{ac}} + \frac{x_w}{x_{ac}} \quad \text{(B-7)}$$

Release rates for minor gaseous products (cesium hydroxide, sodium hydroxide, etc.) depend on their relative abundance in the saltcake and an airborne release fraction, e.g.,

$$f_{NaOH} = \frac{x_{Na}}{x_{ac}} RF_{Na} \qquad \text{(B-8)}$$

where x_{Na} is mass fraction of the dominant condensed phase sodium compound ($Na_2 CO_3$) and RF_{Na} is airborne release fraction.

To evaluate equation (B-4), the shape of the reaction front must be known. Reactions are modeled as if they start at the waste surface and propagate on the surface and normal to the surface. The two propagation velocities can differ. The resulting reaction front is a cone, or conic frustrum, depending on the time of the reaction and the thickness of the saltcake. Figure B-3 illustrates the reaction model.

Figure B-3 shows that the tip of the cone proceeds downward at the "bulk" propagation velocity, while the radius of the reaction front at the surface proceeds with a "surface" propagation velocity.

Figure B-3. Reaction Model Geometry
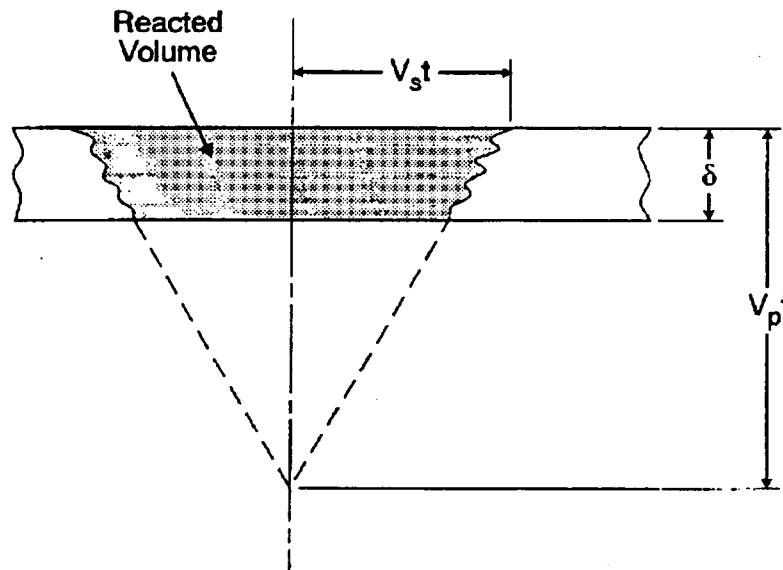
BM965101.CDR 5-21-96

If the tip of the cone has not penetrated the bottom of the saltcake, the volume of reacted waste is simply:

$$V = \frac{\pi}{3} R^2 h \qquad \text{(B-9)}$$

where R is the radius of the reaction front at the saltcake surface, and h is the distance from the surface to the tip of the cone. Cone radius R is related to the surface propagation velocity by,

$$R = R_o + V_s t \qquad \text{(B-10)}$$

and cone height is related to the bulk propagation velocity by,

$$h = R_o + V_p t \qquad \text{(B-11)}$$

where R_o is the initial radius. The initial radius is very small and quickly becomes negligible in relation to the cone radius or cone height. Then, substituting equations (B-10) and (B-11) into equation (B-9),

$$V = \frac{\pi}{3} V_s^2 V_p t^3 \qquad \text{(B-12)}$$

The rate of change with respect to time is:

$$\frac{dV}{dt} = \pi V_s^2 V_p t^2 \qquad \text{(B-13)}$$

If the tip of the cone has penetrated the entire saltcake thickness, the reacted volume is the difference in volume between two virtual cones, as shown in Figure B-3:

$$V = \frac{\pi}{3} V_s^2 V_p t^3 - \frac{\pi}{3} \left(\frac{V_s}{V_p}\right)^2 \left(V_p t - \delta\right)^3 \qquad \text{(B-14)}$$

In this instance, the rate of change with respect to time is:

$$\frac{dV}{dt} = \pi \frac{V_s^2}{V_p} \delta \left(2 V_p t - \delta\right) \qquad \text{(B-15)}$$

These expressions require two propagation velocities. Propagation tube tests demonstrate that the propagation velocity for a condensed phase sodium acetate-sodium nitrate/nitrite reaction is 0.33-0.6 mm/s (Fauske and Epstein, 1995; Fauske, 1996). Clearly, in the saltcake layer interior, this propagation velocity is appropriate. At the saltcake surface, however, a luminous flame at the reaction front may increase the propagation velocity locally. Radiative heat transfer from the flame to saltcake can ignite the saltcake surface. The reaction can then propagate downward, as well as

radially. Figure B-4 illustrates a propagating saltcake reaction in a thin layer. In this figure, V_p represents the "bulk" propagation velocity of 0.6 mm/s. The aim here is to determine if the radiative heat flux q''_o ignites the saltcake surface, and if so, what is the surface propagation velocity.

At any instant, the impact of q''_o is limited because the view factor from the flame to the saltcake decreases rapidly with distance from the flame. If the flame and saltcake are modeled as infinitely long, the problem is two-dimensional, as shown in Figure B-5. The view factor for two infinitely long plates with unequal widths, one common edge, and a 90° angle with respect to each other is given by:

$$F = \frac{1}{2}\left(1 + \frac{w}{h} - \sqrt{1 + \frac{w^2}{h^2}}\right)$$

(B-16)

where h is flame height and w is distance from the flame. This expression has been evaluated for $h = 1$ and various values of w, and the results are listed in Table B-1, which shows that nearly all of the thermal radiation is deposited within two or three flame heights. After three flame heights, the view factor to the saltcake surface barely increases.

Saltcake layers as thin as 1 mm ignite if heated above the ignition temperature. This suggests that the surface propagation velocity is then:

$$V_s = \text{MAX}\left(V_p, \frac{\delta_f}{t_i}\right)$$

(B-17)

where V_p is the bulk propagation velocity, δ_f is a distance of two flame heights, and t_i is the time it takes for the heat flux q''_o to heat 1 mm of saltcake to ignition. This equation stems from the following: (1) if δ_f / t_i is less than V_p, surface effects do not increase propagation velocity, and (2) if δ_f/t_i is greater than V_p, the propagation is δ_f/t_i. The time to heat 1 mm

Figure B-4. Propagating Reaction in a Thin Saltcake Layer
With Surface Effects

q''_o

Surface Propagation
V_s

h

Radial Propagation

V_p

Downward Propagation
V_p

Reaction Front
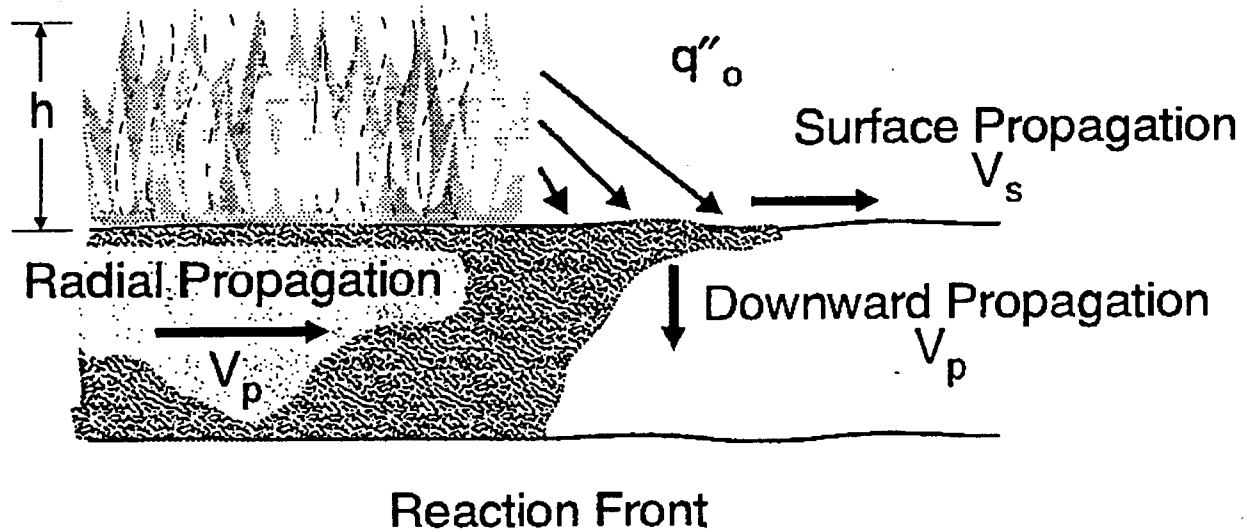
BM965103.CDR 5-21-96

Figure B-5. View Factor Model for Flame and Saltcake
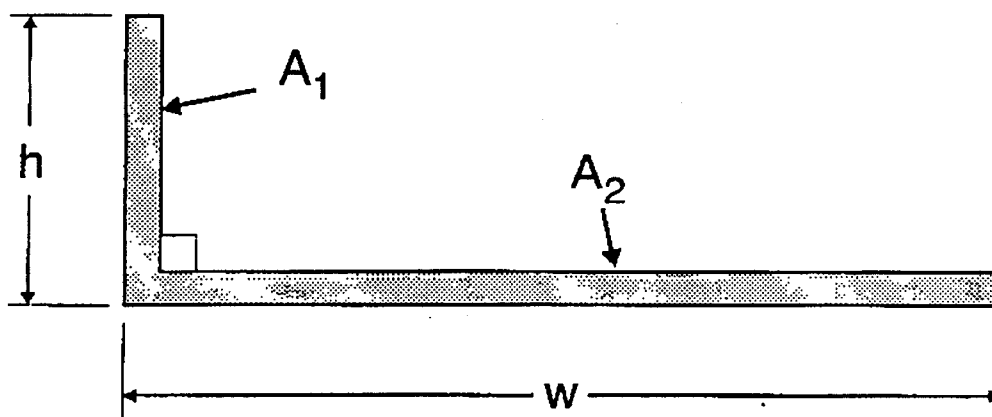
$$F_{12} = \frac{1}{2}\left(1 + \frac{w}{h} - \sqrt{1 + \frac{w^2}{h^2}}\right)$$

BM965107.CDR 5-21-96

Table B-1. View Factor From Flame to Saltcake

Flame Height (h)	Saltcake Width (w)	w/h	F
1	0.01	100.00	0.005
1	0.1	10.00	0.048
1	0.2	5.00	0.090
1	0.3	3.33	0.128
1	0.4	2.50	0.161
1	0.5	2.00	0.191
1	0.6	1.67	0.217
1	0.7	1.43	0.240
1	0.8	1.25	0.260
1	0.9	1.11	0.277
1	1	1.00	0.293
1	1.5	0.67	0.349
1	2	0.50	0.382
1	2.5	0.40	0.404
1	3	0.33	0.419
1	4	0.25	0.438
1	5	0.20	0.450

of saltcake to ignition is given by the solution to the conduction equation for a semi-infinite solid with a constant surface heat flux:

$$T(x,t) = T_o + \frac{2q''_o \sqrt{\frac{\alpha t}{\pi}}}{k} \exp\left(\frac{-x^2}{4\alpha t}\right) - \frac{q''_o x}{k} \operatorname{erfc}\left(\frac{x}{2\sqrt{\alpha t}}\right)$$

(B-18)

where $T(x, t)$ is temperature as a function of distance and time, T_o is the initial temperature, and α and k are the thermal diffusivity and thermal conductivity of the saltcake, respectively. The following saltcake property values are used: $k = 0.5$ W/m·K, $\rho = 1500$ Kg/m^3, and $C_p = 1000$ J/Kg·K. The thermal diffusivity is then 3.3×10^{-7} m^2/s.

To evaluate equation (B-18), the surface heat flux must be determined. If the flame and saltcake are both treated as black bodies, and the flame temperature is equal to the adiabatic reaction temperature,

$$q''_o = \epsilon \sigma F \left(T_r^4 - T_o^4\right)$$

(B-19)

where σ is the Stefan-Boltzmann constant, the emissivity is one, by definition, F is the view factor from the flame to the surface, T_o is the initial surface temperature, and T_r is the adiabatic reaction temperature. Adiabatic temperature rise of the products is given by:

$$\Delta T_r = \frac{x_{ac} \Delta H - x_w \lambda_w}{C_{pr}}$$

(B-20)

where λ_w is the latent heat of water, C_{pr} is the specific heat of the products, and ΔH is the heat of reaction. Assuming the following values,

$$\Delta H = 8 \times 10^6 \ J/Kg$$
$$X_{ac} = 0.24$$
$$X_w = 0.0$$
$$C_{pr} = 2000 \ J/Kg \cdot K$$

Values for ΔH and C_{pr} are discussed in detail by (Fauske and Epstein, 1995) and were used to define the criterion line of Figure B-1. The value for X_{ac} results from $X_{toc} = 0.07$. Adiabatic temperature rise is about 1000 °K. If the initial temperature is 300°K, $T_r = 1260°K$. From Table B-1, $F \approx 0.3$, which results in $q''_o = 42,600 \ W/m^2$.

Equation (B-18) can be solved iteratively to find how long it takes to heat 1 mm of saltcake to the ignition temperature of 250°C (Fauske and Epstein, 1995). With $q''_o = 42,600 \ W/m^2$ and $T_o = 30°C$, it takes 30 seconds to ignite 1 mm of saltcake. Equation (B-18) shows that the time it takes to ignite the saltcake decreases with increasing initial temperature, T_o. The temperature T_o increases during the transient because the headspace gas heats the saltcake surface. If $T_o = 100°C$, the time needed to heat 1 mm to ignition is 17 seconds.

The only remaining parameter needed to evaluate the surface propagation is the flame height. Assume that the flame height is 1 cm and the flame radiation length is 2 cm. This gives a propagation velocity of about 0.7 mm/s, for $T_o = 30°C$ and 1.2 mm/s for $T_o = 100°C$. These results suggest that surface effects might amplify the propagation velocity slightly, relative to 0.6 mm/s. To bound the significant uncertainties associated with this calculation, however, the surface propagation velocity is set equal to 1.2 mm/s, or twice the upper bound for bulk propagation velocity.

B.4.1.2 Vapor/Aerosol Mass and Energy Balances

ORNATE includes a mass and energy balance for the vapor and aerosol state of each gaseous product. This necessitates a partition between aerosol and vapor production for each gaseous product. For each product, aerosol production is simply the gaseous production over and above that needed to reach saturation. To determine the aerosol production rate during a time step, define the extrapolated mass for each product as:

$$M_{xi} = M_i + W_i \Delta t \tag{B-21}$$

where M_i is the mass at the beginning of the time step, W_i the production rate, and Δt is the time step. The extrapolated mass is the total mass of the product at the end of the time step. At saturated conditions, the mass of the product is:

$$M_{si} = V_g \rho_{si} \tag{B-22}$$

where V_g is the region volume and ρ_{si} is the density for saturated vapor. The aerosol production rate is then:

$$W_{ai} = \frac{M_{xi} - M_{si}}{\Delta t} \tag{B-23}$$

and the vapor production rate is:

$$W_{vi} = W_i - W_{ai} \tag{B-24}$$

All products have the adiabatic reaction temperature T_r. For the vapor state of each product, the rate of change of internal energy is then:

$$\frac{dU_{vi}}{dt} = W_{vi}\, h_{vi}\,(T_r) \tag{B-25}$$

where h_{vi} is the saturated vapor specific enthalpy at T_r. Similarly, for the aerosol state:

$$\frac{dU_{ai}}{dt} = W_{ai}\, h_{\ell i}\,(T_r) \tag{B-26}$$

where $h_{\ell i}$ is the saturated liquid specific enthalpy at T_r.

B.4.1.3 Reaction Rate Model Validation

The reaction rate model can be validated by comparing ORNATE results with hand-calculations for the release rates of major products. The ORNATE run considered a single region with a volume of 1000 m^3 and an initial atmosphere of pure oxygen at 300 °K and 100,000 Pa. Inputs to the sludge model were as follows:

$$
\begin{aligned}
R_o &= 0.0, \\
V_s &= 1.2 \text{ mm/s}, \\
V_p &= 0.6 \text{ mm/s}, \\
X_{TOC} &= 7\%, \\
X_w &= 10\%, \\
\delta &= 10 \text{ m, and} \\
\rho &= 1500 \text{ Kg/m}^3.
\end{aligned}
$$

This ORNATE run lasted 500 seconds, with a printout at every 100 seconds. Because there are no outflows, the rate of change of each major product is equal to the production from the reaction model. Output for rate of change of each major gas was compared to hand-calculations using equations (B-4) through (B-7). ORNATE results agreed with hand-calculations to within half a percent.

B.4.2 RELEASE MODELS

B.4.2.1 Introduction and Assumptions

The following assumptions are made in the fission product and toxic material release model:

1. Equilibrium vapor pressures of trace species will be manifest in reacted waste. This is a fair assumption given the high reaction temperatures.

2. All vapors produced at the site of the propagating reaction are released to the headspace. This assumption is conservative because gases released deep within waste may cool or not leave the waste.

3. The reaction product major gases are highly oxidizing, and in far greater abundance (by orders of magnitude) than the vapors considered in the release model. This is an excellent assumption borne out by calculations. As a corollary, equilibrium among major species is unaffected by behavior of the trace species.

4. The exact composition of the reacting condensed phases and the exact composition of the major products is a second order effect. This assumption is quantified in terms of the ratio of condensed to gas phase product moles and the mole fractions of major equilibrium products. It is valid because for a reasonable selection of fuels and oxidizers the equilibrium results are fairly similar.

5. Mutual interaction among trace species is negligible, so the behavior of trace species may be considered independently. This is a typical dilute solution approximation.

6. Trace species will be assumed in ideal solution in the condensed phase.

7. Mechanical formation of aerosols is negligible in comparison to vaporization.

8. Sodium acetate and sodium nitrate/nitrite/hydroxide are chosen as surrogates to evaluate major species equilibrium and to scope the equilibrium of trace species. This surrogate provides a representative amount of oxidizing product gases.

9. The heat of reaction between sodium acetate and nitrate is used to evaluate the adiabatic reaction temperature in release calculations. This is a conservative assumption.

10. Reactions are assumed to take place at 1 atm pressure. Realistically, the model is never applied above about 2 atm, so this assumption is good.

B.4.2.2 Equilibrium Calculations

Two cases with 7% TOC (total organic carbon weight fraction) and 10% TOC are run to determine the impact of fuel content. 7% TOC is chosen as a low value to represent waste capable of sustaining a propagating reaction with a small moisture content, while 10% TOC is chosen as an upper bound of practical interest. Abundances of reactants are:

| Moles of Compound	7% TOC	10% TOC
$NaC_2H_3O_2$	0.212	0.336
$NaNO_2$	0.132	0.036
$NaNO_3$	0.438	0.566
NaOH	0.217	0.062
$CsNO_3$	1.E-5	1.E-5
SrO	1.E-5	1.E-5

Note that the choice of reactants serves only to establish the relative abundance of each element. Relative abundances of interest are the dominance of Na, C, H, and O over traces like Cs and Sr, and the relative amounts of C and Na which eventually determine the amount of CO_2.

Figures B-6 to B-9 show respectively the mole fractions of major products, mole fractions of sodium species, mole fractions of cesium species, and mole fractions of strontium species for the 7% TOC case; Figures B-10 to B-13 show the same results for the 10% TOC case. The major difference between cases is the relative abundance of CO_2 in the gases, which is essentially minor in the 7% TOC case because of the abundance of Na relative to C, allowing Na_2CO_3 to form. A similar trend is observed for Cs and Sr compounds, with the essential result that volatility is higher when the carbonate does not form as in the 7% TOC case.

Note that excess $NaNO_3$ and $NaNO_2$ reacting with CO_2 to form Na_3CO_3 and O_2 is an outcome which differs somewhat from postulated surrogate reactions. However, no matter which set of products exists, the major gas species are highly oxidizing.

The 7% TOC case will be used to guide model development because it is more realistic and because it yields slightly higher volatilities.

Generally, the volatile form a trace species in the waste is either the vapor of the condensed phase present in the waste, or as is more often the case a further oxidized chemical form. A general expression for further oxidation of a trace species present in the waste is:

$$X_1 + a_w H_2 O (g) + a_o O_2 (g) \rightarrow a_2 X_2 (g) \tag{B-27}$$
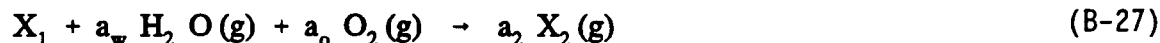
$$k_o = \frac{p^{a_2} (X_2)}{x (X_1) p^{a_w} (H_2O) p^{a_o} (O_2)} \tag{B-28}$$

Figure B-6. Major Species - 7% TOC

File: C:\HSC\GIBBS\TOC07A.OGI
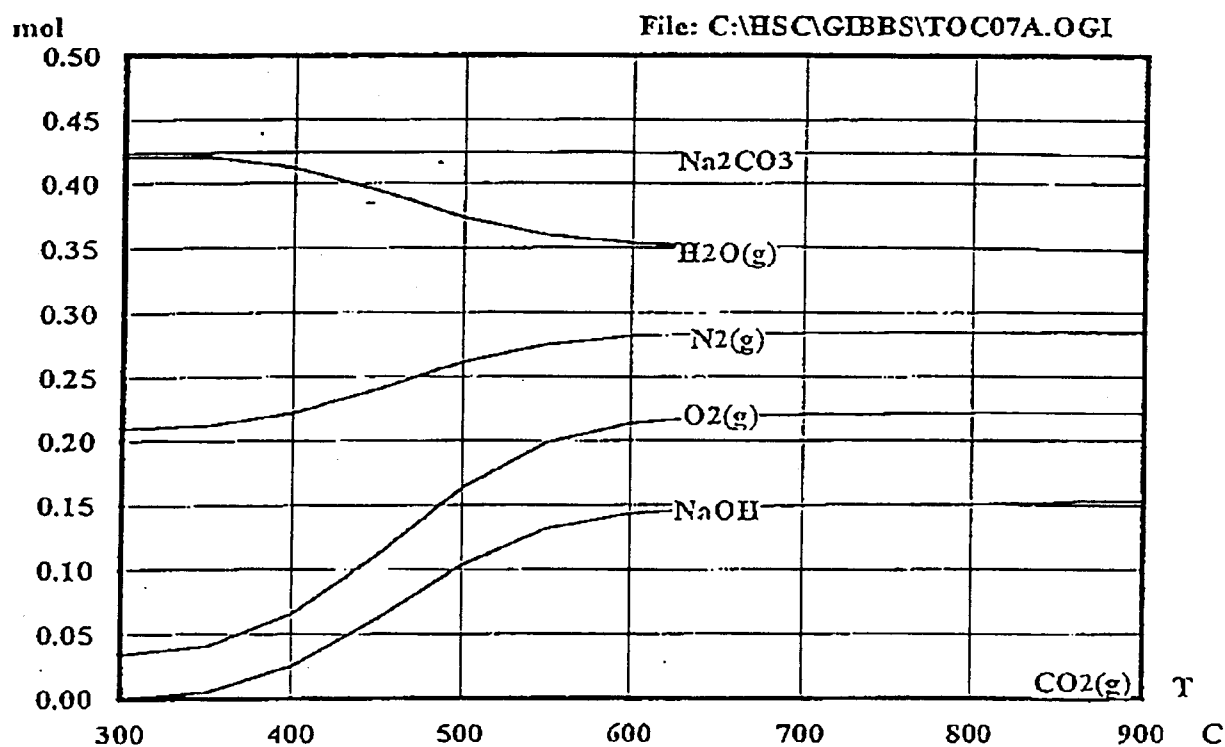
Figure B-7. Sodium Species - 7% TOC

File: C:\HSC\GIBBS\TOC07A.OGI

Log(mol) plot with curves: Na2CO3, NaOH, NaNO3, NaNO2, NaOH(g), Na2O, Na2(OH)2(g). X-axis T (C) from 300 to 900, Y-axis Log(mol) from 0 to -10.
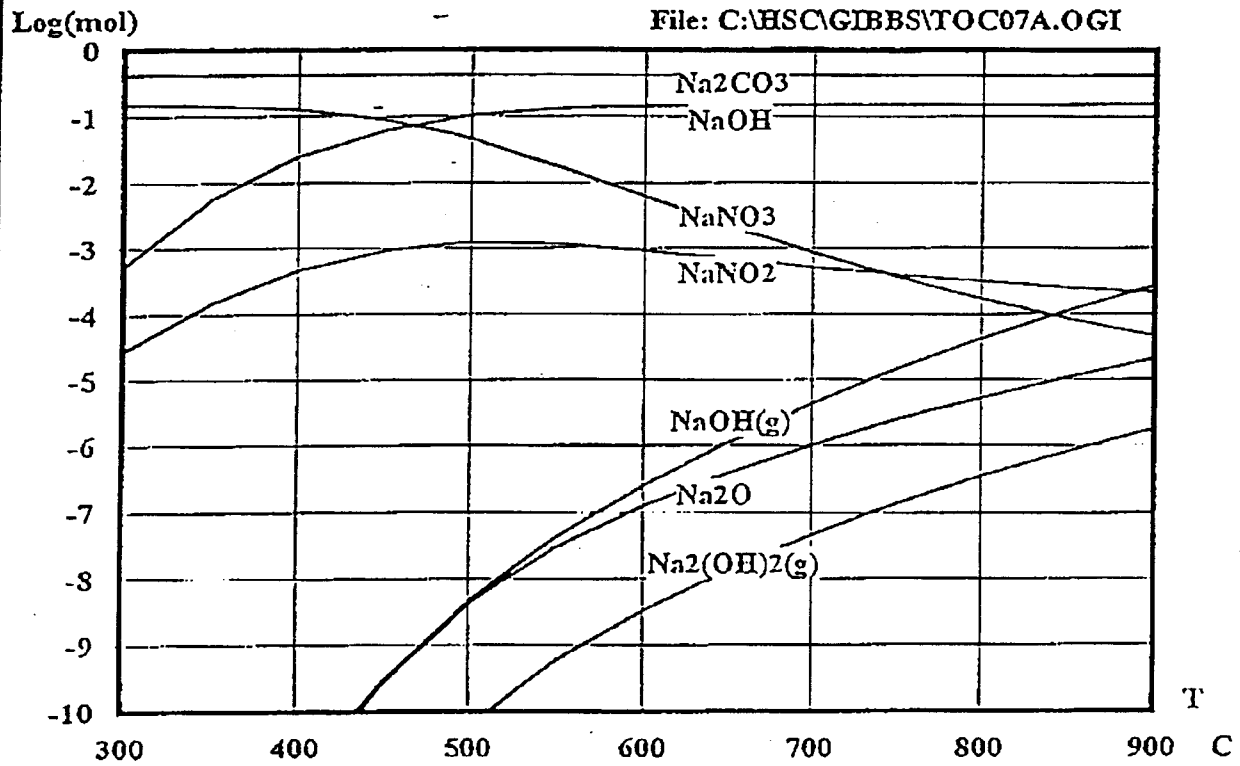
Figure B-8. Cesium Species - 7% TOC
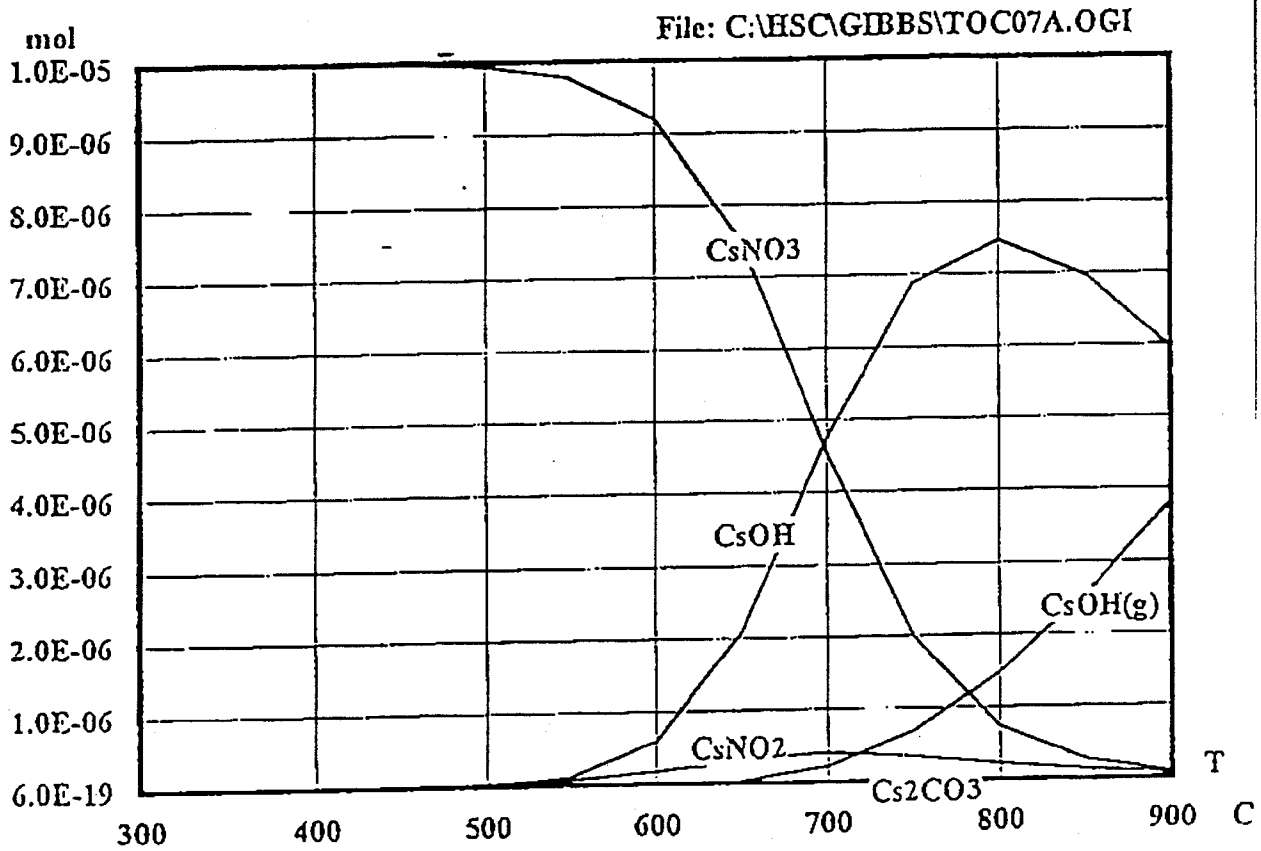
Figure B-9. Strontium Species - 7% TOC

File: C:\HSC\GIBBS\TOC07A.OGI
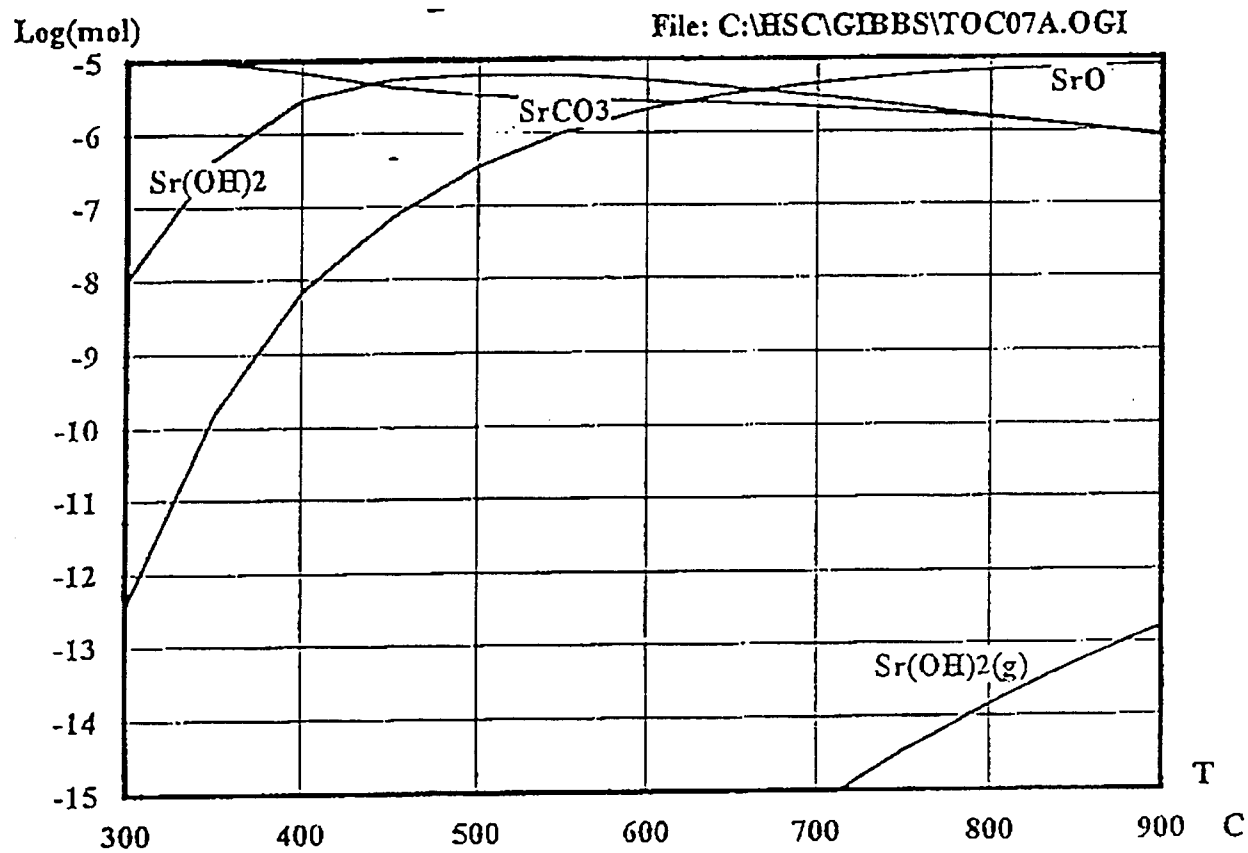
Figure B-10. Major Species - 10% TOC

File: C:\HSC\GIBBS\TOC10A.OGI

mol

- H2O(g)
- Na2CO3
- N2(g)
- CO2(g)
- O2(g)
- NaOH

T

C
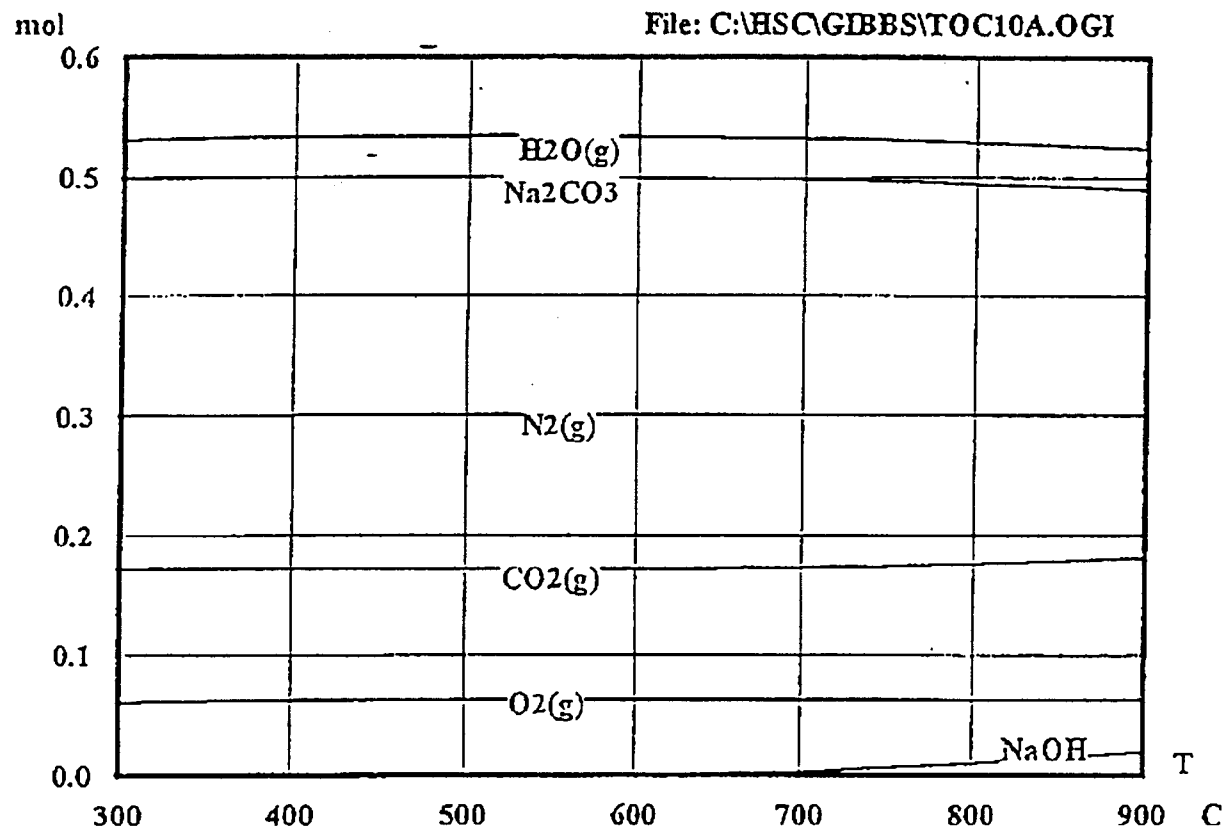
Figure B-11. Sodium Species - 10% TOC

File: C:\HSC\GIBBS\TOC10A.OGI
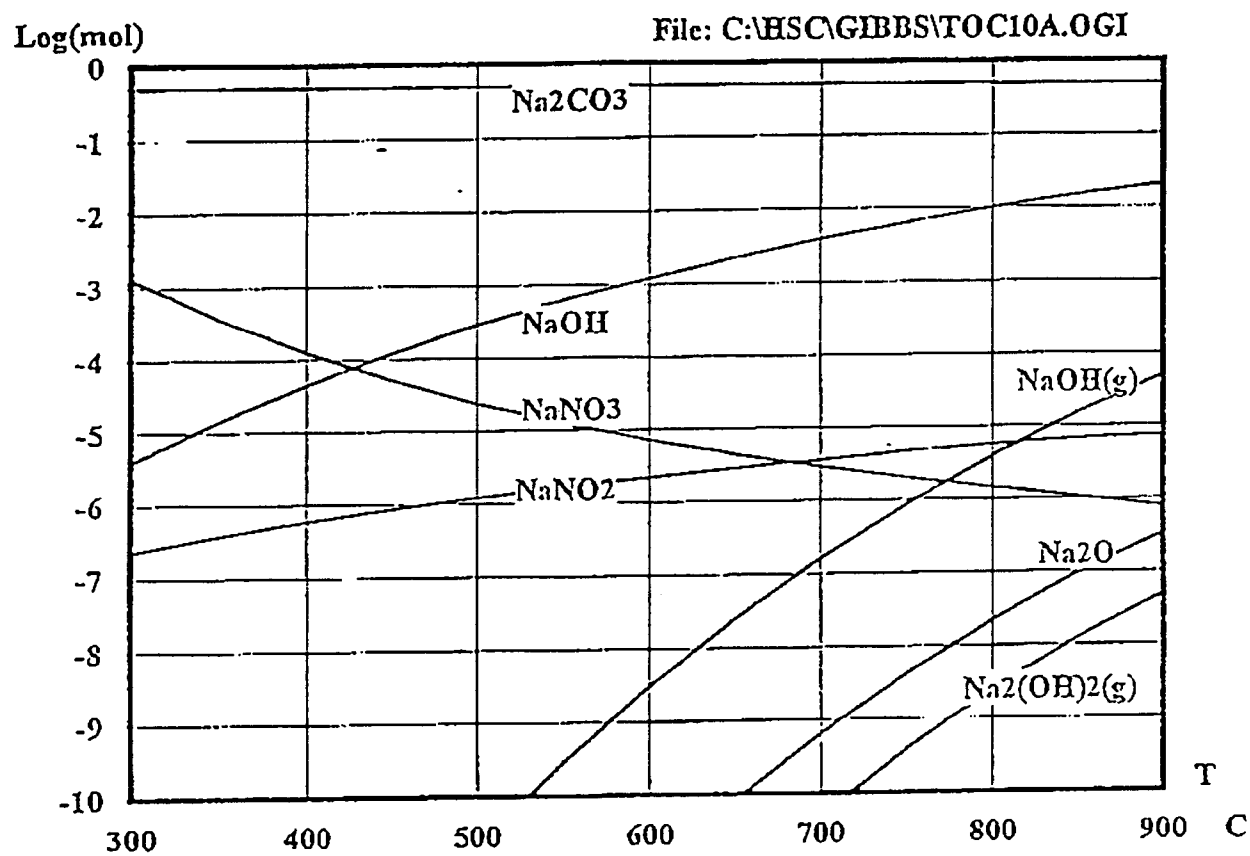
Figure B-12.   Cesium Species – 10% TOC
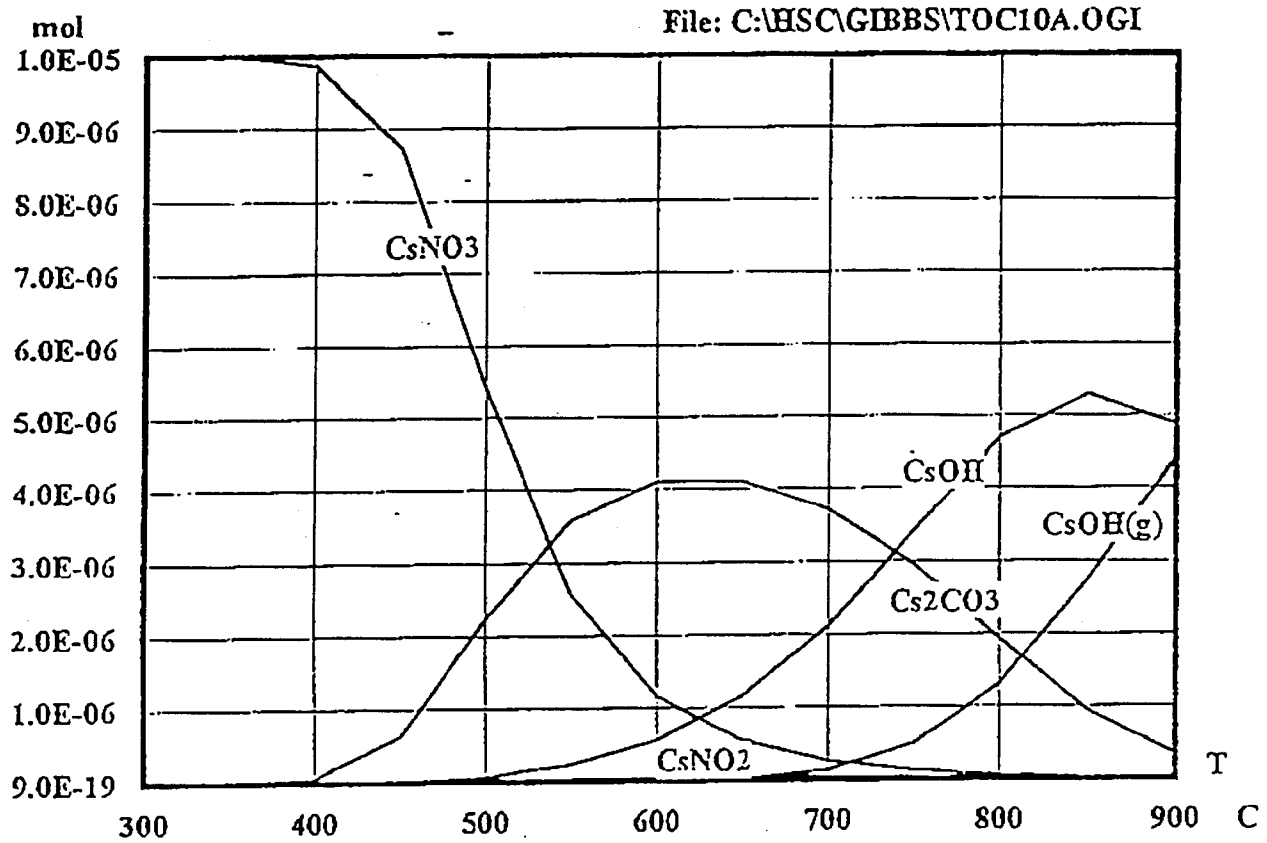
Figure B-13. Strontium Species - 10% TOC

Log(mol)

File: C:\HSC\GIBBS\TOC10A.OGI
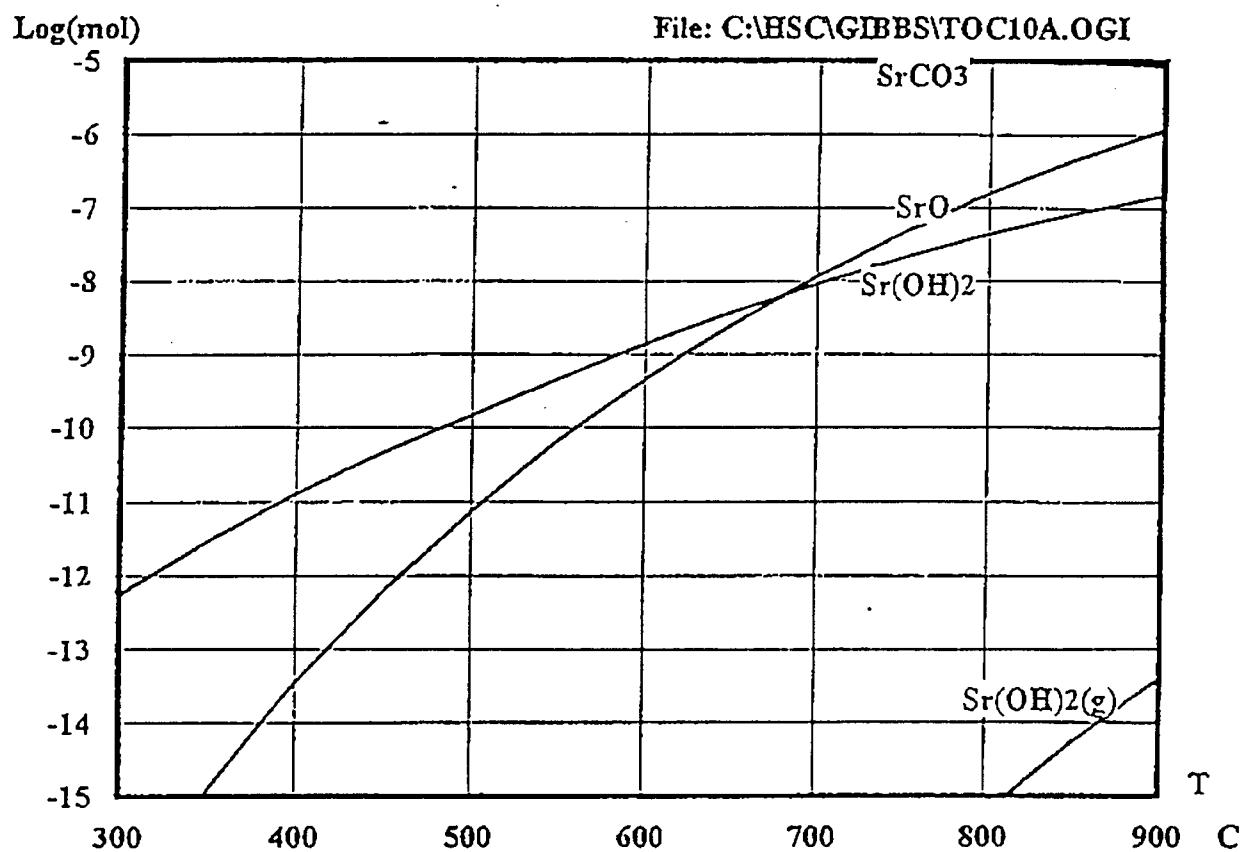
where X_1 = condensed phase oxide,
$\quad a_w$ = stoichiometric coefficient for H_2O,
$\quad a_o$ = stoichiometric coefficient for O_2,
$\quad a_2$ = stoichiometric coefficient for product gas,
$\quad X_2$ = product gas,
$\quad x( )$ = mole fraction, and
$\quad p( )$ = partial pressure.

Assuming reactions in the waste tanks will take place at pressures not grossly greater than one atmosphere total pressure, and assuming that the release fraction is less than about 0.01, the mass action equation may be rearranged to yield the release fraction:

$$RF = \frac{1}{(N/G)} \left[k_o \, p^{a_w}(H_2O) \, p^{a_o}(O_2) \right]^{\frac{1}{a_2}} x \, (X_1)^{\frac{1-a_2}{a_2}} \tag{B-29}$$

For the reference organic-nitrate reaction, the pressures of H_2O and O_2 and the ratio of condensed to gas moles are given above. For each element, the most volatile form must be determined by systematic testing of reactions of the form of equation (B-27).

Thus, release fraction model development requires several parameters whose values are taken from the equilibrium calculation. These are:

N/G	=	0.67 =	Ratio of condensed to gas phase moles in products
n(O2)/G	=	0.26 =	Mole fraction of oxygen in products
n(H2O)/G	=	0.41 =	Mole fraction water vapor in products
n(N2)/G	=	0.33 =	Mole fraction nitrogen in products

These parameters appear in the mass action equations for individual trace species equilibria. The accuracy of the release model depends upon the accuracy of the thermodynamic data for the trace species, the accuracy of the ideal solution assumption, and the accuracy of the parameters above.

Fortunately, these parameters can only realistically vary over a rather small range. The ratio of condensed to gas phase moles in the stoichiometric surrogate sodium acetate-sodium nitrate reaction is 1.3/3.0 = 0.43. The larger parameter value N/G above is due to decomposition of excess sodium nitrate and nitrite. Because volatile species release are directly proportional to this ratio, the larger value is conservative. A realistic range for the parameter is given by the stoichiometric surrogate value at the low end, which neglects decompositions, and the equilibrium value in which all decompositions occur; the variation is on the order 50%. Such variation is considered small for fission product release models.

Similarly the mole fractions of the major gases simply cannot vary over a great range. The mole fraction of water vapor is constrained by the amount of hydrogen in the reacting fuel, the mole fraction of nitrogen is constrained by the amount of nitrogen in the fuel and from decomposition of excess oxidant, and the mole fractions of all major gases must sum to unity (traces are negligible). The mole fraction of water vapor in the stoichiometric surrogate

reaction product gases is 1.5/3.0 = 0.50, only 20% different than the equilibrium value.

Indeed there is no oxygen present in the surrogate reaction products, but that is by definition of the reaction only. Either oxygen or carbon dioxide must be present in the product gases, and more accurately a mixture of both must be present. Both gases are strong oxidizers for the trace species. The tradeoff between these two depends upon the extent of sodium nitrate/ nitrite reaction with carbon dioxide yielding sodium carbonate, oxygen, and nitrogen. The carbonate appears most stable by equilibrium calculations, and yields the most oxygen, maximizing fission product release.

B.4.2.3 Data Sources

Compound data sources are summarized here for convenience. The reference case was calculated using HSC Chemistry for Windows (Roine, 1994). Release models described here are derived by hand calculations and did not require a large equilibrium calculation. Individual species data references are listed in Table B-2.

B.4.2.4 Cesium Release

The equilibrium results suggest a simple release fraction model with two mass action relations for $CsNO_3$, $CsOH$, and $CsOH(g)$. The first relation is

$$CsNO_3 + \frac{1}{2} H_2O \rightarrow CsOH + \frac{1}{2} N_2 + \frac{5}{4} O_2 \tag{B-30}$$
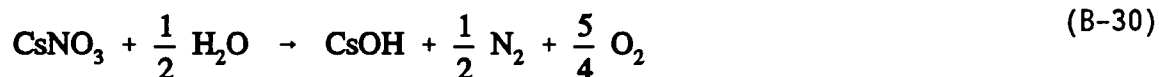
$$k_{Cs1} = \frac{x(CsOH)}{x(CsNO_3)} \left[\frac{p^{1/2}(N_2) \, p^{5/4}(O_2)}{p^{1/2}(H_2O)} \right] \tag{B-31}$$

where symbols are defined in the nomenclature. Note that the bracketed term is a constant for temperatures of interest, and may be regarded as a parameter characteristic of the chosen surrogate. The mass action law may be written as:

$$n_1 = \frac{f_{Cs}}{k_{Cs1}} \, n_2 \tag{B-32}$$

The second mass action relation is

$$CsOH \rightarrow CsOH(g) \tag{B-33}$$

$$k_{Cs2} = \frac{p(CsOH)}{x(CsOH)} \tag{B-34}$$

$$n_2 = \frac{N}{k_2 G} \, n_3 \tag{B-35}$$

Table B-2. References for Species Data

Species	Data Type	Reference
Actinides	K_e	(Krikorian, 1992)
Cd	S_f	(Weast, 1966)
$Cd(OH)_2$ (g)	FEF, G_f	(Jackson, 1971)
CdO	FEF, H_f	(Lamoreaux, 1987)
CoO	H_f, S_f, C_p	(Roine, 1994)
$Co(OH)_2$ (g)	H_f, S_f, C_p	(Roine, 1994)
$CsNO_3$	H_f, S_f, C_p	(Roine, 1994)
CsOH	H_f, S_f, C_p	(Roine, 1994)
CsOH (g)	H_f, S_f, C_p	(Roine, 1994)
$Eu(OH)_3$ (g)	FEF, H_f	(Krikorian, 1982)
Eu_2O_3	FEF, H_f	(Krikorian, 1982)
H_2 (g)	S_f	(Weast, 1966)
H_2O (g)	FEF, H_f	(Chase, 1985)
H_2O (g)	FEF, H_f	(Powers, 1986)
HgO	G_f	(Chase, 1985)
NaOH	H_f, S_f, C_p	(Roine, 1994)
NaOH (g)	H_f, S_f, C_p	(Roine, 1994)
O_2 (g)	S_f	(Weast, 1966)
O_2 (g)	FEF, H_f	(Powers, 1986)
RuO_2	FEF, H_f	(Krikorian, 1982)
$RuO_3(OH)$ (g)	FEF, H_f	(Krikorian, 1982)
SbO_2	H_f, S_f, C_p	(Roine, 1994)
SbO (g)	H_f, S_f, C_p	(Roine, 1994)
SrO	H_f, S_f, C_p	(Roine, 1994)
$Sr(OH)_2$ (g)	H_f, S_f, C_p	(Roine, 1994)
TcO_3	H_f, S_f, C_p	(Roine, 1994)
Tc_2O_7 (g)	H_f, S_f, C_p	(Roine, 1994)
TeO	H_f, S_f, C_p	(Roine, 1994)
TeO_2 (g)	H_f, S_f, C_p	(Roine, 1994)
$Y(OH)_3$ (g)	FEF, H_f	(Krikorian, 1982)
Y_2O_3	FEF, H_f	(Krikorian, 1982)

H_f = Enthalpy of formation at 298°K
K_e = Equilibrium constant
S_f = Entropy of formation at 298°K
FEF = Free Energy Function
G_f = Gibbs energy of formation at 298°K

Closure is achieved by the mass balance

$$n_o = n_1 + n_2 + n_3 \tag{B-36}$$

so the release fraction of Cs becomes

$$RF_{Cs} = \frac{n_3}{n_o} = \left[1 + \left(\frac{N}{k_{Cs2} G} \right) \left(1 + \frac{f_{Cs}}{k_{Cs1}} \right) \right]^{-1} \tag{B-37}$$

For the case of 7% TOC discussed earlier, parameter values are N/G = 0.67 and f_{Cs} = 0.135.

Equilibrium data for the reactions appear in Table B-3. An accurate curve fit to the equilibrium constants is:

$$- \ell n k = A + BT + C \ell n T + D/T \tag{B-38}$$

	A	B	C	D
k_{Cs1}	-147.16	-7.4709E-3	17.657	33.74E3
k_{Cs2}	-46.865	-6.4833E-4	4.5528	19.108E3

where T is degrees Kelvin.

For the example case, the simple model results are:

T, °C	$(CsOH-g)/(CS)_o$	$(CsOH)/(Cs)_o$	$(CsNO_3)/(Cs)_o$
600	5.3E-4	0.071	0.93
700	0.025	0.55	0.43
800	0.16	0.78	0.06
900	0.39	0.60	0.007

These results are in excellent accord with Figure B-8 as expected, and also with Figure B-12 because $CsCO_3$ and $CsNO_3$ equilibria with CsOH are similar.

B.4.2.5 Sodium Release

NaOH and Na_2CO_3 are the only important condensed species in the cases run because $NaNO_2$ and $NaNO_3$ react with the available carbon. The mass action relation between the remaining species is

$$Na_2CO_2 + H_2O \rightarrow 2NaOH + CO_2 \tag{B-39}$$

$$k_{Na1} = \frac{x^2(NaOH)}{x(Na_2CO_3)} \frac{p(CO_2)}{p(H_2O)} \tag{B-40}$$

Table B-3.   Cesium Species Equilibrium Data.

```
===========================================================================
CsOH = CsOH(g)
```

T C	deltaH kJ	deltaS J	deltaG kJ	K
200.00	152.078	142.656	84.581	4.589E-010
300.00	142.937	124.466	71.600	2.980E-007
400.00	135.498	112.071	60.057	2.184E-005
500.00	132.703	108.199	49.049	4.852E-004
600.00	129.956	104.857	38.400	5.042E-003
700.00	127.255	101.928	28.063	3.116E-002
800.00	124.599	99.330	18.003	1.329E-001
900.00	121.987	97.003	8.188	4.319E-001
1000.00	119.420	94.903	-1.405	1.142E+000
1100.00	116.898	92.995	-10.798	2.575E+000
1200.00	114.420	91.253	-20.010	5.123E+000

Formula	FW g/mol	Conc. wt-%	Amount mol	Amount g	Volume l-or-ml
CsOH	149.913	100.000	1.000	149.913	40.793 ml
CsOH(g)	149.913	100.000	1.000	149.913	22.414 l

```
===========================================================================
CsNO3 + 0.5H2O(g) = CsOH + 0.5N2(g) + 1.25O2(g)
```

T C	deltaH kJ	deltaS J	deltaG kJ	K
200.00	207.643	197.684	114.108	2.522E-013
300.00	213.128	208.861	93.419	3.058E-009
400.00	217.030	215.565	71.923	2.621E-006
500.00	201.472	192.823	52.391	2.885E-004
600.00	199.893	190.902	33.207	1.031E-002
700.00	198.335	189.212	14.203	1.728E-001
800.00	196.790	187.701	-4.641	1.682E+000
900.00	195.255	186.333	-23.342	1.095E+001
1000.00	193.728	185.084	-41.912	5.244E+001
1100.00	192.206	183.933	-60.362	1.979E+002
1200.00	190.688	182.866	-78.701	6.177E+002

CsNO3 Extrapolated from 900 K

Formula	FW g/mol	Conc. wt-%	Amount mol	Amount g	Volume l-or-ml
CsNO3	194.910	95.583	1.000	194.910	52.893 ml
H2O(g)	18.015	4.417	0.500	9.008	11.207 l
CsOH	149.913	73.516	1.000	149.913	40.793 ml
N2(g)	28.013	6.869	0.500	14.007	11.207 l
O2(g)	31.999	19.615	1.250	39.999	28.017 l

Since k_{Na1} depends only upon T, at a given T the mole fraction of NaOH varies quickly with the CO_2 pressure due to its exponent. Because the (CO_2/H_2O) ratio is an unknown parameter, knowledge of which determines the NaOH mole fraction, it is best to directly employ the NaOH mole fraction as a parameter.

For NaOH release,

$$k_{Na2} = \frac{p\,(NaOH)}{x\,(NaOH)} \tag{B-41}$$

letting n_2 = moles NaOH and n_3 = moles NaOH(g),

$$n_3 = k_{Na2}\,\frac{n_2}{N}\,G \tag{B-42}$$

But the total condensed phase moles are mostly sodium compounds, and only a negligible fraction of sodium is released. Therefore defining n_o = total sodium moles,

$$RF \equiv \frac{n_3}{n_o} = k_{Na2}\,\frac{n_2}{n_o}\,\frac{G}{N} \tag{B-43}$$

$$RF = k_{Na2}\,\frac{f\,(n_2/n_o)}{(N/G)} \equiv f_{Na}\,k_{Na2} \tag{B-44}$$

The parameter (N/G) used for cesium release appears above with a new parameter n_2/n_o which represents the condensed phase fraction of Na present as NaOH. The definitions used above are valid even if $NaNO_3$ or $NaNO_2$ are present. Because two parameters are multiplied together, for practical purposes a combined parameter f_{Na} may be defined. For the case of 7% TOC, n_2/n_o = 0.15/(0.15 + 0.42) = 0.26 and N/G = 0.67, so f_{Na} = 0.39.

Equilibrium data for NaOH formation appear in Table B-4. A fit to k_{Na2} in the same form as above is

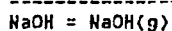|	A	B	C	D
k_{Na2}	-62.046	-1.4764E-3	6.5256	28.628E3

Using this model, NaOH releases are slightly overpredicted. It is thus recommended to set f_{Na} = 0.20 to minimize NaOH production. Note it is conservative to minimize NaOH release because this minimizes in-tank fallout.

Table B-4. Sodium Species Equilibrium Data

```
=======================================================================
Na2CO3 + H2O(g) = 2NaOH + CO2(g)

    T        deltaH      deltaS      deltaG       K
    C          kJ          J           kJ
  200.00     129.440     20.728      119.632    6.191E-014
  300.00     145.884     49.795      117.345    2.017E-011
  400.00     160.166     73.812      110.479    2.669E-009
  500.00     161.102     75.022      103.098    1.081E-007
  600.00     163.678     78.173       95.421    1.955E-006
  700.00     164.841     79.448       87.526    2.002E-005
  800.00     164.579     79.203       79.582    1.337E-004
  900.00     133.658     51.668       73.044    5.590E-004
 1000.00     132.370     50.615       67.929    1.632E-003
 1100.00     130.935     49.531       62.922    4.039E-003
 1200.00     129.354     48.420       58.024    8.758E-003

Formula                   FW      Conc.    Amount      Amount      Volume
----------------------- g/mol --- wt-% ------ mol ------ g ------- l-or-ml ---
Na2CO3                  105.989   85.472    1.000      105.989    41.860 ml
H2O(g)                   18.015   14.528    1.000       18.015    22.414  l
----------------------- g/mol --- wt-% ------ mol ------ g ------- l-or-ml ---
NaOH                     39.997   64.509    2.000       79.994    37.556 ml
CO2(g)                   44.010   35.491    1.000       44.010    22.414  l


=======================================================================
NaOH = NaOH(g)

    T        deltaH      deltaS      deltaG       K
    C          kJ          J           kJ
  200.00     225.958    157.618      151.382    1.934E-017
  300.00     216.104    139.981      135.874    4.130E-013
  400.00     206.380    123.840      123.017    2.841E-010
  500.00     203.172    119.396      110.861    3.232E-008
  600.00     200.084    115.638       99.115    1.175E-006
  700.00     197.110    112.412       87.716    1.956E-005
  800.00     194.247    109.610       76.618    1.864E-004
  900.00     191.490    107.154       65.783    1.177E-003
 1000.00     188.837    104.983       55.178    5.445E-003
 1100.00     186.284    103.052       44.778    1.979E-002
 1200.00     183.830    101.327       34.561    5.949E-002

Formula                   FW      Conc.    Amount      Amount      Volume
----------------------- g/mol --- wt-% ------ mol ------ g ------- l-or-ml ---
NaOH                     39.997  100.000    1.000       39.997    18.778 ml
----------------------- g/mol --- wt-% ------ mol ------ g ------- l-or-ml ---
NaOH(g)                  39.997  100.000    1.000       39.997    22.414  l
```

B.4.2.6 Strontium Release

Strontium forms refractory compounds and is simply not volatile. Its release fraction at 900°C is about 10^{-8}. Release of Sr may be maximized by assuming equilibrium of $Sr(OH)_2$ gas over SrO:

$$SrO + H_2O \rightarrow Sr(OH)_2 \qquad (B\text{-}45)$$

$$k_{Sr} = \frac{p\,(Sr(OH))_2}{x\,(SrO)\;p\,(H_2O)} \qquad (B\text{-}46)$$

Identifying n_3 = moles $Sr(OH)_2$ (g) and n_2 = moles SrO,

$$n_3 = k_{Sr}\,\frac{n_2}{N}\,\frac{n(H_2O)}{G}\,G \qquad (B\text{-}47)$$

Since $n_3 \ll n_2$, RF $= n_3 / n_2$:

$$RF = n_3/n_2 = \frac{k_{Sr}\,[n\,(H_2O)/G]}{(N/G)} \equiv f_{Sr}\,k_{Sr} \qquad (B\text{-}48)$$

The familiar parameter (N/G) appears as does a new parameter which is the fraction of water vapor in the gas phase. For practical purposes, these two parameters are lumped into the multiplier f_{Sr}. For the 7% TOC case, f_{Sr} ≈0.41/0.67 = 0.61.

Table B-5 contains equilibrium constant data for this reaction. A curve fit to the equilibrium constant is:

	A	B	C	D
k_{Sr}	-3.1999	6.1675E-4	-0.64152	28.422E3

Directly using the Table B-5 value at 900°C, the release fraction of Sr as $Sr(OH)_2$(g) is (3.3×10^{-8}) $(0.61) = 2 \times 10^{-8}$. From Figure B-9, the release fraction is approximately 1.5×10^{-8} which is good accord. A conservative result is obtained by setting $f_{Sr} = 1.0$.

B.4.2.7 Cobalt Release

Figure B-14 shows equilibrium cobalt species for the 7% TOC reference case. Its release fraction is small, only 10^{-7} at 1000°C, as the dihydroxide vapor over the oxide. This suggests the simple model:

$$CoO + H_2O \rightarrow Co(OH)_2 \text{ (g)} \qquad (B\text{-}49)$$

$$k_{Co} = \frac{p\,(Co(OH)_2)}{x\,(CoO)\;p\,(H_2O)} \qquad (B\text{-}50)$$

Table B-5. Strontium Species Equilibrium Data

```
=================================================================
SrO + H2O(g) = Sr(OH)2(g)

    T         deltaH     deltaS      deltaG        K
    C          kJ          J          kJ
  200.00     237.847     60.152     209.386    7.628E-024
  300.00     237.784     60.035     203.376    2.908E-019
  400.00     237.651     59.821     197.382    4.813E-016
  500.00     237.430     59.518     191.414    1.166E-013
  600.00     237.109     59.128     185.482    7.998E-012
  700.00     236.683     58.667     179.591    2.288E-010
  800.00     236.155     58.151     173.750    3.485E-009
  900.00     235.524     57.590     167.963    3.318E-008
 1000.00     234.796     56.995     162.233    2.205E-007
 1100.00     233.976     56.375     156.564    1.106E-006
 1200.00     233.072     55.740     150.959    4.435E-006

Formula                    FW      Conc.    Amount    Amount     Volume
----------------------- g/mol--- wt-%------ mol------ g------- l-or-ml---
SrO                       103.619  85.189    1.000    103.619    22.047 ml
H2O(g)                     18.015  14.811    1.000     18.015    22.414 l
----------------------- g/mol--- wt-%------ mol------ g------- l-or-ml---
Sr(OH)2(g)                121.635 100.000    1.000    121.635    22.414 l
```

Figure B-14. Cobalt Species - 7% TOC
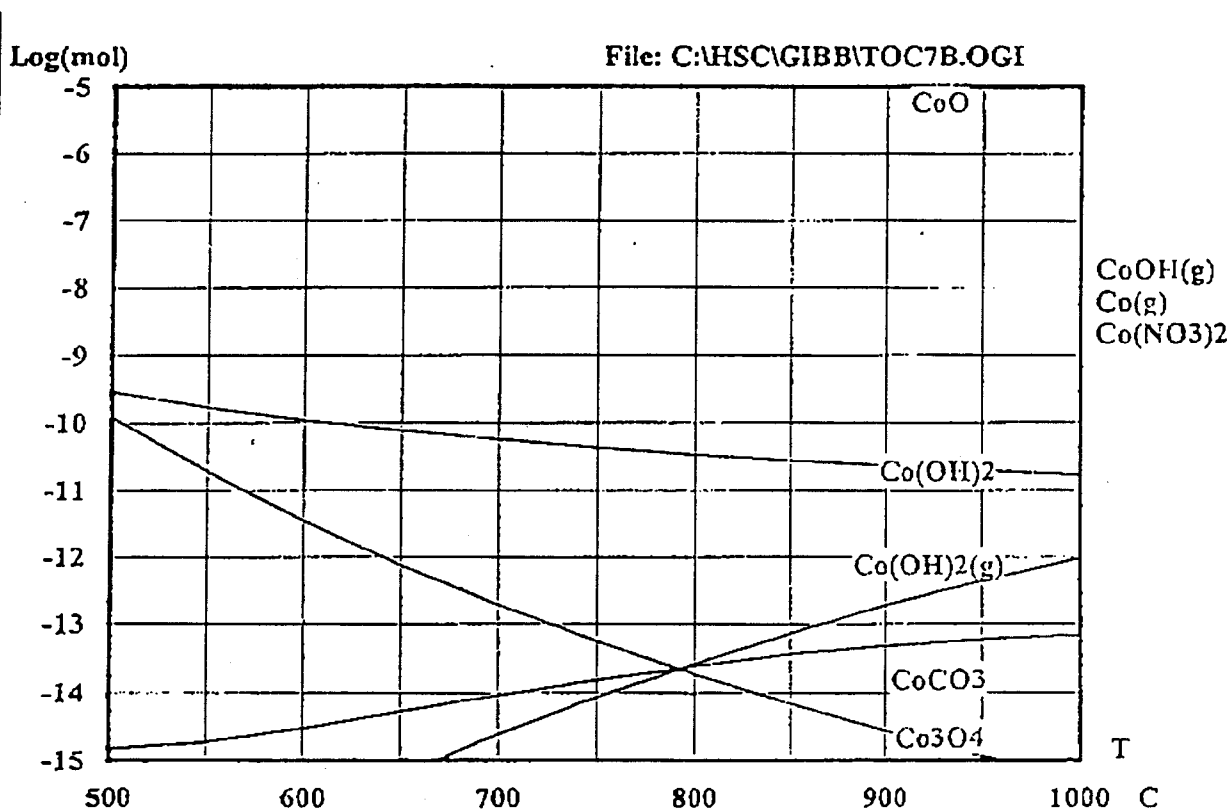
Letting n_1 = moles CoO and n_2 = moles Co(OH)$_2$, noting $n_1 \ll n_2$, so n_0 = moles total cobalt $\simeq n_2$,

$$RF = \frac{n_2}{n_1} = \frac{k_{Co}}{(N/G)}\left[\frac{n(H_2O)}{G}\right] = f_{Co} \, k_{Co} \tag{B-51}$$

Thus, the release fraction depends upon the condensed to gas phase mole ratio (N/G) and the water vapor mole fraction $n(H_2O)/G$. Because two parameters are multiplied, the equivalent parameter f_{co} is created. Its reference case value is f_{co} = 0.61. A value f_{co} = 1.0 is recommended to be conservative.

Equilibrium data for the release reaction are given in Table B-6. At 1000°C, $k = 1.63 \times 10^{-7}$ and RF = 10^{-7} as expected. The equilibrium constant may be fit by:

	A	B	C	D
k_{Co}	-16.742	-6.7107E-5	1.6279	26.501E3

B.4.2.8 Technetium Release

Technetium species are shown in Figure B-15 for the 7% TOC case, suggesting that several percent of this element could be released. A simple model is:

$$TcO_3 + \frac{1}{4}O_2 \rightarrow \frac{1}{2}Tc_2O_7 \text{ (g)} \tag{B-52}$$

$$k_{Tc} = \frac{p\,(TcO_7)^{1/2}}{x\,(TcO_3)\,p\,(O_2)^{1/4}} \tag{B-53}$$

Letting n_1 = moles TcO$_3$, n_2 = moles Tc$_2$O$_7$, and making the conservative approximation $n_2 \ll n_1$,

$$RF = \frac{n_2}{n_1} = \frac{k_{Tc}^2\,(n_1/N)}{(N/G)}\left[\frac{n(O_2)}{G}\right]^{1/2} = f_{Tc}\,k_{Tc}^2\,x_{Tc} \tag{B-54}$$

where x_{Tc} is the mole fraction of TcO$_3$ and the combined parameter f_{Tc} is defined by the remaining groups. Its nominal value is f_{Tc} = 0.76, and a recommended conservative value is 1.0.

Equilibrium data are given in Table B-7 for Tc release. Equilibrium constant fit data are:

	A	B	C	D
k_{Tc}	-17.836	6.4264E-3	1.7959E-1	6.3612E3

Table B-6. Cobalt Species Equilibrium Data

CoO + H2O(g) = Co(OH)2(g)
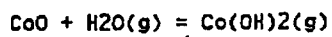
T C	deltaH kJ	deltaS J	deltaG kJ	K
200.00	214.658	43.861	193.905	3.904E-022
300.00	212.992	40.657	189.689	5.141E-018
400.00	211.542	38.322	185.746	3.850E-015
500.00	210.226	36.498	182.008	5.039E-013
600.00	208.982	34.984	178.436	2.111E-011
700.00	207.767	33.667	175.005	4.034E-010
800.00	206.551	32.477	171.698	4.386E-009
900.00	205.311	31.372	168.506	3.138E-008
1000.00	204.026	30.322	165.422	1.631E-007
1100.00	202.681	29.305	162.441	6.611E-007
1200.00	201.260	28.306	159.560	2.197E-006

Figure B-15.   Technetium Species - 7% TOC
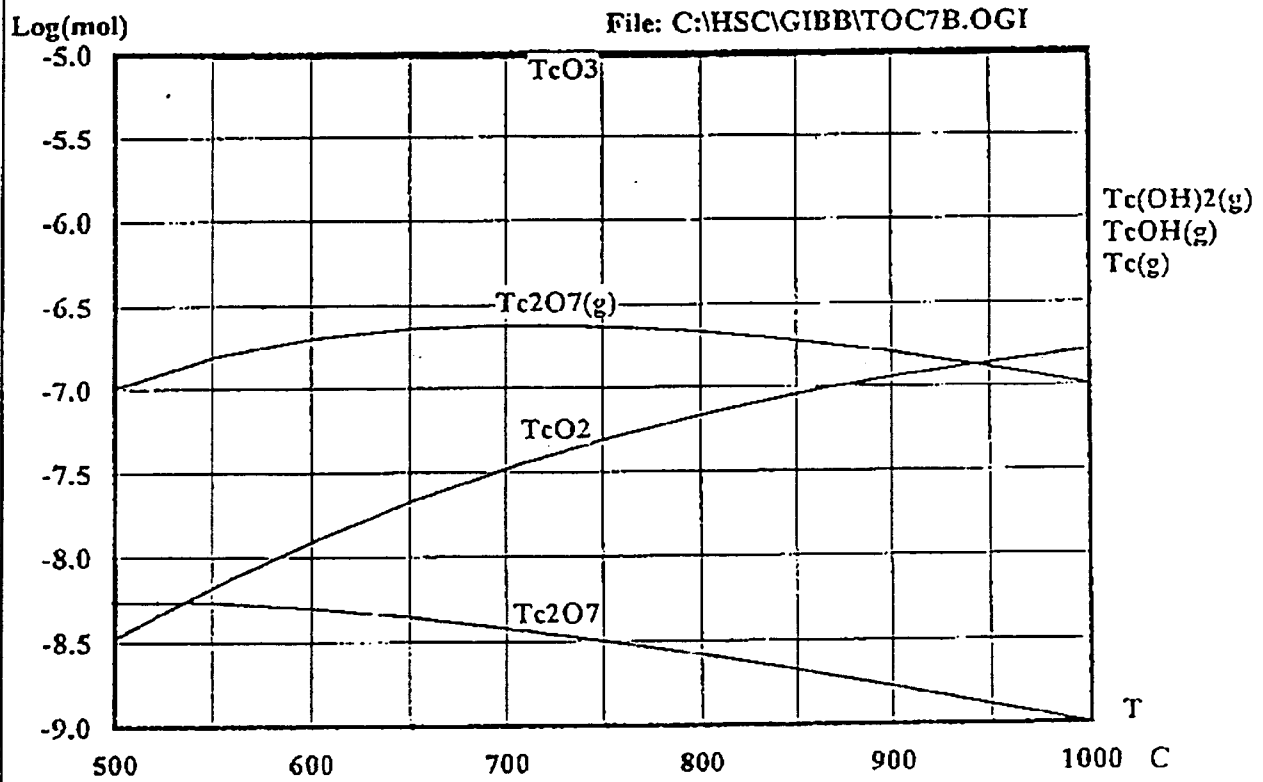
Note, the Tc mole fraction is $10^{-5}/N = 1.75E-5$ in the example case. At 1000°C, $k_{Tc} = 29.24$ and the release fraction is 0.011, in accord with Figure B-15, and at 700°C the release fraction is 0.027, also in accord.

B.4.2.9 Tellurium Release

Tellurium species for the 7% TOC case are shown in Figure B-16, suggesting releases approaching 1% at 1000°C. A simple model is:

$$Te\,O + \frac{1}{2}\,O_2 \rightarrow Te\,O_2 \tag{B-55}$$

$$Te\,O + \frac{1}{2}\,O_2 \rightarrow Te\,O_2 \; (g) \tag{B-56}$$

$$k_{Te1} = \frac{x\,(Te\,O_2)}{x\,(Te\,O)\,p\,(O_2)^{1/2}} \tag{B-57}$$

$$k_{Te2} = \frac{p\,(Te\,O_2)}{x\,(Te\,O)\,p\,(O_2)^{1/2}} \tag{B-58}$$

Letting n_1 = moles TeO, n_2 = moles TeO_2 , n_3 = moles TeO_2 (g), and n_0 = total moles Te. There follows:

$$n_1 = \frac{(N/G)}{k_{Te2}} \left[\frac{G}{n\,(O_2)}\right]^{1/2} n_3 \tag{B-59}$$

$$n_2 = k_{Te1} \left[\frac{n\,(O_2)}{G}\right]^{1/2} n \tag{B-60}$$

$$n_2 = \frac{k_{Te1}}{k_{Te2}}\,(N/G)\,n_3 \tag{B-61}$$

$$n_0 = n_1 + n_2 + n_3 \tag{B-62}$$

Table B-7. Technetium Species Equilibrium Data

TcO3 + 0.25O2(g) = 0.5Tc2O7(g)
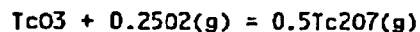
T	deltaH	deltaS	deltaG	K
C	kJ	J	kJ	
200.00	40.346	87.261	-0.941	1.270E+000
300.00	34.506	76.093	-9.107	6.761E+000
400.00	27.678	65.134	-16.167	1.797E+001
500.00	19.817	54.263	-22.136	3.131E+001
600.00	10.897	43.426	-27.020	4.136E+001
700.00	0.904	32.601	-30.822	4.514E+001
800.00	-10.174	21.774	-33.541	4.292E+001
900.00	-22.342	10.940	-35.176	3.684E+001
1000.00	-35.607	0.095	-35.728	2.924E+001
1100.00	-49.972	-10.761	-35.195	2.182E+001
1200.00	-65.441	-21.631	-33.576	1.551E+001

TcO3 Extrapolated from 400 K

Figure B-16. Tellurium Species - 7% TOC
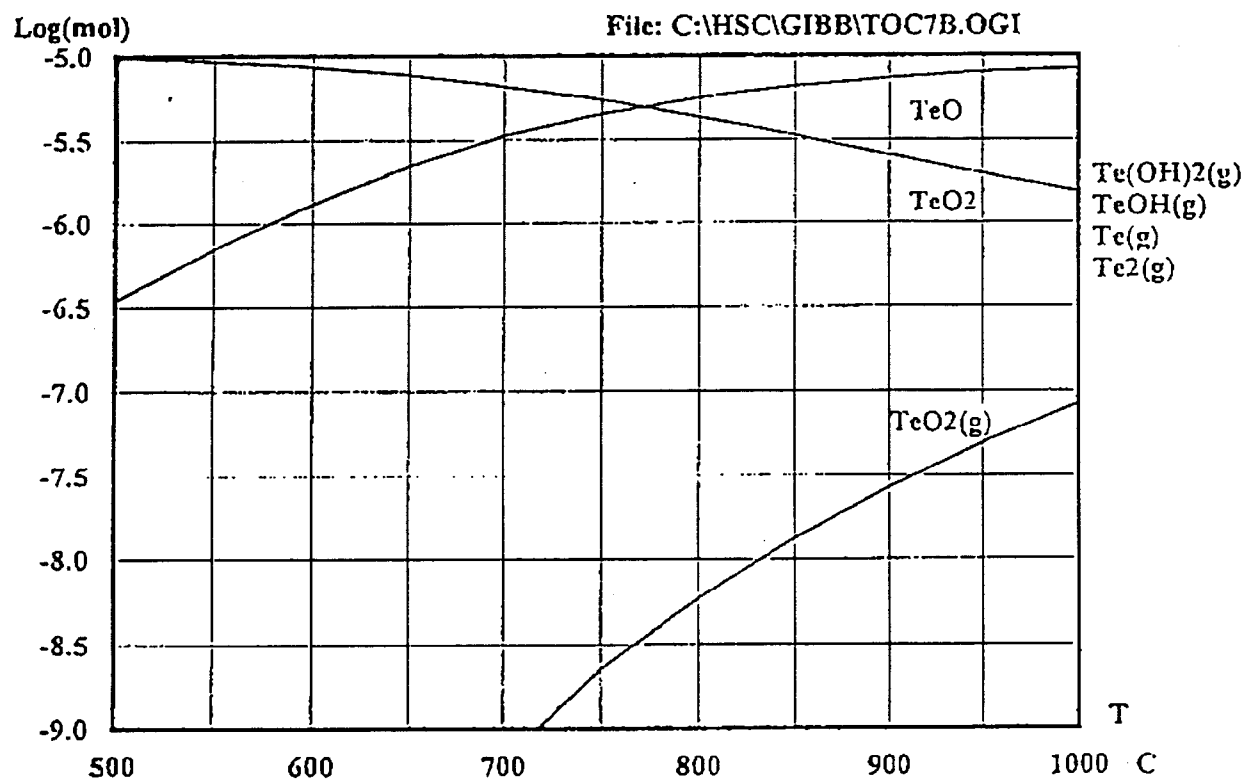
$$RF = \frac{n_3}{n_0} = \left[\frac{(N/G)}{k_{Te2}}\left(\frac{G}{n(O_2)}\right)^{1/2} + \frac{k_{Te1}(N/G)}{k_{Te2}} + 1\right]^{-1} \quad \text{(B-63)}$$

Using reference case data and equilibrium constant data in Table B-8, the terms in brackets may be compared:

Term 1	Term 2	Term 3	
700°C	5300	10^4	1
800°C	1000	750	1
900°C	280	95	1
1000°C	100	18	1

Therefore, using only the first term in brackets will cause overprediction of release by a factor of 3 at 700°C and by less than 20% at 1000°C. This is equivalent to neglecting the presence of condensed Te O_2 and stating $n_3 \ll n_1$, so the simplified release model is:

$$RF \approx \frac{k_{Te2}}{(N/G)}\left[\frac{n(O_2)}{G}\right]^{1/2} = f_{Te} \, k_{Te2} \quad \text{(B-64)}$$

where $f_{Te} = f_{Tc} = 0.76$ from equation (B-54) is evident. Checking the value at 1000°C where $k_{Te2} = 0.0131$ yields RF = 0.0098, just slightly greater than the value from Figure B-16 as expected. Values for the equilibrium constant fit are:

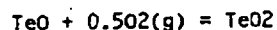|	A	B	C	D
k_{Te2}	27.397	8.2467E-3	-6.8655	19.659E3

B.4.2.10 Antimony Release

Antimony species for the 7% TOC reference case are shown in Figure B-17, indicating high release fractions at high temperatures and suggesting the model:

$$Sb\,O_2 \rightarrow Sb\,O\,(g) + \frac{1}{2}O_2 \quad \text{(B-65)}$$

Table B-8.   Tellurium Species Equilibrium Data

TeO + 0.5O2(g) = TeO2

T C	deltaH kJ	deltaS J	deltaG kJ	K
200.00	-88.074	-80.152	-50.151	3.443E+005
300.00	-87.541	-79.126	-42.190	7.004E+003
400.00	-87.100	-78.415	-34.315	4.602E+002
500.00	-86.768	-77.953	-26.499	6.172E+001
600.00	-86.550	-77.687	-18.718	1.318E+001
700.00	-86.453	-77.580	-10.956	3.874E+000
800.00	-84.844	-75.808	-3.491	1.479E+000
900.00	-81.573	-72.893	3.942	6.675E-001
1000.00	-78.298	-70.214	11.095	3.505E-001
1100.00	-75.017	-67.734	17.991	2.068E-001
1200.00	-71.731	-65.424	24.648	1.337E-001

TeO2 Extrapolated from 1200 K

TeO + 0.5O2(g) = TeO2(g)
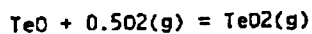
T C	deltaH kJ	deltaS J	deltaG kJ	K
200.00	172.448	111.542	119.671	6.130E-014
300.00	171.053	108.872	108.653	1.250E-010
400.00	169.519	106.408	97.890	2.531E-008
500.00	167.802	104.033	87.369	1.250E-006
600.00	165.877	101.694	77.083	2.445E-005
700.00	163.732	99.371	67.029	2.523E-004
800.00	131.561	67.676	58.935	1.353E-003
900.00	128.980	65.376	52.284	4.697E-003
1000.00	126.420	63.282	45.853	1.314E-002
1100.00	123.880	61.361	39.622	3.109E-002
1200.00	121.357	59.587	33.576	6.447E-002

BEST AVAILABLE COPY

Figure B-17.   Antimony Species - 7% TOC
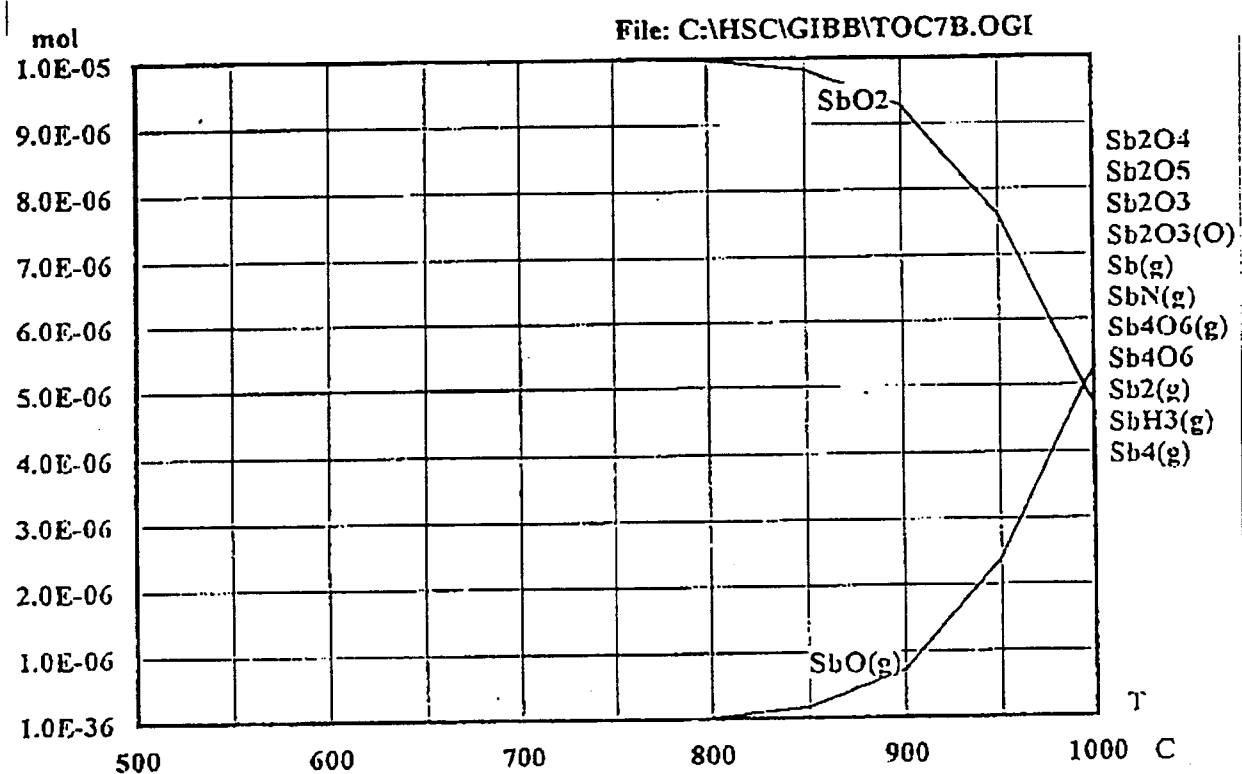
$$k_{Sb} = \frac{p\,(SbO)\,p\,(O_2)^{1/2}}{x\,(SbO_2)} \cdot \tag{B-66}$$

Denoting n_1 = moles SbO_2 and n_2 = SbO with n_0 = total moles Sb. There follows:

$$n_1 = \frac{(N/G)}{k_{Sb}}\left[\frac{n\,(O_2)}{G}\right]^{1/2} n_2 \tag{B-67}$$

$$RF = \frac{n_2}{n_0} = \frac{k_{Sb}}{\left(\dfrac{N}{G}\right)\left[\dfrac{n\,(O_2)}{G}\right]^{1/2} + k_{Sb}} = \frac{k_{Sb}}{f_{Sb} + k_{Sb}} \tag{B-68}$$

which defines the release parameter f_{Sb} whose nominal value is f_{Sb} = (0.67) $(0.26)^{1/2}$ = 0.34. Small values of f_{Sb} are conservative and 0.25 is recommended.

Equilibrium data for antimony release appears in Table B-9. Coefficients for the equilibrium constant are:

	A	B	C	D
k_{Sb}	-36.870	1.2933E-3	0.40216	42.381E3

At 1000°C, k_{Sb} = 0.389 and RF = 0.54 in accord with Figure B-15, and at 900°C RF = 0.073, also in accord.

B.4.2.11 Plutonium and Actinide Release

Krikorian et al. (1992) performed an experiment on Pu volatility in oxidizing environments and found the volatile species to be $PuO_2\,(OH)_2$. Assuming that PuO_2 is the solid species in equilibrium with the H_2O and O_2 vapors present yields the reaction:

$$PuO_2 + H_2O + \frac{1}{2}O_2 \rightarrow PuO_2\,(OH)_2 \tag{B-69}$$
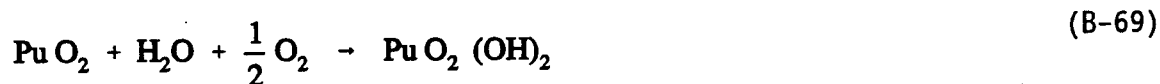
Table B-9. Antimony Species Equilibrium Data

Sb02 = SbO(g) + 0.502(g)

T C	deltaH kJ	deltaS J	deltaG kJ	K
200.00	348.266	272.096	219.523	5.796E-025
300.00	346.924	269.530	192.443	2.884E-018
400.00	345.354	267.011	165.616	1.405E-013
500.00	343.532	264.491	139.041	4.032E-010
600.00	341.444	261.955	112.718	1.804E-007
700.00	339.082	259.396	86.650	2.231E-005
800.00	336.440	256.814	60.840	1.093E-003
900.00	333.516	254.211	35.288	2.683E-002
1000.00	330.306	251.587	9.998	3.888E-001
1100.00	326.809	248.944	-15.029	3.730E+000
1200.00	323.024	246.285	-39.790	2.576E+001

Sb02 Extrapolated from 1200 K

$$k_{Pu} = \frac{p\left(PuO_2(OH)_2\right)}{x\left(PuO_2\right) p\left(H_2O\right) p\left(O_2\right)^{1/2}}$$

(B-70)

The mass action law is rearranged to derive the release fraction:

(B-71)

$$RF = \frac{k_{Pu}}{(N/G)}\left[\frac{n(H_2O)}{G}\right]\left[\frac{n(O_2)}{G}\right]^{1/2} = f_{Pu} k_{Pu}$$

For the 7% TOC reference case, $f_{Pu} = \left(\frac{1}{0.67}\right)(0.41)(0.26)^{1/2} = 0.31$

A linear fit was postulated which includes the points

$$T = 1413°K \qquad \log_{10} k_6 = -7.2$$
$$T = 823°K \qquad \log_{10} k_6 = -11.8$$

yielding the fit parameters:

	A	B	C	D
k_{Pu}	1.355	0.0	0.0	21.35E3

For example, at 1000°C, Krikorian shows $\log_{10} k_{Pu} \cong -8$ so $k_{Pu} = 10^{-8}$, and the present fit yields $k_{Pu} = 1.3 \times 10^{-8}$, which is in accord. The implied release fraction is thus 4×10^{-9}.

Krikorian et al. (1992) presents oxidizing furnace data for plutonium as a function of temperature and also sparse data for Am release based on the observed Pu/Am ratio in gases. A 50/1 ratio was expected for equal release fractions because his sample was 2% Am. Lower and higher values were observed, with the minimum Pu/Am ratio of 11 suggesting a release fraction for Am that is a factor of 5 higher than that of Pu. This is in accord with expectation given the theoretical model (Krikorian 1982).

It is proposed here that Krikorian's experimental results (1992) be retained as the basis for the actinide release model, and that his theoretical results (1982) be used to indicate a scaling basis for releases of other actinides in proportion to Pu. Therefore release fractions of U, Np, Am, and Cm are taken as 5 times that of Pu.

B.4.2.12 Cadmium Release

Cadmium dihydroxide is the single oxidized form of CdO for which data are available:

$$CdO + H_2O \rightarrow Cd(OH)_2 (g)$$

(B-72)

Using the general release fraction formula yields

(B-73)

$$RF = \frac{p(H_2O)}{(N/G)} k_{Cd} = f_{Cd} k_{Cd}$$

The model parameter f_{cd} is defined as the product of parameters available from the reference case equilibrium calculation. Using reference data, $f_{cd} = 0.61$ is the nominal value and a value of 1.0 would be conservative.

Jackson (1971) reports the free energy function, FEF, and Gibbs free energy of formation, which may be used to derive the required enthalpy of formation for the gas. Standard entropy data for the elements in cal/mol are as follows: O_2, 49.0; H_2, 31.21; and Cd, 12.3; yielding the dihydroxide entropy of formation of -23.2 cal/mol. Using $G_f = -82.353$ kcal/mol yields $H_f = -89.28$ kcal/mol = -373.55 kJ/mol. FEF data from references are given in Table B-10 and derived G(T) and k_{cd} values are given in Table B-11.

Table B-10. FEF Data from References

T (K)	FEF = - (G - H$_f$) / T (J/mol/K)		
	H$_2$O	CdO	Cd(OH)$_2$
500	192.69	60.43	297.02
1000	206.74	79.91	324.43
1500	218.52	95.59	347.92
H$_f$ (298) kJ/mol	-241.83	-258.10	-373.55

Table B-11. Equilibrium Constant Derived from Data

T (°K)	G (T) (kJ/mol)				k
	H$_2$O	CdO	Cd(OH)$_2$	ΔG	
500	-338.18	-288.32	-522.06	+104.43	1.23×10^{-11}
1000	-448.57	-338.0	-697.98	88.59	2.36×10^{-5}
1500	-569.61	-401.5	-895.43	75.68	2.31×10^{-3}

A linear fit to the equilibrium constant is chosen using values at 1000 °K and 1500 °K to embrace the temperature range of interest yielding

	A	B	C	D
k_{cd}	-3.093	0.0	0.0	13.74E3

Interpolating for 1000°C for reference, yields $k_{cd} = 4.5 \times 10^{-4}$ and RF = 1.8×10^{-4}. The condition RF < < 1 is satisfied even at 1500 °K.

B.4.2.13 Europium Release

Europium trihydroxide is formed by the oxidation of the oxide:

$$Eu_2O_3 + 3H_2O \rightarrow 2Eu(OH)_3 \tag{B-74}$$

and its release fraction is:

$$RF \ = \ \frac{1}{(N/G)} \ k_{Eu}^{1/2} \ p^{3/2} \ (H_2O) \ X^{-1/2} \ = \ f_{Eu} \ k_{Eu}^{1/2} \ X^{-1/2} \qquad (B\text{-}75)$$

where X represents the mole fraction of condensed oxide. Using reference case data yields $f_{Eu} = 0.38$ and a conservative value would be $f_{Eu} = 1.0$. Data referenced above were used to construct the following fit for the equilibrium constant:

	A	B	C	D
k_{Eu}	-169.261	-1.38860E-2	25.6259	35.2639E3

At 1000°K, the release fraction of Eu is 7.7×10^{-4}. Also considered were $Eu(OH)_2$ and $EuO(OH)$, but these had release fractions three orders of magnitude lower than $Eu(OH)_3$.

B.4.2.14 Yttrium Release

Yttrium has behavior similar to that of Europium suggesting

$$Y_2O_3 \ + \ 3H_2O \ \rightarrow \ 2Y(OH)_3 \ (g) \qquad (B\text{-}76)$$

and the release fraction is given by the formula in equation (B-75). The Y release fraction model parameter is identical to that of Eu, $f_y = 0.38$, and a conservative value would be $f_y = 1.0$.

Reference data were used to construct a fit to the equilibrium constant for Y release k_Y:

	A	B	C	D
k_Y	-164.892	-1.39069E-2	24.5193	77.6429E3

At 1000°C, the Y release fraction is only 2.7×10^{-10}. Release fractions for $YO(OH)$ and $Y(OH)_2$ were 5 and 9 orders of magnitude smaller, respectively.

B.4.2.15 Ruthenium Release

Ruthenium forms many oxidized gases, the most prominent of which for this study is given by:

$$RuO_2 + \frac{1}{2}H_2O + \frac{3}{4}O_2 \rightarrow RuO_3(OH) \qquad (B\text{-}77)$$

$$RF = \frac{k_{Ru}}{(N/G)} p^{1/2}(H_2O) \, p^{3/4}(O_2) = f_{Ru} \, k_{Ru} \qquad (B\text{-}78)$$

where $f_{Ru} = 0.35$ for reference conditions.

Reference data were used to construct a fit to the equilibrium constant k_{Ru}:

	A	B	C	D
k_{Ru}	-42.8913	-2.84264E-3	6.21320	10.3148E3

At 1000 °C, the release fraction of Ru is 8.5×10^{-4}, or nearly 0.1%. Releases of $RuO_2(OH)_2$, $RuO_2(OH)$, and $RuO(OH)_3$ were respectively 3, 4, and 6 orders of magnitude lower, and releases of $RuO(OH)_2$, $RuO(OH)$, $Ru(OH)_4$, $Ru(OH)_3$, and $Ru(OH)_2$ were considerably lower still.

B.4.2.16 Mercury Release

Mercury could either be a metal or an oxide in the waste. Obviously, the metal would be volatile and completely evaporated during an organic-nitrate reaction. JANAF data for HgO show that this compound has a positive free energy of formation above about 750°K, which implies that it is likely to decompose except in a very highly oxidizing environment. At 1000°K, its equilibrium constant of formation, equal to the oxygen pressure to the minus one half power, is about 0.003, implying equilibrium with 10^5 atm oxygen. Therefore mercury is assumed to be in volatile, metallic form following an organic-nitrate reaction, and fully released.

B.4.2.17 Release Fraction Summary

Release fraction models are summarized in Tables B-12 and B-13, which contain a summary of equilibrium constant parameter fits and release fraction formulas.

Results of the release fraction model as a function of temperature are summarized in Table B-14, where for those elements that require a mole fraction a value of 10^{-5} was chosen.

Table B-12. Release Fraction Model Summary

Element	Reaction and Formula	Parameter and Value
Cs	1: $CsNO_3 + \frac{1}{2}H_2O \rightarrow CsOH(l) + \frac{1}{2}N_2 + \frac{5}{4}O_2$ 2: $CsOH(l) \rightarrow CsOH$ $RF = \left[1 + \left(\frac{K_2G}{N}\right)^{-1}\left(1 + \frac{F_{cs}}{K_1}\right)\right]^{-1}$	$f_{cs} = \dfrac{p^{1/2}(N_2)\,p^{5/4}(O_2)}{p^{1/2}(H_2O)}$ $= 0.135$
Na	$NaOH(l) \rightarrow NaOH$ $RF = f_{Na}k$	$f_{Na} = \left(\frac{G}{N}\right)\dfrac{n(NaOH)}{n(NaOH) + n(Na_2CO_3)}$ $= 0.39$
Sr	$SrO + H_2O \rightarrow Sr(OH)_2$ $RF = F_{Sr}k$	$f_{Sr} = \left(\frac{G}{N}\right)\left(\frac{n(H_2O)}{G}\right)$ $= 0.61$
Co	$CoO + H_2O \rightarrow Co(OH)_2$ $RF = f_{Co}k$	$f_{Co} = \left(\frac{G}{N}\right)\left(\frac{n(H_2O)}{G}\right)$ $= 0.61$
Tc	$TcO3 + 1/4O2 \rightarrow 1/2Tc2O7$ $RF = f_{Tc}k^2x_{Tc}$	$f_{Tc} = \left(\frac{G}{N}\right)\left(\frac{n(O_2)}{G}\right)^{1/2}$ $= 0.76$
Te	$TeO + 1/2O_2 \rightarrow TeO_2$ $RF = f_{Te}k$	$f_{Te} = \left(\frac{G}{N}\right)\left(\frac{n(O_2)}{G}\right)^{1/2}$ $= 0.76$
Sb	$SbO_2 \rightarrow SbO + 1/2O_2$ $RF = k\,(f_{Sb} + k)^{-1}$	$f_{Sb} = \left(\frac{G}{N}\right)^{-1}\left(\frac{n(O_2)}{G}\right)^{1/2}$ $= 0.34$
Pu	$PuO_2 + H_2O + 1/2O_2 \rightarrow PuO_2(OH)_2$ $RF = f_{Pu}k$	$f_{Pu} = \left(\frac{G}{N}\right)\left(\frac{n(H_2O)}{G}\right)\left(\frac{n(O_2)}{G}\right)^{1/2}$ $= 0.31$
Eu	$Eu_2O_3 + 3H_2O \rightarrow 2Eu(OH)_3$ $RF = f_{Eu}k^{1/2}x_{Eu}^{-1/2}$	$f_{Eu} = \left(\frac{G}{N}\right)\left(\frac{n(H_2O)}{G}\right)^{3/2}$ $= 0.38$

Table B-12. Release Fraction Model Summary

Element	Reaction and Formula	Parameter and Value
Y	$Y_2O_3 + 3H_2O \rightarrow 2Y(OH)_3$ $RF = f_Y k^{1/2} x_Y^{-1/2}$	$f_Y = \left(\frac{G}{N}\right)\left(\frac{n(H_2O)}{G}\right)^{3/2}$ $= 0.38$
Ru	$RuO_2 + 1/2H_2O + 3/4O_2 \rightarrow RuO_3(OH)$ $RF = f_{Ru}^2 k$	$f_{Ru} = \left(\frac{G}{N}\right)\left(\frac{n(H_2O)}{G}\right)^{1/2}\left(\frac{n(O_2)}{G}\right)^{3/4}$ $= 0.35$
Cd	$CdO + H_2O \rightarrow Cd(OH)_2$ $RF^2 = f_{cd} k$	$f_{cd} = \left(\frac{G}{N}\right)\left(\frac{n(H_2O)}{G}\right)$ $= 0.61$

f = release parameter   G = total gas moles
k = equilibrium constant   N = total condensed moles
n( ) = number of moles   RF = release fraction
x = mole fraction

Table B-13. Equilibrium Constant Temperature-Dependent Fit Parameters

Condensed and Vapor Species	k(T) Parameters*			
	A	B	C	D
CsNO$_3$-CsOH(1)	-147.16 E+0	-7.4709 E-3	17.657 E+0	33.740 E+3
CsOH(1)-CsOH	-46.865 E+0	-6.4833 E-4	4.5528 E+0	19.108 E+3
NaOH(1)-NaOH	-62.046 E+0	-1.4764 E-3	6.5256 E+0	28.628 E+3
SrO-Sr(OH)2	-3.1999 E+0	6.1675 E-4	-6.4152 E-1	28.422 E+3
CoO-Co(OH)2	-16.742 E+0	-6.7107 E-5	1.6279 E+0	26.501 E+3
Tco3-Tc2o7	-17.836 E+0	6.4264 E-3	1.7959 E-1	6.3612 E+3
TeO-TeO2	27.397 E+0	8.2467 E-3	-6.8655 E+0	19.659 E+3
SbO2-SbO	-36.870 E+0	1.2933 E-3	4.0216 E-1	42.381 E+3
PuO2-PuO2(OH)2	1.355 E+0	0.0	0.0	21.350 E+3
Eu2O3-Eu(OH)3	-169.26 E+0	-1.3886 E-2	2.5626 E+1	3.5264 E+4
Y2O3-Y(OH)3	-164.89 E+0	-1.3907 E-2	2.4519 E+1	7.7643 E+4
RuO2-RuO3(OH)	-42.891 E+0	-2.8426 E-3	6.2132 E+0	1.0315 E+4
CdO-Cd(OH)2	-3.093 E+0	0.0	0.0	13.74 E+3

* $-\ln k = A + B * T + C * \ln(T) + D / T$

Table B-14. Fission Product Release Fractions

A. Parameters Values				
FCs: 0.135	FNa: 0.388	FSr: 0.610	FCo: 0.610	
FTc: 0.760	FTe: 0.760	FSb: 0.340	FPu: 0.310	
FEu: 0.390	FY: 0.390	FRu: 0.350	FCd: 0.610	

B. Release Fractions				
T (C)	Rf-Cs	Rf-Na	Rf-Sr	Rf-Co
500.0	1.582 E-06	1.265 E-08	7.171 E-14	3.096 E-13
600.0	5.571 E-04	4.606 E-07	4.911 E-12	1.296 E-11
700.0	2.581 E-02	7.645 E-06	1.404 E-10	2.474 E-10
800.0	1.554 E-01	7.257 E-05	2.136 E-09	2.687 E-09
900.0	3.892 E-01	4.570 E-04	2.033 E-08	1.920 E-08
1000.0	6.297 E-01	2.112 E-03	1.351 E-07	9.977 E-08
1100.0	7.935 E-01	7.686 E-03	6.775 E-07	4.044 E-07
T (C)	Rf-Tc	Rf-Te	Rf-Sb	Rf-Pu
500.0	7.473 E-03	9.998 E-07	1.199 E-09	8.131 E-14
600.0	1.303 E-02	1.858 E-05	5.345 E-07	1.922 E-12
700.0	1.549 E-02	1.734 E-04	6.591 E-05	2.371 E-11
800.0	1.398 E-02	9.775 E-04	3.212 E-03	1.831 E-10
900.0	1.029 E-02	3.765 E-03	7.334 E-02	9.982 E-10
1000.0	6.476 E-03	1.079 E-02	5.346 E-01	4.169 E-09
1100.0	3.609 E-03	2.448 E-02	9.171 E-01	1.414 E-08
T (C)	Rf-Eu	Rf-Y	Rf-Ru	Rf-Cd
500.0	1.841 E-06	1.037 E-17	2.434 E-05	2.574 E-07
600.0	1.057 E-05	1.471 E-15	7.001 E-05	1.970 E-06
700.0	4.202 E-05	7.525 E-14	1.597 E-04	9.926 E-06
800.0	1.300 E-04	1.871 E-12	3.103 E-04	3.700 E-05
900.0	3.372 E-04	2.748 E-11	5.378 E-04	1.102 E-04
1000.0	7.708 E-04	2.718 E-10	8.575 E-04	2.765 E-04
1100.0	1.606 E-03	1.986 E-09	1.285 E-03	6.067 E-04

B.4.2.18 Nomenclature

f   Release fraction multiplier
G   Total gas moles
k   Equilibrium constant
N   Total condensed moles
n( )   Number of moles
n_1 Moles $CsNO_3$
n_2 Moles CsOH, NaOH, or SrO
n_3 Moles CsOH(g), NaOH(g), or $Sr(OH)_2(g)$
n_o Initial Cs moles
p( )   Pressure, atmosphere
RF   Release fraction
x( )   Mole fraction

This page intentionally left blank.

B.5.0 TANK RESPONSE AND TRANSPORT MODELS

B.5.1 MODEL STRUCTURE

The tank response model is designed as a classical state-space representation with mass and energy as state variables and all other quantities such as temperature, pressure, and physical properties as auxiliary variables - an approach consistent with conservation of mass and energy. Thus, the mass of substance *i* in region *r* is a state variable described by the explicit differential equation:

$$\frac{dm_{ir}}{dt} = \sum W_{ijr} + S_{ir} + \sum W_{ipr} \qquad \text{(B-79)}$$

where m_{ir} = mass of compound i region r,

W_{ijr} = flow rate of compound i from j to r,

S_{ir} = source of compound i in r, and

W_{ipr} = flow rate of compound i within region r due to process p.

The total energy is described by

$$\frac{dU_r}{dt} = \sum W_{ijr} h_{ijr} + \sum S_{ir} h_r + \sum W_{ipr} h_p \qquad \text{(B-80)}$$

While these equations are mere bookkeeping, more important is evaluation of the enthalpy and internal energy of a region or source, as described below. The overall scheme into which such an evaluation fits is:

- Initialize State. Given initial conditions, initialize state variables: m_i and U.

- Auxiliary Variables. Get temperature T, pressure P, and physical properties given state variables.

- Rate Laws. Get rates of change for individual processes and assemble into overall derivatives of state variables.

- Integration. Update state variables, and go to Step 2 above.

Initialization of state variables and calculation of auxiliary variables, the first two steps, are discussed under Region Thermodynamics below. Separate sections follow to discuss various phenomena contributing to rate laws: intercompartmental flow, aerosol behavior, and heat trans-fer to structures.

B.5.2 REGION THERMODYNAMICS

B.5.2.1 Thermodynamic Model

Region thermodynamic models serve three functions:

- Initialize state variables - mass and energy,
- Compute pressure and temperatures, and
- Compute aerosol formation/disappearance potential.

For temperatures and pressures of interest, a non-ideal gas model considering the second virial coefficient, temperature-dependent specific heats, and the non-ideal gas contribution to energy is excellent for treating water vapor, the least ideal of the gases. Thus, pressure is given by

$$P = \sum P_i = \sum (R_i T) \left(\frac{1}{v_i} + \frac{B_i}{v_i^2} \right)$$

$$= (RT) \sum \left(\frac{n_i}{V} \right) \left(1 + \frac{B_i M_i n_i}{V} \right)$$

(B-81)

Given the initial pressure, temperature, and mole fractions, equation (B-81) is solved for the total gas moles and then the initial mass of each gas follows. The initial energy is found by

$$U = \sum m_i u_i (T, v_i) = \sum m_i \left(u_{io} (T) + \Delta u_i (T, v_i) \right)$$

(B-82)

where the term u_{io} represents the integral of the temperature-dependent specific heat, including a reference value, and Δu_i represents the contribution arising from a nonzero B_i.

When mass and total energy are known, equation (B-82) is solved iteratively for the temperature, and subsequently equation (B-81) is solved for the pressure.

When aerosols are present, the term

$$\sum m_{ai} u_{ai} (T)$$

(B-83)

is added to the total energy. In general, the resulting temperature can represent a nonequilib-rium state for vapor species, i.e., it may be true that the vapor pressure exceeds saturation, in which case aerosols (fog) should form, or it may be that aerosols exist but the calculated vapor pressure is less than saturation, in which case the aerosols should evaporate. Rates of aerosol formation and disappearance are discussed later, but the model requires the equilibrium state. The equilibrium state is found by solving equation (B-82) together with the constraints:

$$P_i \leq P_{sat,i} (T)$$

(B-84a)

$$m_{i,tot} = m_i + m_{ai}$$

(B-84b)

which means that the aerosol and gas masses are adjusted during the iteration for temperature, and the resulting equilibrium values are saved for reference by the aerosol models.

B.5.2.2 Validation

Essential thermodynamic model features requiring validation are:

- Constitutive Relations. An increment in system internal energy should yield the correct increment in pressure and temperature.

- Aerosol Equilibrium. An initially nonequilibrium state requiring forma-tion or depletion of aerosols should evolve to the correct equilibrium state.

- Dynamic Evolution. A system with mass inflows and outflows should have the correct pressure and temperature history, illustrating correct conservation laws and property calculations.

Constitutive relations are validated for the non-ideal gas steam by using steam table data. A reference state is defined, and states with the same specific volume at higher energies are identified as shown in Table B-15. By initializing a region to the reference state and then adding an energy source, the higher energy states should be duplicated. The precision of this procedure depends upon the integral agreement between the curve fits for $c_v(T)$ and B(T) with the steam table values (Keenan et al. 1978). Very good agreement is shown in Table B-15 over a large temperature range from an initially supersaturated state to a high super-heated state. It is also notable that the non-ideal gas contribution to the internal energy is about 20% of the ideal contribution for the initial condition, so the model must be correct in order for agreement to be achieved.

The fog (aerosol) formation model is checked by a sample problem with an initially supersaturated vapor (relative humidity greater than 100%). When fog forms, the gas temperature increases and at equilibrium the relative humidity is 100%. The temperature rise and aerosol mass are given by:

$$\Delta T = \frac{m_{io} (RH - 1) / RH}{\dfrac{C_o}{u_{fg}} + \dfrac{m_{io} \theta}{RH}}$$

(B-85a)

$$m_{ai} = \frac{C_o}{u_{fg}} \Delta T$$

(B-85b)

Table B-15. Constitutive Relation Validation				
A. Steam Table State (Keenan et al. 1978)				
v (m^3/kg)	P (MPa)	T (°C)	u (kJ/kg)	Δu (kJ/kg)
0.4011	0.46	145	2551.8	0
0.4010	0.72	360	2895.6	343.8
0.4011	1.00	600	3296.8	745.0
0.4034	1.80	1300	4679.5	2127.7

B. Calculated State		
$\Delta U = \Delta u/v$ (kJ)	P (MPa)	T (°C)
0.0	0.46	145
857.4	0.721	363
1857.9	1.00	604
5306.0	1.81	1305

$$\theta = \frac{1}{P_{sat}} \frac{d\,P_{sat}}{dT} - \frac{1}{T}$$

(B-85c)

where m_{io} = Initial vapor mass, kg,
 RH = Relative humidity,
 C_o = Gas heat capacity, J/K, and
 u_{fg} = Energy change of vaporization, J/kg.

Table B-16 contains the sample problem initial conditions, analytical solution, and output of the calculation, illustrating very good agreement. The reason for a few percent error is that the derivative dP_{sat}/dT varies over the range of ΔT so that the linear analytical extrapolation is imperfect.

Table B-16. Fog Formation Sample Problem

A.	Initial Quantities			
	Temperature	T_o	323	°K
	Saturation Pressure	P_{sat}	12350	Pa
	Pressure Derivative	dP_{sat} / dT	636	Pa/°K
	Internal Energy Change	u_{fg}	2.23	MJ/kg
	Steam Mole Fraction		0.15	
	Nitrogen Mole Fraction		0.85	
	Steam Specific Heat		1409.	J/kg-°K
	Nitrogen Specific Heat		739.	J/kg-°K
	Steam Mass	m_{io}	0.1006	kg
	Relative Humidity	RH_{io}	1.2	
	Nitrogen Mass		0.8871	kg
	Gas Heat Capacity	C_o	798	J/°K
B.	Analytical Solution			
	Parameter	θ	4.840E-2	
	Temperature Rise		3.80	°K
	Aerosol Mass		1.36E-3	kg
C.	Code Output			
	Temperature Rise		3.74	°K
	Aerosol Mass		1.39E-3	kg

B.5.2.3 Nomenclature

B_i Second virial coefficient, m^3/kg,
m_{ai} Mass of aerosol i, kg,
m_i Mass of gas i, kg,
M_i Molecular weight, gas i, kg/kg·mole,
n_i Moles of gas i,
P Total pressure, Pa,
P_i Partial pressure of gas i, Pa,
R_i Gas constant, gas i,
T Temperature, K,
u_i Internal energy gas i, J/kg,
u_{ia} Internal energy aerosol i, J/kg,
V Volume, m^3, and
v_i Specific volume of gas i, m^3/kg.

B.5.3 SURFACE HEAT TRANSFER MODEL

B.5.3.1 Finite Difference Solution for Heat Sink Temperature

ORNATE includes a model for heat transfer from a gas region to a passive heat sink, such as the tank sidewalls or dome. Using an implicit finite difference formulation, the model solves the one-dimensional conduction equation subject to the boundary conditions specified for each heat sink surface. Pertinent features of the model are as follows:

- Up to ten heat sinks are allowed.
- Heat sinks can be planar or cylindrical.
- Each heat is subdivided into as many as 10 slabs.
- Volumetric heat generation can be included.

For a plane wall heat sink with constant thermal properties, the one-dimensional conduction equation is written as:

$$\frac{\partial^2 T}{\partial x^2} + \frac{Q}{k} = \frac{1}{\alpha}\frac{\partial T}{\partial t} \tag{B-86}$$

where Q is the volumetric heat generation rate, k is the thermal conductivity, and α is the thermal diffusivity. For a cylinder with constant thermal properties, the one-dimensional conduction equation is:

$$\frac{1}{r}\frac{\partial}{\partial r}\left(r\frac{\partial T}{\partial r}\right) + \frac{Q}{k} = \frac{1}{\alpha}\frac{\partial T}{\partial t} \tag{B-87}$$

A finite difference formulation of either equation is:

$$A_n T_{n-1} + B_n T_n + C_n T_{n+1} = D_n \tag{B-88}$$

where, for an implicit solution, the temperatures are at the end of the time step.

Once the coefficients in equation (B-88) are known, the temperature distribution is found by standard tridiagonal matrix inversion routines. There are fourteen different sets of coefficients, depending on the geometry: planar or cylindrical; the type of slab: inner surface, interior node, or outer surface; and boundary conditions at the inner and outer surfaces: convective, adiabatic, or constant temperature. Table B-17 lists the coefficient values for interior nodes (nodes 2 through 9) for both planar and cylindrical geometries. Table B-18 lists the coefficient values for the inner surface (node 10) of the heat sink, for both geometries and all three boundary conditions. Table B-19 lists the coefficient values for the outer surface (node 1) of the heat sink, for both geometries and all three boundary conditions.

Table B-17. Implicit Finite Difference Temperature Coefficients
- Interior Nodes

	A_n	B_n	C_n	D_n
Planar	$- 1.0$	$2 + F_o$	$- 1.0$	$T_q + F_o T'_n$
Cylindrical	$-\left(r + \dfrac{\Delta r}{2}\right)/$	$2 + F_o$	$-\left(r - \dfrac{\Delta r}{2}\right)/$	$T_q + F_o T'_n$

NOTES:

(1)
$$F_o = \frac{\Delta x^2}{2 \alpha \Delta t}$$

(2)
$$T_q = \frac{Q}{K \Delta x^2}$$

(3) T'_n is the temperature at the current time step.

(4) r is the radius of the center of the node.

B.5.3.2 Heat Transfer to Heat Sink Surfaces

The finite difference scheme described above requires net heat transfer to inner and outer heat surfaces as part of the boundary conditions. First, it must be decided whether condensation can occur for any of the species in the region. For each gas, condensation occurs if:

$$P_{sat}(T_w) < Min(P_i, P_{sat}(T_g)) \tag{B-89}$$

where $P_{sat}(T_g)$ is the saturation pressure at the bulk gas temperature, $P_{sat}(T_w)$ is the saturation pressure at the wall temperature, and P_i is the partial pressure.

If condensation cannot occur, heat transfer from the gas to the wall is based only on natural convection and radiation. A single heat transfer correlation is used:

$$Nu = 0.12 (Pr \cdot Gr)^{0.33} \tag{B-90}$$

where Pr is the Prandtl number, and Gr is the Grashof number. The Prandtl number is defined as,

$$Pr = \frac{\mu_g C_{pg}}{k_g} \tag{B-91}$$

Table B-18. Implicit Finite Difference Temperature Coefficients - Inner Surface

	T_a	h_a	T_{qa}	A_n	B_n	C_n	D_n
Planar - Convection	T_g	0.0	$\dfrac{Q_{wa}}{A\Delta xK}$	0.0	$Bi_a + \dfrac{F_o}{2} + 1.0$	-1.0	$Bi_a T_a + \dfrac{T'_n F_o}{2} + \dfrac{T_q}{2} + T_{qa}$
Planar - Insulated	273.15K	0.0	0.0	0.0	$Bi_a + \dfrac{F_o}{2} + 1.0$	-1.0	$Bi_a T_a + \dfrac{T'_n F_o}{2} + \dfrac{T_q}{2} + T_{qa}$
Planar - Fixed Temp.	T_o	10^6	0.0	0.0	$Bi_a + \dfrac{F_o}{2} + 1.0$	-1.0	$Bi_a T_a + \dfrac{T'_n F_o}{2} + \dfrac{T_q}{2} + T_{qa}$
Cylindrical -	T_g	0.0	$\dfrac{Q_{wa}}{A\Delta xK}$	0.0	$Bi_a \dfrac{r_i}{r} + \dfrac{F_o}{2} + \left(r - \dfrac{\Delta r}{4}\right)/r$	$-\left(r - \dfrac{\Delta r}{4}\right)/r$	$Bi_a \dfrac{r_i}{r} T_a + \dfrac{F_o T'_n}{2} + \dfrac{T_q}{2} + T_{qa}$
Cylindrical - Insulated	273.15K	0.0	0.0	0.0	$Bi_a \dfrac{r_i}{r} + \dfrac{F_o}{2} + \left(r - \dfrac{\Delta r}{4}\right)/r$	$-\left(r - \dfrac{\Delta r}{4}\right)/r$	$Bi_a \dfrac{r_i}{r} T_a + \dfrac{F_o T'_n}{2} + \dfrac{T_q}{2} + T_{qa}$
Cylindrical - Fixed	T_o	10^6	0.0	0.0	$Bi_a \dfrac{r_i}{r} + \dfrac{F_o}{2} + \left(r - \dfrac{\Delta r}{4}\right)/r$	$-\left(r - \dfrac{\Delta r}{4}\right)/r$	$Bi_a \dfrac{r_i}{r} T_a + \dfrac{F_o T'_n}{2} + \dfrac{T_q}{2} + T_{qa}$

Notes:

(1) T_a is the bulk gas temperature.
(3) h_a is the heat transfer coefficient.
(5) A is the one-sided heat sink area.
(7) Bi_a is the slab Biot number, $h_a A\Delta x/K$.
(9) T'_n is the current temperature.

(2) T_g is the region gas temperature.
(4) Q_{wa} is the total heat transfer rate from gas to wall.
(6) T_o is the fixed temperature.
(8) r_i is the radius of the inner surface of the heat sink.

Table B-19. Implicit Finite Difference Temperature Coefficients - Outer Surface

	T_b	h_b	T_{qb}	A_n	B_n	C_n	D_n
Planar - Convection	T_g	0.0	$\frac{Q_{wb}}{A\Delta x K}$	-1.0	$Bi_b + \frac{F_o}{2} + 1.0$	0.0	$Bi_b T_b + \frac{F_o}{2} T'_n + \frac{T_g}{2} + T_{qb}$
Planar - Insulated	273.15K	0.0	0.0	-1.0	$Bi_b + \frac{F_o}{2} + 1.0$	0.0	$Bi_b T_b + \frac{F_o}{2} T'_n + \frac{T_g}{2} + T_{qb}$
Planar - Fixed Temp.	T_o	10^6	0.0	-1.0	$Bi_b + \frac{F_o}{2} + 1.0$	0.0	$Bi_b T_b + \frac{F_o}{2} T'_n + \frac{T_g}{2} + T_{qb}$
Cylindrical -	T_g	0.0	$\frac{Q_{wb}}{A\Delta x K}$	$-\left(r + \frac{\Delta r}{4}\right)/r$	$Bi_b \frac{r_o}{r} + \frac{F_o}{2} + \frac{r+(\Delta r/4)}{r}$	0.0	$Bi_b \frac{r_o}{r} T_b + \frac{F_o}{2} T'_n + \frac{T_g}{2} + T_{qb}$
Cylindrical - Insulated	273.15K	0.0	0.0	$-\left(r + \frac{\Delta r}{4}\right)/r$	$Bi_b \frac{r_o}{r} + \frac{F_o}{2} + \frac{r+(\Delta r/4)}{r}$	0.0	$Bi_b \frac{r_o}{r} T_b + \frac{F_o}{2} T'_n + \frac{T_g}{2} + T_{qb}$
Cylindrical - Fixed	T_o	10^6	0.0	$-\left(r + \frac{\Delta r}{4}\right)/r$	$Bi_b \frac{r_o}{r} + \frac{F_o}{2} + \frac{r+(\Delta r/4)}{r}$	0.0	$Bi_b \frac{r_o}{r} T_b + \frac{F_o}{2} T'_n + \frac{T_g}{2} + T_{qb}$

Notes:
(1) T_b is the bulk gas temperature.
(2) T_g is the region gas temperature.
(3) h_b is the heat transfer coefficient.
(4) Q_{wb} is the total heat transfer rate from gas to wall.
(5) A is the one-sided heat sink area.
(6) T_o is the fixed temperature.
(7) Bi_b is the slab Biot number, $h_b A \Delta x / K$.
(8) r_o is the radius of the outer surface of the heat sink.
(9) T'_n is the current temperature.

where μ_g is the dynamic viscosity of the gas, C_{pg} is the specific heat of the gas, and k_g is the thermal conductivity of the gas. The Grashof number is

$$Gr = \frac{g \beta (T_w - T_g) L^3}{\left(\frac{\mu_g}{\rho_g}\right)^2} \qquad (B-92)$$

where g is the acceleration of gravity, β is the ideal gas expansion coefficient, T_g is the gas temperature, T_w is the wall temperature, L is the heat sink characteristic dimension, and ρ_g is the gas density. The natural convection heat transfer coefficient is then:

$$h_c = \frac{Nu \, k_g}{L} \qquad (B-93)$$

Radiation heat transfer from the gas to the heat sink is described by the following heat transfer coefficient:

$$h_r = \sigma \epsilon \left(T_g^2 + T_w^2\right) \left(T_g + T_w\right) \qquad (B-94)$$

where σ is the Stefan-Boltzmann constant, and ϵ is the heat sink emissivity. Net heat transfer to the heat sink is then:

$$Q_w = \left(h_c + h_r\right) A \left(T_g - T_w\right) \qquad (B-95)$$

where A is the heat sink one-sided surface area.

If condensation occurs, the condensate film interface temperature is found iteratively. The gas-to-interface heat transfer rate must be equal to the sum of the conduction heat transfer rate through the liquid and the energy carried by the film:

$$Q_g \left(T_f\right) = Q_w \left(T_f\right) + Q_f \left(T_f\right) \qquad (B-96)$$

where Q_g is the heat transfer from the gas to the film, including convection, radiation, and condensation; Q_w is conduction through the liquid layer; and Q_f is the energy carried away by the film. This can be re-written

$$F \left(T_f\right) = Q_g \left(T_f\right) - Q_w \left(T_f\right) - Q_f \left(T_f\right) \qquad (B-97)$$

and equation (B-96) is true if F approaches zero.

The iterative scheme proceeds as follows:

1. Guess the interface temperature.

2. Calculate convective and radiative sensible heat transfer in the same manner as the case described above with no condensation; i.e., equation (B-95).

3. Use log-mean pressure difference P_{am}, if the atmosphere is not pure:

$$P_{am} = \frac{P_i - P_{sat}}{\log\left(\dfrac{P - P_{sat}}{P - P_i}\right)} \tag{B-98}$$

    where P is the total pressure and P_{sat} is the saturation pressure.

4. Define the Schmidt number, Sc, by

$$Sc = \frac{\mu_g \, v_g}{D} \tag{B-99}$$

    where μ_g is the viscosity, v_g is the specific volume, and D is the diffusivity.

5. Calculate the Prandtl number, as defined by equation (B-91).

6. Evaluate the mass transfer coefficient using the Reynold's analogy between heat and mass transfer:

$$h_m = \frac{h_c \left(\dfrac{Pr}{Sc}\right)^{0.66}}{C_{pg} \, P_{am} \, M_w} \tag{B-100}$$

    where M_w is the molecular weight.

7. Repeat 1 through 6 for each gas.

8. Total condensation rate is then:

$$W_c = \sum_{j=1}^{N} h_{mj} \, A \, (P_j - P_{satj}) \tag{B-101}$$

    where N is the number of gases.

9. Total energy of the film is:

$$Q_f = \sum_{j=1}^{N} W_{cj} \left[i_{\ell j} - \frac{3}{4} C_{p\ell j} (T_f - T_w) \right] \tag{B-102}$$

where i_ℓ is the specific enthalpy of liquid, and $C_{p\ell}$ is the liquid specific heat.

10. Total heat transfer rate from the gas to the film is:

$$Q_g = (h_c + h_r) A (T_g - T_f) + \sum_{j=1}^{N} i_{gj} A (P_j - P_{satj}) h_{gj} \tag{B-103}$$

where i_{gj} is the specific enthalpy of gas j.

11. Conduction heat transfer through the liquid is given by:

$$Q_w = 0.943 \left[\frac{g \, \rho_\ell (\rho_\ell - \rho_g) \, k_\ell^3 \, i'_{fg}}{L \, \mu_\ell} \right]^{\frac{1}{4}} (T_f - T_w)^{\frac{3}{4}} A \tag{B-104}$$

where g is the acceleration of gravity,
        ρ_ℓ is the liquid density,
        ρ_g is the gas density,
        k_ℓ is the liquid conductivity,
        i'_{fg} is equal to $i_{fg} + 3/8 \, C_{p\ell} (T_f - T_w)$,   (B-105)
        i_{fg} is latent heat of evaporation,
        $C_{p\ell}$ is the liquid specific heat,
        μ_ℓ is the dynamic viscosity of the liquid, and
        T_w is the wall temperature.

12. The residual, F, is given by:

$$F = Q_g - Q_w - Q_f \tag{B-106}$$

13. The derivative of the residual with respect to temperature is used to update T_{fi} and is given by:

$$\frac{dF}{dT} = \frac{dQ_g}{dT} - \frac{dQ_w}{dT} - \frac{dQ_f}{dT} \tag{B-107}$$

14. An updated guess for T_{fi} is given by the well-known Newton method.

$$T_{fi} = T_{fi}^{old} - F \, (dF/dT)^{-1} \tag{B-108}$$

15. Repeat 1 through 14 until the energy imbalance is less than 0.001%, or the temperature resolution is better than 0.0001%, or 30 iterations have passed.

Because the film consists of an arbitrary number of species, liquid properties must be appropriate averages based on the pure liquid properties. The film mixture specific heat, latent heat of vaporization, and specific volume are based on a mass fraction weighted-average. For example, the specific heat of the film mixture is:

$$C_{p\ell} = \sum_{j=1}^{N} C_{p\ell j} \, x_j \tag{B-109}$$

where
$$x_j = \frac{W_{cj}}{\sum_{j=1}^{N} W_{cj}} \tag{B-110}$$

Film mixture values for kinematic viscosity and thermal conductivity are slightly more complicated. Film mixture kinematic viscosity is based on a mole fraction weighted-average:

$$\nu_\ell = \exp \left\{ \sum_{j=1}^{N} n_j \, \log \nu_{\ell j} \right\} \tag{B-111}$$

where n_j is defined as:

$$n_j = \frac{\dfrac{W_{cj}}{MW_j}}{\sum_{j=1}^{N} \dfrac{W_{cj}}{MW_j}} \tag{B-112}$$

The Li equation gives the film mixture thermal conductivity (Reid et al. 1987):

$$k_\ell = \sum_{i=1}^{N} \sum_{j=1}^{N} \phi_i \, \phi_j \, k_{\ell ij} \tag{B-113}$$

where (B-114)

$$k_{\ell ij} = \frac{2}{\dfrac{1}{k_{\ell i}} + \dfrac{1}{k_{\ell j}}}$$

and ϕ_i (or ϕ_j) is the volume fraction of pure liquid i (or j). Volume fraction is given by:

(B-115)

$$\phi_i = \frac{n_i \dfrac{MW_i}{\rho_{\ell i}}}{\sum_{i=1}^{N} \dfrac{n_i MW_i}{\rho_{\ell i}}}$$

B.5.3.3 Heat Transfer Model Validation

The model for heat transfer to passive heat sinks can be validated using the problem of a one-dimensional slab exposed at time zero to a fluid at constant temperature T_∞ on one surface, and insulated on the other. The slab has thickness L, uniform initial temperature T_i, thermal conductivity k, specific heat c, and density ρ. Consider the following values for the validation problem:

```
L    =  10 cm,
T∞   =  100°C,
Tᵢ   =  200°C,
k    =  0.5 W/m·K,
c    =  500 J/kg·K,
ρ    =  5000 kg/m³, and,
α    =  2.0E-7 m²/s.
```

ORNATE simulation of this problem uses a single region with one plane wall heat sink. Models for junction flow, organic-nitrate reactions, aerosol settling, etc., are neglected. The region volume is made extremely large (1 x 10^{10} m³) to keep the temperature constant regardless of any heat transfer to/from the heat sink. Initial gas temperature is 100°C, initial pressure is 100,000 Pa, and the region is 80% oxygen, 20% nitrogen by volume. The heat sink has the dimensions and thermal properties noted above, with no volumetric heat generation. Characteristic height, which is used to determine the natural convection heat transfer coefficient, is 10 m, and the heat sink one-sided surface area is 100 m².

Analytical solutions to this problem are approximate because the heat transfer coefficient is a function of the surface temperature. ORNATE's model gives the heat transfer coefficient, h, to the fluid as the combined sum of the natural convection heat transfer coefficient given by equation (B-93) and the radiation heat transfer coefficient given by equation (B-94). The approach here is to compare ORNATE results against approximate analytical solutions

using a constant heat transfer coefficient. Initially, the slab temperature profile can be approximated by the solution for a semi-infinite slab exposed at time zero to a fluid with constant h (Incropera, 1981):

$$\frac{T(x, t) - T_i}{T_\infty - T_i} = \text{erfc}\left(\frac{x}{2\sqrt{\alpha t}}\right) - \left[\exp\left(\frac{hx}{k} + \frac{h^2\alpha t}{k^2}\right)\right]\left[\text{erfc}\left(\frac{x}{2\sqrt{\alpha t}} + \frac{h\sqrt{\alpha t}}{k}\right)\right]$$

(B-116)

Equation (B-116) applies if the transient time is much less than the time constant for conduction (L^2 / α), which is 50,000 seconds. The heat transfer coefficient h is evaluated using equations (B-93) and (B-94), assuming T_∞ = 100°C, T_i = 200°C, and the thermal properties of the gas are the thermal properties of air at 400 K. The natural convection heat transfer coefficient is 5 W/m^2·K, and the radiative natural convection is 12 W/m^2·K, for a total of 17 W/m^2·K. For the first 50,000 seconds of the transient, Table B-20 compares the surface temperature as predicted by equation (B-116) against ORNATE results. For the first 10,000 seconds, the two sets of results are in good agreement. Afterwards, the slab is no longer semi-infinite and the heat transfer coefficient is no longer 17 W/m^2·K.

If the heat sink no longer behaves as if it were semi-infinite, Heisler charts can be used to estimate the temperature at the adiabatic surface and the temperature distribution in the heat sink. For the problem statement, Heisler charts give a non-dimensional solution assuming h is constant (Incropera and Dewitt 1981). Non-dimensional temperature at the adiabatic surface, θ_L, is defined by:

(B-117)

$$\theta_L = \frac{T_L - T_\infty}{T_i - T_\infty}$$

Table B-20. Comparison of the Semi-Infinite Slab Solution for Surface
Temperature (T_o) with ORNATE Results

Time (seconds)	ORNATE (°C)	Analytical (°C)	Absolute Error[1] (%)
0	200.000	200.000	0.00
100	189.114	184.915	0.92
200	182.145	179.706	0.54
300	177.370	176.052	0.29
400	173.879	173.179	0.16
500	171.177	170.792	0.09
600	168.986	168.743	0.06
700	167.143	166.943	0.05
800	165.549	165.338	0.05
900	164.143	163.888	0.06
1000	162.880	162.565	0.07
2000	154.448	153.387	0.25
3000	149.454	147.797	0.39
4000	145.928	143.829	0.50
5000	143.225	140.788	0.59
10000	135.135	131.826	0.82
20000	126.662	124.023	0.66
30000	120.804	120.130	0.17
40000	116.295	117.680	− 0.35
50000	112.791	115.954	− 0.81

[1] Absolute error is defined as:

$$\frac{\text{ORNATE Temp.} - \text{Analytical Temp.}}{\text{Analytical Temp.} + 273.15 \text{ K}}$$

where T_L is the temperature at the adiabatic surface. Values for θ_L are plotted as a function of the Fourier number ($\alpha t/L^2$) and the inverse Biot number (k/hL). Temperature distribution through the slab is expressed non-dimensionally as

$$\theta = \frac{T - T_\infty}{T_L - T_\infty}$$

(B-118)

Heisler charts express θ as a function of the inverse Biot number and the non-dimensional coordinate, x/L.

Initially, the inverse Biot number is 0.3, but it increases over the course of the transient as the natural convection and radiation heat transfer coefficients decrease. Assuming T_o = 110°C, the natural convection heat transfer coefficient is 2.3 W/m²·K, and the radiation heat transfer coefficient is 8.6 W/m²·K, for a total of 10.9 W/m²·K. Inverse Biot number is then 0.45. During the course of the transient, the inverse Biot number starts at 0.30 and approaches 0.45, roughly.

Table B-21 shows a comparison of ORNATE results with analytical results using the Heisler charts. Results are in good agreement, although the comparison is limited by the ability to read the charts and the assumption of constant heat transfer coefficient. Nevertheless, Tables B-20 and B-21 validate the ORNATE heat transfer model.

B.5.4 AEROSOL MODEL

B.5.4.1 Mass Balance Approach

Aerosol transport and deposition are modeled via mass balance equations for the total aerosol mass in each control volume. The particle size distribution of aerosols is considered implicitly by the deposition models through a correlation technique (Epstein and Ellison 1988)

Table B-21. Comparison of ORNATE Results With Analytical Results Obtained
from Heisler Charts

Time (seconds)	ORNATE Results T_o (°C)	ORNATE Results T_L (°C)	F_o	Bi^{-1}	Analytical Results T_o (°C)	Analytical Results T_L (°C)
50,000	130.523	112.791	1	0.3	130	111.
100,000	108.673	103.920	2	0.4	109	104.
150,000	102.636	101.250	3	0.4	103	101.
200,000	100.833	100.408	4	0.4	100.6	100.2
250,000	100.266	100.133	5	0.4	100.2	100.1

as explained below. Validation of the method is abundantly described in the
references (Vaughan and von Arx 1988) and an example with the present code is
presented here.

The mass balance of aerosols of compound i is written

$$\frac{dm_i}{dt} = - \lambda_{dep} \, m_i - \lambda_{out} \, m_i + \sum \lambda_{in} \, m_{i,don} + S_i \tag{B-119}$$

where
m_i = Mass of aerosol compound i, kg,
λ_{dep} = Deposition rate constant, 1/s,
λ_{out} = Outflow rate constant, 1/s,
λ_{in} = Inflow rate constant on a given flow path, 1/s,
$m_{i,don}$ = Donor region aerosol mass, kg, and
S_i = Source, kg/s.

Note that, when required, information on the particle size is encoded into
λ_{dep}.

B.5.4.2 Transport and Condensation

For transport between volumes, the rate constant is simply the fractional
volumetric flow rate, hence, it is independent of particle size:

$$\lambda_{out} = \frac{W_g}{\rho_g \, V_{don}} \tag{B-120}$$

where
W_g = Flow rate along path, kg/s,
ρ_g = Density, kg/m³, and
V_{don} = Volume of donor region, m³.

The equation applies for inflow and outflow.

Aerosol deposition in tanks occur by condensation and sedimentation. Condensation removal is independent of particle size and is written as

$$\lambda_{cond} = \frac{W_{cond}}{\rho_g V} \tag{B-121}$$

B.5.4.3 Sedimentation

Aerosol sedimentation is particle-size dependent and correlations that implicitly account for particle size are used for two dimensionless rate constants, chosen based on the source strength (Epstein and Ellison 1988):

$$\lambda_{sed}^{ss} = C_\lambda \Lambda_{sed}^{ss} \tag{B-122a}$$

$$\lambda_{sed}^{D} = C_\lambda \Lambda_{sed}^{D} \tag{B-122b}$$

where

λ_{sed}^{ss} = Steady-state sedimentation rate,

λ_{sed}^{D} = Decay sedimentation rate,

C_λ = Scaling factor for λ, and

Λ = Dimensionless sedimentation rate.

The dimensionless rates are correlated to a dimensionless mass:

$$\Lambda_{sed}^{ss} = 0.226 \, M^{0.282} (1 + 0.189 \, M^{0.8})^{0.695} \tag{B-123a}$$

$$\Lambda_{sed}^{D} = 0.528 \, M^{0.235} (1 + 0.473 \, M^{0.754})^{0.786} \tag{B-123b}$$

and the dimensionless mass is related to the <u>total</u> aerosol mass

$$m = C_m \, M \tag{B-124}$$

Note that the total aerosol mass m ultimately is correlated to λ_{sed} and the same λ_{sed} is used for all compounds present as aerosols. This is the results of two important modeling assumptions:

- Intimate coagulation/homogeneous aerosol. All aerosol particles are regarded as having the same chemical composition due to the rapidity of coagulation versus settling.

- Polydisperse universal size distribution. The aerosol size distribution is assumed to conform to one of two universal, source-independent dimensionless distributions, which is usually an excellent approximation.

The difference between a "steady-state" and "decaying" aerosol, and the choice between correlations, remain to be explained. A steady-state aerosol is one in equilibrium with its source, so that

$$\frac{dm}{dt} \approx 0 \qquad \text{and} \qquad \lambda_{sed}^{ss} m \approx S \qquad \text{(B-125a)}$$

A decaying aerosol is one with a negligible source, so that its mass must decrease, i.e., decay with time:

$$\frac{dm}{dt} \approx -\lambda_{sed}^{D} m \qquad \text{(B-125b)}$$

A choice between, or an interpolation between, the steady-state and decay distribution is made as follows. When the source exceeds the fallout rate in equation (B-119a), λ_{sed}^{ss} is selected, and when the source is very weak as in equation (B-119b), λ_{sed}^{D} is selected. Interpolation occurs when the fallout rate is near the source rate. When outflow of aerosols is strong, the deposition rate is influenced as described by (Epstein and Ellison 1988) and the formulas for λ_{sed} are adjusted.

B.5.4.4 Validation

Implementation of the aerosol modeling is validated by comparison to the well-known AB-5 experiment conducted at Hanford (Hilliard et al. 1983). In this experiment, a sodium vapor source reacted to produce sodium oxide aerosol during a source period of 900 s into a volume of 850 m^3 at a rate of 0.444 kg/s.

Figure B-18 illustrates the suspended mass versus time as both measured and using the present code and correlation technique. Results are considered very good - within a factor of two for a suspend mass history spanning four orders of magnitude.

B.5.5 GAS FLOW MODEL

B.5.5.1 Model Equations

Gas flow between compartments or to the environment is calculated using the standard compressible flow equation for pressure-driven flow and accounting for the possibility of

Figure B-18.   Suspended Mass History for AB-5 Data (boxes) and Prediction (line).
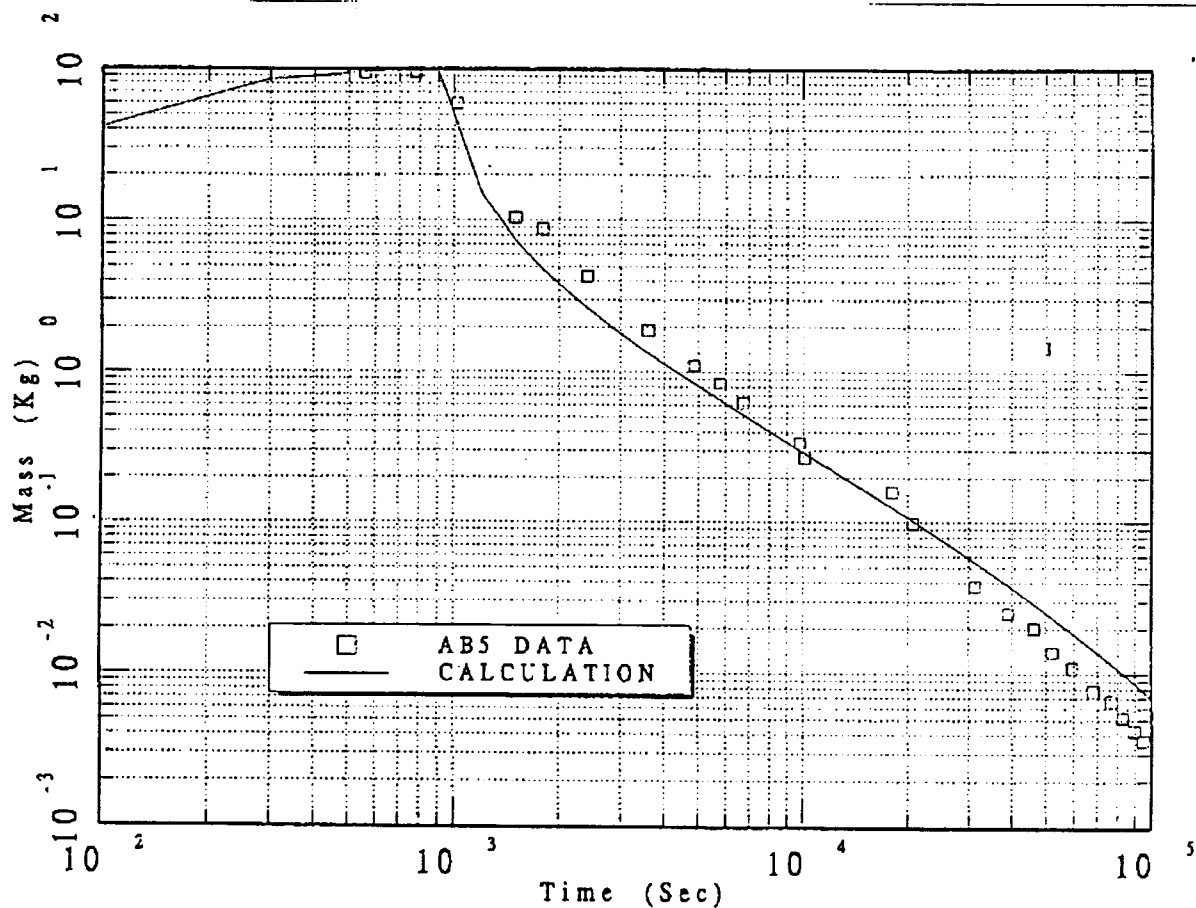
choking. A rather complex numerical scheme is employed to assure numerical stability because multiple flow paths may exist from a given region (for example, there may be several vent lines on a tank). Flow occurs between the region of higher upstream pressure P_{up} to the region of lower downstream pressure P_{dn} and is choked when the pressure ratio P_{up}/P_{dn} is less than the critical pressure ratio:

$$r_{crit} = \left(\frac{2}{1+\gamma}\right)^{\frac{\gamma}{\gamma-1}}$$ (B-126)

The pressure ratio used is the minimum:

$$r = \min\left(r_{crit}, \; P_{dn}/P_{up}\right)$$ (B-127)

and the mass flowrate is given by:

$$W_j = C_o A \left[\frac{2\gamma P_{up} \rho}{\gamma-1} \; r^{2/\gamma}\left(1 - r^{\frac{\gamma-1}{\gamma}}\right)\right]^{\frac{1}{2}}$$ (B-128)

where C_o is the loss coefficient and γ and ρ are upstream quantities.

All flowrates through junctions between regions are solved simultaneously by recasting the single-junction flow equation as

$$P_{upj} - P_{dnj} = K_j W_j \left|W_j\right|$$ (B-129)

where the effective coefficient K_j is derived from the compressible formula for W_j and the known pressure difference. Flowrates are found so that the equation above is true for end of timestep pressures, for example,

$$P_{upj} = P\left(m_{upj}^{ex}, \; U_{upj}^{ex}\right) - \rho_{upj}^{ex} g \, z_{upj}$$ (B-130)

where the superscript ex indicates an extrapolated value and the pressure in the region is corrected for static head at the junction elevation through the second term.

Extrapolated gas masses and energies are found by incrementing the beginning of timestep values using known source rates and the current guess for the flowrate of each junction. Extrapolated pressure and temperature are found by the same technique normally used for a control volume. Newton's method is used to converge on the flowrates.

B.5.5.2 Model Validation

An integral check of the junction flow model, conservation of mass and energy, and correct property calculations for flow between compartments is prediction of the pressure history for a region with a fixed inlet source rate and a fixed outlet downstream pressure. Rates of change of mass temperature and pressure for an ideal gas in an adiabatic region with these flows are:

$$\frac{dm}{dt} = W_s - W_o \tag{B-131}$$

$$\frac{dT}{dt} = \left(\frac{W_s}{m}\right)(\gamma T_s - T) + \left(\frac{W_o}{m}\right)(\gamma - 1)\, T \tag{B-132}$$

$$\frac{dP}{dt} = \left(\frac{\gamma RT}{MV}\right)\left(W_s \frac{T_s}{T} - W_o\right) \tag{B-133}$$

where W_s and T_s are the constant source flowrate and temperature, W_o is the outlet flowrate found from the compressible flow relation, and the ideal gas of molecular weight M and specific heat ratio γ applies to the source and the region initial conditions. The preceding simple equations are easily solved numerically (pressure dependence of W_o makes analytic solution impossible) and are verifiable because the pressure equation is redundant (the ideal gas law provides P given m and T).

A test case is defined in Table B-22 illustrating an "overdriven" source wherein a maximum in pressure is obtained because the outflow rate depends upon both gas density and pressure. Figure B-2 shows the pressure history and achievement of a steady-state with equal region and source temperatures and a pressure high enough to equate source and vent flows. ORNATE results are identical to the simplified equations. From the test case data, the ideal gas law, and final pressure, the final region density is 0.1886 kg/m^3, the pressure ratio is 0.893, and in the calculation $\gamma = 1.4$. The corresponding outflow rate from equation (B-128) is 1.01 kg/s, indicating close approach to the steady-state as expected.

Table B-22. Test Case Values

Parameter	Value	Units
Volume	850	m^3
Pressure	10^5	Pa
Temperature	300	°K
Specific heat	830	J/kg·°K
Molecular weight	28	kg/kg·mole
Sink Pressure	10^5	Pa
Vent area	0.03	m^2
Vent coefficient	0.5345	$(1/\sqrt{3.5})$
Source rate	1.0	Kg/s
Source temperature	2000	°K

Figure B-19.   Pressure History for Ideal Gas Source and Outflow Test Case –
Program and Simple Model Results are Identical
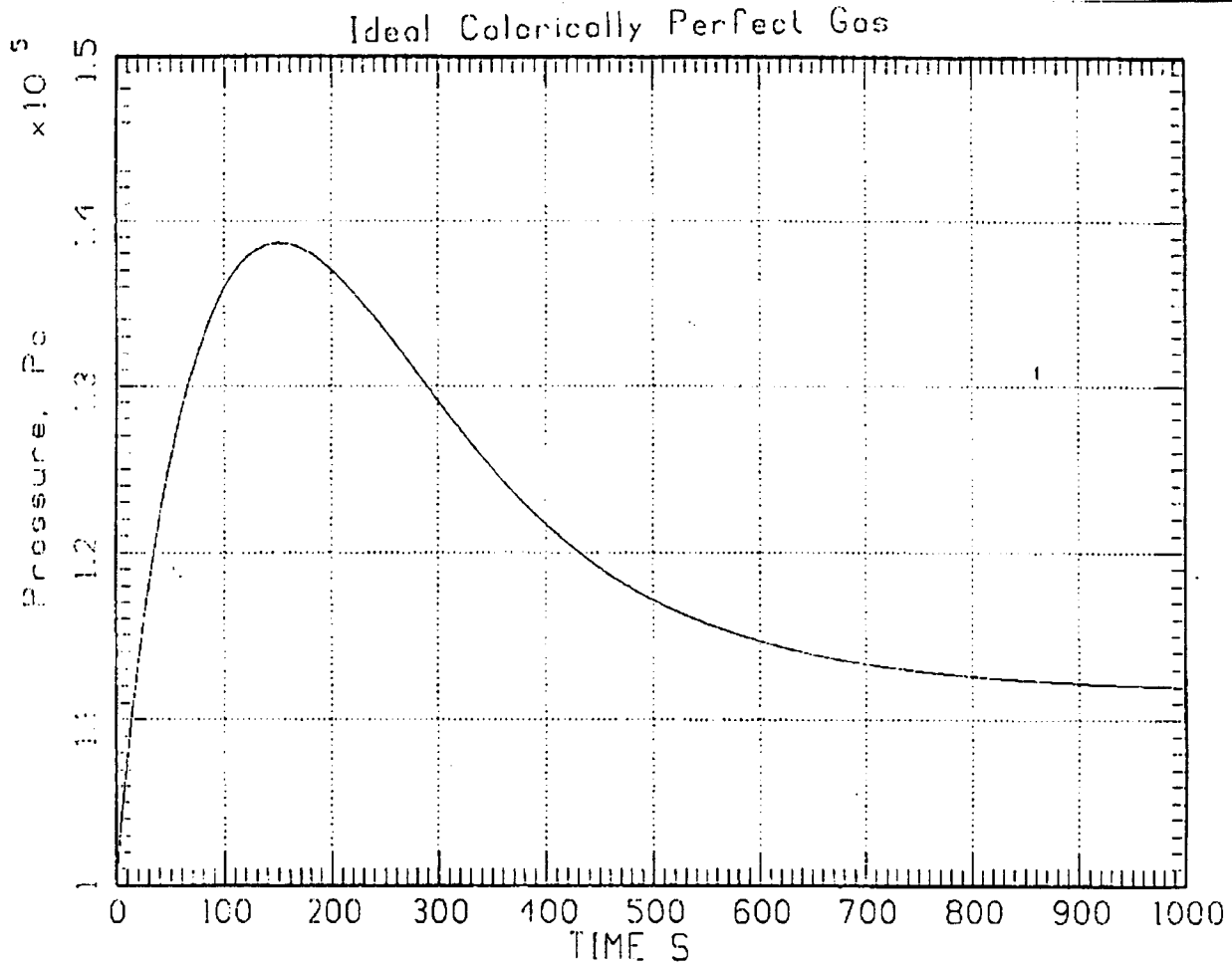
B.6.0 EXAMPLE CALCULATIONS

B.6.1 SST RESPONSE CALCULATIONS

A parametric study of single shell tank (SST) response to a condensed phase organic-nitrate reaction and a detailed example transient are presented here. Key parameters varied were: the volume of the reactive waste, TOC and moisture level in the reactive waste, and the headspace volume. Parameters were selected to represent 100-series SSTs and hypothetical reactive waste in them. The 200-series tanks, which are considerably smaller, are not considered here. Key outputs of interest are the release fraction of each radioactive and toxic specie and whether the tank pressurizes sufficiently to pop out the HEPA filter (0.1 bar overpressure) or to fail the dome (0.75 bar overpressure). First, the parametric run results are presented. Then, an example transient is discussed in detail. The example transient is also repeated with additional venting through a twelve-inch riser and a cascade line.

B.6.2 RELEASES INTO AN SST HEADSPACE

The release fraction of each specie depends only on the reaction temperature, which in turn is determined by the TOC and moisture content of the waste. Table B-23 summarizes reaction temperatures for eleven pairs of TOC and moisture level and corresponding release fractions for each specie. The eleven pairs were selected to envelop a range of TOC and moisture in reactive waste. As expected, high TOC and low moisture yields high reaction temperature. In fact, the reaction temperature is closely tied to the reaction propagation criteria. In this parametric study, the reaction temperature varied from $1060°K$ (6% TOC and 5% moisture) to $1410°K$ (9% TOC and 10% moisture). The corresponding variation in CsOH release fraction was 18% to 87%.

Table B-23. Release Fraction from Reaction.

TOC	H2O	Tslud	Cs	Sr	Co	Tc	Sb	Pu	Eu	Y	Ru	Cd	Na	Hg
0.06	0.05	1060.0	1.8E-01	2.5E-09	3.3E-09	6.7E-08	2.7E-03	1.4E-10	1.8E-03	5.8E-11	8.2E-04	3.3E-09	2.9E-05	1.0
0.07	0.05	1196.7	5.2E-01	5.4E-08	4.8E-08	4.4E-08	1.7E-01	1.4E-09	6.7E-03	2.2E-09	1.7E-03	4.8E-08	3.5E-04	1.0
0.07	0.10	1136.7	3.6E-01	1.5E-08	1.6E-08	5.5E-08	3.5E-02	5.6E-10	3.9E-03	4.9E-10	1.3E-03	1.6E-08	1.3E-04	1.0
0.07	0.15	1076.7	2.1E-01	3.8E-09	4.8E-09	6.5E-08	4.9E-03	2.0E-10	2.2E-03	9.4E-11	9.1E-04	4.8E-09	4.0E-05	1.0
0.08	0.05	1333.3	7.9E-01	6.0E-07	3.9E-07	2.2E-08	8.6E-01	8.9E-09	1.9E-02	4.2E-08	3.1E-03	3.9E-07	2.4E-03	1.0
0.08	0.10	1273.3	7.0E-01	2.2E-07	1.6E-07	3.0E-08	6.1E-01	4.2E-09	1.2E-02	1.2E-08	2.5E-03	1.6E-07	1.1E-03	1.0
0.08	0.15	1213.3	5.7E-01	7.4E-08	6.3E-08	4.1E-08	2.5E-01	1.8E-09	7.7E-03	3.3E-09	1.9E-03	6.3E-08	4.5E-04	1.0
0.08	0.20	1153.3	4.1E-01	2.2E-08	2.2E-08	5.2E-08	5.6E-02	7.3E-10	4.5E-03	7.6E-10	1.4E-03	2.2E-08	1.7E-04	1.0
0.09	0.10	1410.0	8.7E-01	1.9E-06	1.1E-06	1.3E-08	9.7E-01	2.1E-08	3.3E-02	1.8E-07	4.2E-03	1.1E-06	6.1E-03	1.0
0.09	0.15	1350.0	8.1E-01	7.8E-07	4.9E-07	2.0E-08	9.0E-01	1.1E-08	2.2E-02	5.8E-08	3.4E-03	4.9E-07	3.0E-03	1.0
0.09	0.20	1290.0	7.3E-01	3.0E-07	2.1E-07	2.8E-08	7.0E-01	5.2E-09	1.4E-02	1.8E-08	2.6E-03	2.1E-07	1.4E-03	1.0

Released Amount = * *Amount in the Reacted Waste*
* *Release Fraction from Reaction*
* *Release Fraction from Tank*

B.6.3 RELEASES TO THE ENVIRONMENT

Only a fraction of released material entering the headspace gets released to the environment. This release fraction from the tank depends on the specific sequence but is the same for all species because species in aerosol form are coagglomerated.

Figures B-20 to B-30 show the family of curves for release fraction from a tank as a function of reacted waste volume for various headspace volumes. The release fraction from tank is only a few percent when the reacted waste volume is a tenth of a cubic meter and approaches one hundred percent as reacted waste volume reaches tens of cubic meter. Thus, the tank can trap significant portion of airborne aerosol when the reaction is less extensive but relieves most of the airborne aerosol for a large reaction.

Plotted on the same graphs are the points where the HEPA filter pops out and where the dome fails. Although the exact amounts vary depending on the TOC and moisture pair and the headspace volume, in general, HEPA filter pops out when about a tenth of a cubic meter of waste is reacted and the dome fails when about twenty cubic meters of waste are reacted.

B.6.4 OVERALL RELEASE FRACTIONS

The waste release fraction table and the family of curves for release fraction from tank completely characterize the source term from condensed phase reactions. That is, the amount of a particular specie released to the environment can be determined by:

Released Amount = Amount in the Reacted Waste x Release Fraction from Reaction x Release Fraction from Tank

Consider for example a case of two cubic meters of reactive waste with 7% TOC and 10% moisture in a tank with a 1657 m^3 headspace volume. We would like to determine how much Cesium-137 will be released to the environment due to a condensed phase reaction. The super-tank activity concentration for Cesium-137 is 7.5E10 Bq/L (or 2000 curie/m^3). In two cubic meters of waste, we have 1.5E14 Bq (or 4100 curie) of Cesium-137 activity. From Table B-23 the reaction temperature is 1136.7 K and the corresponding CsOH release fraction is 36%. The release fraction from the tank can be read from Figure B-26 as 25%. Hence, the activity of Cesium-137 released to environment due to a solid phase reaction is 1.5E14 x 0.36 x 0.25 = 1.4E13 Bq (or 365 curie). Also, from Figure B-26 we determine that the HEPA filter has failed.

Figure B-20. Release Fraction from Tank, TOC = 0.06, H_2O = 0.05

Figure B-21. Release Fraction from Tank, TOC = 0.07, H_2O = 0.05

Fig. 6-2 Release Fraction from Tank, TOC=0.07 H2O=0.05

Figure B-22. Release Fraction from Tank, TOC = 0.07, H_2O = 0.10

Fig. 6-3   Release Fraction from Tank, TOC=0.07   H2O=0.10

Figure B-23.   Release Fraction from Tank, TOC = 0.07, H_2O = 0.15
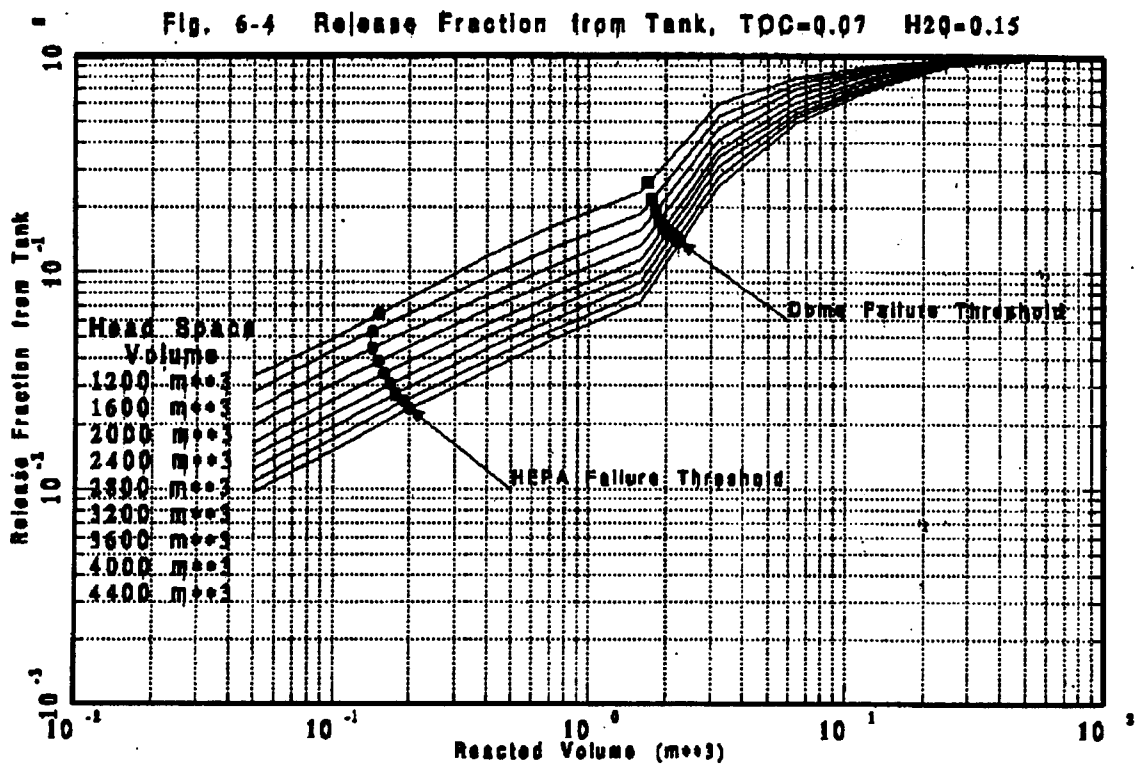
Figure B-24.   Release Fraction from Tank, TOC = 0.08, H_2O = 0.05
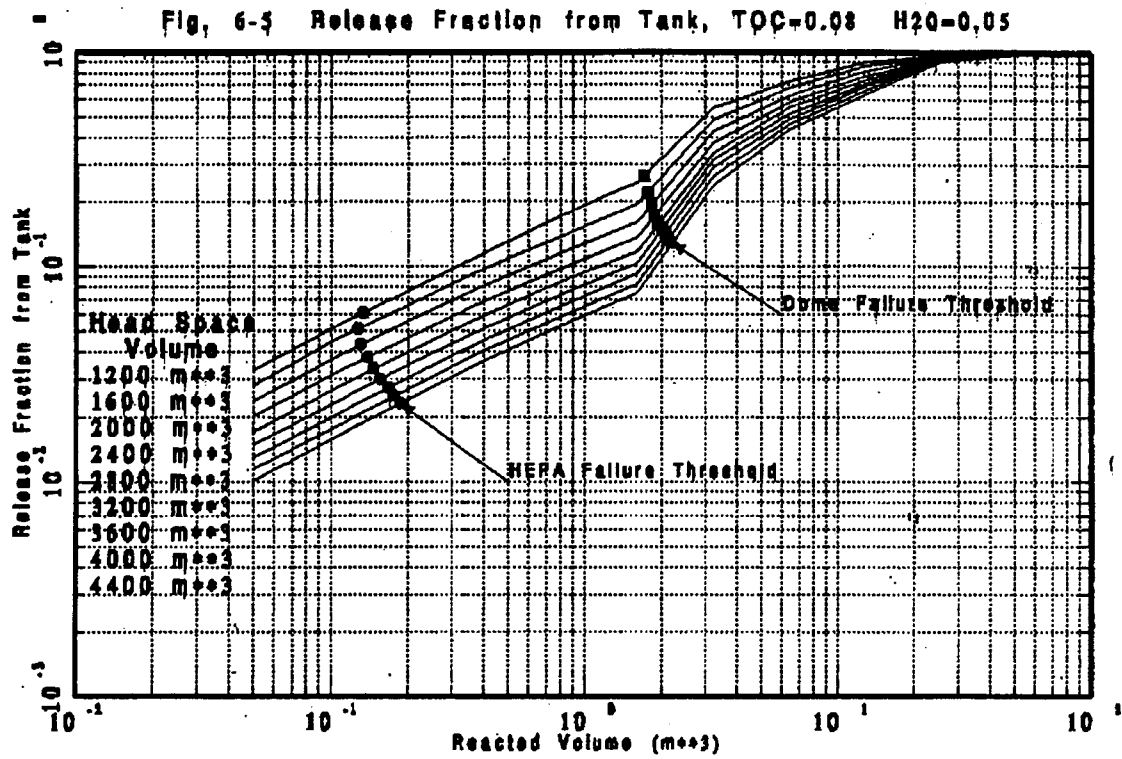
Figure B-25.   Release Fraction from Tank, TOC = 0.08, H_2O = 0.10
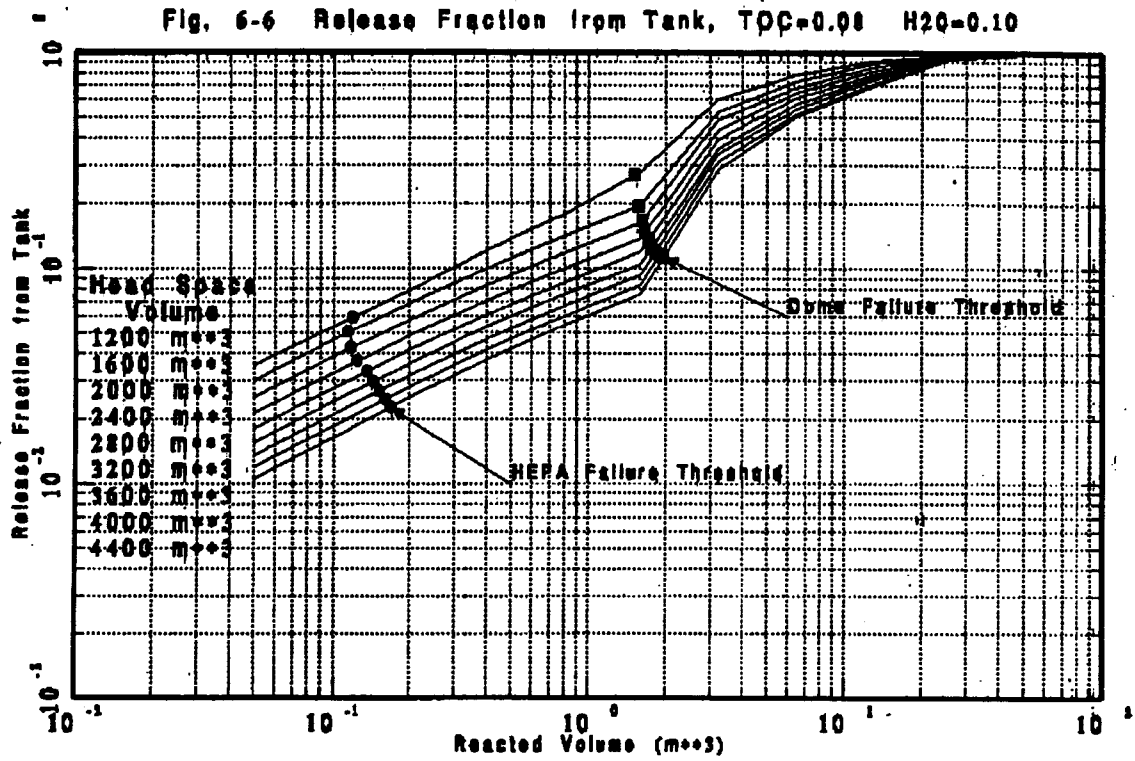
Figure B-26.   Release Fraction from Tank, TOC = 0.08, H_2O = 0.15
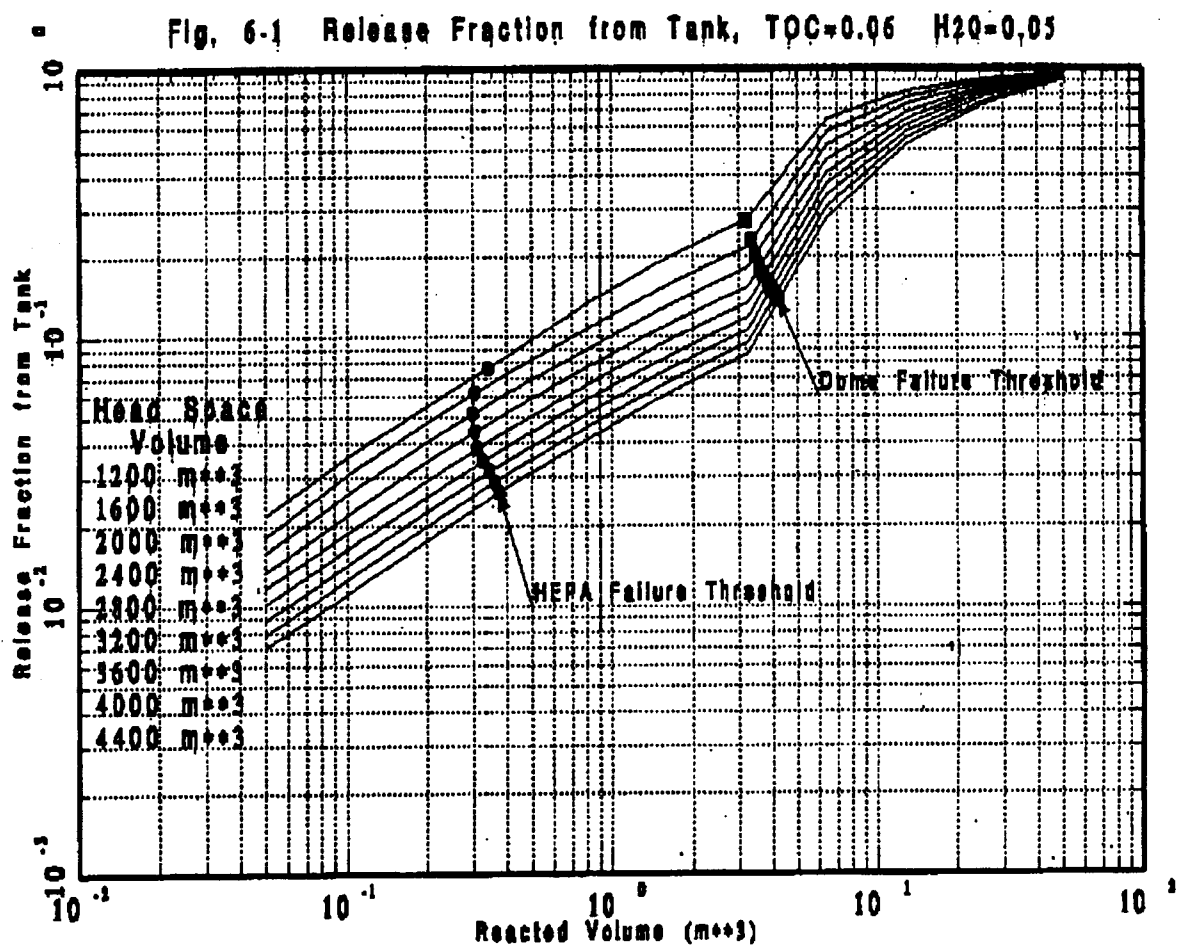
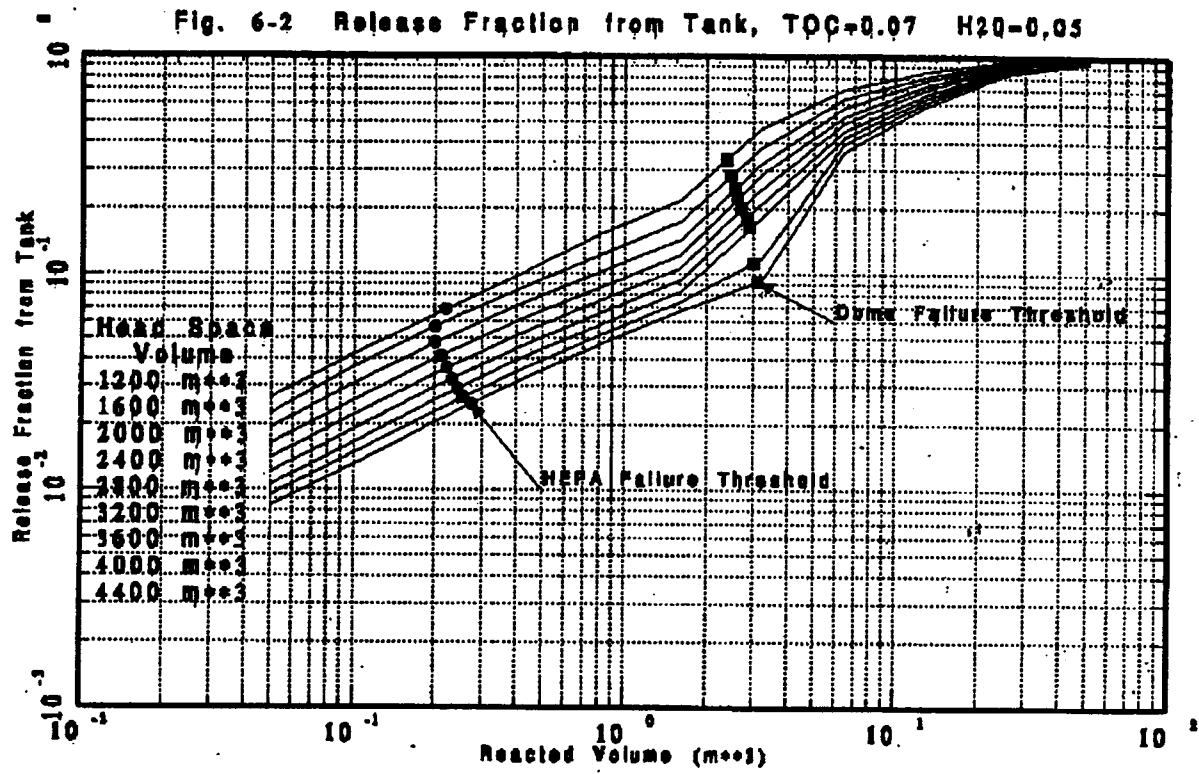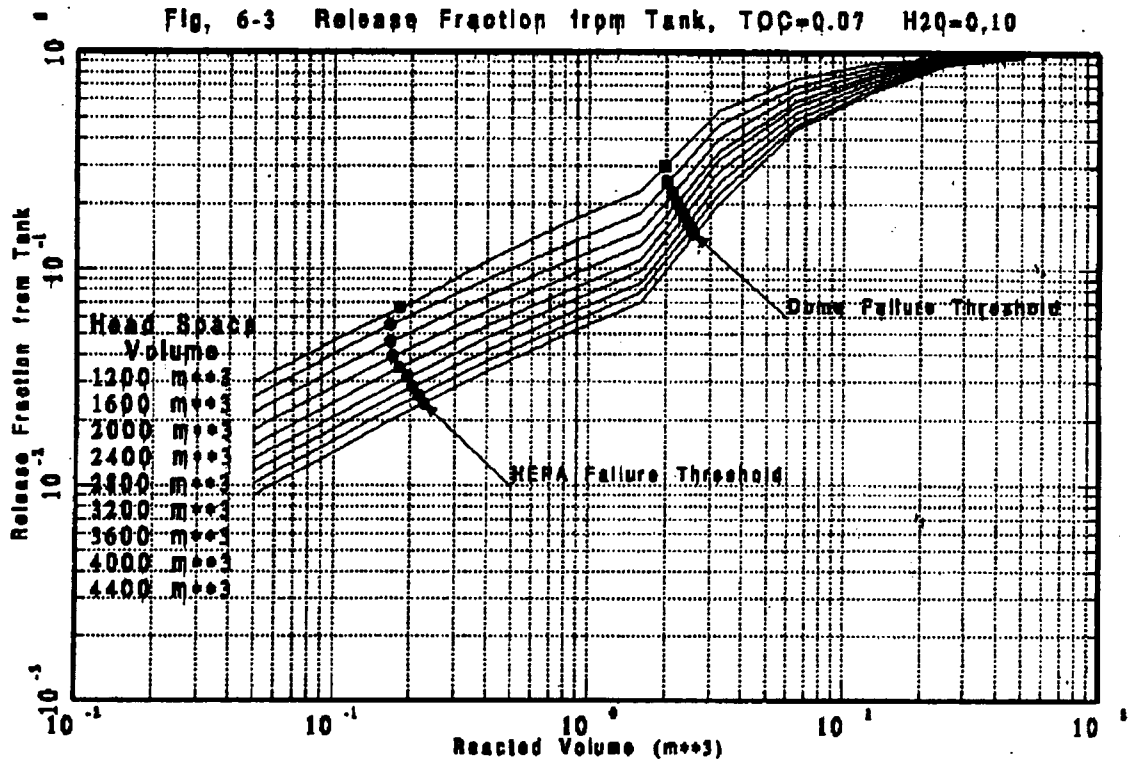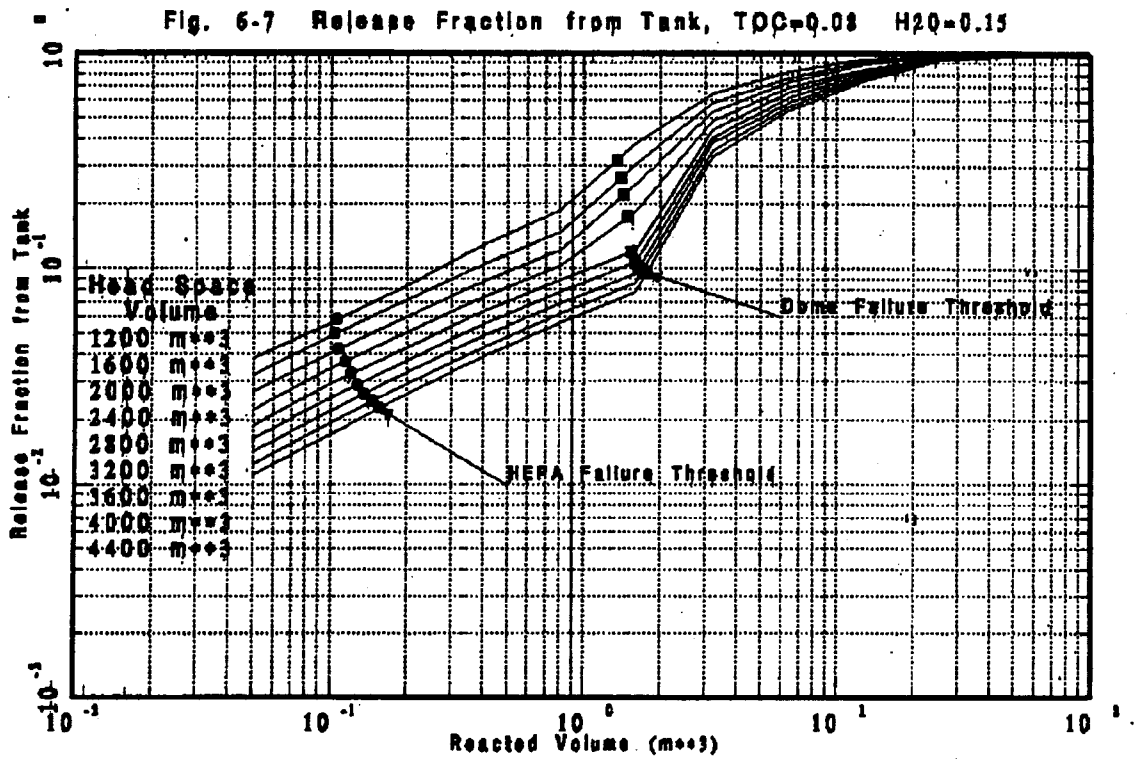Figure B-27. Release Fraction from Tank, TOC = 0.08, H_2O = 0.20
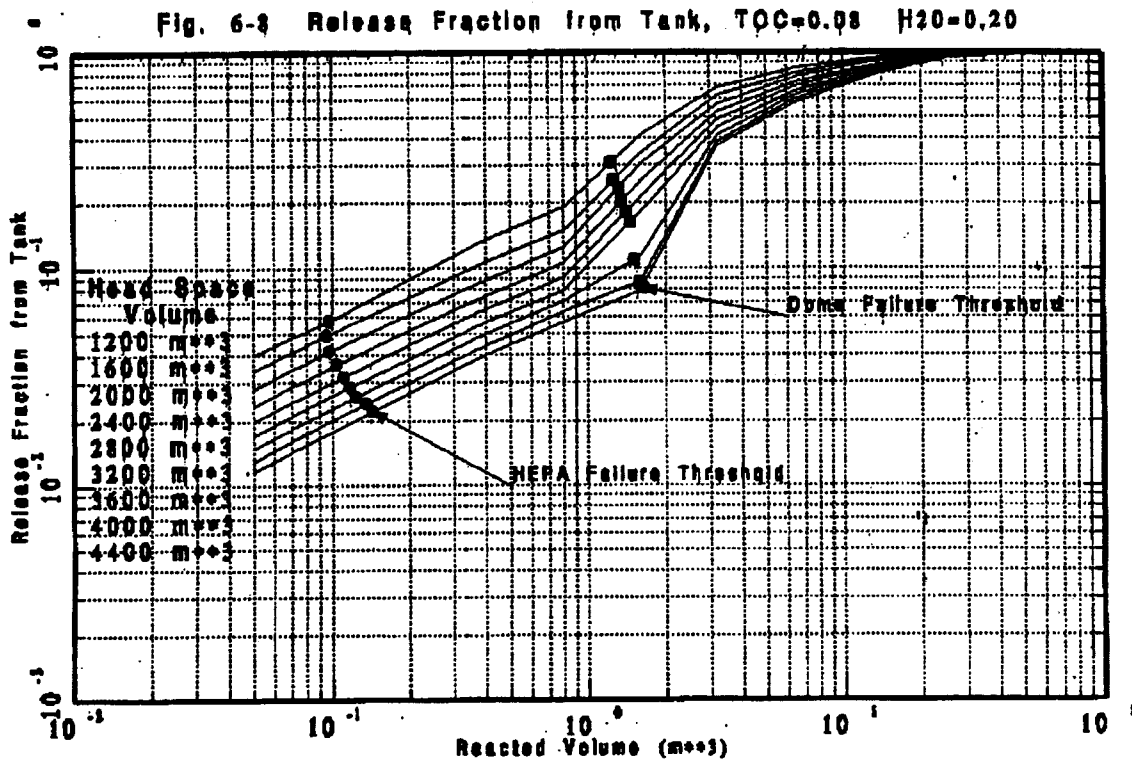
Figure B-28. Release Fraction from Tank, TOC = 0.09, H_2O = 0.10
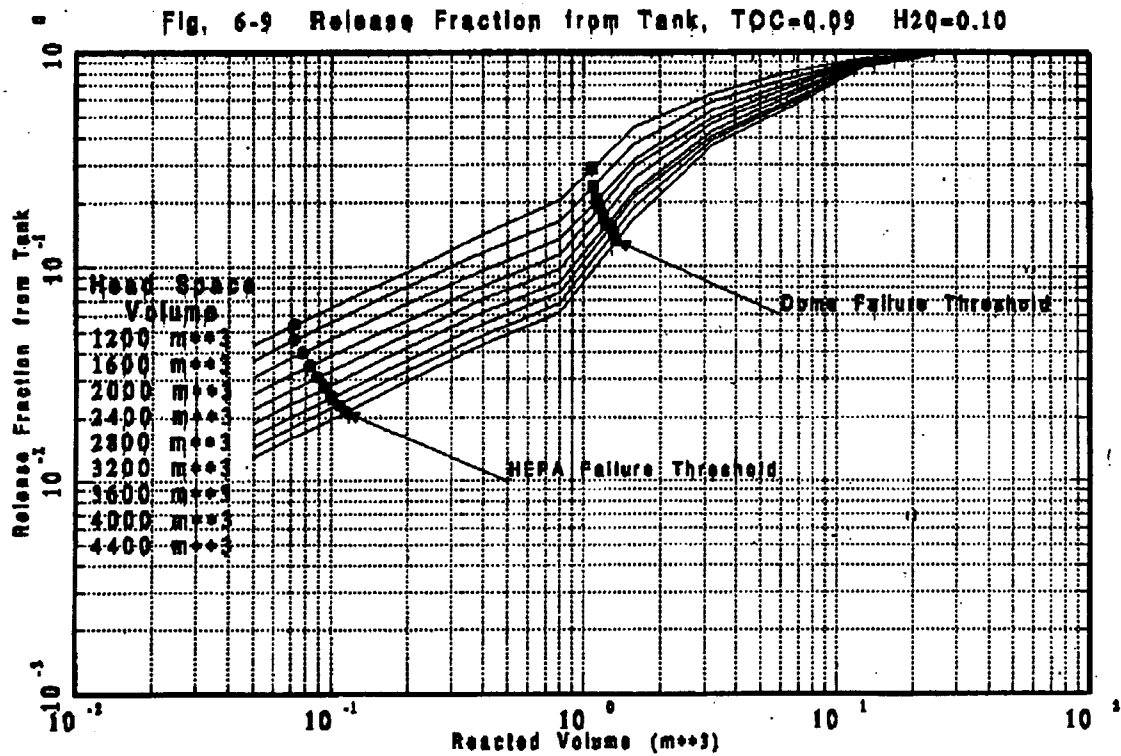
Figure B-29. Release Fraction from Tank, TOC = 0.09, H_2O = 0.15
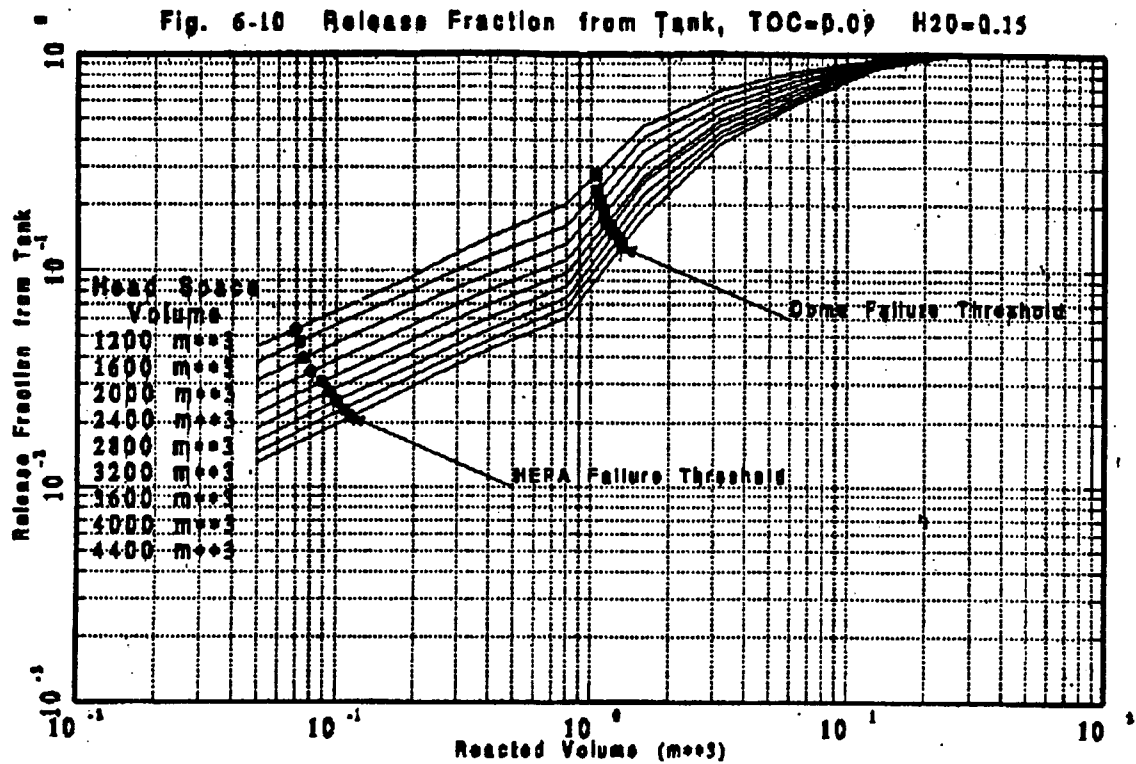
Figure B-30.   Release Fraction from Tank, TOC = 0.09, H_2O = 0.20
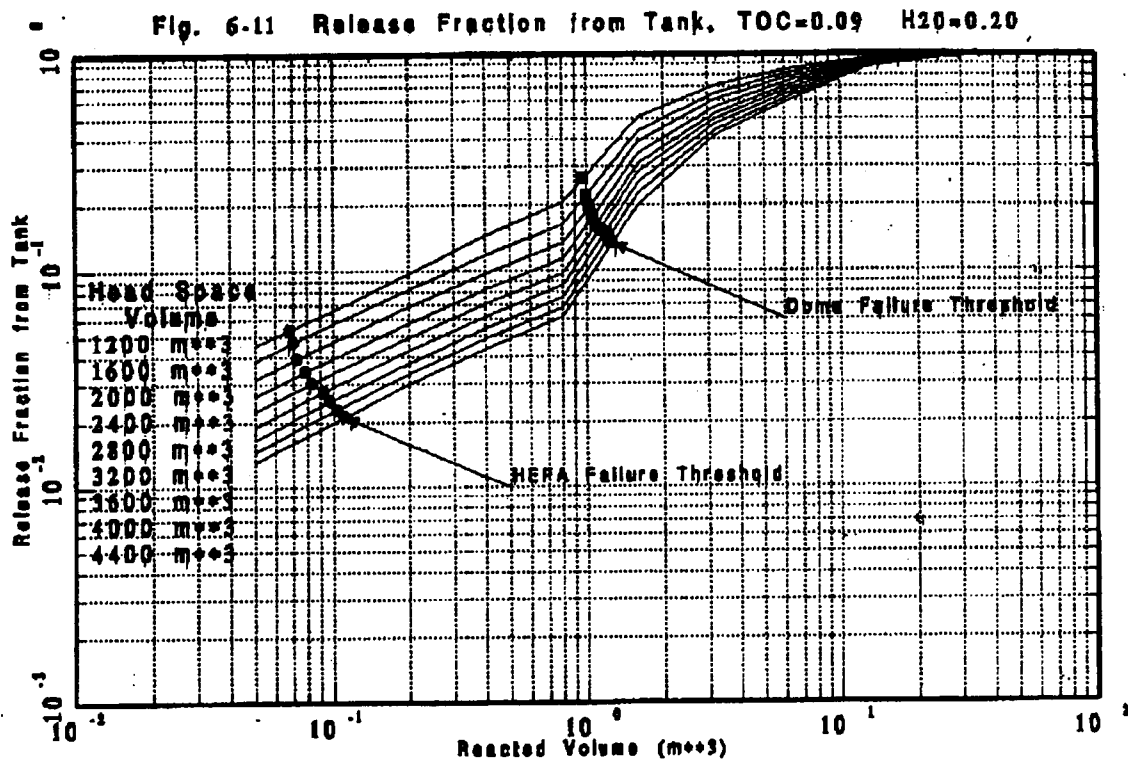
B.6.5 DETAILED TRANSIENT DESCRIPTION

Detailed response of tank U-105 to a condensed phase reaction and the corresponding fission product aerosol behavior are analyzed here to provide a complete description of an organic-nitrate reaction scenario. U-105 has a headspace volume of 1657 m^3 and a total waste volume of 1582 m^3. Two cases selected by WHC were analyzed: In the first case, only 0.058% of the waste, or 0.92 m^3 is assumed to be reactive. In the second case, 1.6% of the total waste, or 25.3 m^3, is assumed to be reactive. The average TOC and moisture content of the reactive portion of the waste were assumed to be 7.0% and 10.0%, respectively. The reaction is assumed to propagate radially outward at 1.2 mm/sec and downward at 0.6 mm/sec in accord with the earlier discussion. CsOH is selected to demonstrate aerosol behavior in the tank, although eleven total aerosol species are tracked in the calculation.

For a given reacted volume, tank headspace response depends upon the headspace volume, heat sink area, and total pressure relief capacity. Only a single filtered riser is credited here for pressure relief. Flow occurs through a two-inch diameter bypass line until the tank pressure is sufficient to fail the HEPA filter, after which venting occurs through a four-inch flowpath. In reality, tank U-105 is connected by cascade lines to two neighbor tanks, but no credit is taken for these relief paths because it is not known whether they are still open. Also, tank U-105 and its neighbors may each have a twelve-inch riser in a service pit covered only by a movable metal lid which would easily lift during pressurization, but no credit is taken for this vent path either. The impact of the cascade line and large riser vent paths is overall to reduce the source term, so the current calculation is conservative.

Figures B-31 through B-33 show results for the first case. Tank pressure increases as the reaction accelerates, and at 570 seconds, the HEPA filter fails. The pressure keeps increasing and reaches the peak pressure of 1.36E+05 Pa (5.04 psig) when the reactive waste is exhausted and the reaction stops at 1,010 seconds. Subsequently the tank depressurizes due to gas outflow and heat transfer to the dome wall and the saltcake. Depressurization slows down when water fog starts to form at 1,120 seconds. Peak temperatures reached during the transient in the headspace gas, on the wall, and on the saltcake surface are 396°K, 324°K and 318°K, respectively.

The airborne aerosol builds up monotonically in the tank until the reaction stops. Some airborne aerosols are settled in the tank and some are released to the ambient. The aerosol settlement potential is determined by total suspended mass and until the water fog forms both sodium and cesium hydroxide dominate aerosol. Leakage to the ambient continues and stops only when the tank is fully depressurized. Note that when steam fog starts to form, it coagglomerates with aerosols from the reaction and the total deposition rate is increased. At the end of the transient, 3.8E-03 kg of CsOH remains airborne in the tank, 3.8E-03 kg has been settled in the tank, and 1.6E-03 kg has been released to the ambient. Hence, the fraction of CsOH released from saltcake that is released to the environment is about 17%.

Figures B-34 through B-36 show results for the second case. In this case, there is enough reactive waste volume to cause dome failure; the tank pressure reaches the dome failure pressure of 1.75E+05 Pa (11 psig) at 1,350 seconds.

The dome starts to crack, and strains sufficiently to relieve the excess pressure in the tank. Hence, the pressure is maintained constant at the tank failure pressure up until all reactive waste is exhausted and the reaction stops at 2,770 seconds. The tank quickly depressurizes. The headspace heats up because the effluent gases enter the headspace at the reaction temperature of 1,137 K. The hot headspace gas in turn transfers heat to the dome and unreacted saltcake by radiation and convection. When the surface temperature of the saltcake exceeds 500°K, the entire saltcake ignites. The peak temperatures predicted for headspace and the dome wall are 1,030°K and 580°K, respectively.

After the dome starts to crack, the airborne aerosol concentration remains nearly constant, and fallout of airborne aerosol is minuscule compared to leakage to the environment. This is because, due to the high outflow, the aerosols do not have sufficient time to coagulate and settle by gravity. At the end of the transient, 1.1E-02 kg of CsOH remains airborne in the tank, 2.2E-03 kg has settled in the tank, and 2.3E-01 kg has been released to the ambient. Hence, the fraction of CsOH released from saltcake that is released to the ambient is 95%.

Release fractions for toxic and radiological species are summarized below in Table B-24. It should be noted that the release fraction reported herein is based on the inventory of each specie in the total waste volume, not on the reacted portion of the waste.

Table B-24. U-105 Example Release Fractions

	0.92 m^3	25.3 m^3
Cs-137	3.6E-05	5.5E-03
Sr-90	1.5E-12	2.3E-10
Y-90	4.9E-14	7.5E-12
Co-60	1.67E-12	2.4E-10
Tc-99	5.5E-12	8.4E-10
Sb-125	3.4E-06	5.3E-04
Eu-154	3.9E-07	5.9E-05
Pu-239	5.5E-14	8.5E-12
Ru-106	1.3E-07	1.9E-05
Cd	1.2E-08	1.9E-06
Hg	9.9E-05	1.5E-02
NaOH	1.2E-08	1.9E-06
HEPA Failed?	Yes	Yes
Dome Failed?	No	Yes

Figure B-31. Tank Pressure for TOC = 0.07, H_2O = 0.10, Waste Burn Volume = 4m ^{3}, Headspace Volume = 2400m^3

Figure 6-12   Tank Pressure,TOC=0.07,H2O=0.10,Vwaste=4 m**3,Vhead=2400 m**3.
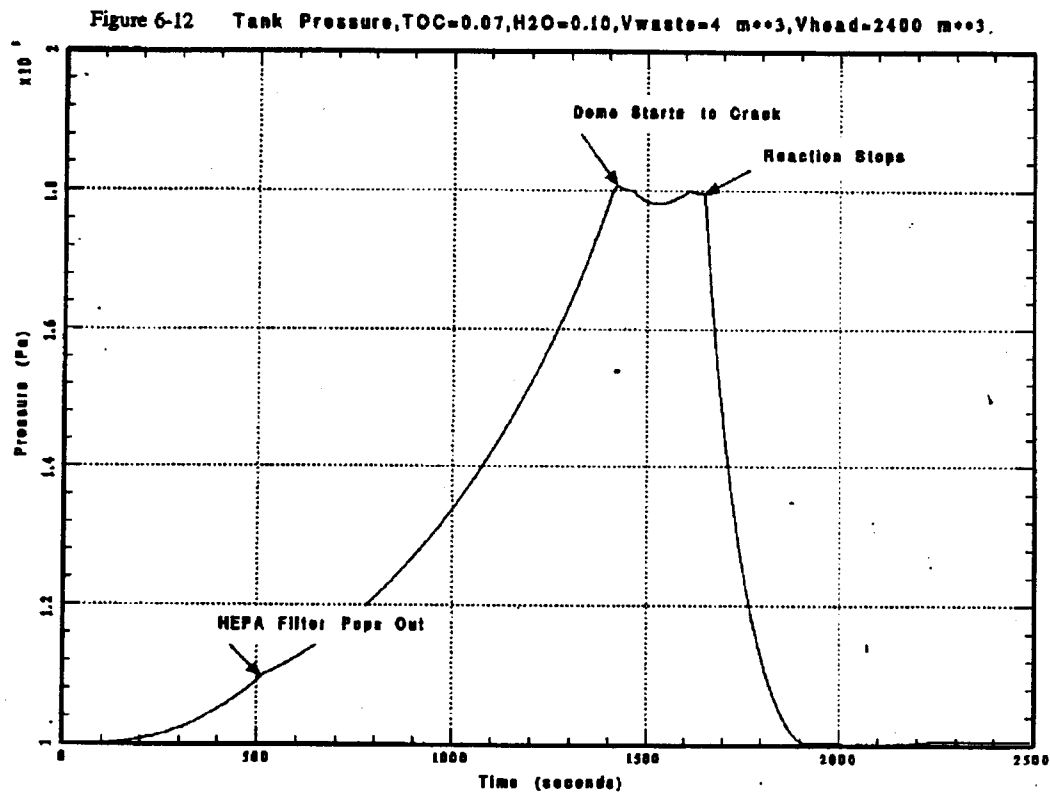
Figure B-32. Temperature for TOC = 0.07, H_2O = 0.10, Waste Burn Volume = 4m^3, Headspace Volume = 2400m^3

Figure 6-13   Temperatures,TOC=0.07,H2O=0.10,Vwaste=4 m++3,Vhead=2400
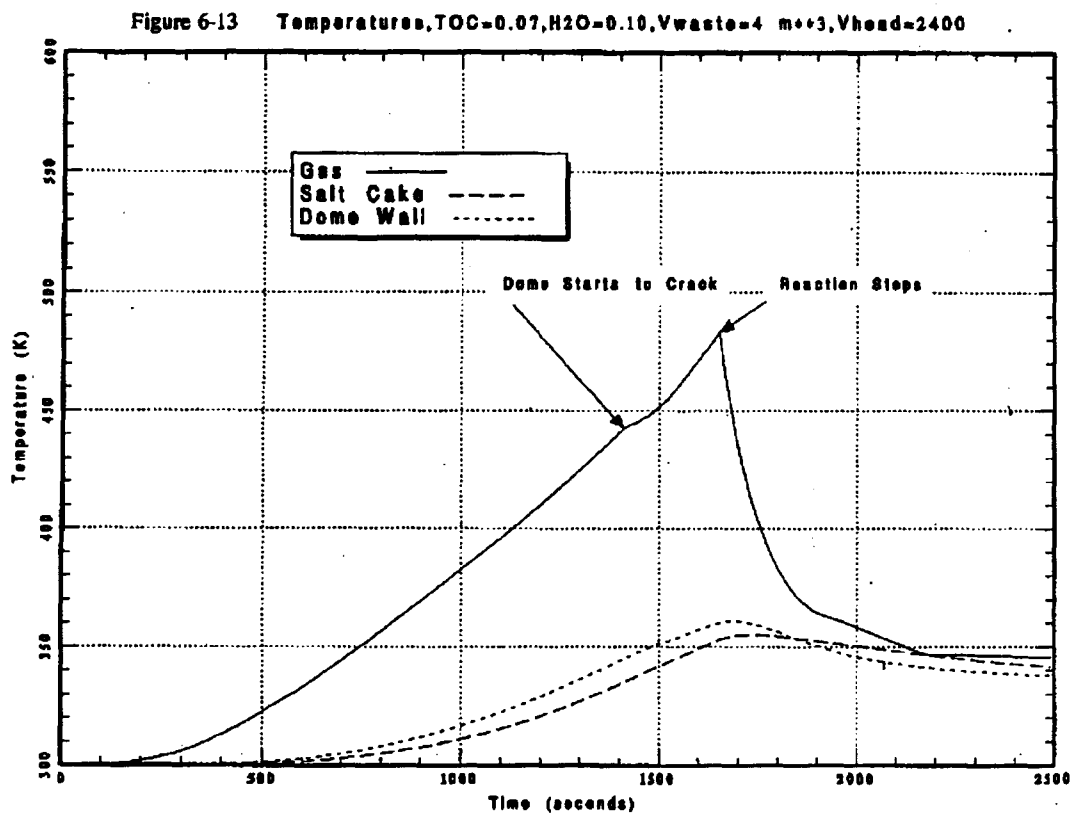
Figure B-33. Aerosol Distribution for TOC = 0.07, H_2O = 0.10, Waste Burn
Volume = 4m^3, Headspace Volume = 2400m^3

Figure 6-14 Aerosol Distribution,TOC=0.07,H2O=0.1,Vwaste=4 m**3,Vhead=2400 m**3

Cs Aerosol in Tank ——
Steam Aerosol in Tank ————
Total Aerosol in Tank ....
Cs Settled in Tank —■—
Water in Tank —■—
Cs Released to Ambient —▲—

Fog Forms
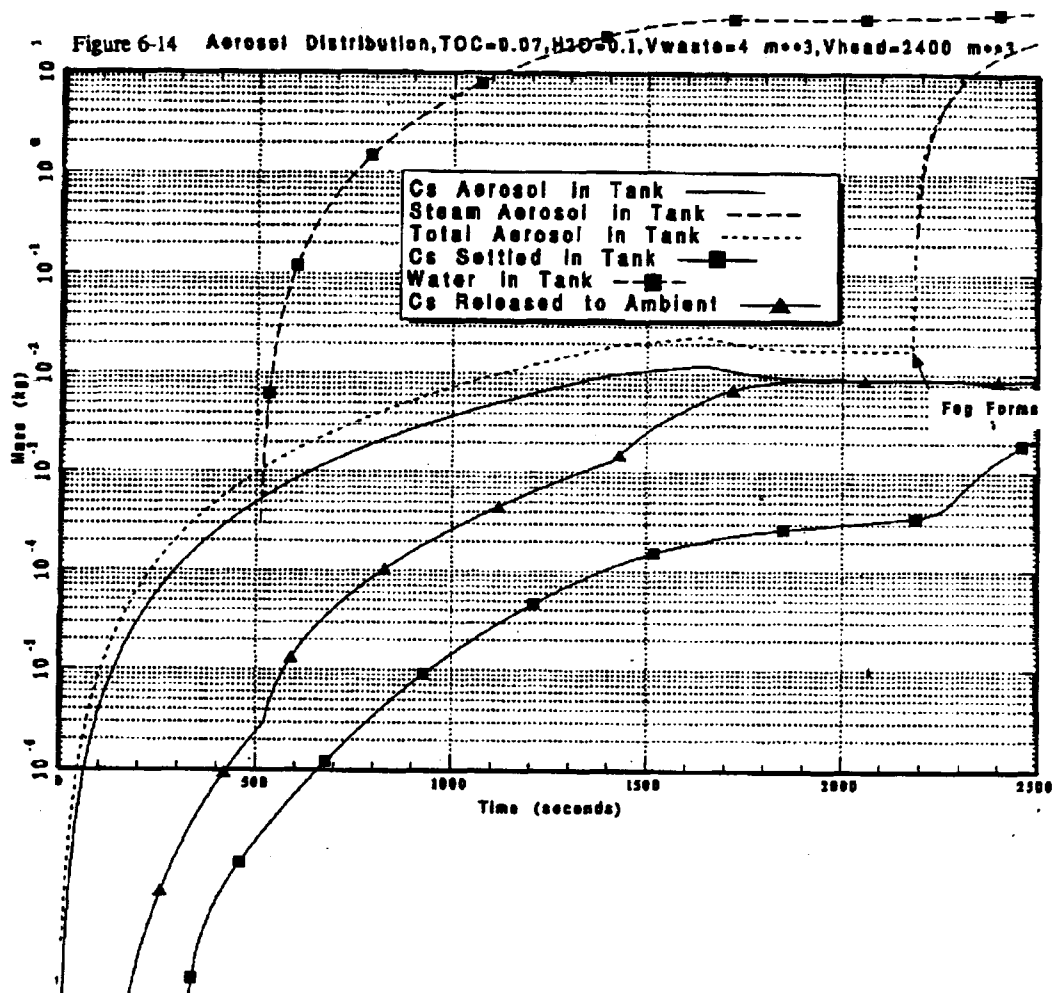
Figure B-34. Tank Pressures for Two Cascaded Tanks

Figure 6-15   Tank Pressures for Two Cascaded Tanks
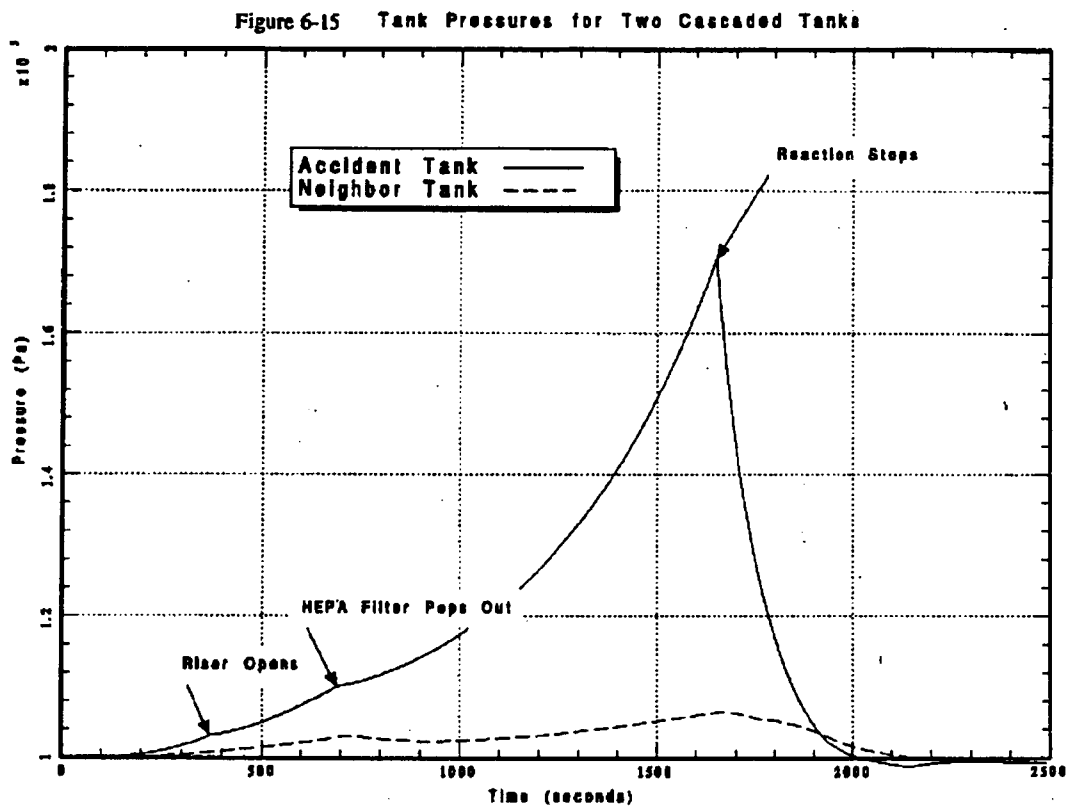
Figure B-35.   Gas Temperatures for Two Cascaded Tanks

Figure 6-16   Gas Temperatures for Two Cascaded Tanks
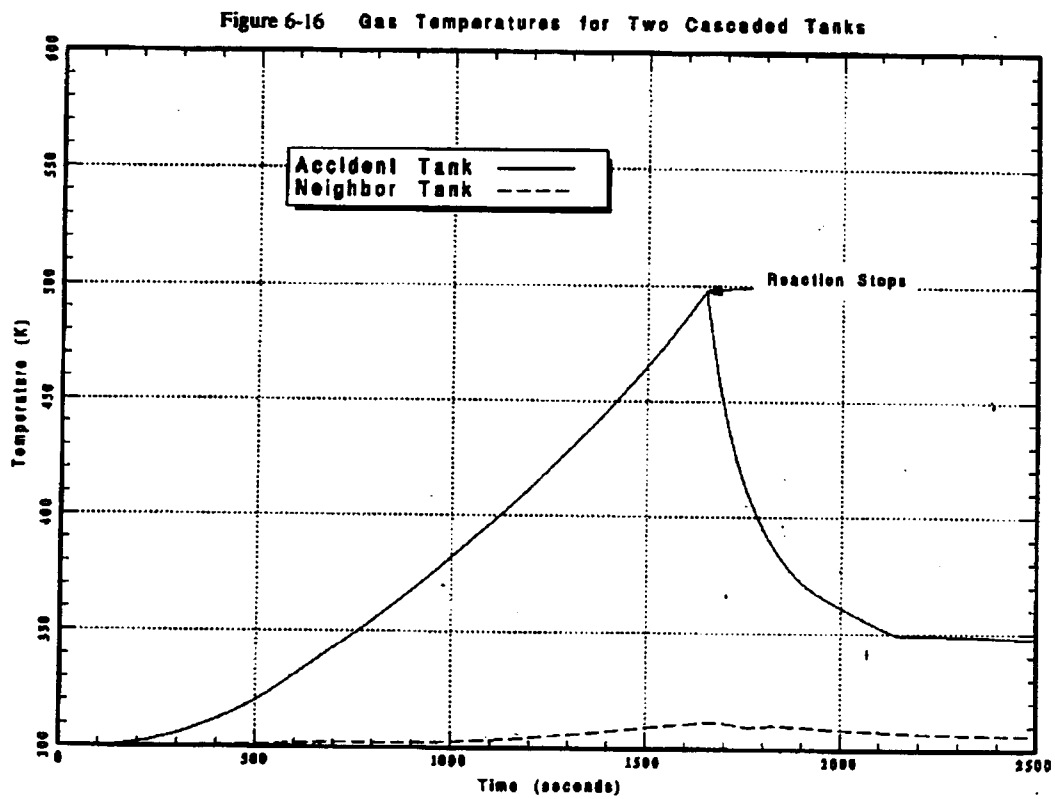
Figure B-36.   Aerosol Distribution for Two Cascaded Tanks
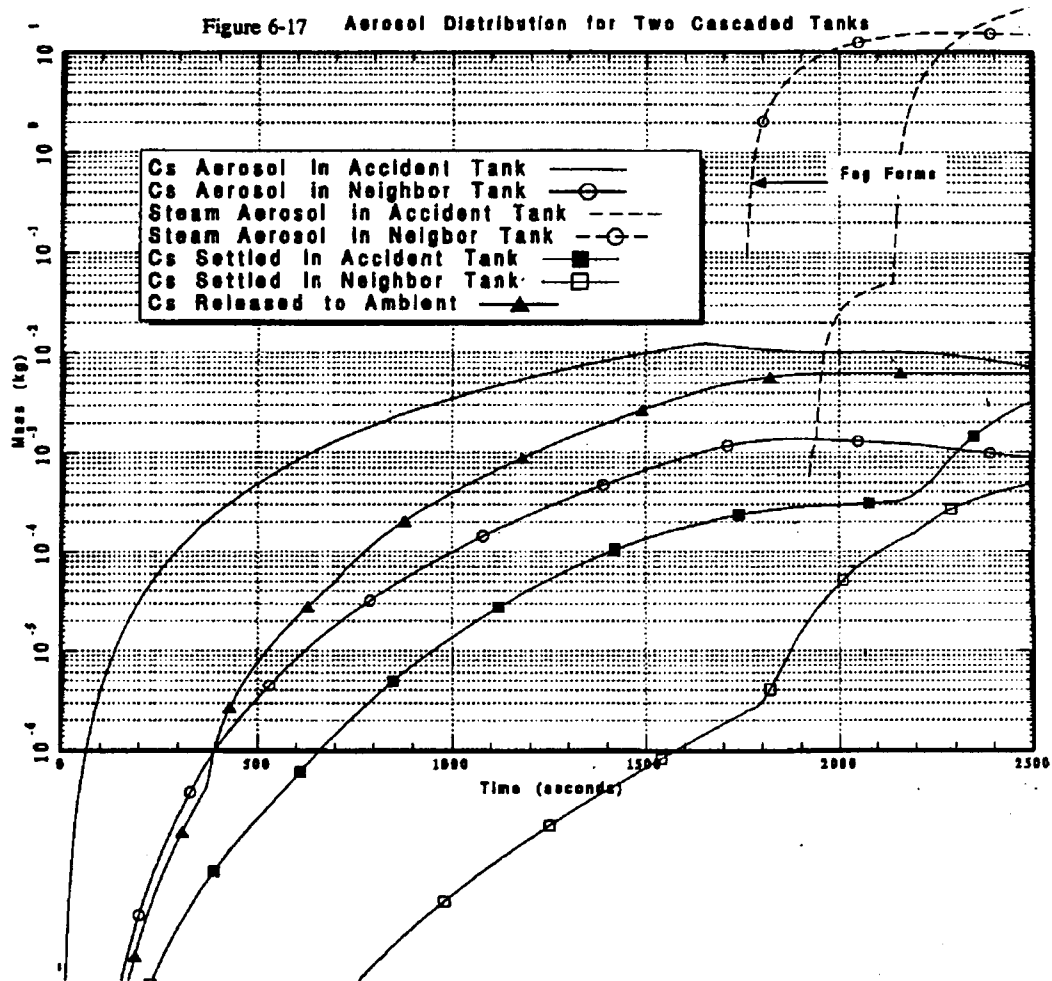
B.7.0 INPUT DECK DESCRIPTION

```
*
* Control input file:  CONTRL.DAT
*
* 1.  Keyword-based input. Non-keywords are comments.  Order of
*     keywords or keyword groups is arbitrary.
* 2.  Keyword groups contain only group-specific keywords. Order arbitrary.
*     No comments allowed within keyword groups.
* 2.  TITLE / END keyword group. Case title defined between these.
* 3.  ACTIVE MODELS / END keyword group.  Separate keywords here
*     to activate models.
* 4.  PLOT / END keyword group.  Defines variables to plot
* 5.  SOURCES / END keyword group. Defines mass & energy sources.
*
'TITLE'
*
* SINGLE TANK TEST
*
END     note the word end must appear without quotes starting in column 1
*
'TSTART'     0.0           ! Start time
'TLAST'      501.          ! End time
'DTMIN'      1.0           ! Minimum timestep
'DTMAX'      1.0           ! Maximum timestep
'DTPRIN'     100.          ! Print interval
*
'ACTIVE MODELS'            ! PARAMETER KEYWORD SECTION 1=on, 0=off
'IVALID'  1                ! 1=Validation case, 0=multi-tank cases
'IJUNC'   1                ! 1=Use junction models
'IHSINK'  1                ! 1=Use heat sink models
'ICNDS'   1                ! 1=Use condensation models
'IASED'   1                ! 1=Use aerosol sedimentation models
'IALEAK'  1                ! 1=Use aerosol flow between compartments
'IFOG'    1                ! 1=Use fog formation/evaporation models
'ISRC'    0                ! 1=Use source models
'ISLDG'   1                ! 1=Use waste reaction models
'IRELMD'  1                ! 1=Use release models
'END'                      ! END ACTIVE MODELS
*
* The PLOT keyword is followed by the plot time interval
* Plot syntaxes:
* 1. variable type, # of regions to plot, list of regions
*     types: PRESSURE, GAS-T, HS-T
* 2. variable type, species, # regions to plot, list of regions
*     types: GAS-MASS, AER-MASS, LIQ-MASS
*
'PLOT'  10.                ! PLOT KEYWORD GROUP and plot interval time.
PRESSURE     1   1         ! Plot pressure from 1 region, region #1.
GAS-T        1   1
HS-T         1   1
```

```
AER-MASS    NAOH     2  1  2        ! Plot NAOH aerosol mass from two
AER-MASS    CSOH     2  1  2        !       regions, regions 1 and 2 etc.
AER-MASS    STEAM    1  1
LIQ-MASS    NAOH     1  1
LIQ-MASS    CSOH     1  1
LIQ-MASS    STEAM    1  1
'END'
*
* The SOURCES keyword is followed by the # of source vs time tables
* The SOURCES / END keyword group contains that # of REGION / END groups
* Each REGION / END group has
*    1. REGION keyword followed by Region # and # of source species
*    2. Names of the source species
*    3. Table of:  Time, Temperature, flowrates per species, Power
* Sources are not used for tank cases - waste inputs are.
* Sources are used for validation purposes.
*
'SOURCES'    2             ! BEGIN SOURCES GROUP, 2 GROUPS OF REGION SOURCES
'REGION'         1  2      ! REGION 1 HAS 2 GASES
'STEAM' 'CARBON DIO'
0.0    600.0  1.E0  1.E0 0.E0      ! Time, Temperature, flowrate of two gases,
10.    600.0  1.E0  1.E0 0.E0              additional energy flow (zero)
10.02 300.0  0.E0  0.E0 0.E0
20.02 300.0  0.E0  0.E0 0.E0
'END'                       ! End REGION table group
'REGION'         2  1      ! REGION 2 HAS 1 GAS - A DUMMY
'STEAM'
0.0    300.0  0.E0    185.8E3       ! Energy source only J/s (zero flowrate)
10.    300.0  0.E0    185.8E3
10.02 300.0  0.E0    0.E0
20.02 300.0  0.E0    0.E0
'END'                       ! End REGION table group
'END'                       ! END SOURCES GROUP
```

```
*
* Region input file REGINI.DAT:  Region geometry and initialization.
*
* 1. Comment lines are non-keyword lines.
* 2. REGIONS keyword defines the number of regions (columns) expected.
*    Other keywords can follow in any order, except the GASES group.
*    MKS units.
* 3. GASES keyword defines the number of rows for gas mole fractions,
*    which must immediately follow.  Input gas names must be in the
*    gas property data file.  ·
* 4. AEROSOLS keyword works the same as GASES, defines kg/m^3 aerosol.
*
*              TANK          ENVIRN

*

'REGIONS'      2

'VOLUME'       2400.0        1.0E6

'SED AREA'     410.4            0.0

'ELEVATION'    0.0           0.0

'TEMP_GAS'     300.0         300.0

'PRESSURE'     1.0E5         1.0E5

'GASES'        3

'STEAM'        0.01776       0.00000

'NITROGEN'     0.77597       0.79000

'OXYGEN'       0.20627       0.21000
```

```
C
C    FLOWPATH DATA FOR ORNATE:  JUNC.DAT
C
C    1.   Comments begin with C
C    2.   Input for junctions is one line per junction.  MKS units.
C    3.   Each input line begins with the junction type keyword:
C         NORMAL is always open
C         HEPA changes area once at a specific delta P
C         COVER changes area:  lifts at high delta P, resets at low,
C             based on input mass and area
C    4.   NORMAL junction inputs in order are:
C         'NORMAL'  LITERALLY
C         IUP: UPSTREAM REGION
C         IDN: DOWNSTREAM REGION
C         AJN: AREA
C         ZUP: ELEVATION UPSTREAM WRT FLOOR
C         ZDN: ELEVATION DOWNSTREAM WRT FLOOR
C         CJN: LOSS COEFF (MULTIPLIES 1/2 RHO*U*U)
C    5.   HEPA junctions add the following after AJN:
C         ABYP:  BYPASS AREA = AREA AFTER BLOWOUT
C         PHEPA: BLOWOUT PRESSURE DIFFERENCE
C    6.   COVER junctions add the following after AJN:
C         ACOV:  AREA OF COVER THAT OPENS
C         MCOV:  MASS OF COVER
C
C TYPE          IUP IDN     AJN     ABYP     PHEPA     ZUP     ZDN     CJN

   'HEPA'        1   2     0.0075  0.0020  10000.0    5.0    10.0    3.50
```

```
C
C HEAT SINK INPUT FOR ORNATE:   HSINI.DAT
C
C  1. Comment lines begin with C
C  2. One line per heat sink.  MKS units.
C  3. Inputs supplied sequentially are:
C     IGEOM 1=Planar, 2=Cylindrical
C     RHO    Density
C     K      Thermal conductivity
C     CP     Specific heat
C     QV     Volumetric heat generation
C     XRI    Inner radius
C     XRO    Outer radius (outer minus inner is thickness)
C     AHS    Area
C     TIINIT Initial inside surface temperature
C     TOINIT Initial outside surface temperature
C     NT     Number of temperature points
C     IREGI  Region index on inside surface
C     TIHS   Temperature for constant T boundary condition inside if nonzero
C     IREGO  Region index on outside surface
C     TOHS   Temperature for constant T boundary condition outside if nonzero
C     XL     Length used in nat. convection correlation
C
C IGEOM RHO K CP QV XRI XRO  AHS  TIINIT  TOINIT NT IREGI TIHS IREGO  TOHS XL
    1 1500. 0.5 1500. 300.0  0.0  0.25  410.4  26.85 26.85 10  1 0.0  0 0.0 22.0

    1 2000. 1.0  500.   0.0  0.0  0.25  599.2  26.85 26.85 10  1 0.0  0 0.0 22.0
```

```
*
*   REACTION AND SOURCE INPUT:   WASTE.DAT
*
*   All inputs are keywords.  MKS units.
*   Comments are non-keywords.

*

'TREACO'          0.0          ! Reaction start time
'PTHRES'          2.0E5        ! Threshold pressure to end reaction
'RZONEO'          0.001        ! Initial reaction zone size
'VPROP'           0.6E-3       ! Propagation velocity into waste
'GUS'             2.0          ! Ratio of surface/inside velocity
'DSLUD'           1500.        ! Waste density
'MFTOC'           0.06         ! TOC
'MFH2O'           0.05         ! Moisture
'XLSLUD'          8.788        ! Layer depth
'HRACE'           8.E6         ! Acetate heat of reaction J/kg
'CPSLUD'          2000.        ! Effective specific heat
'LHH2O'           2.4E6        ! Water latent heat
'TSLUDO'          300.         ! Initial temperature
'TSLUD'           0.0          ! If nonzero, reaction temperature
'TIGNTN'          500.0        ! Temperature to ignite surface
'VZONEF'          1.E6         ! Volume threshold to end reaction
'VWASTE'          3607.        ! Waste volume
'MFCSSL'          .21E-04      ! CsOH mass fraction
'MFNASL'          .14E+00      ! NaOH mass fraction
'MFSRSC'          .38E-03      ! SrO  mass fraction
'MFCOSC'          .97E-08      ! CoO  mass fraction
'MFTCSC'          .41E-10      ! TcO3 mass fraction
'MFSBSC'          .48E-08      ! SbO2 mass fraction
'MFPUSC'          .47E-03      ! PuO2 mass fraction
'MFEUSC'          .16E-07      ! Eu2O3 mass fraction
'MFYSC'           .10E-06      ! Y2O3 mass fraction
'MFRUSC'          .13E-11      ! RuO2 mass fraction
'MFCDSC'          .11E-02      ! CdO mass fraction
'MFHGSC'          .36E-01      ! HgOH mass fraction
```

```
C
C      Gas Property Input File:  GASINP.DAT
C
C      1. Keyword-based input defines content of line.
C      2. Non-keyword lines are comments.
C      3. Keywords following a species name define properties
C         for that input species - MKS units in general
C      4. GAS Species name keyword followed by:
C         Species name, formula weight, heat of formation (J/mol)
C      5. PV Vapor Pressure (Pa) keyword followed by:
C         Critical Temperature, Pressure at Tcrit, coefficients:
C         PV=exp(A + B/T + C*lnT + D*T^E)
C      6. CV Specific Heat (J/kg/K) keyword followed by:
C         Example temperature, Value at that temperature, coefficients:
C         CV= A + B*T + C*T^2 + D*T^3 + E*T^4
C      7. BV Virial Coefficient (m3/kg) keyword followed by:
C         Example temperature, Value at that temperature, coefficients:
C         BV= A + B/T + C/T^3 + D/T^8 + E/T^9
C      8. HFG Heat of Vaporization (J/kg) keyword followed by:
C         Example temperature, Value at that temperature, coefficients:
C         HFG= A*(1-Tr)^B + C*Tr + D*Tr^2 + D*Tr^3
C      9. RL Density (kg/m^3) of Liquid keyword followed by::
C         Example temperature, Value at that temperature, coefficients:
C         DL= A + B*T
C     10. MUG Vapor Viscosity Keyword followed by:
C         Example temperature, Value at that temperature, coefficients:
C         VV= A +  ( T^B / (1 + C/T + D/T^2) )
C     11. DFG Diffusion Coefficient Keyword followed by:
C


'GAS'  'STEAM'          1.80000E+01      -2.41820E+08
'CVG' 1.57320E+03      2653.             1.33579E+03    -4.37917E-03    8.40632E-04
-4.06859E-07      6.03749E-11
'BV'   3.23000E+02      -0.04E0          2.295514E-3    -2.024448E+0    -8.778481E+5
-3.00507E+18      5.79857E+20
'PV'   647.290E+00      2.1977E7         7.25500E+01    -7.20670E+03    -7.13850E+00
4.04600E-06      2.0E0
'HFG' 300.E0            2.4376E6         3.184381E6     0.571707E0      -0.289795E0
-0.182469E0      0.295616E0
'RL'   300.E0           1.E3             1.E3           1.E0            1.E0
0.E0             0.E0
'CVL' 300.E0            4200.E0          4200.E0        0.E0            0.E0
0.E0             0.E0
'MUG' 370.E0            1.1946E-5        7.619E-8       9.2758E-1       2.116E2
-4.67E3
'DFG' 2.52E0           775.             1.0E0


'GAS'  'CARBON DIO'     4.40100E+01      -3.93520E+08
'CVG' 1.50000E+03      1140.             2.84515E+02    1.55345E+00     -1.14113E-03
4.02762E-07      -5.30735E-11
'BV'   1.52100E+03      6.835E-4         1.23636E-03    -8.26136E-01    -3.40000E+04
1.95227E+15      -3.17500E+17
```

```
'PV'   204.E0              7.3617E6      8.55300E+01   -3.48130E+03   -1.13360E+01
2.15050E-02      1.0E0
'HFG' 300.                 0.4E6         0.4E6         1.E0           0.E0
0.E0              0.E0
'RL'  300.                 0.4E6         0.77E3        1.E0           1.E0
0.E0              0.E0
'CVL' 300.                 0.4E6         800.E0        0.E0           0.E0
0.E0              0.E0
'MUG' 1500.                5.2032E-5     2.148E-6      4.6E-1         2.9E2
0.E0
'DFG' 3.941                195.2         0.E0


'GAS' 'NITROGEN'           2.80130E+01   0.00000E+00
'CVG' 1.50000E+03    947.                7.42319E+02   -1.38235E-01   4.78640E-04
-2.57728E-07      4.14112E-11
'BV'  1.40000E+03    0.0001286           1.66786E-03   -5.33929E-01   -2.18321E+03
2.87500E+12     -1.65357E+14
'PV'  126.100E+00    3.3818E6            5.9826E1      -1.0976E3      -8.6689E0
4.6346E-2        1.0E0
'HFG' 300.                 0.E0          0.E0          0.E0           0.E0
0.E0              0.E0
'RL'  300.                 1.E-3         1.E-3         1.E0           1.E0
0.E0              0.E0
'CVL' 300.                 1.E3          1.E3          0.E0           0.E0
0.E0              0.E0
'MUG' 1.5E3                5.3917E-5     7.632E-7      5.8823E-1      6.775E1
0.E0
'DFG' 3.798                71.4          0.E0


'GAS' 'OXYGEN'             3.20000E+01   0.00000E+00
'CVG' 1.50000E+03    881.                5.32655E+02   4.41600E-01    -1.54996E-04
4.29830E-09      4.29767E-12
'BV'  1.40000E+03    0.000871            1.21875E-03   -4.85625E-01   -2.65000E+03
5.12500E+12     -3.59375E+14
'PV'  154.580E+00    5.0416E6            5.2486E1      -1.2134E3      -6.7062E0
2.9764E-2        1.0E0
'HFG' 300.                 0.E0          0.E0          0.E0           0.E0
0.E0              0.E0
'RL'  300.                 1.E-3         1.E-3         1.E0           1.E0
0.E0              0.E0
'CVL' 300.                 1.E3          1.E3          0.E0           0.E0
0.E0              0.E0
'MUG' 1.5E3                6.3987E-5     8.038E-7      6.0478E-1      7.03E1
0.E0
'DFG' 3.467                106.7         0.E0


'GAS' 'CSOH'               149.91274     -2.59408E+08
'CVG' 300.E0         276.5E0             2.12857E+02   3.33181E-01    -4.90431E-04
3.38981E-07     -8.44686E-11
'BV'  300.                 0.0           0.0           0.0            0.0
0.0               0.0
'PV'  1.30619E+03    .101325E6           4.18806E+01   -1.87360E+04   -3.83793E+00
3.16319E-04     -1.00000E+00
```

'HFG'	298.E0	146.562E6	146.56E6	0.E0	0.E0
0.E0		0.E0			
'RL'	300.E0	1.E3	1.E3	1.E0	1.E0
0.E0		0.E0			
'CVL'	300.E0	4200.E0	4200.E0	0.E0	0.E0
0.E0		0.E0			
'MUG'	370.E0	1.1946E-5	7.619E-8	9.2758E-1	2.116E2
-4.67E3					
'DFG'	2.52E0	775.	1.0E0		
'GAS'	'NAOH'	39.99711	-1.97757E+08		
'CVG'	300.E0	1003.E0	6.94773E+02	1.60345E+00	-2.32827E-03
1.57271E-06		-3.85667E-10			
'BV'	300.	0.0	0.0	0.0	0.0
0.0		0.0			
'PV'	2.10578E+03	.101325E6	5.08838E+01	-2.77488E+04	-4.92736E+00
7.22433E-04		-1.00000E+00			
'HFG'	298.E0	219.121E6	219.121E6	0.E0	0.E0
0.E0		0.E0			
'RL'	300.E0	1.E3	1.E3	1.E0	1.E0
0.E0		0.E0			
'CVL'	300.E0	4200.E0	4200.E0	0.E0	0.E0
0.E0		0.E0			
'MUG'	370.E0	1.1946E-5	7.619E-8	9.2758E-1	2.116E2
-4.67E3					
'DFG'	2.52E0	775.	1.0E0		
'GAS'	'SROH2'	121.62	-1.0E8		
'CVG'	300.E0	1000.0	1000.0	0.0	0.0
0.0		0.0			
'BV'	300.	0.0	0.0	0.0	0.0
0.0		0.0			
'PV'	1.30619E+03	.101325E6	-46.0	0.0	0.0
0.0		0.0			
'HFG'	298.E0	1.0E6	1.0E6	0.0	0.0
0.0		0.E0			
'RL'	300.E0	1.E3	1.E3	1.E0	1.E0
0.E0		0.E0			
'CVL'	300.E0	4200.E0	4200.E0	0.E0	0.E0
0.E0		0.E0			
'MUG'	370.E0	1.1946E-5	7.619E-8	9.2758E-1	2.116E2
-4.67E3					
'DFG'	2.52E0	775.	1.0E0		
'GAS'	'COOH2'	93.	-1.0E8		
'CVG'	300.E0	1000.0	1000.0	0.0	0.0
0.0		0.0			
'BV'	300.	0.0	0.0	0.0	0.0
0.0		0.0			
'PV'	1.30619E+03	.101325E6	-46.0	0.0	0.0
0.0		0.0			
'HFG'	298.E0	1.0E6	1.0E6	0.0	0.0
0.0		0.E0			

```
'RL'   300.E0          1.E3            1.E3            1.E0            1.E0
  0.E0            0.E0
'CVL'  300.E0          4200.E0         4200.E0         0.E0            0.E0
  0.E0            0.E0
'MUG'  370.E0          1.1946E-5       7.619E-8        9.2758E-1       2.116E2
-4.67E3
'DFG'  2.52E0          775.            1.0E0

'GAS'  'TC207'         308.            -1.0E8
'CVG'  300.E0          1000.0          1000.0          0.0             0.0
  0.0             0.0
'BV'   300.            0.0             0.0             0.0             0.0
  0.0             0.0
'PV'   1.30619E+03     .101325E6       -46.0           0.0             0.0
  0.0             0.0
'HFG'  298.E0          1.0E6           1.0E6           0.0             0.0
  0.0             0.E0
'RL'   300.E0          1.E3            1.E3            1.E0            1.E0
  0.E0            0.E0
'CVL'  300.E0          4200.E0         4200.E0         0.E0 .          0.E0
  0.E0            0.E0
'MUG'  370.E0          1.1946E-5       7.619E-8        9.2758E-1       2.116E2
-4.67E3
'DFG'  2.52E0          775.            1.0E0

'GAS'  'SBO'           137.75          -1.0E8
'CVG'  300.E0          1000.0          1000.0          0.0             0.0
  0.0             0.0
'BV'   300.            0.0             0.0             0.0             0.0
  0.0             0.0
'PV'   1.30619E+03     .101325E6       -46.0           0.0             0.0
  0.0             0.0
'HFG'  298.E0          1.0E6           1.0E6           0.0             0.0
  0.0             0.E0
'RL'   300.E0          1.E3            1.E3            1.E0            1.E0
  0.E0            0.E0
'CVL'  300.E0          4200.E0         4200.E0         0.E0            0.E0
  0.E0            0.E0
'MUG'  370.E0          1.1946E-5       7.619E-8        9.2758E-1       2.116E2
-4.67E3
'DFG'  2.52E0          775.            1.0E0

'GAS'  'PUO2OH2'       308.            -1.0E8
'CVG'  300.E0          1000.0          1000.0          0.0             0.0
  0.0             0.0
'BV'   300.            0.0             0.0             0.0             0.0
  0.0             0.0
'PV'   1.30619E+03     .101325E6       -46.0           0.0             0.0
  0.0             0.0
'HFG'  298.E0          1.0E6           1.0E6           0.0             0.0
  0.0             0.E0
'RL'   300.E0          1.E3            1.E3            1.E0            1.E0
  0.E0            0.E0
```

'CVL' 300.E0	4200.E0	4200.E0	0.E0	0.E0
0.E0 0.E0				
'MUG' 370.E0	1.1946E-5	7.619E-8	9.2758E-1	2.116E2
-4.67E3				
'DFG' 2.52E0	775.	1.0E0		
'GAS' 'EUOH3'	205.	-1.0E8		
'CVG' 300.E0	1000.0	1000.0	0.0	0.0
0.0 0.0				
'BV' 300.	0.0	0.0	0.0	0.0
0.0 0.0				
'PV' 1.30619E+03	.101325E6	-46.0	0.0	0.0
0.0 0.0				
'HFG' 298.E0	1.0E6	1.0E6	0.0	0.0
0.0 0.E0				
'RL' 300.E0	1.E3	1.E3	1.E0	1.E0
0.E0 0.E0				
'CVL' 300.E0	4200.E0	4200.E0	0.E0	0.E0
0.E0 0.E0				
'MUG' 370.E0	1.1946E-5	7.619E-8	9.2758E-1	2.116E2
-4.67E3				
'DFG' 2.52E0	775.	1.0E0		
'GAS' 'YOH3'	141.	-1.0E8		
'CVG' 300.E0	1000.0	1000.0	0.0	0.0
0.0 0.0				
'BV' 300.	0.0	0.0	0.0	0.0
0.0 0.0				
'PV' 1.30619E+03	.101325E6	-46.0	0.0	0.0
0.0 0.0				
'HFG' 298.E0	1.0E6	1.0E6	0.0	0.0
0.0 0.E0				
'RL' 300.E0	1.E3	1.E3	1.E0	1.E0
0.E0 0.E0				
'CVL' 300.E0	4200.E0	4200.E0	0.E0	0.E0
0.E0 0.E0				
'MUG' 370.E0	1.1946E-5	7.619E-8	9.2758E-1	2.116E2
-4.67E3				
'DFG' 2.52E0	775.	1.0E0		
'GAS' 'RUO3OH'	171.	-1.0E8		
'CVG' 300.E0	1000.0	1000.0	0.0	0.0
0.0 0.0				
'BV' 300.	0.0	0.0	0.0	0.0
0.0 0.0				
'PV' 1.30619E+03	.101325E6	-46.0	0.0	0.0
0.0 0.0				
'HFG' 298.E0	1.0E6	1.0E6	0.0	0.0
0.0 0.E0				
'RL' 300.E0	1.E3	1.E3	1.E0	1.E0
0.E0 0.E0				
'CVL' 300.E0	4200.E0	4200.E0	0.E0	0.E0
0.E0 0.E0				

'MUG' 370.E0	1.1946E-5	7.619E-8	9.2758E-1	2.116E2
-4.67E3				
'DFG' 2.52E0	775. ·	1.0E0		
'GAS' 'CDOH2'	146.4	-1.0E8		
'CVG' 300.E0	1000.0	1000.0	0.0	0.0
0.0 0.0				
'BV' 300.	0.0	0.0	0.0	0.0
0.0 0.0				
'PV' 1.30619E+03	.101325E6 ·	-46.0	0.0	0.0
0.0 0.0				
'HFG' 298.E0	1.0E6	1.0E6	0.0	0.0
0.0 0.E0				
'RL' 300.E0	1.E3	1.E3	1.E0	1.E0
0.E0 0.E0				
'CVL' 300.E0	4200.E0	4200.E0	0.E0	0.E0
0.E0 0.E0				
'MUG' 370.E0	1.1946E-5	7.619E-8	9.2758E-1	2.116E2
-4.67E3				
'DFG' 2.52E0	775.	1.0E0		
'GAS' 'HG'	200.6	-1.0E8		
'CVG' 300.E0	1000.0	1000.0	0.0	0.0
0.0 0.0				
'BV' 300.	0.0	0.0	0.0	0.0
0.0 0.0				
'PV' 1.30619E+03	.101325E6	-46.0	0.0	0.0
0.0 0.0				
'HFG' 298.E0	1.0E6	1.0E6	0.0	0.0
0.0 0.E0				
'RL' 300.E0	1.E3	1.E3	1.E0	1.E0
0.E0 0.E0				
'CVL' 300.E0	4200.E0	4200.E0	0.E0	0.E0
0.E0 0.E0				
'MUG' 370.E0	1.1946E-5	7.619E-8	9.2758E-1	2.116E2
-4.67E3				
'DFG' 2.52E0	775.	1.0E0		

B.8.0 REFERENCES

Chase, M. W., et al, 1985, *JANAF Thermochemical Tables*, Third Edition, Journal of Physical Chemistry Reference Data, Vol. 14, Supplement 1.

Epstein, M., and P. G. Ellison, 1988, *Correlations of the Rate of Removal of Coagulating and Depositing Aerosols for Application to Nuclear Reactor Safety Problems*, Nuclear Engineering and Design, Vol. 107, pp. 327-344.

Fauske, H. K., and M. Epstein, 1995, *The Contact-Temperature Ignition (CTI) Criterion for Propagating Chemical Reactions Including the Effect of Moisture and Application to Hanford Waste*, FAI/94-103(a), Burr Ridge, Illinois.

Fauske, H. K., 1996, *Assessment of Chemical Vulnerabilities in the Hanford High-Level Waste Tanks*, WHC-SD-WM-ER-543, Westinghouse Hanford Company, Richland, Washington.

Hilliard, R. K., J. D. McCormack, and A. K. Postma, 1983, *Results and Code Predictions for ABCOVE Aerosol Code Validation - Test AB5*, HEDL-TME 83-16, Hanford Engineering Development Laboratory, Richland, Washington.

Incropera, F. P., and D. P. Dewitt, 1981, *Fundamentals of Heat Transfer*, John Wiley and Sons, New York, New York.

Jackson, D. D., 1971, *Thermodynamics of the Gaseous Hydroxides*, UCRL-51137, Lawrence Livermore Laboratory, Livermore, California.

Keenan, J. H., et al, 1978, *Steam Tables*, John Wiley & Sons, New York, 1978.

Krikorian, O. H., 1982, *Predictive Calculations of Volatilities of Metals and Oxides in Steam-Containing Environments*, High Temperatures - High Pressures, Vol. 14, pp. 387-397.

Krikorian, O. H., et al., 1992, *Evaluation of Actinide Volatilities in Mixed Waste Processors: Interim Report*, UCRL-ID-111352, Lawrence Livermore National Laboratory, Livermore, California.

Lamoreaux, R. H., D. L. Hildenbrand, and L. Brewer, 1987, *High-Temperature Vaporization Behavior of Oxides II. Oxides of Be, Mg, Ca, Sr, Ba, B, Al, Ga, In, Tl, Si, Ge, Sn, Pb, Zn, Cd, and Hg*, Journal of Physical Chemistry Reference Data, Vol. 16, No. 3.

Powers, D. A., J. E. Brockmann, and A. W. Shriver, 1986, *VANESA: A Mechanistic Model of Radionuclide Release and Aerosol Generation During Core Debris Interactions with Concrete*, NUREG/CR-4308, SAND85-1370, Los Alamos National Laboratory, Los Alamos, New Mexico.

Reid, R. C., J. M. Prausnitz, and B. E. Poling, 1987, *The Properties of Liquids and Gases*, Fourth Edition, McGraw-Hill, New York, New York.

Roine, A., 1994, *Outokumpu HSC Chemistry for Windows*, Outokumpu Research Oy, Finland.

Vaughan, E. V., and A. V. von Arx, 1988, *Evaluation of Aerosol Correlations*, EPRI NP-5602, Electric Power Research Institute, Palo Alto, California.

Weast, R. C., and S. M. Selby, 1966, *CRC Handbook of Chemistry and Physics*, 47th Edition, Chemical Rubber Company, Cleveland, Ohio.

This page intentionally left blank.

APPENDIX C

CALCULATION NOTES FOR DOSE CONSEQUENCES

This page intentionally left blank.

APPENDIX C

CALCULATION NOTES FOR DOSE CONSEQUENCES

C.1.0 PURPOSE

This package provides the onsite and offsite radiological and toxilogical dose consequences as a function of amount of waste combusted.

C.2.0 METHODOLOGY

Radiological and toxicological dose calculations were performed according to standard methods based upon the quantities of released radionuclides and toxicological chemicals. These methods are briefly described below.

C.2.1. RADIOLOGICAL DOSE CALCULATION PROCESS

The dose to an onsite or offsite receptor for an isotope is given by the equation:

$$Dose = \frac{X}{Q} * BR * V * (RF_i * Q_i * DCF_i) * 1000 \frac{L}{m^3} * 1000 \frac{mSv}{Sv} \qquad (C-1)$$

where,

X/Q = atmospheric dispersion coefficient (0.0341 s/m^3 for the onsite receptor; 2.83E-05 s/m^3 for the offsite receptor). These X/Q values are calculated for the tank farm areas relative to the site boundary, now taken as the Columbia River to the north of the tank farms.

BR = breathing rate (3.3E-04 m^3/s),

V = volume of waste in tank (m^3),

Rf_i = Release fraction for ith isotope,

Q_i = Activity concentration for ith isotope in Bq/L based on the bounding tank source term for all SST solids,

DCF_i = dose conversion factor for ith isotope (Sv/Bq).

C.2.2 TOXICOLOGICAL EXPOSURE CALCULATION PROCESS

A method of comparison to guidelines for individual toxic chemicals is given by the equation:

$$FC = C * RF * RR * \frac{X}{Q} * \frac{1000}{ERPG} \tag{C-2}$$

where,

FC = Fraction of risk acceptance guideline

C = Concentration of toxic material in waste (g/L)

RF = Release fraction

RR = rate of material being released from tank (L/s)

X/Q = atmospheric dispersion coefficient (s/m^3)

ERPG = Emergency Response Planning Guideline (mg/m^3)

The 1000 is a unit conversion (mg/g).

Each toxic chemical has three ERPGs: ERPG-1, ERPG-2 and ERPG-3; plus a fourth limit PEL-TWA. The limit used depends on the frequency class of the receptor and the whether the onsite or offsite receptor is being considered. ERPG-1 is a level at which most people will experience no permanent effects, exceeding ERPG-2 can result in permanent damage, and exceeding ERPG-3 can result in life threatening effects.

The toxic evaluation requires adding up the sum of the concentration of the toxics (Cd, Hg, and U) divided by the appropriate limit; the sum of the corrosives (NaOH) divided by the appropriate limit; and the particulate concentration divided by the appropriate limit.

Particulates are evaluated since it possible that a large enough concentration of even nontoxic particulates can cause choking. The particulates are compared to the limits by the following equation:

$$SOF = D * Q' * \frac{X}{Q'} * \frac{1E+06}{RG} \tag{C-3}$$

where,

SOF = Sum of fractions

d = density of solids (usually taken at 1.6 g/cm^3)

Q' = release rate (L/s)

X/Q' = atmospheric dispersion coefficient (s/m^3).

RG = risk guideline (appropriate PEL or ERPG, mg/m^3)

The 1E+06 is a unit conversion.

The limits for particulates are:

$$
\begin{aligned}
\text{PEL-TWA} &= 10 \ mg/m^3 \\
\text{ERPG-1} &= 30 \ mg/m^3 \\
\text{ERPG-2} &= 50 \ mg/m^3 \\
\text{ERPG-3} &= 100 \ mg/m^3
\end{aligned}
$$

The procedure requires that the largest sum of fractions in the three categories be examined. If the largest is less than 1, the Risk Guidelines are met.

C.3.0 ASSUMPTIONS

Two reference cases were analyzed. A best estimate case was based upon analyzing 0.92 m^3 of reacted waste in tank U-105. A bounding case based upon analyzing 25.3 m^3 of reacting waste in tank U-105 was analyzed as the second case. Both reference cases specify the average TOC and moisture of the reacted waste as 7 wt% TOC and 10 wt% moisture respectively. U-105 contains 1582 m^3 of total waste and has a headspace volume of 1652 m^3.

(1) From thermodynamic calculations (Fauske 1996), a reaction temperature of 800 °C was used for this analysis. A large fraction of the cesium, mercury, and sodium hydroxide are volatilized at this temperature. These compounds dominate the radiological, toxicological, and corrosives releases.

(2) The respirable fraction is the fraction of the material which is released that is in the respirable range. Because this material is formed as a vapor at temperature and will eventually condense to form aerosols as it leaves the tank, or shortly thereafter, it is expected that a majority of the material will be in the respirable particle size range. For the purposes of this dose calculation, the respirable fraction is taken as 1.0. That is, it is assumed that all of the radionuclides of interest reach the maximum exposed individual as respirable particles.

(3) When the gas pressure in the tank exceeds the HEPA filter pressure capabilities, the HEPA filter will rupture and disperse a significant fraction of its burden. The rupture pressure of the HEPA filter is taken to be 0.1 atm overpressure (10 kPa or 1.47 psig). HEPA filters with active ventilation accumulate more activity and hence give a larger dose at blowout. Filters are changed based on accumulation of material on the filter (as back calculated from the direct radiation dose rate). For purposes of this analysis, the additional inhalation dose attributed

to the mechanical failure of the HEPA is (Cowley 1996a): Onsite 15 mSv and Offsite 0.013 mSv.

(4) The doses given are based on an onsite receptor X/Q of 0.0341 s/m^3 and an offsite receptor X/Q of 2.83E-05 s/m^3 (Cowley 1996b). Values are given for bounding conditions (99.5% meteorology). These X/Q values are calculated for the tank farm areas relative to the nearest boundary, now taken as the Columbia River to the north of the tank farms.

(5) The assumed breathing rate is 3.3E-04 m^3/s.

C.4.0 INPUT DATA

The release fractions for toxic and radiological species are summarized below. It should be noted that the release fraction is based on the inventory of each specie in the total waste volume, not on the reacted portion of the waste. The release fraction calculations are shown in Appendix B.

Bounding radionuclide and toxic concentrations were assumed for U-105 (Tables C-2 and C-3, respectively). The radionuclide concentrations are from Cowley (1996a), and the toxic concentrations are from Van Keuren (1996).

Table C-1. Release Fractions for Tank U-105

Analyte	Release Fraction (0.92 m^3 Combusted)	Release Fraction (25 m^3 Combusted)
Cs-137	3.6E-05	5.5E-03
Sr-90	1.5E-12	2.3E-10
Y-90	4.9E-14	7.5E-12
Co-60	1.6E-12	2.4E-10
Tc-99	5.5E-12	8.4E-10
Sb-125	3.4E-06	5.3E-04
Eu-154	3.9E-07	5.9E-05
Pu-239	5.5E-14	8.5E-12
Cd	1.2E-08	1.9E-06
Hg	9.9E-05	1.5E-02
NaOH	1.2E-08	1.9E-06

Table C-2. Bounding Radionuclide Concentrations and Conversion Factors

Isotope	Dose Conversion Factor (Sv/Bq)	Concentration (Bq/L)	Sv/L
Cs-137	8.63E-09	1.01E+11	8.72E+02
Sr-90	6.47E-08	1.63E+12	1.05E+05
Y-90	2.28E-09	1.63E+12	3.72E+03
Co-60	5.91E-08	4.18E+08	2.47E+01
Tc-99	2.25E-09	1.20E+10	2.70E+01
Sb-125	3.30E-09	2.80E+08	9.24E-01
Eu-154	7.73E-08	5.75E+09	4.44E+02
Pu-239	1.16E-04	4.40E+08	5.10E+04

Table C-3. Bounding Toxic Concentrations

Analyte	Concentration (g/L)
Cadmium	1.7
Mercury	54
Sodium Hydroxide	210
Uranium	280

Additional dose from HEPA failure (Cowley 1996a):

Onsite	15 mSv
Offsite	0.013 mSv

The doses calculated are based on an onsite receptor X/Q of 0.0341 s/m3 and an offsite receptor X/Q of 2.83E-05 s/m^3 (Cowley 1996b). Values are given for bounding conditions (99.5% meteorology). These X/Q values are calculated for the tank farm areas relative to the nearest boundary, now taken as the Columbia River to the north of the tank farms.

The assumed breathing rate is 3.3E-04 m^3/s (Cowley 1996b).

C.5.0 CALCULATIONS

An Excel worksheet was used to automate the dose calculations. A table of the worksheet is included in the Results section. An example radiological dose calculation follows.

The dose contribution for Cs-137 in Tank U-105 is calculated to be:

$$TWV = 1582 \text{ m}^3$$
$$X/Q = 0.034 \text{ s/m}^3 \text{ (onsite)}$$
$$BR = 3.3 \text{ E-04 m}^3/\text{s}$$
$$RF = 3.6 \text{ E-05}$$
$$Qi = 1.01 \text{ E+11 Bq/L}$$
$$DCF = 8.63 \text{ E-09 Sv/Bq}$$

Dose = 1582 m^3 x 0.034 s/m^3 x 3.3 E-04 m^3/s x 3.6 E-05 x 1.01 E+11 Bq/L
x 8.63 E-09 Sv/Bq x 1000 L/m^3 x 1000 mSv/Sv

= 5.57 E+02 mSv dose contribution of Cs-137 for Tank U-105.

This identical calculation is performed for each of the 11 isotopes of interest. The contributions are then summed to produce an onsite dose of 5.62E+02 mSv.

The offsite calculation is performed the same way, except that the X/Q used is 1.9E-05 s/m^3. The dose due to the Cs-137 is shown to dominate the results, as has been shown in previous reports and dose calculations.

The dose contributions from the HEPA filter blowout and the dome collapse are then added to the inhalation/dispersion dose calculated herein, in cases where the HEPA filter is determined to fail. The additional dose due to the HEPA blowout has been estimated (Cowley 1996a) to be 15 mSv onsite and 0.013 mSv offsite. At deadline, no firm estimate of dome collapse dose was available; therefore the spreadsheet shows a zero adder for this term. The summary columns in the Summary Table indicate dose due to dispersion/inhalation only and combined dispersion/inhalation dose plus mechanical HEPA filter failure dose adder.

The doses given are based on an onsite receptor X/Q of 0.0341 s/m^3 and an offsite receptor X/Q of 2.83E-05 s/m^3 (Cowley 1996b). Values are given for bounding conditions (99.5% meteorology). These X/Q values are calculated for the tank farm areas relative to the nearest boundary, now taken as the Columbia River to the north of the tank farms. The assumed breathing rate is 3.3E-04 m^3/s.

For toxicological doses, a sample calculation is given below for Hg:

$$FC = C*RF*RR*\frac{X}{Q}*\frac{1000}{ERPG} \tag{C-4}$$

2.87 E+03 = (54 * 1582/0.92 * 1000) * (9.9E-05) * (.92/1006) * (.0341) * 1000/0.1

Summing up the toxics of concern, mercury dominates the other species; i.e.,

Cd + U + Hg = 1.09E-03 + 4.3E-07 + 2.87E+03 for the total toxic dose result. The total is equal to the mercury dose contribution, for practical purposes.

C.6.0 RESULTS

Table C-6 is the worksheet used to automate the dose calculations. The pertinent summary dose consequences are extracted from this worksheet and summarized in Tables C-4 and C-5.

Table C-4. Summary of Dose Consequences for Tank U-105

Combustible Waste Volume (m³)	Radiological Dose: Dispersion Only		Radiological Dose: Dispersion + HEPA Adder Dose	
	Onsite (mSv)	Offsite (mSv)	Onsite (mSv)	Offsite (mSv)
0.92	5.62E+02	4.66E-01	5.77E+02	4.79E-01
25.30	8.58E+04	7.12E+01	8.58E+04	7.12E+01

Table C-5. Toxic Dose Sum of Fractions, Hg + U + Cd

Waste Combusted (m³)	Limit Category	Onsite	Limit Category	Offsite
0.92	ERPG-1	3.82E+03	PEL-TWA	4.76E+00
	ERPG-2	2.87E+03	ERPG-1	3.17E+00
	ERPG-3	2.05E+01	ERPG-2	2.38E+00
25.30	ERPG-1	1.92E+05	PEL-TWA	2.39E+02
	ERPG-2	1.44E+05	ERPG-1	1.59E+02
	ERPG-3	1.03E+03	ERPG-2	1.19E+02

The radiological dose consequences are also depicted graphically in Figures C-1 and C-2. The onsite radiological doses exceed the risk evaluation guidelines by a large degree, as shown in Figure C-1. The offsite radiological doses are acceptable for the 0.92 m³ case when compared to risk evaluation guidelines as depicted below the offsite risk evaluation curve on Figure C-1. Both the offsite radiological doses and offsite toxicological exposures greatly exceed the risk evaluation guidelines as shown in Figure C-2.

Figure C-1.   Comparison of Consequences to Radiological Guidelines for 0.92 m³ Combustion Event in Tank U-105
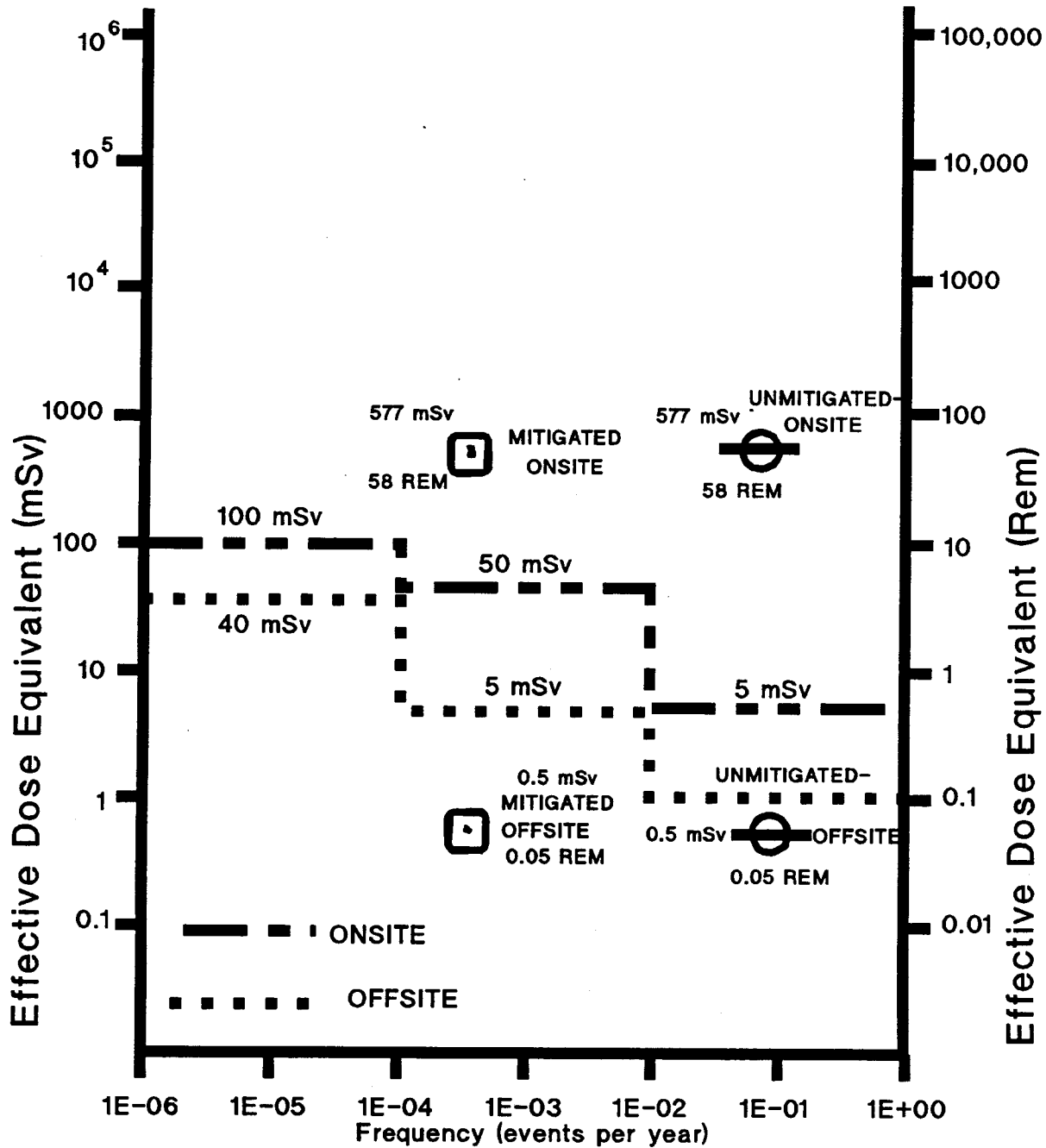

AAARAG13.GAL/960819/ABW

Figure C-2.   Comparison of Consequences to Radiological Guidelines for 25 m³
Combustion Event in Tank U-105

AAARAG14.GAL/960826/ABW
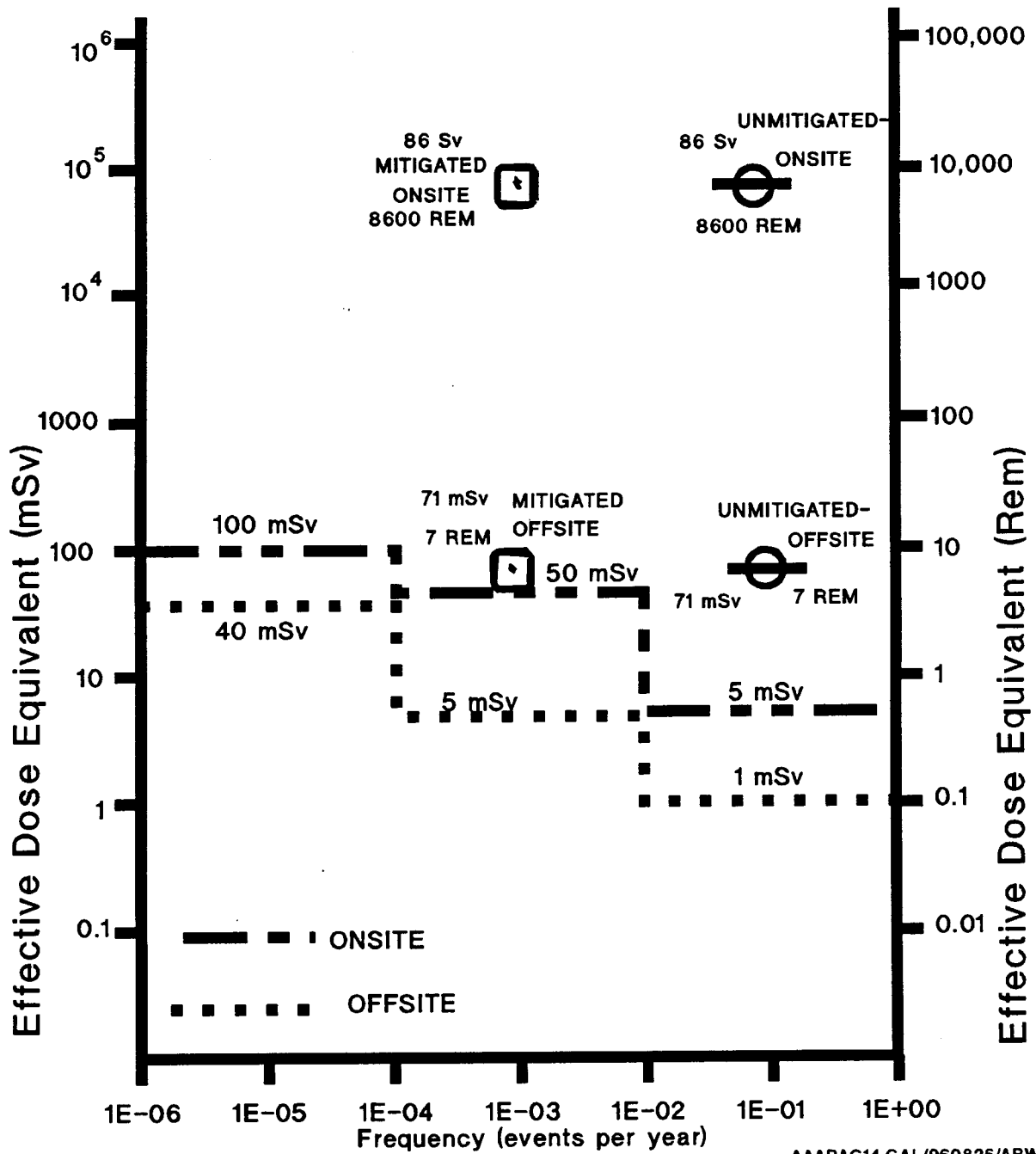
Table C-6. Radiological and Toxicological Dose Work Sheet (Page 1 of 4)

Mechanical Dose From HEPA Failure			Mechanical Dose From Dome Collapse						X/Q Meteorology Toggle	
Onsite	15	mSv	Onsite	0	mSv				Onsite	Offsite
Offsite	0.013	mSv	Offsite	0	mSv		50th		5.33E-03	4.43E-06
						X	"95th"		3.41E-02	2.83E-05

NEW SITE BOUNDARY; X/Q "95th" Percentile			Concentration (g/L)	PEL-TWA (mg/m3)	ERPG-1 (mg/m3)	ERPG-2 (mg/m3)	ERPG-3 (mg/m3)	Agnew (g/M)		Source Term Toggle (use "1")
	Onsite	Offsite	Cd	1.70E+00	5.00E-03	2.00E-01	1.00E+00	1.00E+01			Agnew for Cs, Hg; SuperTank Otherwise
X/Q	3.41E-02	2.83E-05	Hg	5.40E+01	5.00E-02	7.50E-02	1.00E-01	1.40E+01	200.59	1	Super Tank
BR	3.30E-04	3.30E-04	NaOH	2.10E+02	2.00E+00	2.00E+00	4.00E+01	1.00E+02			
X/Q*BR	1.13E-05	9.34E-09	U	2.80E+02	2.00E-01	1.00E+00	1.00E+01	2.00E+01			Offsite INGi Toggle

									No	Yes
SOURCE TERM: Super Tank						INCLUDE OFFSITE INGESTION:	No		X	

Isotope	DCFi (Sv/Bq)	Qi (Bq/L)	Agnew (Bq/Ci)	Onsite Dose Term: Qi*DCFi (Sv/L)	Agnew Onsite Term (Sv/Ci)	Offsite: INGi (Sv-m3 /Bq-s)	Offsite Dose Term: Qi* [(DCFi *BR) +INGi] (Sv-m3/L-s)	Agnew Term: (Sv-m3 /Ci-s)		Half-Life (yrs.)	Percent Remaining after 50 yrs	No (Zero)	Offsite: INGi (Sv-m3 /Bq-s)
Co-60	5.91E-08	4.18E+08		2.47E+01		0.00E+00	8.15E-03		Co-60	5.272	0.14%	0.00E+00	4.90E-13
Sr-90	6.47E-08	1.63E+12		1.05E+05		0.00E+00	3.48E+01	Agnew	Sr-90	29	30.27%	0.00E+00	2.30E-12
Y-90	2.28E-09	1.63E+12		3.72E+03		0.00E+00	1.23E+00	Term:	Y-90*	NA	30.27%	0.00E+00	2.00E-13
Tc-99	2.25E-09	1.20E+10		2.70E+01		0.00E+00	8.91E-03	(Sv-m3	Tc-99	213000	99.98%	0.00E+00	4.20E-14
Sb-125	3.30E-09	2.80E+08		9.24E-01		0.00E+00	3.05E-04	/Ci-s)	Sb-125	2.76	0.00%	0.00E+00	5.10E-14
Cs-137	8.63E-09	1.01E+11	3.70E+10	8.72E+02	3.19E+02	0.00E+00	2.88E-01	1.05E-01	Cs-137	30.17	31.70%	0.00E+00	9.00E-13
Eu-154	7.73E-08	5.75E+09		4.44E+02		0.00E+00	1.47E-01		Eu-154	8.5	1.70%	0.00E+00	1.80E-13
Np-237	1.46E-04	3.02E+07		4.41E+03		0.00E+00	1.46E+00		Np-237	2.14E+06	100.00%	0.00E+00	9.90E-11
Pu-238	1.06E-04	1.87E+08		1.98E+04		0.00E+00	6.54E+00		Pu-238	87.74	67.37%	0.00E+00	6.10E-11
Pu-239	1.16E-04	4.40E+08		5.10E+04		0.00E+00	1.68E+01		Pu-239	24110	99.86%	0.00E+00	6.80E-11
Pu-241	2.23E-06	3.22E+09		7.18E+03		0.00E+00	2.37E+00		Pu-241	14.4	9.01%	0.00E+00	1.30E-12
Am-241	1.20E-04	2.29E+08		2.75E+04		0.00E+00	9.07E+00		Am-241**	432.2	163.00%	0.00E+00	6.90E-11
Cm-244	6.70E-05	2.29E+06		1.53E+02		0.00E+00	5.06E-02		Cm-244	18.11	14.75%	0.00E+00	3.80E-11

Table C-6. Radiological and Toxicological Dose Work Sheet (Page 2 of 4)

																		Onsite Dose	
Release Fractions from SUMMRY1C Threshold Values from THRSHLDB																			
TANK ID	EVENT	TOT WASTE VOL.	REACTED VOL.	Cs Agnew (Ci/L)	Hg Agnew (M/L)	DURATION	CO RF	SR RF	Y RF	TC RF	SB RF	CS RF	EU RF	PU RF	CD RF	HG RF	NA RF	Dispersion +Mech.	Dispersion
U105	(15*HEPA+DOME)/16	1582	0.233	0.255	1.00E-05	640	1.20E-15	5.80E-16	6.60E-18	8.40E-13	1.10E-10	1.60E-07	4.30E-09	8.80E-17	9.20E-11	1.20E-05	1.30E-11	1.75E+01	2.52E+00
U105	(13*HEPA+3*DOME)/16	1582	0.423	0.255	1.00E-05	780	3.40E-15	1.60E-15	1.80E-17	2.30E-12	3.10E-10	4.30E-07	1.20E-08	2.40E-16	2.50E-10	3.30E-05	3.50E-11	2.18E+01	6.77E+00
U105	(5*HEPA+3*DOME)/8	1582	0.707	0.255	1.00E-05	925	7.70E-15	3.60E-15	4.10E-17	5.20E-12	7.20E-10	9.80E-07	2.70E-08	5.50E-16	5.80E-10	7.50E-05	8.00E-11	3.04E+01	1.54E+01
U105		1582	0.92			1006	1.60E-12	1.50E-12	4.90E-14	5.50E-12	3.40E-06	3.60E-05	3.90E-07	5.50E-14	1.20E-08	9.90E-05	1.20E-08	5.77E+02	5.62E+02
U105	(HEPA+ 3*DOME)/4	1582	1.275	0.255	1.00E-05	1125	1.90E-14	8.80E-15	1.00E-16	1.30E-11	1.70E-09	2.40E-06	6.50E-08	1.30E-15	1.40E-09	1.80E-04	2.00E-10	5.28E+01	3.78E+01
U105	2*DOME	1582	3.312	0.255	1.00E-05	1545	1.30E-13	6.00E-14	6.80E-16	8.60E-11	1.20E-08	1.60E-05	4.40E-07	9.10E-15	9.50E-09	1.20E-03	1.30E-09	2.67E+02	2.52E+02
U105	4.5*DOME	1582	7.415	0.255	1.00E-05	2020	3.90E-13	1.80E-13	2.10E-15	2.60E-10	3.60E-08	4.90E-05	1.30E-06	2.80E-14	2.90E-08	3.80E-03	4.00E-09	7.86E+02	7.71E+02
U105	9*DOME	1582	14.846	0.255	1.00E-05	2545	8.70E-13	4.10E-13	4.70E-15	5.90E-10	8.10E-08	1.10E-04	3.00E-06	6.30E-14	6.50E-08	8.50E-03	9.10E-09	1.75E+03	1.73E+03
U105		1582	25.3			3035	2.40E-10	2.30E-10	7.50E-12	8.40E-10	5.30E-04	5.50E-03	5.90E-05	8.50E-12	1.90E-06	1.50E-02	1.90E-06	8.58E+04	8.58E+04
U105	18*DOME	1582	29.703	0.255	1.00E-05	2953.8	1.90E-12	8.70E-13	9.90E-15	1.30E-09	1.70E-07	2.40E-04	6.40E-06	1.30E-13	1.40E-07	1.80E-02	1.90E-08	3.79E+03	3.77E+03
U105	36*DOME	1582	59.342	0.255	1.00E-05	3073.3	3.80E-12	1.80E-12	2.00E-14	2.60E-09	3.50E-07	4.80E-04	1.30E-05	2.70E-13	2.80E-07	3.70E-02	3.90E-08	7.57E+03	7.55E+03
U105	72*DOME	1582	118.65	0.255	1.00E-05	3309.5	7.60E-12	3.60E-12	4.10E-14	5.20E-09	7.10E-07	9.70E-04	2.60E-05	5.40E-13	5.70E-07	7.40E-02	7.90E-08	1.53E+04	1.53E+04
U105	144*DOME	1582	237.266	0.255	1.00E-05	3770.3	1.50E-11	7.20E-12	8.10E-14	1.00E-08	1.40E-06	1.90E-03	5.30E-05	1.10E-12	1.10E-06	1.50E-01	1.60E-07	2.99E+04	2.99E+04

Table C-6. Radiological and Toxicological Dose Work Sheet (Page 3 of 4)

		Decayed 50 Years				Cd						U					
		Onsite Dose		Offsite Dose		Onsite			Offsite			Onsite			Offsite		
Offsite Dose																	
Disp +Ing +Mech.	Dispersion + Ingestion	Dispersion +Mech.	Dispersion	Disp +Ing +Mech.	Dispersion + Ingestion	ERPG-1	ERPG-2	ERPG-3	PEL-TWA	ERPG-1	ERPG-2	ERPG-1	ERPG-2	ERPG-3	PEL-TWA	ERPG-1	ERPG-2
1.51E-02	2.09E-03	1.58E+01	7.88E-01	1.37E-02	6.54E-04	6.59E-05	1.32E-05	1.32E-06	2.19E-06	5.47E-08	1.09E-08	1.04E-08	1.04E-09	5.19E-10	4.31E-11	8.62E-12	8.62E-13
1.86E-02	5.62E-03	1.71E+01	2.12E+00	1.48E-02	1.76E-03	1.47E-04	2.94E-05	2.94E-06	4.88E-06	1.22E-07	2.44E-08	2.32E-08	2.32E-09	1.16E-09	9.64E-11	1.93E-11	1.93E-12
2.58E-02	1.28E-02	1.98E+01	4.82E+00	1.70E-02	4.00E-03	2.88E-04	5.75E-05	5.75E-06	9.54E-06	2.39E-07	4.77E-08	4.49E-08	4.49E-09	2.25E-09	1.86E-10	3.73E-11	3.73E-12
4.79E-01	4.66E-01	1.92E+02	1.77E+02	1.60E-01	1.47E-01	5.47E-03	1.09E-03	1.09E-04	1.82E-04	4.54E-06	9.08E-07	4.13E-06	4.13E-07	2.07E-07	1.71E-08	3.43E-09	3.43E-10
4.43E-02	3.13E-02	2.68E+01	1.18E+01	2.28E-02	9.81E-03	5.71E-04	1.14E-04	1.14E-05	1.89E-05	4.74E-07	9.47E-08	8.73E-08	8.73E-09	4.36E-09	3.62E-10	7.24E-11	7.24E-12
2.22E-01	2.09E-01	9.38E+01	7.88E+01	7.84E-02	6.54E-02	2.82E-03	5.64E-04	5.64E-05	9.36E-05	2.34E-06	4.68E-07	4.45E-07	4.45E-08	2.22E-08	1.85E-09	3.69E-10	3.69E-11
6.53E-01	6.40E-01	2.56E+02	2.41E+02	2.13E-01	2.00E-01	6.58E-03	1.32E-03	1.32E-04	2.19E-04	5.46E-06	1.09E-06	1.05E-06	1.05E-07	5.23E-08	4.34E-09	8.69E-10	8.69E-11
1.45E+00	1.44E+00	5.57E+02	5.42E+02	4.62E-01	4.49E-01	1.17E-02	2.34E-03	2.34E-04	3.89E-04	9.72E-06	1.94E-06	1.87E-06	1.87E-07	9.35E-08	7.76E-09	1.55E-09	1.55E-10
7.12E+01	7.12E+01	2.71E+04	2.71E+04	2.25E+01	2.25E+01	2.87E-01	5.74E-02	5.74E-03	9.53E-03	2.38E-04	4.76E-05	2.11E-04	2.11E-05	1.06E-05	8.78E-07	1.76E-07	1.76E-08
3.15E+00	3.13E+00	1.20E+03	1.18E+03	9.94E-01	9.81E-01	2.17E-02	4.35E-03	4.35E-04	7.21E-04	1.80E-05	3.61E-06	3.32E-06	3.32E-07	1.66E-07	1.38E-08	2.76E-09	2.76E-10
6.28E+00	6.27E+00	2.38E+03	2.36E+03	1.97E+00	1.96E+00	4.18E-02	8.36E-03	8.36E-04	1.39E-03	3.47E-05	6.93E-06	6.64E-06	6.64E-07	3.32E-07	2.75E-08	5.51E-09	5.51E-10
1.27E+01	1.27E+01	4.79E+03	4.78E+03	3.98E+00	3.96E+00	7.90E-02	1.58E-02	1.58E-03	2.62E-03	6.55E-05	1.31E-05	1.23E-05	1.23E-06	6.16E-07	5.11E-08	1.02E-08	1.02E-09
2.48E+01	2.48E+01	9.37E+03	9.35E+03	7.78E+00	7.76E+00	1.34E-01	2.68E-02	2.68E-03	4.44E-03	1.11E-04	2.22E-05	2.20E-05	2.20E-06	1.10E-06	9.14E-08	1.83E-08	1.83E-09

Table C-6.   Radiological and Toxicological Dose Work Sheet (Page 4 of 4)

| Hg | | | | | | Toxic Total | | | | | | Na | | | | | |
| Onsite | | | Offsite | | | Onsite | | | Offsite | | | Onsite | | | Offsite | | |
ERPG-1	ERPG-2	ERPG-3	PEL-TWA	ERPG-1	ERPG-2	ERPG-1	ERPG-2	ERPG-3	PEL-TWA	ERPG-1	ERPG-2	ERPG-1	ERPG-2	ERPG-3	PEL-TWA	ERPG-1	ERPG-2
7.28E+02	5.46E+02	3.90E+00	9.07E-01	6.04E-01	4.53E-01	7.28E+02	5.46E+02	3.90E+00	9.07E-01	6.04E-01	4.53E-01	1.15E-04	5.75E-06	2.30E-06	9.55E-08	9.55E-08	4.77E-09
1.64E+03	1.23E+03	8.80E+00	2.05E+00	1.36E+00	1.02E+00	1.64E+03	1.23E+03	8.80E+00	2.05E+00	1.36E+00	1.02E+00	2.54E-04	1.27E-05	5.08E-06	2.11E-07	2.11E-07	1.05E-08
3.15E+03	2.36E+03	1.69E+01	3.92E+00	2.61E+00	1.96E+00	3.15E+03	2.36E+03	1.69E+01	3.92E+00	2.61E+00	1.96E+00	4.90E-04	2.45E-05	9.80E-06	4.07E-07	4.07E-07	2.03E-08
3.82E+03	2.87E+03	2.05E+01	4.76E+00	3.17E+00	2.38E+00	3.82E+03	2.87E+03	2.05E+01	4.76E+00	3.17E+00	2.38E+00	6.76E-02	3.38E-03	1.35E-03	5.61E-05	5.61E-05	2.80E-06
6.21E+03	4.66E+03	3.33E+01	7.74E+00	5.16E+00	3.87E+00	6.21E+03	4.66E+03	3.33E+01	7.74E+00	5.16E+00	3.87E+00	1.01E-03	5.03E-05	2.01E-05	8.36E-07	8.36E-07	4.18E-08
3.02E+04	2.26E+04	1.62E+02	3.76E+01	2.50E+01	1.88E+01	3.02E+04	2.26E+04	1.62E+02	3.76E+01	2.50E+01	1.88E+01	4.77E-03	2.38E-04	9.53E-05	3.96E-06	3.96E-06	1.98E-07
7.31E+04	5.48E+04	3.91E+02	9.10E+01	6.06E+01	4.55E+01	7.31E+04	5.48E+04	3.91E+02	9.10E+01	6.06E+01	4.55E+01	1.12E-02	5.61E-04	2.24E-04	9.31E-06	9.31E-06	4.65E-07
1.30E+05	9.73E+04	6.95E+02	1.61E+02	1.08E+02	8.07E+01	1.30E+05	9.73E+04	6.95E+02	1.61E+02	1.08E+02	8.07E+01	2.03E-02	1.01E-03	4.05E-04	1.68E-05	1.68E-05	8.40E-07
1.92E+05	1.44E+05	1.03E+03	2.39E+02	1.59E+02	1.19E+02	1.92E+05	1.44E+05	1.03E+03	2.39E+02	1.59E+02	1.19E+02	3.55E+00	1.77E-01	7.09E-02	2.94E-03	2.94E-03	1.47E-04
2.37E+05	1.78E+05	1.27E+03	2.95E+02	1.96E+02	1.47E+02	2.37E+05	1.78E+05	1.27E+03	2.95E+02	1.96E+02	1.47E+02	3.64E-02	1.82E-03	7.29E-04	3.02E-05	3.02E-05	1.51E-06
4.68E+05	3.51E+05	2.51E+03	5.82E+02	3.88E+02	2.91E+02	4.68E+05	3.51E+05	2.51E+03	5.82E+02	3.88E+02	2.91E+02	7.19E-02	3.59E-03	1.44E-03	5.97E-05	5.97E-05	2.98E-06
8.68E+05	6.51E+05	4.65E+03	1.08E+03	7.21E+02	5.41E+02	8.68E+05	6.51E+05	4.65E+03	1.08E+03	7.21E+02	5.41E+02	1.35E-01	6.76E-03	2.70E-03	1.12E-04	1.12E-04	5.61E-06
1.55E+06	1.16E+06	8.28E+03	1.92E+03	1.28E+03	9.62E+02	1.55E+06	1.16E+06	8.28E+03	1.92E+03	1.28E+03	9.62E+02	2.40E-01	1.20E-02	4.81E-03	1.99E-04	1.99E-04	9.97E-06

C.7.0 CONCLUSIONS

The onsite consequences are excessive from both the best estimate and bounding safety analyses. The offsite consequences are acceptable only for the best estimate radiological calculations.

C.8.0 REFERENCES

Cowley, W. L., 1996a, *Development of Radiological Concentrations and Unit Liter Doses for TWRS FSAR Radiological Consequence Calculations*, WHC-SD-WM-SARR-037, Rev. 0, Westinghouse Hanford Company, Richland, Washington.

Cowley, W. L., 1996b, *Tank Waste Compositions and Atmospheric Dispersion Coefficients for Use in ASA Consequence Assessments*, WHC-SD-WM-SARR-016, Rev. 2, Westinghouse Hanford Company, Richland, Washington.

Fauske, H. K., 1996, *An Assessment of Requirements for Organic-Nitrate Propagating Reactions Including RSST and Tube Progation Test Results With Waste Simulants*, FAI/96-48, Rev. 0, Fauske and Associates, Inc., Burr Ridge, Illinois.

Van Keuren, J. C., 1996, *Toxic Chemical Considerations for Tank Farm Releases*, WHC-SD-WM-SARR-011, Rev. 2, Westinghouse Hanford Company, Richland, Washington.

DISTRIBUTION

<u>Number of copies</u>

   <u>OFFSITE</u>

6   <u>U.S. Department of Energy</u>
EM-38, Trevion II
12800 Middlebrook Road
Germantown, MD 20874

Harry Calley (4)
Maureen Hunemuller
Ken Lang

<u>U.S. Department of Energy</u>
Forrestal Building
1000 Independence Avenue SW
Washington, DC 20585

Shirley Campbell, EH-71
John Kaysak, EM-25

1   Charles S. Abrams
1987 Virginia
Idaho Falls, ID 83404

1   David O. Campbell
102 Windham Road
Oak Ridge, TN 37830

1   Fred N. Carlson
6965 North 5th West
Idaho Falls, ID 83401

1   Billy C. Hudson
202 Northridge Court
Lindsborg, KA 67456

1   Thomas S. Kress
102-B Newridge Road
Oak Ridge, TN 37839

DISTRIBUTION (Continued)

<u>Number of copies</u>

   <u>OFFSITE</u>

1	Thomas E. Larson 2711 Walnut Street Los Alamos, NM 87544
1	<u>Air Products & Chemicals, Inc.</u> 7201 Hamilton Blvd Allentown, PA 18195-1501 George E. Schmauch
1	<u>Brookhaven National Laboratory</u> Upton, NY 11973 Kamal K. Bandyopadhyay
2	<u>Fauske and Associates, Inc.</u> 16W070 W. 83rd St. Burr Ridge, IL 60521 Michael Epstein Hans K. Fauske
1	<u>G & P Consulting, Inc.</u> 3640 Ballard Road Dallas, OR 97338 Arlin K. Postma
1	<u>Harvard University</u> 295 Upland Avenue Newton Highlands, MA 02161 Melvin W. First

DISTRIBUTION (Continued)

<u>Number of copies</u>

<u>OFFSITE</u>

1   <u>MIT/Department of Nuclear Engineering</u>
     77 Massachusetts Ave.
     Room 24-102
     Cambridge, MA   02139

     Mujid S. Kazimi

1   <u>Nuclear Consulting Services, Inc</u>.
     P.O. Box 29151
     Columbus, OH   43229-0151

     J. Louis Kovach

     <u>Oak Ridge National Laboratory</u>

1   Emory D. Collins
     P.O. Box 2008
     7930, MS-6385
     Oak Ridge, TN   37831-6385

1   Charles W. Forsberg
     P.O. Box 2008
     MS-6495
     Oak Ridge, TN   37831-6495

1   <u>Rice University</u>
     5211 Paisley
     Houston, TX   77096

     Andrew S. Veletsos

2   <u>Sandia National Laboratories</u>
     P.O. Box 5800
     Albuquerque, NM   87185

     Dana A. Powers, MS-0744
     Scott E. Slezak, MS-0741

DISTRIBUTION (Continued)

Number of copies

OFFSITE

3   Science Applications International Corporation
      20300 Century Blvd, Suite 200-B
      Germantown, MD 20874

      Paul Hogroian (3)

      State of Washington - Department of Ecology

1   Robert C. King
      P. O. Box 47600
      Olympia, WA 98504-7600

1   Alex B. Stone
      1315 W. 4th Avenue
      Kennewick, WA 99336

1   Waste Policy Institute
      555 Quince Orchard Road, Suite 600
      Gaitherburg, MD 20878-1437

      Donald T. Oakley

ONSITE

7   U.S. Department of Energy,
      Richland Operations Office

D. H. Irby (2)	S7-54
W. F. Hendrickson	S7-54
A. G. Krasopoulos	A4-81
Public Reading Room	H2-53
RL Docket File (2)	B1-17

DISTRIBUTION (Continued)

4   <u>Pacific Northwest Laboratory</u>

       J. W. Brothers   K5-22
       R. T. Hallen   P8-38
       M. A. Lilga   P8-38
       Hanford Technical Library   P8-55

34   <u>Westinghouse Hanford Company</u>

       H. Babad   S7-14
       M. V. Berriochoa   B3-30
       J. B. Billetdeaux   S7-15
       J. F. Bores   S1-57
       W. S. Callaway   S3-90
       R. J. Cash (2)   S7-14
       M. D. Crippen   L5-31
       R. D. Crowe   H0-32
       M. L. Dexter   R1-51
       D. R. Dickinson   L5-31
       G. T. Dukelow   S7-14
       J. M. Grigsby   A3-37
       M. N. Islam   R3-08
       D. W. Jeppson   L5-31
       N. W. Kirch   R2-11
       C. A. Kuhlman   B3-30
       L. L. Lockrem   S3-90
       J. E. Meacham (5)   S7-14
       N. J. Milliken   A3-37
       S. R. Moreno   B3-06
       F. R. Reich   L5-55
       E. F. Riedel   S3-90
       B. C. Simpson   R2-12
       L. E. Thomas   R3-08
       Central Files   A3-88
       Correspondence Processing   A3-01
       EDMC   H6-08
       DPC   A3-94

This page intentionally left blank.